ISSN 2413-5577

№ 2 Апрель – Июнь 2025

Экологическая безопасность прибрежной и шельфовой зон моря

Ecological Safety of Coastal and Shelf Zones of Sea

No. 2 April – June 2025

ecological-safety.ru

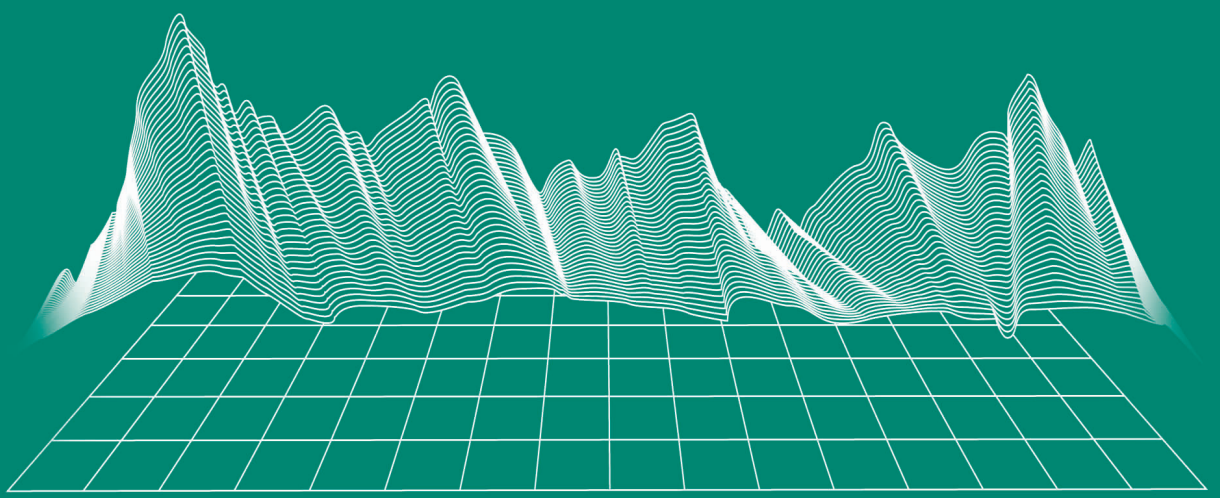

ISSN 2413-5577

No. 2, 2025
April – June

Publication frequency:
Quarterly

16+

ECOLOGICAL SAFETY OF COASTAL AND SHELF ZONES OF SEA

Scientific and theoretical peer reviewed journal

FOUNDER AND PUBLISHER:
Federal State Budget Scientific Institution
Federal Research Centre
"Marine Hydrophysical Institute of RAS"

The Journal publishes original research results, review articles (at the editorial board's request) and brief reports.

The Journal aims at publication of results of original scientific research concerning the state and interaction of geospheres (atmosphere, lithosphere, hydrosphere, and biosphere) within coastal and shelf areas of seas and oceans, methods and means of study thereof, ecological state of these areas under anthropogenic load as well as environmental protection issues.

The Journal's editorial board sees its mission as scientific, educational and regulatory work to preserve the ecological balance and restore the resource potential of coastal and shelf areas believing that despite the geographical limitations of the areas under study, the processes taking place within them have a significant impact on the waters of the seas and oceans and economic activity.

The Journal publishes original research materials, results of research performed by national and foreign scientific institutions in the coastal and shelf zones of seas and oceans, review articles (at the editorial board's request) and brief reports on the following major topics:
- Scientific basis for complex use of shelf natural resources
- Marine environment state and variability
- Coastal area state and variability; coast protection structures
- Monitoring and estimates of possible effects of anthropogenic activities
- Development and implementation of new marine environment control and monitoring technologies

The outcome of the research is information on the status, variability and possible effects of anthropogenic activities in the coastal and shelf marine areas, as well as the means to perform calculations and to provide information for making decisions on the implementation of activities in the coastal zone.

e-mail: ecology-safety@mhi-ras.ru

website: http://ecological-safety.ru

Founder, Publisher and Editorial Office address:
2, Kapitanskaya St.,
Sevastopol, 299011, Russia

Phone, fax: + 7 (8692) 54-57-16

EDITORIAL BOARD

РЕДАКЦИОННАЯ КОЛЛЕГИЯ

CONTENTS

No. 2. 2025 April – June, 2025

Shokurova I. G., Nikolsky N. V , Chernyshova E. D. Frontal Zones as Boundaries of Areas with Different Ranges of Sea Surface Temperature Seasonal Variability in the North Atlantic 6

Melnikov V. V., Serebrennikov A. N., Masevich A. V., Chudinovskikh E. S. The Main Patterns of the Black Sea Ecosystem Long-Term Changes 19

Lukashova O. A., Belokopytov V. N. Thermohaline Structure of Western Crimea Shelf Waters. 36

Kuznetsov A. S., Garmashov A. V. Estimation of the Characteristics of the Wind Field Seasonal Variability Near the Southern Coast of Crimea from Measurements with High Temporal Discreteness 53

Lomakin P. D., Ryabtsev Yu. N., Chepyzhenko A. I. Upwelling in the Black Sea Water Area near Cape Lukull Based on Numerical Modeling and Observational Data 67

Manilyuk Yu. V., Belokon A. Yu., Bagaev A. V., Yurovsky Yu. Yu., Lazorenko D. I. Resonance Properties of Water Areas Based on Mathematical Modelling Results: A Case of Sevastopol Bays (the Black Sea) 80

Widada S., Kunarso, Indrayanti E., Widiaratih R., Ismanto A., Zainuri M., Hadibarata T., Anindita M. A., Tristanova T., Jihadi M. S. Assessment and Characterization of Microplastics in Aquatic Environments near Pekalongan (Indonesia) 99

Pospelova N. V., Shchurov S. V., Kovrigina N. P., Lisitskaya E. V., Troshchenko O. A. Ecological State of Waters of the Sevastopol Seashore (Western Crimea) and its Influence on the Dynamics of Plankton Communities 118

Zaripova K. M., Demidova E. A., Tikhonova E. A., Burdiyan N. V., Doroshenko Yu. V., Basova E. D. The Abundance and Distribution of Individual Bacterial Groups in Coastal Waters of the Kamchatka Peninsula 135

Karpova E. P., Abliazov E. R. Distribution of the Chestnut Goby *Chromogobius quadrivittatus* (Steindachner, 1863) in the Black Sea and the Problem of its Range Expansion 149

Gogoberidze G. G., Rumiantceva E. A., Lednova I. A., Efimenko E. A. Natural and Technogenic Risks Assessment of Arctic Nature Use for the Murmansk Region Coastal Zone 159

СОДЕРЖАНИЕ

№ 2. 2025 Апрель – Июнь, 2025

Шокурова И. Г., Никольский Н. В., Чернышова Е. Д. Фронтальные зоны как границы областей с разным диапазоном сезонной изменчивости поверхностной температуры воды в Северной Атлантике 6

Мельников В. В., Серебренников А. Н., Масевич А. В., Чудиновских Е. С. Основные закономерности многолетних изменений экосистемы Черного моря 19

Лукашова О. А., Белокопытов В. Н. Термохалинная структура вод шельфа Западного Крыма 36

Кузнецов А. С., Гармашов А. В. Оценка характеристик сезонной изменчивости поля ветра у Южного берега Крыма по данным измерений с высокой временной дискретностью 53

Ломакин П. Д., Рябцев Ю. Н., Чепыженко А. И. Апвеллинг в акватории Черного моря у мыса Лукулл на основе численного моделирования и данных наблюдений 67

Манилюк Ю. В., Белоконь А. Ю., Багаев А. В., Юровский Ю. Ю., Лазоренко Д. И. Резонансные свойства акваторий севастопольских бухт (Черное море) по результатам математического моделирования 80

Widada S., Kunarso, Indrayanti E., Widiaratih R., Ismanto A., Zainuri M., Hadibarata T., Anindita M. A., Tristanova T., Jihadi M. S. Assessment and Characterization of Microplastics in Aquatic Environments near Pekalongan (Indonesia) 99

Поспелова Н. В., Щуров С. В., Ковригина Н. П., Лисицкая Е. В., Трощенко О. А. Экологическое состояние вод Севастопольского взморья (Западный Крым) и его влияние на динамику планктонных сообществ 118

Зарипова К. М., Демидова Е. А., Тихонова Е. А., Бурдиян Н. В., Дорошенко Ю. В., Басова Е. Д. Численность и распределение отдельных групп бактерий в воде прибрежной акватории полуострова Камчатка 135

Карпова Е. П., Аблязов Э. Р. Распространение четырехполосого бычка *Chromogobius quadrivittatus* (Steindachner, 1863) в Черном море и проблема расширения его ареала 149

Гогоберидзе Г. Г., Румянцева Е. А., Леднова Ю. А., Ефименко Е. А. Оценка природных и техногенных рисков арктического природопользования для береговой зоны Мурманской области 159

ISSN 2413-5577, Ecological Safety of Coastal and Shelf Zones of Sea, 2025, No. 2, pp. 6–18.

Original paper

Frontal Zones as Boundaries of Areas with Different Range of Sea Surface Temperature Seasonal Variability in the North Atlantic

I. G. Shokurova *, N. V. Nikolsky, E. D. Chernyshova

Marine Hydrophysical Institute of RAS, Sevastopol, Russian Federation
* *e-mail: igshokurova@mail.ru*

Abstract
The paper analyses the position of the oceanic temperature frontal zones in comparison with the spatial distribution of the amplitude of the seasonal variability of water temperature and gradients of amplitude in the North Atlantic. The paper also considers the change in the amplitude of the water temperature seasonal variability along meridional surface transects through the Gulf Stream front, Subtropical and Arctic Fronts. The authors use data on the potential water temperature at 0.5 m depth of the ORAS5 ocean reanalysis (1958–2021). The position of frontal zones is determined based on the calculation of horizontal water temperature gradients. The amplitude of the water temperature seasonal variability is calculated as half of the difference between the maximum and minimum temperature in the mean annual cycle. It is noted that high values of the amplitude of water temperature seasonal variations are observed in the mid-latitudes, decreasing in the northern and southern directions. In the equatorial zone, Tropical Atlantic and Arctic, the range of water temperature seasonal variability is minimal. The extended areas with a sharp change in the amplitude of the water temperature seasonal variations were found to coincide with the position of temperature frontal zones. The correlation coefficient between the spatial distribution of temperature gradients and gradients of its seasonal variation amplitude was 0.93. The Gulf Stream front bordering the waters of the Labrador Current separates the regions with the largest difference in the water temperature seasonal variability. The difference in the amplitude of the water temperature seasonal variations in the areas located on both sides of the Gulf Stream, Subtropical and Arctic fronts was mainly due to the winter temperature difference. The obtained results show that the frontal zones in the ocean separate regions not only with different thermohaline characteristics, but also with different amplitudes of the seasonal variability of surface water temperature.

Keywords: water temperature, frontal zones, amplitude of water temperature annual variations, temperature gradient, seasonal variability, North Atlantic

Acknowledgements: The work was carried out under state assignment of MHI RAS no. FNNN-2024-0014 “Fundamental studies of interaction processes in the sea–air system that form the physical state variability of the marine environment at various spatial and temporal scales”.

For citation: Shokurova, I.G., Nikolsky, N.V. and Chernyshova, E.D., 2025. Frontal Zones as Boundaries of Areas with Different Range of Sea Surface Temperature Seasonal Variability in the North Atlantic. *Ecological Safety of Coastal and Shelf Zones of Sea*, (2), pp. 6–18.

Фронтальные зоны как границы областей с разным диапазоном сезонной изменчивости поверхностной температуры воды в Северной Атлантике

И. Г. Шокурова *, Н. В. Никольский, Е. Д. Чернышова

Морской гидрофизический институт РАН, Севастополь, Россия
** e-mail: igshokurova@mail.ru*

Аннотация
Анализируется положение среднемноголетних океанических температурных фронтальных зон в сравнении с пространственным распределением амплитуды сезонной изменчивости температуры воды и градиентов амплитуды в Северной Атлантике. Рассматривается изменение амплитуды сезонного хода температуры воды вдоль меридиональных поверхностных разрезов через фронт Гольфстрима, Субтропический и Арктический фронты. Используются данные о потенциальной температуре воды на глубине 0.5 м океанического реанализа *ORAS*5 (1958–2021 гг.). Положение фронтальных зон определяется на основе расчета горизонтальных градиентов температуры воды. Амплитуда сезонной изменчивости температуры воды вычисляется как половина разницы между максимальной и минимальной температурой в климатическом годовом ходе. Отмечается, что высокие значения амплитуды сезонного хода температуры воды наблюдаются в средних широтах, уменьшаясь в северном и южном направлениях. В экваториальной зоне, в Тропической Атлантике и в Арктике диапазон сезонной изменчивости температуры воды минимальный. Получено, что протяженные области, на которых происходит резкое изменение амплитуды сезонного хода температуры воды, совпадают с положением температурных фронтальных зон. Коэффициент корреляции между пространственным распределением градиентов поверхностной температуры воды и градиентов амплитуды ее сезонного хода равен 0.93. Фронт Гольфстрима, граничащий с водами Лабрадорского течения, разделяет области с наибольшей разницей в сезонной изменчивости температуры воды. Различие амплитуд сезонного хода температуры воды в областях, расположенных с двух сторон фронта Гольфстрима, Субтропического и Арктического фронтов, в основном обусловливается зимней разницей температуры. Полученные результаты показывают, что фронтальные зоны в океане разделяют области не только с разными термохалинными характеристиками, но и с разной амплитудой сезонной изменчивости поверхностной температуры воды.

Ключевые слова: температура воды, фронтальные зоны, амплитуда годового хода температуры воды, градиент температуры, сезонная изменчивость, Северная Атлантика

Благодарности: работа выполнена в рамках темы государственного задания ФГБУН ФИЦ МГИ FNNN-2024-0014 «Фундаментальные исследования процессов взаимодействия в системе океан-атмосфера, формирующих изменчивость физического состояния морской среды на различных пространственно-временных масштабах».

Для цитирования: *Шокурова И. Г., Никольский Н. В., Чернышова Е. Д.* Фронтальные зоны как границы областей с разным диапазоном сезонной изменчивости поверхностной температуры воды в Северной Атлантике // Экологическая безопасность прибрежной и шельфовой зон моря. 2025. № 2. С. 6–18. EDN AEMNOT.

Introduction

Extended areas of high temperature and salinity gradients at the ocean surface indicate the presence of ocean fronts, i. e. boundaries of water masses with different thermohaline characteristics [1]. The areas within which the front position changes on daily, seasonal and interannual time scales are defined as frontal zones. The study of processes in frontal zones is connected with many branches of oceanological science such as physical, biological, climate, etc. Fronts play an important role in the processes of vertical mixing in the ocean and eddy formation [1, 2], atmosphere and ocean interaction [3]. Marine frontal zones are areas of high bioproductivity. They are important for both fisheries and nature conservation, which determines the applied importance of their study [4–8]. Long-term changes in the characteristics of frontal zones can be used to monitor and predict climatic changes in the ocean [9].

Presently, the study of fronts is the most intensive research domain, with investigations being conducted in various scientific disciplines and on different spatial and temporal scales. This is due to the emergence of multi-year series of satellite data and reanalyses on a regular grid with high spatial resolution. In our study, we address general issues related to ocean fronts, such as the position of large-scale temperature frontal zones, gradient values, and consider the distinctive properties of areas separated by frontal zones in the North Atlantic.

Large-scale fronts of various types are present in this region. They include fronts at the boundaries of the Gulf Stream, North Atlantic, Labrador, East Greenland and Norwegian currents carrying water with characteristics different from those of the surrounding waters; fronts in the areas of equatorial and coastal upwelling near West Africa. The subtropical front is that characterised by the interaction of colder waters transported from the north by Ekman transport and influenced by westerly winds, and warmer waters transported from the south by trade winds. The Arctic Front, located in the Atlantic sector of the Arctic, serves to delineate the boundary between the Atlantic and Arctic waters. The polar front of the ice zone boundary, otherwise known as the East Greenland Polar Front, and estuarine saline fronts, such as the Amazon River outflow front, are also of significance [2].

The position of the temperature fronts in the North Atlantic, as determined by calculations of surface temperature gradients, is outlined in [2, 10–13]. In the Atlantic sector of the Arctic, temperature fronts have been the focus in [14–16] and numerous other works. The highest recorded horizontal gradients of surface temperature are observed in the frontal zone of the Gulf Stream. A significant seasonal variability of temperature gradients is also noted here [13]. It has been observed

that the area under discussion also exhibits the highest amplitude of seasonal variability in surface water temperature [17, 18]. The question of interest is whether the spatial variation in the amplitude of the seasonal cycle is related to the position of frontal zones. Temperature fronts along large-scale currents are present throughout the year, and the difference in the characteristics of the annual temperature variations in the surrounding waters is not obvious.

The aim of this work is to compare the spatial distribution of the amplitude of the seasonal temperature cycle with the position of frontal zones, and to analyse the change in amplitude at the crossing of frontal zones in the North Atlantic.

Research data and methods

Monthly averaged data from the ocean reanalysis ORAS5 on potential temperature θ (°C) at 0.5 m depth with a spatial resolution of about 0.25° (decreasing to 9 km in polar regions) for 1958–2021 were used in the work [19].

To determine the position of frontal zones, the absolute values of potential temperature horizontal gradients $\nabla\theta = \left(\frac{\partial\theta}{\partial x}, \frac{\partial\theta}{\partial y}\right)$ (°C/100 km) were calculated:

$$|\nabla\theta| = \sqrt{\left(\frac{\partial\theta}{\partial x}\right)^2 + \left(\frac{\partial\theta}{\partial y}\right)^2}.$$

Gradient vector components were calculated using the central difference scheme. When calculating gradients, the latitude of the place was taken into account.

The amplitude of water temperature seasonal variability (AMP) was calculated as half of the difference between the maximum and minimum temperature values in the long-term mean annual variations for each grid node. In order to analyse changes in amplitude by space quantitatively, its horizontal gradients were calculated. Areas with high values of gradients were defined as boundaries between areas with different amplitudes of seasonal variability.

The spatial variability of the amplitude of the annual variations of water temperature and temperature gradients was considered on the examples of meridional surface transects crossing the frontal zones of the Subtropical Front, the Gulf Stream Front and the Arctic Front.

Results

Temperature gradients in large-scale temperature fronts in the North Atlantic. Large-scale temperature fronts are located in areas with extreme changes in water temperature (Fig. 1, *a*) which is manifested in high values of horizontal gradients (Fig. 1, *b*). According to long-term mean data, the highest temperature gradients exceeding 1°C/100 km are observed in the frontal zones of large-scale currents, e.g., the current systems of the Gulf Stream, the North Atlantic and

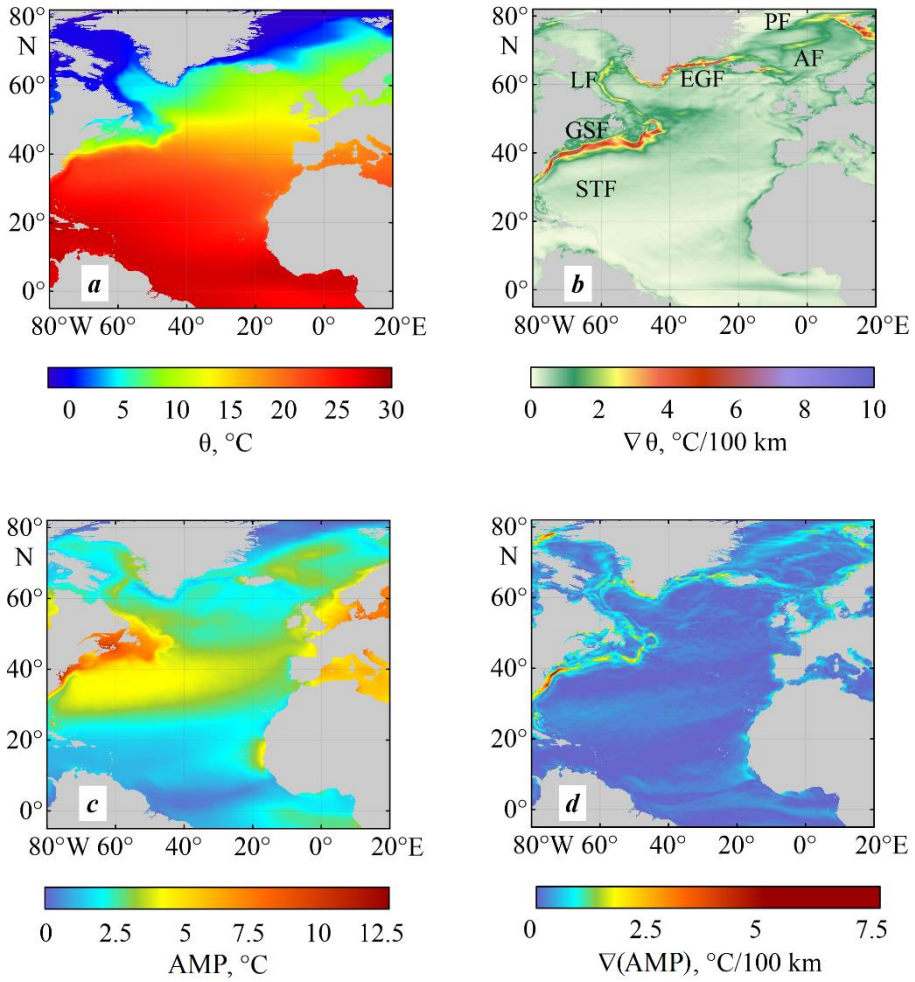

Fig. 1. Long-term mean potential temperature θ at a depth of 0.5 m (*a*), its gradients (*b*), amplitude of the seasonal variations AMP (*c*) and its gradients (*d*). Notations: GSF – Gulf Stream Front, LF – Labrador Current Front, EGF – East-Greenland Current Front, AF – Arctic Front, PF – Polar Front, STF – Subtropical Front

the Norwegian currents, transporting warm water from more southern latitudes to northern ones, and northern – the East Greenland, West Greenland and Labrador – currents which carry cold water from the Arctic Ocean to the Atlantic Ocean. Fronts along these currents are present throughout the year. The maximum values of gradients are observed in the Gulf Stream front [13]. Here, the average annual gradient values range from 4 to 10°C/100 km (Fig. 1, *b*).

In the areas of coastal upwelling along the African coast and equatorial upwelling in the eastern part of the equator, the mean annual gradients in the frontal zones are about 1°C/100 km. In the subtropical front, the gradients do not exceed 1°C/100 km. In the Atlantic sector of the Arctic, in the Polar Front mainly manifested in summer during the period of ice melting, the mean annual gradient values are 1–2°C/100 km and in the Arctic Front (Jan Mayen – Mohns Ridge), they are 2–2.5°C/100 km. It should be taken into account that the real values may be higher than those obtained from the reanalysis data, which are rather smooth.

Amplitude of water temperature seasonal variability. The spatial distribution of the amplitude of seasonal variations in surface water temperature exhibits distinct zonality (Fig. 1, *c*). High values of the amplitude of the seasonal temperature variations are observed in the middle latitudes, decreasing in the northern and southern directions. The amplitude of the annual temperature variations is minimal in the equatorial zone, Tropical Atlantic and Arctic.

At the same time, the zonal direction shows pronounced features in the amplitude distribution. The region with the highest amplitude of seasonal temperature changes exceeding 3°C is located in the western part of the ocean between 25° and 55° N, narrowing to the east to 30°–50° N (Fig. 1, *c*). The largest amplitude reaching 10°C is located in the area of the Labrador Current branch spreading southward along the coast of Canada and the USA and bordering the Gulf Stream.

An extensive area with an amplitude of seasonal temperature variability exceeding 3°C is located in the Atlantic sector of the Arctic. The Polar and Arctic fronts are adjacent to this area. A high range of seasonal temperature variations is also observed off the coast of Africa in the area of the Canary upwelling and the equatorial upwelling. The results obtained correspond to the data given in [18].

Spatial gradients of the amplitude of water temperature seasonal variability. In order to determine the position of the areas of sharp changes in the amplitude of the annual variation of water temperature more precisely, the amplitude gradients were calculated (Fig. 1, *d*). The delineation of areas exhibiting divergent ranges of seasonal variability is facilitated by elevated gradient values. A comparison of the position of the gradients of the seasonal variability amplitude with the distribution of temperature gradients demonstrates that the areas with a sharp change in the amplitude of seasonal variability correspond to the position of large-scale temperature fronts. The spatial correlation was found to be 0.93.

Thus, frontal zones are located in places with a sharp transition from the area with a high range of seasonal temperature variability to the area with a low range. The obtained result can be defined as a property of frontal zones – they are the boundaries of areas with different ranges of seasonal variability.

The highest values of the gradients of the seasonal variation amplitude are observed in the areas of frontal zones of narrow western currents, including the Gulf Stream, the Labrador Current and the coastal branches of the West Greenland and East Greenland Currents (Fig. 1, *d*). In the subtropical and tropical zones, the amplitude gradients are minimal, as are the amplitude values themselves (Fig. 1, *c*, *d*).

Changes in the amplitude of the annual variations of water temperature along transects through the frontal zone of the Gulf Stream, Subtropical and Arctic fronts. As examples, let us consider changes in the amplitude of seasonal water temperature variability and temperature gradients on meridional transects through the subtropical frontal zone at 55° W, the Gulf Stream frontal zone at 61° W, and the Arctic front at 0° W (Fig. 2, *a* – *c*). Temperature values pre-averaged along the transect within ±0.5° of the selected longitude were used for the amplitude calculations.

Subtropical Front. The Subtropical Front (STF) or Subtropical Convergence Zone (STCz) crosses the subtropical gyre in a broad band, shifting northwards in the eastern part of the ocean (Fig. 1, *b*). The front occurs at the boundary between colder waters transported from the north by Ekman transport under the influence of westerly winds and warmer waters transported from the south under the influence of trade winds [11].

Temperature gradients in the front in the transect area are low and do not exceed 0.5°C/100 km on average (Fig. 1, *a*). From winter to spring, gradients increase reaching a maximum in spring (Fig. 2, *d*). In summer, as a result of water warming, the front weakens, narrows and the zone of increased gradients shifts northwards (Fig. 2, *d, g*) [11, 13].

Across the front (along the meridional transect at 55° W), the amplitude of the seasonal variations of surface water temperature changes insignificantly. North of the front, the amplitude at point A (36° N) is 4.2°C, and south of the front, at point B (22° N), it is 1.8°C (Fig. 3, *a, d*). Between points A and B, the change in amplitude is small, about 0.2°C per 1° latitude.

Gulf Stream Front. The Gulf Stream Front (GSF) has the highest horizontal temperature gradients in the North Atlantic due to high temperature difference between the warm waters of the Gulf Stream and the cold waters of the Labrador Current (Figs. 1, *a*, *b*; 2, *b*). In the region of the meridional transect at 61° W, the temperature gradients in the front increase in winter (January – March) up to 6°C/100 km and decrease in summer (July – August) (Fig. 2, *e*) up to 3°C/100 km due to summer warming (Fig. 2, *h*).

The amplitude of seasonal temperature variability along the transect decreases southwards. At point A (44° N), located in the cold waters of the Labrador Current, it is 8.0°C, and at point B (38.5° N) south of the front, the amplitude is 4.3°C (Fig. 3, *b, e*). The change of the amplitude relative to the distance between the points is 0.7°C per 1° latitude.

Arctic Front. The Arctic Front (AF) is located between the deep-water basins of the Norwegian and Greenland Seas (see Fig. 1, *b*), in the area of the Jan Mayen, Mohns Ridge, Knipovich Ridge submarine ridges [15, 16, 20].

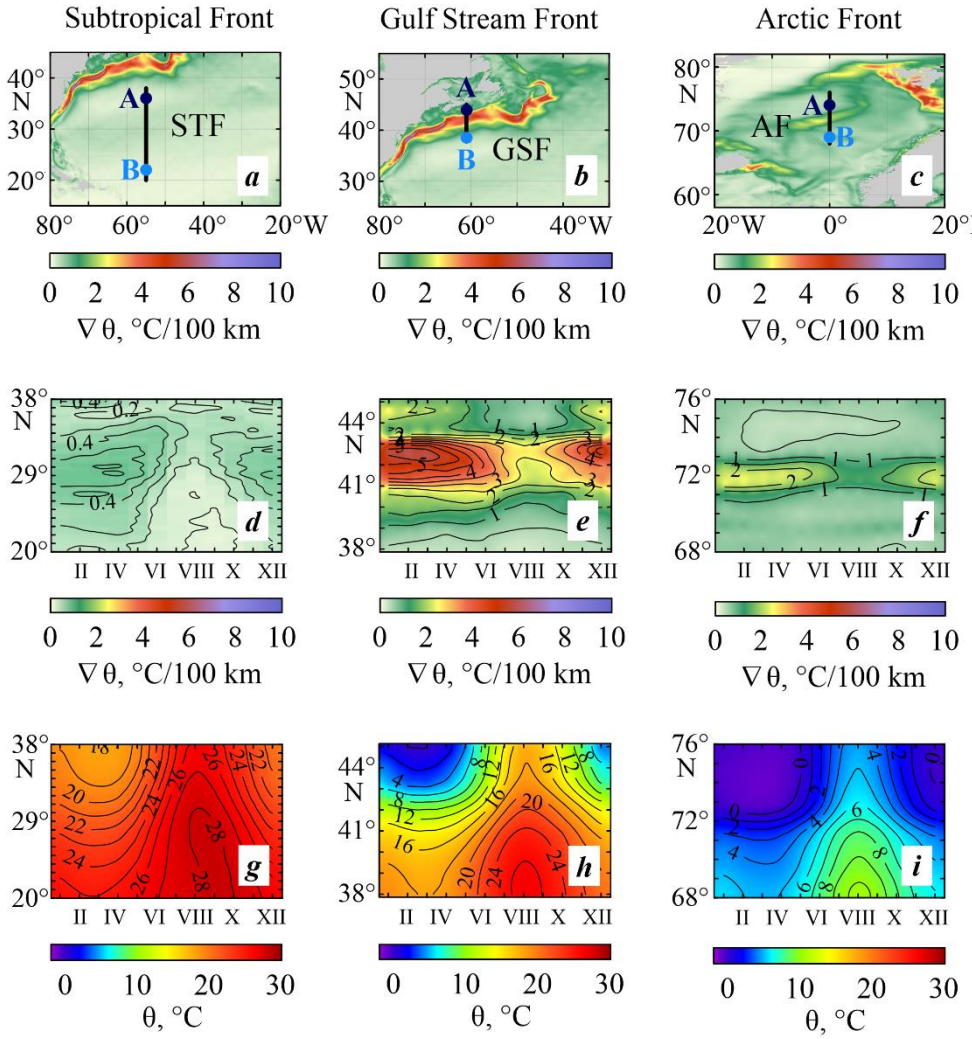

Fig. 2. Position of surface meridional transects through the frontal zones of the Subtropical Front (*a*), Gulf Stream (*b*), Arctic Front (*c*), seasonal variations of horizontal gradients of water temperature (*d* – *f*) and temperature (*g* – *i*) along the transects. Roman numerals denote months

This front is often divided into separate elements – frontal zones: the Jan Mayen zone, the zones of Mohns Ridge, Greenland and Norwegian Seas [14]. The front separates the warmer salty Atlantic waters of the Norwegian Atlantic Front Current (one of the branches of the continuation of the North Atlantic Current) and colder, fresher waters of the East Greenland Current mixed with the return Atlantic waters carried by the West Spitsbergen Current [15, 21].

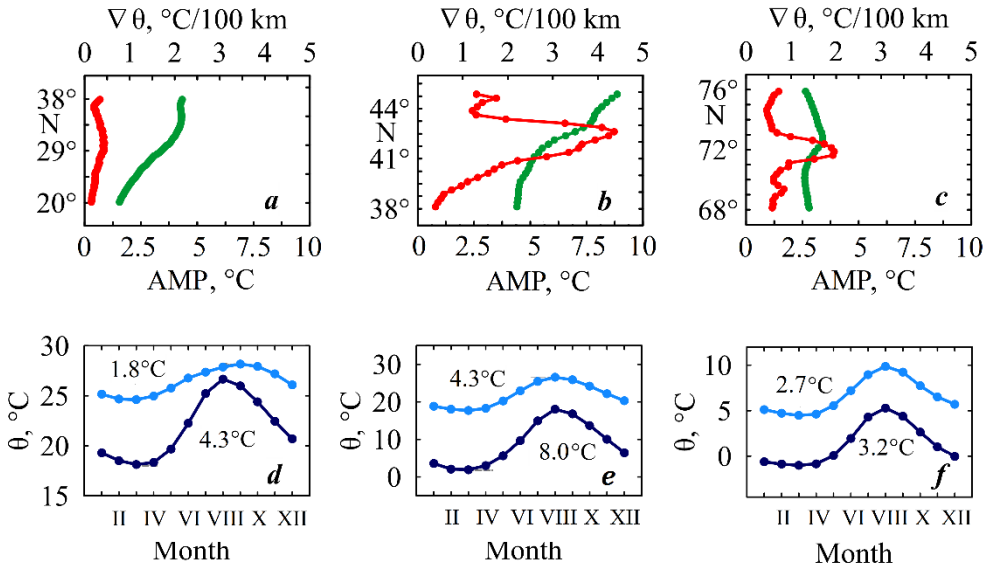

Fig. 3. Amplitude of seasonal variability (green curves) and gradient (red curves) of water temperature (*a* – *c*), annual variations of water temperature at points A and B on the cold (dark blue curves) and warm (light blue curves) sides of the front (*d* – *f*) along meridional transects through the frontal zones of the Subtropical Front (*a*, *d*), Gulf Stream (*b*, *e*), and Arctic Front (*c*, *f*). The figures indicate the amplitude at points A and B (see Fig. 2)

Water temperature gradients in the frontal zone in the area of the 0° W meridional transect increase to 3°C/100 km in winter and decrease to 1.5–2°C/100 km by summer (see Fig. 2, *f*). The minimum value is reached in August with a maximum water temperature of 6°C (see Fig. 2, *i*).

When crossing this front, the amplitude of the annual variations of water temperature decreases from 3.2°C at point A located on the cold side of the front (74° N) to 2.7°C at point B (69° N) south of the front (Fig. 3, *c*, *f*). The change in amplitude with respect to the distance between A and B is about 0.1°C per 1° latitude.

The northern boundary of the front (73° N) is characterized by a local maximum of the seasonal temperature variations and the southern side – by a local minimum (Fig. 3, *c*). In winter, water temperatures decrease on the northern side of the front, while the warm Atlantic waters continue to arrive on the southern side of the front, resulting in a strengthening of the front (see Fig. 2, *f*). In summer, the water warms up and the front weakens. The higher difference in water temperature between the cold and warm sides of the front in winter is accompanied by a difference in the magnitude of the seasonal temperature variations.

The analysed examples demonstrate that the most significant alterations in the amplitude of the seasonal variability of water temperature are observed in the frontal zone of the Gulf Stream at the boundary between warm water originating from low latitudes and cold water arriving with the Labrador Current from the Arctic. The highest water temperature gradients are also observed here (see Fig. 2). The Subtropical and Arctic fronts separate waters with a smaller difference in seasonal temperature variations compared to the Gulf Stream Front (Figs. 2, 3).

The greatest difference between water temperature on the cold and warm sides of the front is achieved in winter when the temperature on the cold side of the front decreases more than on the warm side, which, in turn, is accompanied by an increase in gradients. In summer, due to seasonal warming, the difference between the water temperature on both sides of the front decreases and contributes less to the difference in the seasonal variations. In addition, summer warming is accompanied by a decrease of gradients in the frontal zones. Thus, the cases under consideration show that the difference in the amplitude of the seasonal variations on both sides of the front is mainly related to the winter temperature difference between the cold and warm sides of the front.

Discussion

It is known that the formation of ocean fronts is the result of complex interaction of various physical and dynamic processes, such as wind forcing leading to currents, vertical rise and fall of water, spatial and temporal variability of heat fluxes on the ocean surface, ice melting, river runoff and ocean mixing processes [1, 2, 22]. Different regions have their own predominant processes leading to the emergence of temperature and salinity fronts.

Seasonal variability of these factors can lead to strengthening, weakening or complete disappearance of fronts. Summer heating weakens all temperature fronts, including those along the stationary large-scale currents. Weakening of westerly winds and trade winds in summer leads to weakening of the Subtropical Front, its narrowing and shift to the north.

These factors and their variability, heat reserve in the mixed layer [22] and proximity of coasts influence the temperature conditions on each side of the front. Thus, high seasonal range of water temperature on the cold side of the Gulf Stream Front corresponds to high seasonal range of air temperature along the coast of Nova Scotia [18]. It should be taken into account that the nearby continental regions have continental climate with low temperatures in winter and high temperatures in summer [23]. Moving away from temperate latitudes to the north and south, the amplitude of the seasonal variations decreases [17, 18]. Furthermore, the difference between the amplitude on both sides of the front decreases, as can be observed in the Arctic and Subtropical fronts.

Another aspect of the considered issue is the relative isolation of the areas separated by frontal zones. Thus, it is noted in [1] that frontal partitions are elements of the complex three-dimensional structure of ocean waters associated with local closure of individual elements of the general circulation. The difference not only

in temperature values but also in its seasonal variations emphasizes the isolation of the areas on the cold and warm sides of the front.

An important manifestation of the isolation of the areas on both sides of the front are different hydrological and hydrochemical conditions of marine organisms, species composition and different indicators of water productivity [24–27]. An increase in the amplitude of the seasonal variations generally indicates lower winter temperatures on the cold side of the ocean front (Fig. 3, *d* – *f*), which can be accompanied by the predominance of cold-water marine species in this area [28].

Conclusion

Based on the ORAS5 ocean reanalysis data on the temperature at 0.5 m depth, the spatial position of temperature fronts and the distribution of the amplitude of the annual variations of surface water temperature were compared. It was obtained that the mean annual temperature fronts, which by definition are bands with high gradients of sea water temperature, were also the boundaries of areas with different ranges of seasonal variability of water temperature. The division of the ocean into areas with different amplitudes of seasonal variations can be characterised as one of the properties of frontal zones. The difference in the ranges of seasonal temperature variability emphasizes the local closure of the areas in the ocean separated by frontal zones.

The largest difference between the amplitudes of the seasonal variability of surface water temperature is noted in the areas located on both sides of the Gulf Stream frontal zone. In the subpolar, subtropical and tropical zones, the fronts separate areas with a smaller difference in the amplitudes of the annual temperature variations.

The difference in the amplitudes of the seasonal variations of water temperature on both sides of the Gulf Stream, Subtropical and Arctic fronts is mainly stipulated by the difference in temperature values on the cold and warm sides of the front in winter. At this time, the difference between the water temperature on the northern cold and southern warm sides of the front increases. In summer, due to seasonal warming, the difference between the water temperature values on both sides of the front decreases and contributes less to the magnitude of the annual variations.

The results obtained can be taken into account in climate studies, in marine biology, in the analysis of meteorological conditions in different regions of the ocean.

REFERENCES

1. Fedorov, K.N., 1986. *The Physical Nature and Structure of Oceanic Fronts*. New York: Springer-Verlag, 333 p.
2. Belkin, I.M., Cornillon, P.C. and Sherman, K., 2009. Fronts in Large Marine Ecosystems. *Progress in Oceanography*, 81(1–4), pp. 223–236. https://doi.org/10.1016/j.pocean.2009.04.015
3. Kida, S., Mitsudera, H., Aoki, S., Guo, X., Ito, S., Kobashi, F., Komori, N., Kubokawa, A., Miyama, T. [et al.], 2015. Oceanic fronts and jets around Japan: a review. *Journal of Oceanography*, 71, pp. 469–497. https://doi.org/10.1007/s10872-015-0283-7
4. Olson, D.B., Hitchcock, G.L., Mariano, A.J., Ashjian, C.J., Peng, G., Nero, R.W. and Podestá, G.P., 1994. Life on the Edge: Marine Life and Fronts. *Oceanography*, 7(2), pp. 52–60. https://doi.org/10.5670/oceanog.1994.03

5. Bakun, A., 2006. Fronts and Eddies as Key Structures in the Habitat of Marine Fish Larvae: Opportunity, Adaptive Response and Competitive Advantage. *Scientia Marina*, 70(2), pp. 105–122. https://doi.org/10.3989/scimar.2006.70s2105
6. Taylor, J.R. and Ferrari, R., 2011. Ocean Fronts Trigger High Latitude Phytoplankton Blooms. *Geophysical Research Letters*, 38(23), L23601. https://doi.org/10.1029/2011GL049312
7. Scales, K.L., Miller, P.I., Hawkes, L.A., Ingram, S.N., Sims, D.W. and Votier, S.C., 2014. On the Front Line: Frontal Zones as Priority At-Sea Conservation Areas for Mobile Marine Vertebrates. *Journal of Applied Ecology*, 51(6), pp. 1575–1583. https://doi.org/10.1111/1365-2664.12330
8. Haëck, C., Lévy, M., Mangolte, I. and Bopp, L., 2023. Satellite Data Reveal Earlier and Stronger Phytoplankton Blooms over Fronts in the Gulf Stream Region. *Biogeosciences*, 20(9), pp. 1741–1758. https://doi.org/10.5194/bg-20-1741-2023
9. Yang, K., Meyer, A., Strutton, P.G. and Fischer, A.M., 2023. Global Trends of Fronts and Chlorophyll in a Warming Ocean. *Communications Earth & Environment*, 4, 489. https://doi.org/10.1038/s43247-023-01160-2
10. Artamonov, Yu.V. and Skripaleva, E.A., 2005. The Structure and Seasonal Variability of the Large-Scale Fronts in the Atlantic Ocean on the Basis of Satellite Data. *Issledovaniye Zemli iz Kosmosa*, (4), pp. 62–75 (in Russian).
11. Ullman, D.S., Cornillon, P.C. and Shan, Z., 2007. On the Characteristics of Subtropical Fronts in the North Atlantic. *Journal of Geophysical Research: Oceans*, 112(C1), C01010. https://doi.org/10.1029/2006JC003601
12. Kazmin, A.S., 2017. Variability of the Climatic Oceanic Frontal Zones and Its Connection with the Large-Scale Atmospheric Forcing. *Progress in Oceanography*, 154, pp. 38–48. https://doi.org/10.1016/j.pocean.2017.04.012
13. Shokurova, I.G., Nikolsky, N.V. and Chernyshova, E.D., 2024. Seasonal Variability of Horizontal Gradients in the North Atlantic Large-Scale Thermohaline Frontal Zones. *Ecological Safety of Coastal and Shelf Zones of Sea*, (2), pp. 23–38.
14. Kostianoy, A.G. and Nihoul, J.C.J., 2009. Frontal Zones in the Norwegian, Greenland, Barents and Bering Seas. In: J. C. J. Nihoul and A. G. Kostianoy, eds., 2009. *Influence of Climate Change on the Changing Arctic and Sub-Arctic Conditions*. Springer, Dordrecht, pp. 171–190. https://doi.org/10.1007/978-1-4020-9460-6_13
15. Raj, R.P., Chatterjee, S., Bertino, L., Turiel, A. and Portabella, M., 2019. The Arctic Front and Its Variability in the Norwegian Sea. *Ocean Science*, 15(6), pp. 1729–1744. https://doi.org/10.5194/os-15-1729-2019
16. Akhtyamova, A.F. and Travkin, V.S., 2023. Investigation of Frontal Zones in the Norwegian Sea. *Physical Oceanography*, 30(1), pp. 62–77. https://doi.org/10.29039/1573-160X-2023-1-62-77
17. Umoh, J.U. and Thompson, K.R., 1994. Surface Heat Flux, Horizontal Advection, and the Seasonal Evolution of Water Temperature on the Scotian Shelf. *Journal of Geophysical Research: Oceans*, 99(C10), pp. 20403–20416. https://doi.org/10.1029/94JC01620
18. Yashayaev, I.M. and Zveryaev, I.I., 2001. Climate of the Seasonal Cycle in the North Pacific and the North Atlantic Oceans. *International Journal of Climatology: A Journal of the Royal Meteorological Society*, 21(4), pp. 401–417. https://doi.org/10.1002/joc.585
19. Zuo, H., Balmaseda, M.A., Tietsche, S., Mogensen, K. and Mayer, M., 2019. The ECMWF Operational Ensemble Reanalysis-Analysis System for ocean and Sea Ice: a Description of the System and Assessment. *Ocean Science*, 15(3), pp. 779–808. https://doi.org/10.5194/os-15-779-2019

20. Volkov, D.L., Belonenko, T.V. and Foux, V.R., 2013. Puzzling over the Dynamics of the Lofoten Basin-a sub-Arctic Hot Spot of Ocean Variability. *Geophysical Research Letters*, 40(4), pp. 738–743. https://doi.org/10.1002/grl.50126
21. Walczowski, W., 2013. Frontal Structures in the West Spitsbergen Current Margins. *Ocean Science*, 9(6), pp. 957–975. https://doi.org/10.5194/os-9-957-2013
22. Dong, S. and Kelly, K.A., 2004. Heat Budget in the Gulf Stream Region: The Importance of Heat Storage and Advection. *Journal of Physical Oceanography*, 34(5), pp. 1214–1231. https://doi.org/10.1175/1520-0485(2004)034<1214:HBITGS>2.0.CO;2
23. Kottek, M., Grieser, J., Beck, C., Rudolf, B. and Rubel, F., 2006. World Map of the Köppen-Geiger Climate Classification Updated. *Meteorologische Zeitschrift*, 15(3), pp. 259–263. https://doi.org/10.1127/0941-2948/2006/0130
24. Dafner, E., Mordasova, N., Arzhanova, N., Maslennikov, V., Mikhailovsky, Y., Naletova, I., Sapozhnikov, V., Selin, P. and Zubarevich, V., 2003. *Journal of Geophysical Research: Oceans*, 108(C7), 3227. https://doi.org/10.1029/1999JC000288
25. Børsheim, K.Y., Milutinović, S. and Drinkwater, K.F., 2014. TOC and Satellite-Sensed Chlo-Rophyll and Primary Production at the Arctic Front in the Nordic Seas. *Journal of Marine Systems*, 139, pp. 373–382. https://doi.org/10.1016/j.jmarsys.2014.07.012
26. Acha, E.M., Piola, A., Iribarne, O. and Mianzan, H., 2015. *Ecological Processes at Marine Fronts: Oases in the Ocean*. Cham: Springer, 68 p. https://doi.org/10.1007/978-3-319-15479-4
27. Qu, B. and Gabric, A.J., 2022. The Multi-Year Comparisons of Chlorophyll and Sea Ice in Greenland Sea and Barents Sea and Their Relationships with the North Atlantic Oscillation. *Journal of Marine Systems*, 231, 103749. https://doi.org/10.1016/j.jmarsys.2022.103749
28. Mugo, R.M., Saitoh, S.-I., Takahashi, F., Nihira, A. and Kuroyama, T., 2014. Evaluating the Role of Fronts in Habitat Overlaps Between Cold and Warm Water Species in the Western North Pacific: A Proof of Concept. D*eep Sea Research Part II: Topical Studies in Oceanography*, 107, pp. 29–39. https://doi.org/10.1016/j.dsr2.2013.11.005

Submitted 15.10.2024; accepted after review 19.01.2025;
revised 25.03.2025; published 30.06.2025

About the authors:

Irina G. Shokurova, Senior Research Associate, Marine Hydrophysical Institute of RAS (2 Kapitanskaya Str., Sevastopol, 299011, Russian Federation), Ph.D. (Geogr.), **ORCID ID: 0000-0002-3150-8603**, *igshokurova@mail.ru*

Nikolay V. Nikolsky, Junior Research Associate, Marine Hydrophysical Institute of RAS (2 Kapitanskaya Str., Sevastopol, 299011, Russian Federation), **ORCID ID**: **0000-0002-3368-6745**, *n.nikolsky@mhi-ras.ru*

Elena D. Chernyshova, Senior Research Engineer, Marine Hydrophysical Institute of RAS (2 Kapitanskaya Str., Sevastopol, 299011, Russian Federation), **ORCID ID: 0009-0005-4607-8190**, *alenaksendzik@rambler.ru*

Contribution of the authors:

Irina G. Shokurova – original draft writing, literature review, editing, analysis and synthesis of the results

Nikolay V. Nikolsky – numerical calculations, visualization, editing, analysis and synthesis of the results

Elena D. Chernyshova – visualization, literature review, editing, analysis and synthesis of the results

All the authors have read and approved the final manuscript.

Original paper

The Main Patterns of the Black Sea Ecosystem Long-Term Changes

V. V. Melnikov [1] *, **A. N. Serebrennikov** [2], **A. V. Masevich** [3], **E. S. Chudinovskikh** [1]

[1] *A. O. Kovalevsky Institute of Biology of the Southern Seas of Russian Academy of Sciences, Sevastopol, Russian Federation*
[2] *Institute of Natural and Technical Systems, Sevastopol, Russian Federation*
[3] *Marine Hydrophysical Institute of RAS, Sevastopol, Russian Federation*
* *e-mail: sevlin@ibss-ras.su*

Abstract
This study examines long-term changes in the Black Sea ecosystem, including the warming of its waters amid anthropogenic pollution and eutrophication. The aim of the study is to describe structural shifts in water masses and biotopes, as well as to assess alterations in key ecosystem components. Through the analysis of multi-year hydrological datasets, mathematical modelling, and hydrobiological studies, it has been demonstrated that a comprehensive understanding of the Black Sea's ecosystem changes requires consideration not only of climate warming, anthropogenic pollution, and eutrophication but also of chorological changes in water mass structure and associated biotopes. Ongoing deoxygenation is reducing the habitat layer for cold-water species, while warming has already caused the disappearance of the cold intermediate layer – with which these species are associated – dissolving it into surrounding waters at temperatures around 9 °C. Further warming of surface waters may lead to the degradation of cold-water species assemblages that form the trophic foundation of the Black Sea's current ecosystem. A significant transformation is expected due to the increasing dominance of warm-water and eurythermic species.

Keywords: Black Sea, ecosystem, climate change, deoxygenation, water masses, biotopes

Acknowledgements: The research is performed under state assignment on IBSS RAS topic no. 124030100137-6, on MHI RAS topic no. FNNN-2025-0001, and on IPTS topic no. 124020100120-9.

For citation: Melnikov, V.V., Serebrennikov, A.N., Masevich, A.V. and Chudinovskikh, E.S., 2025. The Main Patterns of the Black Sea Ecosystem Long-Term Changes. *Ecological Safety of Coastal and Shelf Zones of Sea*, (2), pp. 19–35.

Основные закономерности многолетних изменений экосистемы Черного моря

В. В. Мельников [1] *, А. Н. Серебренников [2], А. В. Масевич [3], Е. С. Чудиновских [1]

[1] *Институт биологии южных морей имени А. О. Ковалевского РАН, Севастополь, Россия*
[2] *Институт природно-технических систем, Севастополь, Россия*
[3] *Морской гидрофизический институт РАН, Севастополь, Россия*
* *e-mail: sevlin@ibss-ras.su*

Аннотация
Анализируются многолетние изменения экосистемы Черного моря, выражающиеся, кроме прочего, в потеплении вод на фоне антропогенного загрязнения и эвтрофикации. Цель работы заключается в описании структурных изменений водных масс, биотопов, а также в оценке изменений ключевых компонентов экосистемы. На основе анализа многолетних массивов данных о гидрологии, математического моделирования и гидробиологических исследований показано, что для полного понимания изменений экосистемы Черного моря необходимо учитывать не только потепление климата, антропогенное загрязнение и эвтрофикацию, но и хорические изменения структуры водных масс и связанных с ними биотопов. Продолжающаяся деоксигенация сокращает слой обитания холодноводных видов, а потепление уже привело к тому, что холодный промежуточный слой, с которым эти виды ассоциированы, исчез и растворился в окружающих водах при температуре около 9 °С. Дальнейшее потепление поверхностных вод может привести к деградации комплекса холодноводных видов, создающих трофическую основу современной экосистемы Черного моря. Следует ожидать ее существенной трансформации вследствие увеличения роли тепловодных и эвритермных видов.

Ключевые слова: Черное море, экосистема, изменения климата, деоксигенация, водные массы, биотопы

Благодарности: работа выполнена в рамках государственных заданий ФИЦ ИнБЮМ РАН по теме 124030100137-6, ФГБУН ФИЦ МГИ по теме FNNN-2025-0001 и ФГБУН ИПТС № 124020100120-9.

Для цитирования: Основные закономерности многолетних изменений экосистемы Черного моря / В. В. Мельников [и др.] // Экологическая безопасность прибрежной и шельфовой зон моря. 2025. № 2. С. 19–35. EDN SUIYJB.

Introduction

Around 130 years ago, N. I. Andrusov [1)] was the first to demonstrate that the Black Sea (BS) was a two-layered system consisting of a thin (80–200 m) "living" oxygen layer and a hydrogen sulphide zone. Until the end of the 20th century, it was believed that a layer of co-existing oxygen and hydrogen sulphide waters, or a C-layer, existed between these two layers. The first publications about the absence of this layer were met with scepticism [1]. However, new techniques introduced at the end of the 20th century revealed that ideas about the C-layer were

[1)] Andrusov, N.I., 1890. [Preliminary Report on Participation in a Black Sea Deep-Water Expedition]. *Izvestiya Russkogo Geografocheskogo Obshchestva*, 26(5), pp. 398–409 (in Russian).

erroneous [1–3]. A water mass measuring between 30 and 50 m deep composed of transformed Mediterranean water ($O_2 < 10$ μM, $H_2S < 3$ μM), or the Suboxic Layer (SOL), was found to exist between the oxygen zone and the hydrogen sulphide layer [1, 2]. The position of this layer within the water column is determined by the intensity of vertical water exchange and the concentration of dissolved organic matter. The Danube, Dnieper and Don rivers experienced a tenfold increase in nutrient inputs between the 1960s and 1990s, leading to anthropogenic eutrophication and the formation of large amounts of sinking organic matter [2]. The vertical water exchange did not provide sufficient aeration to compensate for the aeration needed to oxidise the large amount of organic matter, and the oxygen layer of the sea began to "shrink" [2, 4]. The depth to which oxygen penetrated the upper boundary of the SOL decreased from 130 m in 1955 to 90 m in 2013 [5]. Although eutrophication of the sea decreased by the beginning of the 21st century [6], deoxygenation of the depths continued due to the increase in surface water temperature [7].

Consequently, there have been significant changes in the composition of biotopes in the BS deep-water zone in recent years, which have had a considerable impact on the living conditions of plankton and fish. It is important to recognise that understanding the contemporary shifts within the BS ecosystem necessitates a comprehensive approach encompassing not only the impact of climate change, anthropogenic pollution and eutrophication but also the substantial alterations in the hydrological-hydrochemical and chorological characteristics of water masses and biotopes. (Chorological changes of water masses (from Greek *chora* – "place") are observed when a water mass changes its spatial position and acquires different ecological properties under the influence of a different combination of external factors in a new location [8].)

The existing hydrological-hydrochemical understanding of the structure of surface water masses in the BS deep waters can be described as follows:

1. Upper Black Sea Water Mass (UBSWM): $T > 20$°C, $S = 18.0…18.4$ PSU, $\sigma_t < 14$ [2), 3)].

2. Cold Intermediate Layer (CIL): $T < 8$°C, $S = 18.0…19.0$ PSU, $\sigma_t = 14.0…14.8$ [2), 3)].

3. Suboxic Layer (SOL): $T > 8$°C, $\sigma_t = 15.8…16.2$ [2, 3].

4. Intermediate Black Sea Water Mass (IBSWM): $T > 8$°C, $S > 20$ PSU, $\sigma_t = 16.2…17.9$ [2), 3)]. (The coastal and deep-water masses are not discussed in this paper as only the surface water of the deep-water zone is discussed.)

The biotope structure in the BS deep waters can be presented as follows:

1. Surface film biotope (aerocontour): community of aerobic organisms of the surface film – neuston. Composition – permanent or temporary inhabitants of 0–5 cm layer: bacteria and protozoa, phytoplankton, zooplankton, eggs and larvae of invertebrates and fish [9, 10].

---

2) Beznosov, V.N., 2000. [*Environmental Effect of Marine Destratification. Extended Abstract of DSc Thesis, Biological Sciences*]. Moscow: MSU, 42 p. (in Russian).

3) Belokopytov, V.N., 2017. [Climate Changes of the Black Sea Hydrological Regime. *DSc Thesis, Geographical Sciences*]. Sevastopol: MHI RAS, 377 p. (in Russian).

2. UBSWM biotope (aerobic zone): a community of aerobic organisms above a seasonal thermocline, epibiota. (We used the terms "epibiota" and "bathybiota" following T. S. Petipa [4)] who first described epi- and bathyplankton.) Composition – thermophilic and eurythermal species inhabiting the upper water mass: phytoplankton, epiplankton, macroplankton and the main mass of fish (*Engraulis encrasicolus* Linnaeus, 1758, etc.) [4)] [6, 11].

3. CIL biotope (aerobic zone): community of aerobic organisms under a seasonal thermocline, bathybiota [4)]. Composition: bathyplankton and cold-water fishes (*Sprattus sprattus* (Linnaeus, 1758), etc.), eurythermal plankton species [4), 5)] [11–14].

4. SOL biotope (anaerocontour): community of aerobic and anaerobic microorganisms of the Suboxic Layer. (The term "anaerocontour" was first introduced by V. V. Melnikov [14].) Composition: aerobic and anaerobic species of cyanobacteria, denitrifying bacteria, methanotrophs, methanogens, iron-reducing bacteria, manganese-reducing bacteria [14].

5. IBSWM biotope (anaerobic zone): community of anaerobic microorganisms of the hydrogen sulphide zone. Composition: thione bacteria (up to 40% of the biomass of all bacterioplankton), purple and fermenting bacteria, methanotrophs, methanogens, manganese-reducing bacteria, anammoxibacteria and various archaea [6)] [14]. The coastal and deep-water masses are not discussed because only the surface waters of the deep-water zone are discussed.

Recent studies indicate that the above-described ideas about the structure of water masses and biotopes no longer correspond to the real situation due to prolonged warming of surface waters [7)]. To date, deoxygenation has reduced deep-sea oxygen concentrations by 44% [5]. The CIL temperatures began to rise and by 2019 this water mass had disappeared [15]. Information about this catastrophic event for the BS ecosystem, of course, requires verification using different data series. Continued warming of surface waters could cause cascading changes throughout the BS ecosystem, since cold-water copepods form the bulk of the forage zooplankton that constitutes the main part of the diet of small plankton-feeding fish in the BS [12–16]. In addition, one of the fundamental questions remains unresolved as to how the reduction of the total oxygen layer thickness in the deep sea has affected chorological changes in the structure of pelagial habitats. The present study fills this gap to some extent.

The aim of the work is to analyse the basic processes of long-term changes in the BS ecosystem under the influence of warming, anthropogenic pollution,

---

[4)] Petipa, T.S., 1967. [*Life Forms of Pelagic Copepods and the Structure of Trophic Levels in the Structure and Dynamics of Aquatic Communities and Populations*]. Kiev: Naukova Dumka, pp. 108–119 (in Russian).

[5)] Flint, M.V., 1989. Vertical Distribution of the mass Mesoplankton Species in Connection with the Oxygen Field Structure. In: M. E. Vinogradov and M. V. Flint, eds., 1989. [*Structure and Production Characteristics of Plankton Communities of the Black Sea*]. Moscow: Nauka, pp. 187–212 (in Russian).

[6)] Sorokin, Yu.I., 1982. [*Black Sea. Nature. Resources*]. Moscow: Nauka, 216 p. (in Russian).

[7)] Masevich, A.V., 2022. [*Oxygen Dynamics in the Main Pycnocline of the Black Sea. Extended Abstract of PhD Thesis. Geographical Sciences*]. Sevastopol: MHI RAS, 24 p. (in Russian).

eutrophication and changes in the structure of water masses and to assess changes in key ecosystem components.

Materials and methods

The hydrodynamic analysis was derived from the NEMO ocean circulation model version 3.6 [8]. This model was implemented in the BS region with a horizontal resolution of 0.037° × 0.028° and 31 irregularly spaced vertical levels. The online model is linked to the OceanVar assimilation scheme [17, 18]. The BS-REA includes observations of temperature/salinity (T/S) profiles derived *in situ* from SeaDataNet and CMEMS INS TAC, as well as sea level anomalies. A summary of all available observations from ships (SYNOP SHIP), bathythermographs (BATHY) and drifting buoys (DRIBU) as well as data sourced from the ECMWF operational archive is provided.

In this paper, we examined the spatial and temporal variations in the temperature of the CIL and its surrounding waters over the past 30 years. Long-period and spatial variations of sea surface temperature (SST) were calculated from daily satellite maps with a resolution of 0.05° × 0.05° covering a 40-year period from 1982 to 2021. All information was obtained from the Copernicus marine environmental monitoring service (https://www.copernicus.eu) [9]. In addition, we used new data obtained during the recent large-scale expeditions of the Collective Use Center R/V *Professor Vodyanitsky* of the A. O. Kovalevsky Institute of Biology of the Southern Seas of RAS in 2017–2023 (using an Idronaut Ocean Seven 320Plus M CTD probe).

Materials from the BS western central part were used to investigate long-term changes in the vertical position of the SOL density boundaries. As the distribution of hydrochemical parameters in the deep sea has quasi-permanent isopycnic distributions, the assessment of long-term changes in the vertical position of the SOL boundaries was carried out on the conditional density scale. On average, these boundaries correspond to isopycnic surfaces: σ_t = 15.8 to upper boundary and σ_t = 16.2 to lower one [2, 3]. This approach solves two important methodological problems:

1) deficit of hydrochemical data: data on the hydrochemistry of the western deep-water zone are clearly insufficient to assess their long-term shifts (with almost an order of magnitude more hydrological stations);

2) influence of random factors on assessment accuracy: the use of density characteristics makes it possible to minimise the impact of random processes and obtain more reliable quantitative assessments of the evolution of the BS waters ecological structure.

---

[8] Gurvan, M., Bourdalle-Badie, R., Bouttier, P.-A., Bricaud, C., Bruciaferri, D., Calvert, D., Chanut, J., Clementi, E., Coward, A. [et al.], 2016. *NEMO ocean engine*. France: IPSL, 412 p. (Note du Pôle de modélisation de l'Institut Pierre-Simon Laplace; No. 27). https://doi.org/10.5281/zenodo.3248739

[9] SST_BS_SST_L4_REP_OBSERVATIONS_010_022 / E.U. Copernicus Marine Service Information (CMEMS). Marine Data Store (MDS). https://doi.org/10.48670/moi-00160

The western part of the sea was chosen because the seasonal dynamics of the isopycnic vertical position in this circulation is insignificant (~5 m) compared to the eastern circulation where it reaches 20 m. Considering that the interannual variability is also greater in the eastern circulation, density characteristics for determining long-term shifts in the western central part of the sea are more statistically reliable.

Data for calculations were collected in oceanographic cruises of research vessels of the USSR, Russia, Ukraine, Turkey, Bulgaria and Romania. Data sets from the databases of WOD18 [10], SeaDataNet, Coriolis Ocean Dataset, Marine Hydrophysical Institute and Institute of Biology of the Southern Seas as well as from other sources were used for the reanalysis. The boundaries of the central and western high salinity zones are taken as follows: 42.5–43.5°N, 30–32.5°E. A total of 1453 hydrological stations were sampled by research vessels in 154 cruises and seven Argo buoys during the summer period from 1957 to 2021 (June–August). The highest annual number of observations dates back to the 1980s, when up to 120 were recorded in the summer. Recently, however, the number of summer observations in the western open Black Sea has not exceeded 20, similar to the situation in the 1960s. Data from each expedition were checked for reliability and obviously false values (outliers that did not correspond to similar features in the distribution of other environmental parameters) were rejected.

Based on this, the average conditional density profiles were calculated. Averaging was performed by the inverse distance method followed by additional smoothing by low-pass filtering. Vertical density profiles (EOS-80 formulas) were interpolated with 1 m depth resolution using the method described in [19], then a search for a given isopycnic level was performed based on minimum deviation. Quality control including filtration jumps and vertical density inversions is performed before isopycnic levels are calculated. Further time series of calculated isopycnic levels were filtered using the 3σ statistical criterion and then averaged over the summer periods of each year. The averaging procedure serves as a specific low-pass filter to reduce the intra-seasonal variability that is inherent in this layer due to the influence of mesoscale eddies. The vertical discretisation of the raw data has increased significantly since the 1990s so this part of the time series has more reliable values of isopycnic levels and exhibits less mesoscale “noise”. The mesoscale variability estimated as standard deviations calculated over summer periods over the last 30 years is almost half the total interannual variability, which improves estimates of the current linear trend.

Predictive analyses were conducted using MS Excel forecasting functions using the AAA version of the exponential smoothing algorithm (ETS), which in Excel is based on the AAA (additive error, additive trend and additive seasonality)

---

[10] Mishonov, A.V., Boyer, T.P., Baranova, O.K., Bouchard, C.N., Cross, S., Garcia, H.E., Locarnini, R.A., Paver, C.R., Reagan, J.R. [et al.], 2024. *World Ocean Database 2023*. NOAA Atlas NESDIS 97, 207 p. Available at: https://www.ncei.noaa.gov/products/world-ocean-database [Accessed: 16 August 2024].

version of the exponential triple smoothing (ETS) algorithm which smooths out small deviations in past data trends by identifying patterns of seasonality and confidence intervals. This forecasting method is optimal for non-linear data models with seasonal or other recurring patterns.

Results and discussion

Structural shifts in water masses

Fig. 1 presents averaged data on the long-term variability of the CIL vertical structure in the whole deep-sea zone from June to October in 1993–2023. The data reveal that in 2019, the upper and lower boundaries of the CIL merged at an average depth of about 70 m and this water mass, sustained the existence of the BS relict boreal species of forage zooplankton and planktivorous fish, had disappeared. This process did not occur overnight but as a result of a gradual warming of the CIL core over the last 20 years. The water renewal of its core decreased due to a succession of warm winters (Fig. 2) which recurring approximately every five years: in 1996, 2000, 2005, 2010, 2015, 2020 (based on the winters by SST calculated as the average for December–February). This is strongly evidenced by the high

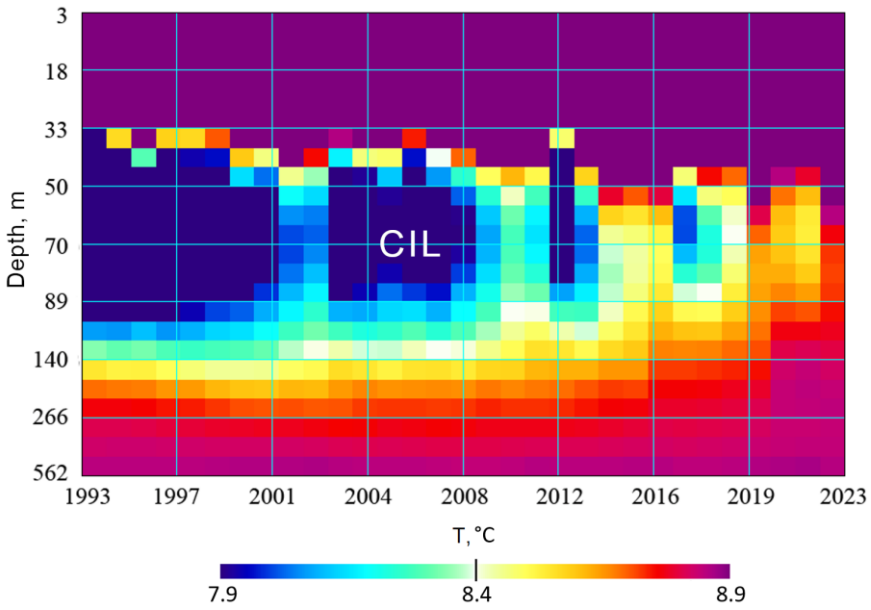

F i g . 1 . Long-term variability of the cold intermediate layer (CIL)

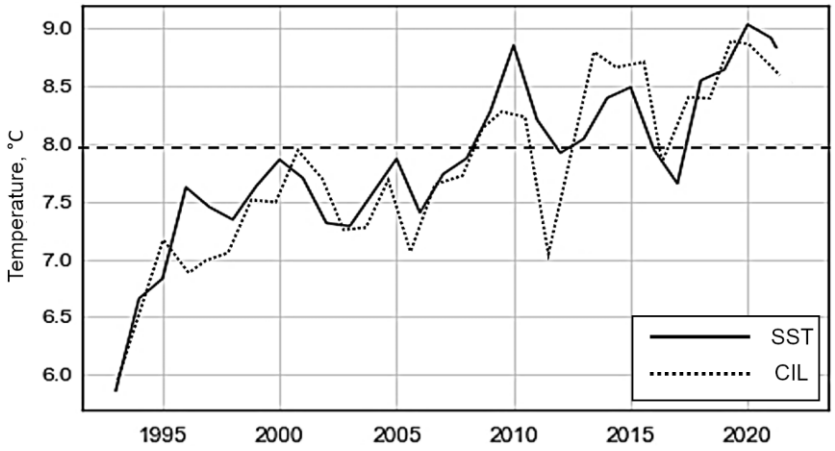

Fig. 2. Average seasonal (winter) values of sea surface temperature, calculated as the average values for January, February and December, and the base value of the CIL in August for 1993–2022

rank Spearman correlation coefficient [20] between annual SST and CIL values, which is ~0.85 (Pearson correlation coefficient is ~0.89). The non-parametric rank correlation method is applied here because SST and CIL are not normally distributed according to the Shapiro–Wilk test [20]. The convergence of the upper and lower CIL boundaries has also led to an increase in the salinity of the surface layer. In 2023, at a depth of 50 m which usually corresponds to the position of the CIL core, salinity reached a maximum value of 19 PSU, which was previously observed only in the 60–70 m layer, i. e. at the average position of the lower boundary in summer.

Thus, a new stratification of water masses and associated biotopes had been emerged throughout the deep sea by 2021. Analysis of data from 84 hydrological profiles across the entire deep-water zone (0–150 m) revealed isothermia (~ 8.7 °C) under the thermocline at all depths up to the hydrogen sulphide zone (Fig. 3, *a*).

The distribution of water density characteristics in the same layer revealed the SOL and the associated anaerocontour biotope were located in the 85–115 m layer. Its upper boundary corresponded to the middle of the main pycnocline (σ_t = 15.8). The SOL average density boundaries are given in accordance with [2, 3]. Above it, the plankton and fish habitat was located in the oxygen zone (Fig. 3, *b*) in the 0–85 m layer (UBSWM and CIL). The maximum depth of zooplankton with a concentration [5)] of 10 μM, or 0.2 ml/L, coincided precisely with the upper boundary of the anaerocontour at the 85 m isobath (Fig. 3, *c*). At a depth of 115 m (with water density σ_t = 16.2), trace oxygen concentrations had disappeared completely and the chemocline layer began with a concentration of H_2S ~3 μM.

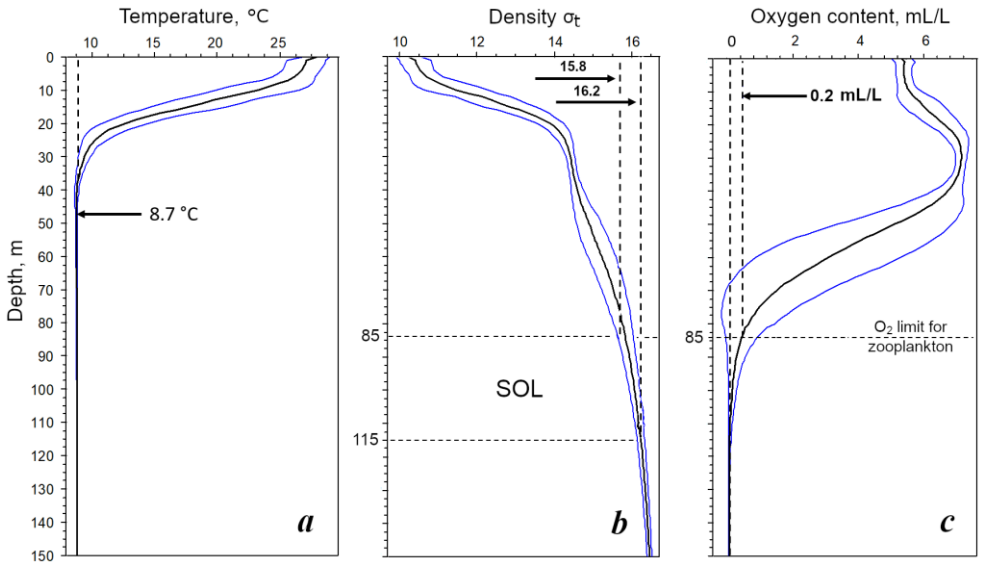

Fig. 3. Average vertical profile of temperature (*a*), density anomaly (*b*) and oxygen content (*c*) in the 0–150 m layer in July and August 2021 in the central deep regions of the Black Sea, according to data from the 117th cruise of R/V *Professor Vodyanitsky*. Blue lines are SD, black lines are mean values

Structural shifts of biotopes

Fig. 3, *b* shows that the zone of daily accumulations of bathyplankton in 2021 aligned precisely with the upper boundary (at a depth of 85 m) of the biotope [12] of the anaerocontour. The study of the multiyear vertical dynamics of the vertical position of the anaerocontour from 1957 to 2021 was based on the fact that the average position of this contact zone corresponded to the upper boundary of the SOL at conditional density $\sigma_t = 15.8$ [2, 3].

The results of the study (Fig. 4) confirm that the upper boundary of this biotope ($\sigma_t = 15.8$) has moved 35 m closer to the surface over 60 years while its lower boundary ($\sigma_t = 16.2$) has risen from a depth of 165 to 115 m. This means that in 1983, the upper anaerocontour boundary (Fig. 4, white circles) rose to the isobath of 100 m which is the maximum depth of the Black Sea sprat *S. sprattus* habitat. Since then, deep accumulations of cold-water (forage) zooplankton concentrated near the upper anaerocontour boundary have appeared in the zone of accumulations of cold-water planktivorous fish. The lower anaerocontour boundary rise (Fig. 4, black circles) indicates that the chemocline, i. e. the hydrogen sulphide zone, has risen 50 m upwards.

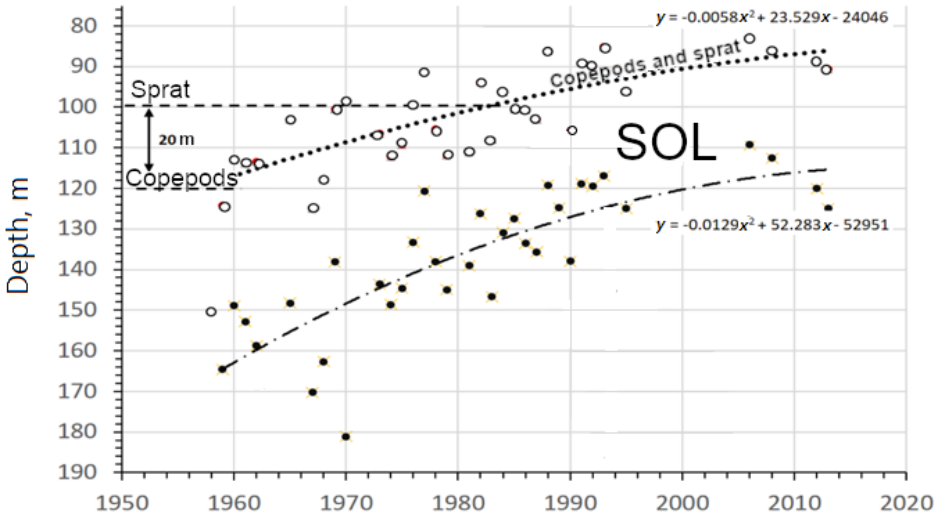

Fig. 4. Dynamics of the anaerocontour rise to the surface for 1957–2021, in summer in the western central deep-sea zone of the Black Sea: white circles are the upper anaerocontour boundary (σ_t = 15.8), black circles are the lower one (σ_t = 16.2). Average data by year: dotted line – upper contact zone; dashed-dotted line – lower contact zone; dashed lines – second-degree polynomial trends

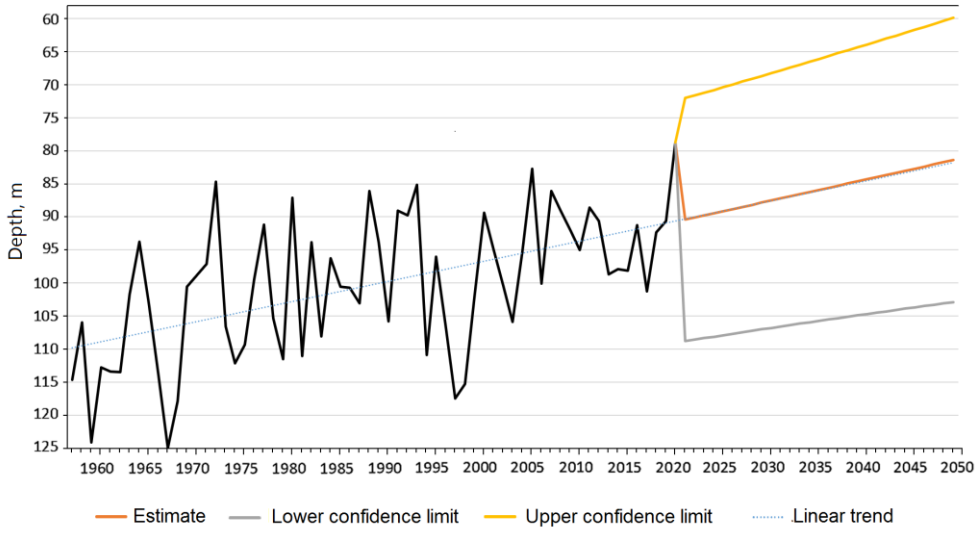

Fig. 5. Dynamics of the upper limit of the Suboxic Layer until 2050 (σ_t = 15.8) in the center of the western Black Sea (42.5–43.5° N, 30–32.5° E)

Knowledge of the dynamics and variability of SOL density boundaries makes it possible to calculate the approximate position of anaerocontour boundaries over the next 25 years. Analysis of hydrological data from the central part of the western cyclonic circulation for 1957–2021 has shown that the upper boundary of the anaerocontour defined by isopycnic σ_t = 15.8 (O_2 = 10 μM) was characterised by a steady tendency to rise to the surface (Fig. 5). In 1959, the average position of the upper boundary of the anaerocontour corresponded to a depth of 124 m. In 1982, this contact zone rose to a depth of 91 m, i. e. almost 33 m higher (compared to 1959), and at present, the upper SOL boundary in the center of the western circulation is located at a depth of 79 m, which is almost 50 m higher than the level observed in 1959. Calculations showed that the estimated shift of the upper SOL boundary could be a further 9 m by 2050 (Fig. 5, dashed line).

Discussion

Trends in changes to the ecological properties of water masses

1. *UBSWM*. It has been established that at the end of the last century the winter SST in the deep-sea zone was about 5.8°C, now its average value has risen almost to 9°C (see Fig. 2). The SST growth rate in the BS is equal to about 0.6°C/10 years. This is consistent with the data of the authors of [21] that the SST increase in 1982 and 2020 was 0.40 ± 0.21 and 0.71 ± 0.19°C/10 years, respectively. Modelling [22] showed that from 1980–1999 to 2080–2099, the SST would increase by a further 3.7°C. According to our calculations, in recent years, the salinity in the UBSWM has started to increase: from 18.0–18.4 PSU [3)] [8] to 18.61–18.8 PSU.

2. *CIL*. We confirm the information of E. V. Stanev et al. [15] that by 2019 warming caused the disappearance of the CIL. In the water layer between the middle of the seasonal thermocline and that of the pycnocline, main environmental parameters changed significantly (Figs. 1, 6). Between 1993 and 2023, temperature changed from 6.0–7.8 to 9°C, salinity – from 18.0–19.0 to 18.8–20.4 PSU and conditional density σt – from 14.0–14.8 to 14.3–15.8.

3. *SOL*. The rise of the Suboxic Layer to the surface has been a steady trend over the last 60 years (Figs. 4, 6). Its upper boundary (σ_t = 15.8) in the deep sea was at a depth of 115 m in 1957, rising to 85 m by 2021; its lower boundary (σ_t = 16.2) was at a depth of 165 m in 1957, rising to 115 m by 2021.

4. *IBSWM*. The upper boundary of this water mass is the chemocline, from which the hydrogen sulphide layer extends deep to the bottom. The results of the present work (Fig. 6) indicate that during 60 years, the hydrogen sulphide layer has risen approximately 50 m upwards.

Trends of major changes in the structure of biotopes

1. *Surface film biotope* (neuston [9]). Currently, the number of neuston copepods of the family Pontellidae has decreased by 50–70%. Their occurrence has decreased so much that they are listed in the Black Sea Red Book [10]. A further increase in SST by almost 4°C [22] by the end of this century can not only lead to a change in the taxonomic composition of traditional neuston species, but also affect the biology of merohyponeuston organisms.

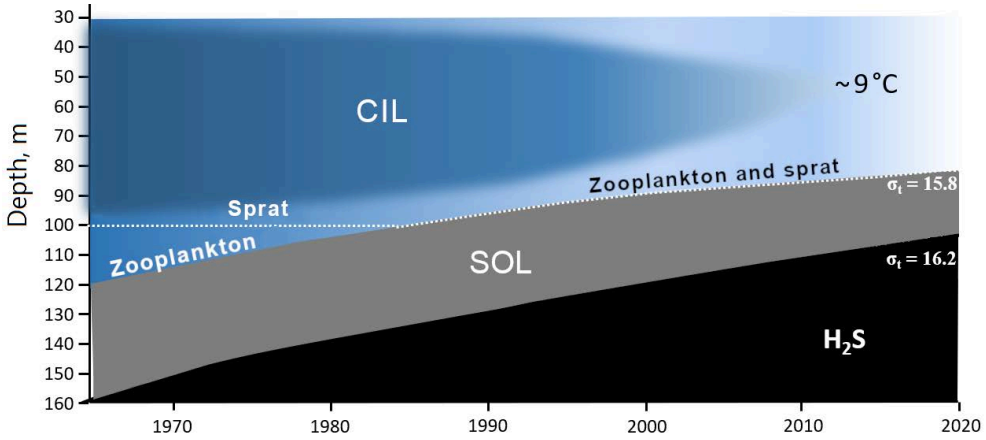

Fig. 6. Changes in the structure of water masses, biotopes and vertical distribution of zooplankton and fish aggregations at the lower boundary of the oxygen layer in the central deep waters of the Black Sea in 1960–2020 (day-time, in summer) in the 30–160 m layer

2. *UBSWM biotope* (epibiota). The bulk of works on anthropogenic and climatic changes in the BS ecosystem were published mainly on the basis of data on changes in the biota of this layer [6, 11, 23, 24]. Therefore, we will only note that under warming conditions over the last few decades, the UBSWM biota began to change significantly due to the appearance of warm-water species and their intentional or unintentional introduction. Now, more than 300 invasive species have been recorded in the BS, the appearance of which has accelerated, especially in recent years [25]. At first, 26 new invasive species were described [26], then their number increased to 59. By 2009, 156 non-indigenous species had been described, most of them from the Mediterranean [27]. In 2017, 261 invasive species were described [28].

3. *CIL biotope* (bathybiota). An increase resulting in temperature values more than 8°C leads to serious disturbances in the spawning phenology of moderately cold-water fish species which start spawning in late September instead of December and finish in May. In recent years, the ontogenetic development cycle of the sprat *S. sprattus* from egg to hatching has almost halved (from seven to two to three days), and the average size of larvae at hatching and their transition to external feeding has decreased [29].

This is also obviously the case with other cold-water species. For example, it is known that the development time of *Calanus euxinus* Hulsemann, 1991 is up to 66 days (from egg to adult) at 8°C, whereas at 18°C this period is almost halved [30]. The compression of the habitat layer of this species due to deoxygenation of the depths has resulted in the disruption of trophic relationships. In 1960–1970s,

the habitat (volume of the environment occupied by the population [30]) of *C. euxinus* in summer occupied the entire thickness of the CIL water mass to a depth of 130 m, where 10 μM isooxygene was located [5], while the habitat of the Black Sea sprat *S. sprattus* occupied only the upper CIL part to a depth of 100 m. The Black Sea sprat feeds on copepods only during the day, either in the zone where they migrate vertically or in the hypoxic zone where they gather near the upper boundary of the Suboxic Layer.

The deeper the copepods concentration layer at the lower boundary of the anaerocontour, the fewer fish are able to descend into it to feed [12]. In the 1960–1970s, the Black Sea sprat could intercept copepods only during their daily vertical migrations (Fig. 6). In recent years, the entire population of *C. euxinus* (including diapause individuals) throughout the deep-water zone of the BS is in the habitat layer of the Black Sea sprat. The merger of their habitats [11)] took place in 1985 (see Fig. 4), which could cause a tenfold increase in sprat stocks at its maximum fat content [31]. It was during these years that *C. euxinus* began to dominate the food boli of these fish. In the near future, due to the disappearance of the CIL, the amount of cold-water zooplankton in the central deep-water areas can decrease significantly because such species as *Oithona similis* Claus, 1866 and *Pseudocalanus elongatus* (Brady, 1865) prefer temperatures below 8°C [31].

4. *SOL biotope* (anaerocontour). Shifts in the position of vertical boundaries of this biotope are the main mediator of climatic changes in the BS ecosystem. The results of the present study show that during the last decades, the upper boundary of the anaerocontour with oxygen concentration of 0.2 ml/L and density σ_t = 15.8 has risen by almost 40 m (see Fig. 4). It is estimated that the habitat of plankton and fish can be reduced by a further 10 m in the deep sea by 2050 (see Fig. 5).

5. *IBSWM biotope*. In the next 25 years, further rise of the hydrogen sulphide zone to the surface by another 10 m can occur in the BS deep waters (see Fig. 5). In the long term, this could lead to the release of anaerobic waters to the surface, which could cause serious damage to the ecosystem, fisheries, recreational and bioclimatic resources of the Black Sea coast.

Conclusion

Thus, the results of the present study have shown statistically significant shifts in the structure of water masses and associated hydrobiont biotopes of the Black Sea pelagic zone over the last decades. Habitat conditions for cold-water species have become particularly complex in the CIL mixed with the surrounding warmer waters under the influence of warming. It is likely that this water mass can reappear under the influence of long-term hydrological cycles and cold-water organisms will not disappear. The variability of the intensity of atmospheric circulation

[11)] Beklemishev, K.V., 1969. [*Ecology and Biogeography of the Pelagic Zone*]. Moscow: Nauka, 291 p. (in Russian).

over the North Atlantic, which affects the balance between the inflow of high-salinity water masses from the Mediterranean Sea (averaging ~170 km^3 per year) and river runoff into the sea (averaging ~370 km^3 per year), plays a huge role here. This balance depends on the difference in levels between the seas, on currents, including drift currents caused by wind action, and thus can also depend on atmospheric circulation and climate change. Accordingly, the SOL represented by transformed Mediterranean water is also related to climate change.

Changes in river runoff volumes are also one of the important consequences of climatic change that determine the intensity of renewal of the CIL waters. The number of baby fish, biomass and catches of the Black Sea sprat *S. sprattus* were found to be in direct dependence on the dynamics of the runoff volumes of the Danube and Dnieper rivers. Apparently, the increase in runoff leads to the removal of large volumes of dissolved organic matter (especially in the area of the north-western shelf), which ensures the development of phyto- and zooplankton. This can create favourable conditions for feeding young pelagic fish species or lead to hypereutrophication and extensive fish kill. It is shown that the increase in the BS water temperature is likely to have an unfavourable effect on the reproduction and catches of cold-water predators, including sprat, whiting, horse mackerel and bottom benthophagous species such as halibut and mullet. The paper describes the process of the warming-induced disappearance of the CIL, which is the habitat of the BS cold-water pelagic species. This process can serve as a precursor of large-scale ecological shifts in other regions of the World Ocean.

REFERENCES

1. Murray, J., Jannasch, H., Honjo, S., Anderson, R.F., Reeburgh, W.S., Top, Z., Friederich, G.E., Codispoti, L.A. and Izdar, E., 1989. Unexpected Changes in the Oxic/Anoxic Interface in the Black Sea. *Nature*, 338, pp. 411–413. https://doi.org/10.1038/338411a0
2. Konovalov, S., Murray, J. and Luther, G., 2005. Basic Processes of Black Sea Biogeochemistry. *Oceanography*, 16(2), pp. 24–35. https://doi.org/0.5670/oceanog.2005.39
3. Eremeev, V.N. and Konovalov, S.K., 2006. On the Budget and the Distribution of Oxygen and Sulfide in the Black Sea Water. *Marine Ecological Journal*, 5(3), pp. 5–29 (in Russian).
4. Friedrich, J., Janssen, F., Aleynik, D., Bange, H.W., Boltacheva, N., Çagatay, M.N., Dale, A.W., Etiope, G., Erdem, Z. [et al.], 2014. Investigating Hypoxia in Aquatic Environments: Diverse Approaches to Addressing a Complex Phenomenon. *Biogeosciences*, 11(4), pp. 1215–1259. https://doi.org/10.5194/bg-11-1215-2014
5. Capet, A., Stanev, E.V., Beckers, J.-M., Murray, J. W. and Grégoire, M., 2016. Decline of the Black Sea Oxygen Inventory. *Biogeosciences*, 13(4), pp. 1287–1297. https://doi.org/10.5194/bg-13-1287-2016
6. Mikaelyan, A.S., Zatsepin, A.G. and Chasovnikov, V.K., 2013. Long-term changes in nutrient supply of phytoplankton growth in the Black Sea. *Journal of Marine Systems*, 117–118, pp. 53–64. https://doi.org/10.1016/j.jmarsys.2013.02.012
7. Vidnichuk, A.V. and Konovalov, S.K., 2021. Changes in the Oxygen Regime in the Deep Part of the Black Sea in 1980–2019. *Physical Oceanography*, 28(2), pp. 180–190. https://doi.org/10.22449/1573-160X-2021-2-180-190
8. Mamayev, O.I., Arkhipkin, V.S. and Tuzhilkin, V.S., 1994. TS-Analysis of the Black Sea Waters. *Okeanologiya*, 34(2), pp. 178–192 (in Russian).

9. Zaytsev, Yu.P., 2015. *Scientific Issues Ternopil Volodymyr Hnatiuk National Pedagogical University Series: Biology*, 3–4(64), pp. 309–313 (in Russian).
10. Harcotă, G.-E., Țotoiu, A., Bișinicu, E., Tabarcea, C., Boicenco, L. and Timofte, F., 2022. Abundance and Distribution of the Hyponeustonic Copepods *Anomalocera patersonii* and *Pontella mediterranea* in the South-western Part of the Black Sea. *Turkish Journal of Fisheries and Aquatic Sciences*, 22(5), TRJFAS18987. https://doi.org/10.4194/TRJFAS18987
11. Yunev, O.A., Konovalov, S.K. and Velikova, V., 2019. *Anthropogenic Eutrophication in the Black Sea Pelagic Zone: Long-Term Trends, Mechanisms, Consequences*. Moscow: GEOS, 164 p. (in Russian).
12. Melnikov, V., Pollehne, F., Minkina, N. and Melnik, L., 2021. Distribution of *Sprattus sprattus phalericus* (Risso, 1827) and Zooplankton near the Black Sea Redoxcline. *Journal of Fish Biology*, 99(4), pp. 1393–1402. https://doi.org/10.1111/jfb.14848
13. Hubareva, E.S. and Anninsky, B.E., 2022. State of Population of *Calanus euxinus* (Copepoda) in the Open Pelagial and on the Shelf of The Black Sea Near Crimea in Autumn 2016. *Marine Biological Journal*, 7(3), pp. 17–27. https://doi.org/10.21072/mbj.2022.07.3.02
14. Melnikov, V.V., 2023. Anaeroconture of the Black Sea. *Izvestia of Samara Scientific Center of the Russian Academy of Sciences*, 25(5), pp. 203–218. https://doi.org/10.37313/1990-5378-2023-25-5-203-218
15. Stanev, E.V., Peneva, E. and Chtirkova, B., 2019. Climate Change and Regional Ocean Water Mass Disappearance: Case of the Black Sea. *Journal of Geophysical Research: Oceans*, 124(7), pp. 4803–4819. https://doi.org/10.1029/2019JC015076
16. Oven, L.S., Shevchenko, N.F. and Volodin, S.V., 1996. Sprats Nutrition in Different Regions of the Black Sea. In: Konovalov, S.M., ed., 1996. *The Modern State of Black Sea Ichtyophauna: Collection of Scientific Papers*. Sevastopol: IBSS, pp. 34–38 (in Russian).
17. Dobricic, S. and Pinardi, N., 2008. An Oceanographic Three-Dimensional Variational Data Assimilation Scheme // *Ocean Modelling*, 22(3–4), pp. 89–105. https://doi.org/10.1016/j.ocemod.2008.01.004
18. Strorto, A., Martin, M.J., Dereble, B. and Masina, S., 2018. Strongly Coupled Data Assimilation Experiments with Linearized Ocean-Atmosphere Balance Relationships. *Monthly Weather Review*, 146(4), pp. 1233–1257. https://doi.org/10.1175/MWR-D-17-0222.1
19. Reiniger, R.F. and Ross, C.K., 1968. A Method of Interpolation with Applications to Oceanographic Data. *Deep-Sea Research*, 15(2), pp. 185–193. https://doi.org/10.1016/0011-7471(68)90040-5
20. Shapiro, S.S. and Wilk, M.B., 1965. An Analysis of Variance Test for Normality (Complete Samples). *Biometrika*, 52(3–4), pp. 591–611. https://doi.org/10.2307/2333709
21. Mohamed, B., Ibrahim, O. and Nagy, H., 2022. Sea Surface Temperature Variability and Marine Heatwaves in the Black Sea. *Remote Sensing*, 14(10), pp. 2383. https://doi.org/10.3390/rs14102383
22. Cannaby, H., Fach, B. A., Arkin, S.S. and Salihoglu, B., 2015. Climatic controls on biophysical interactions in the Black Sea under present day conditions and a potential future (A1B) climate scenario. *Journal of Marine Systems*, 141, pp. 149–166. https://doi.org/10.1016/j.jmarsys.2014.08.005
23. Oguz, T., Dippner, J.W. and Kaymaz, Z., 2006. Climatic Regulation of the Black Sea Hydro-Meteorological and Ecological Properties at Interannual-to-Decadal Time Scales. *Journal of Marine Systems*, 60(3–4), pp. 235–254. https://doi.org/10.1016/j.jmarsys.2005.11.011

24. Öztürk, B., 2021. *Non-Indigenous Species in the Mediterranean and the Black Sea*. Rome: FAO, 106 p. Series Studies and reviews (General Fisheries Commission for the Mediterranean). No. 87. https://doi.org/10.4060/cb5949en

25. Zaitsev, Y. and Mamaev, V., 1997. *Marine Biological Diversity in the Black Sea. A Study of Change and Decline*. New York: United Nations Publications. Black Sea Environmental Series No. 3. 1997. 208 p.

26. Zaitsev, Y. and Öztürk, B., 2001. *Exotic Species in the Aegean, Marmara, Black, Azov and Caspian Seas*. Istanbul: Turkish Marine Research Foundation, 261 p.

27. Shiganova, T. and Öztürk, B., 2009. Trend on Increasing Mediterranean Species Arrival into the Black Sea. In: F. Briand, ed., 2009. *Climate forcing and its impacts on the Black Sea marine biota*. Monaco: CIESM, No. 39, pp. 75–91.

28. Alexandrov, B., Minicheva, G. and Zaitsev, Y., 2017. Black Sea Network of Marine Protected Areas: European Approaches and Adaptation to Expansion and Monitoring in Ukraine. In: P. D. Groriup, ed., 2017. *Management of Marine Protected Areas: A Network Perspective*. Chichester, John Wiley & Sons. 2017. pp. 227–246. https://doi.org/10.1002/9781119075806.ch12

29. Klimova, T.N., Vdodovich, I.V., Anninsky, B.E., Subbotin, A.A., Podrezova, P.S. and Melnikov, V.V., 2021. Effect of Certain Abiotic and Biotic Factors on Spawning of the European Sprat *Sprattus sprattus* (Linnaeus, 1758) in the Black Sea in November 2016–2017. *Oceanology*, 61(1), pp. 58–68. https://doi.org/10.1134/S0001437021010082

30. Sazhina, L.I., 1973. [Growth of Black Sea Mass Copepods Under Laboratory Conditions]. *Biologiya Morya*, 28, pp. 41–51 (in Russian).

31. Shulman, G.E., Nikolsky, V.N., Yuneva, T.V., Shchepkina, A.M., Bat, L. and Kideys, A.E., 2007. Influence of Global Climatic and Regional Anthropogenic Factors on Small Pelagic Fishes of the Black Sea. *Marine Ecological Journal*, 6(4), pp. 18–30 (in Russian).

Submitted 29.08.2024; accepted after review 05.03.2025;
revised 25.03.2025; published 30.06.2025

About the authors:

Viktor V. Melnikov, Leading Research Associate, A.O. Kovalevsky Institute of Biology of the Southern Seas of RAS (2 Nakhimov Av., Sevastopol, 299011, Russian Federation), PhD (Biol.), **ORCID ID: 0000-0001-6856-0467, ResearcherID: N-9219-2014, Scopus Author ID: 57197396948**, *sevlin@ibss-ras.su*

Alexander N. Serebrennikov, Research Associate, Institute of Natural and Technical Systems (28 Lenina St., Sevastopol, 299011, Russian Federation), **ORCID ID: 0000-0002-8650-8168; ResearcherID: K-4059-2018; Scopus Author ID: 57203430266,** *swsilv@gmail.com*

Anna V. Masevich, Research Associate, Marine Hydrophysical Institute of RAS (2 Kapitanskaya Str., Sevastopol, 299011, Russian Federation), PhD (Geogr.), **ORCID ID: 0000-0002-0889-020X; ResearcherID: AAO-2592-2020; Scopus Author ID: 58544083700,** *anna_vidnichuk@mhi-ras.ru*

Elena S. Chudinovskykh, Junior Research Associate, A.O. Kovalevsky Institute of Biology of the Southern Seas of RAS (2 Nakhimov Av., Sevastopol, 299011, Russian Federation), **ORCID ID: 0000-0003-4962-7333, ResearcherID: HQZ-6164-2023, Scopus Author ID: 57895036400,** *chudhel@yandex.ru*

Contribution of the authors:

Viktor V. Melnikov – problem statement, processing, analysis and description of research results, correction of the text of the article.

Alexander N. Serebrennikov – obtaining field data, processing measurement data, preparing graphic material.

Anna V. Masevich – analysis of the literature on the research problem, discussion of the results of the work.

Elena S. Chudinovskykh – obtaining and processing of field data discussion of the results.

All the authors have read and approved the final manuscript.

Original paper

Thermohaline Structure of Western Crimea Shelf Waters

O. A. Lukashova, V. N. Belokopytov *

Marine Hydrophysical Institute of RAS, Sevastopol, Russian Federation
***** *e-mail: belokopytov.vn@mhi-ras.ru*

Abstract
The paper uses oceanographic observations and climatic values at the grid $10' \times 15'$ for 1950–2023 to investigate spatial distribution and seasonal course of the thermohaline structure of Western Crimea shelf waters. In the cold season, the regional spatial thermal structure had a pronounced zonal distribution with cold northern and warm southern parts. During the spring–summer period, the relative location of warm/cold zones changed to the meridional one. The regional haline structure was characterized by a saltier tongue spreading from the open sea and separating brackish waters of the north-western shelf and coastal waters. Over the greater part of the year, the coastal zone was colder and less saline than the outer shelf part. The opposite distribution, when the coastal zone was warmer than the outer shelf part, was observed in the surface layer in April–May and below the seasonal thermocline in the summer–autumn period. Due to frequent upwelling events in summer, salinity in the subsurface layers of the coastal zone from May to September becomes higher than in the outer shelf part. In general, in terms of the thermohaline water structure, the Western Crimea shelf is an intermediate zone between the north-western shelf and the deep part of the Black Sea, the water exchange with which depends of the intensity of the Rim Current and the Sevastopol anticyclonic eddy. Regional water masses or sub-types of main Black Sea water masses were not identified in the study area.

Keywords: thermohaline structure, sea temperature, salinity, climate, shelf, coastal zone, Western Crimea

Acknowledgments: The work was performed under state assignment of MHI RAS on topic FNNN-2024-0014 “Fundamental studies of interaction processes in the sea-air system that form the physical state variability of the marine environment at various spatial and temporal scales”.

For citation: Lukashova, O.A. and Belokopytov, V.N., 2025. Thermohaline Structure of Western Crimea Shelf Waters. *Ecological Safety of Coastal and Shelf Zones of Sea*, (2), pp. 36–52.

Термохалинная структура вод шельфа Западного Крыма

О. А. Лукашова, В. Н. Белокопытов *

Морской гидрофизический институт РАН, Севастополь, Россия

** e-mail: belokopytov.vn@mhi-ras.ru*

Аннотация

На основе рассчитанного по данным наблюдений климатического массива температуры и солености на сетке 10′ × 15′ для 1950–2023 гг. рассмотрены пространственное распределение и сезонная изменчивость термохалинной структуры вод шельфа Западного Крыма. Пространственная термическая структура района в холодный период года имеет явно выраженное зональное распределение с холодной северной и теплой южной частями. В весенне-летний период относительное расположение теплых/холодных областей изменяется на меридиональное. Для халинной структуры вод района характерно наличие клина соленых вод открытого моря, разделяющего распресненные воды прибрежной зоны и северо-западного шельфа. Прибрежная зона на протяжении большей части года является более холодной и распресненной, чем мористая часть шельфа. Обратное распределение, когда прибрежная зона теплее мористой части шельфа, наблюдается в поверхностном слое в апреле – мае, а также в слое глубже сезонного термоклина в летне-осенний период. Частые апвеллинги в летний сезон способствуют тому, что соленость в подповерхностных слоях прибрежной зоны с мая по сентябрь становится выше, чем в мористой части шельфа. В целом по характеристикам термохалинной структуры вод шельф Западного Крыма является промежуточной зоной между северо-западным шельфом и глубоководной частью Черного моря, водообмен с которой зависит от интенсивности Основного Черноморского течения и Севастопольского антициклона. Региональные водные массы или подтипы основных черноморских водных масс в исследуемом районе не выделены.

Ключевые слова: термохалинная структура, температура воды, соленость, климат, шельф, прибрежная зона, Западный Крым

Благодарности: работа выполнена в рамках государственного задания ФГБУН ФИЦ МГИ по теме FNNN-2024-0014 «Фундаментальные исследования процессов взаимодействия в системе океан-атмосфера, формирующих изменчивость физического состояния морской среды на различных пространственно-временных масштабах».

Для цитирования: *Лукашова О. А., Белокопытов В. Н.* Термохалинная структура вод шельфа Западного Крыма // Экологическая безопасность прибрежной и шельфовой зон моря. 2025. № 2. С. 36–52. EDN JFOUEO.

Introduction

The sea area adjacent to the city of Sevastopol and the western districts of the Republic of Crimea constitutes a natural component of the region, playing an important role in its economic development. Regional reference books highlighting climatic conditions and the current state of the environment, including the thermohaline structure of the waters, are needed to solve applied problems.

General features of the hydrology of the area adjacent to the western coast of Crimea are presented in varying degrees of detail in generalized works describing all shelf areas or the Black Sea as a whole [1–4] as well as in works [1), 2)].

[1)] Vinogradov, K.A., Rozengurt, M.Sh. and Tolmazin, D.M., 1966. [*Atlas of Hydrological Characteristics of the North-Western Black Sea (for Fishery Purposes)*]. Kiev: Naukova Dumka, 94 p. (in Russian).

In the above studies, the Western Crimea shelf was not distinguished as a discrete region; rather, it was considered part of the extensive north-western shelf. Its proximity to the deep-water segment of the Black Sea is noteworthy with respect to the similarity of conditions.

The characteristics of various oceanographic phenomena and processes specific to the area have been addressed in works [3), 4)] [6–12]. Much research is devoted to the circulation of waters of the north-western shelf in general and the Sevastopol anticyclonic eddy in particular (e. g., works [2), 5)] as well as [2–4, 13–21]). The advection of waters affects the thermohaline structure significantly, especially at the boundaries of areas with different hydrological structure of waters.

The regional description of the seasonal variability of the thermohaline structure of waters related to this area was published more than 20 years ago on the basis of archival data available at that time and was limited to the Sevastopol seaside [12].

The aim of the work is to describe the seasonal variability of the thermohaline structure of Western Crimea shelf waters based on the observation data for 1950–2023 with an assessment of the main differences between the open and coastal parts of the study area.

Materials and methods of study

The shelf area adjacent to the western coast of Crimea is one of the areas of the Black Sea with a fairly high availability of oceanographic data. In total, the data bank of Marine Hydrophysical Institute of RAS includes 37,046 oceanographic stations (1460 sets/cruises) made in the study area (44° 20′–45° 30′ N, 32°–33° 35′ E) in 1910–2023 [6)] (Fig. 1). The 1950–2023 period covering two World Climate Organization climate periods was chosen for the calculation of climate values (10,673 stations) (Fig. 2).

Climatic estimates of temperature and salinity were calculated based on decade profiles from the thermohaline field reanalysis array, which are interpolated values of primary measurements at the regular grid 10′ × 15′ using the methodology described in [22]. The relative degree of coverage of the study area with interpolated values reached 90% in 1960–1980, 20% in 1995–2015 and 40% after 2016. For 1950–2023, monthly temperature and salinity values at grid nodes were calculated and taken as climatic normals.

---

2) Nelepo, B.A., ed., 1984. [*Variability of Hydrophysical Fields of the Black Sea*]. Leningrad: Gidrometeoizdat, 240 p. (in Russian).

3) Ilyin, Yu.P. and Grishin, G.A., 1988. [The Summer Spreading of the North-Western Black Sea and the Possibility of its Control by Satellite Video Data]. In: Vasiliev, L.N., 1988. [*Geographic Interpretation of Aerospace Data*]. Moscow: Nauka, pp. 119–125 (in Russian).

4) Tuzhilkin, V.S., 2008. [*Seasonal and Multiyear Variability of the Thermohaline Structure of the Black Sea and Caspian Sea Waters and the Processes of its Formation. Extended Abstract of DSc Thesis. Geographical Sciences*]. Moscow, 46 p. (in Russian).

5) Bolshakov, V.S., 1970. [*Transformation of River Waters in the Black Sea*]. Kiev: Naukova Dumka, 328 p. (in Russian).

6) Godin, E.A., Belokopytov, V.N., Ingerov, A.V., Plastun, T.V., Galkovskaya, L.K., Kasianenko, T.E., Zhuk, E.V. and Isaeva, E.A., 2019. *The Black Sea: Hydrology. 2018* [Database]. Moscow. State Registration No. 2019621008 (in Russian).

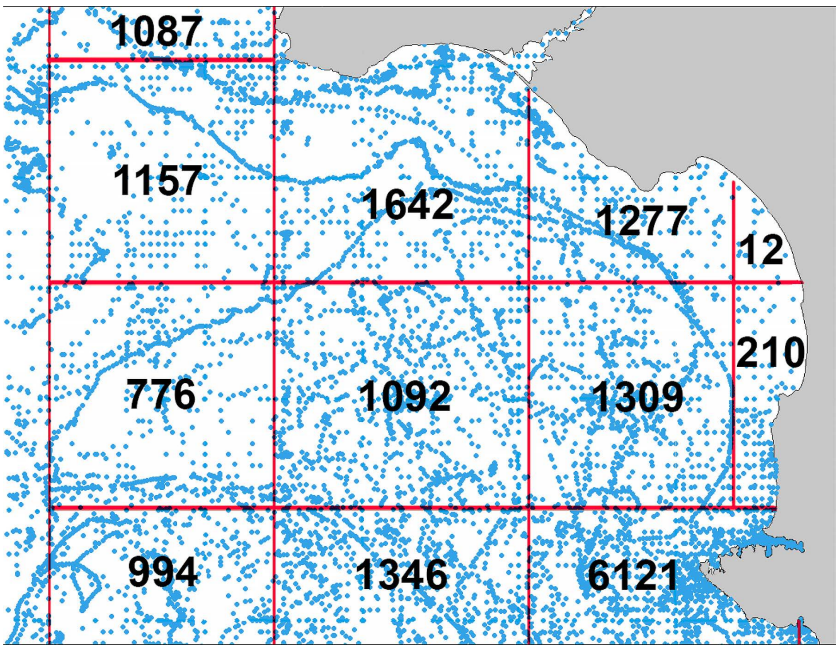

Fig. 1. Location of oceanographic casts in the shelf area near the Western Crimea coast in 1910–2023 and number of stations in 20′ × 30′ squares

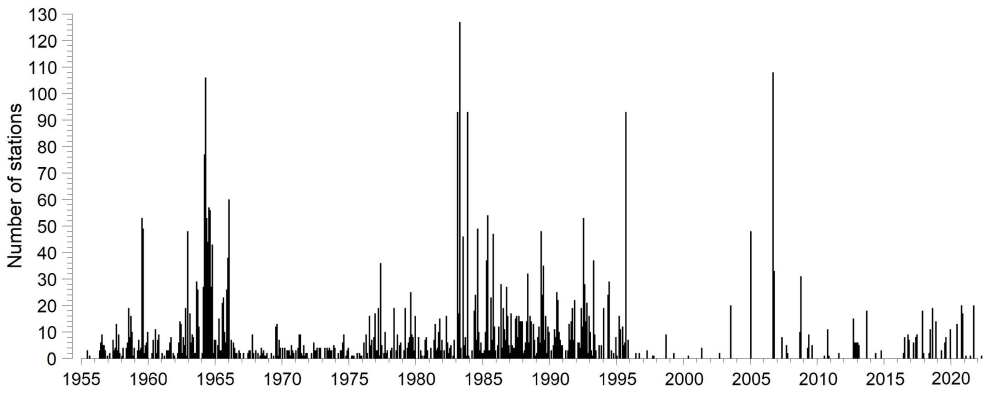

Fig. 2. Time-series of monthly number of oceanographic stations in the study area

Results and discussion

Water temperature

The seasonal course of the vertical thermal structure of the waters in the study area is generally characteristic of the Black Sea. From January to March, the water temperature remains consistent throughout the layer. From May to August, a sharp thermocline develops, and the frequency of occurrence of the upper mixed layer during this period of the year is minimal. A phase delay of the seasonal cycle is observed with depth (Figs. 3, 4).

To separate the open and coastal segments of the shelf, an isobath of 50 m was adopted. From January to April, the coastal zone in the entire layer is colder than the rest of the shelf; the difference in temperature between the waters of the coastal zone and the outer shelf part reaches 0.8°C and does not change sign with depth

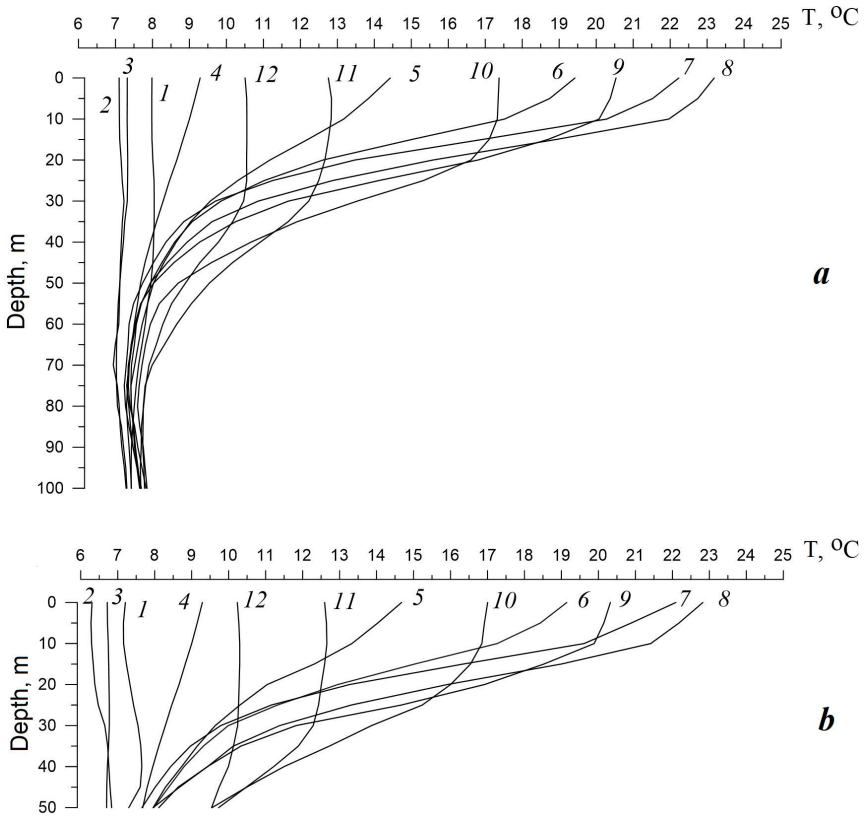

Fig. 3. Climatic monthly vertical temperature profiles in the South-Western Crimea shelf area: in the outer shelf part (*a*), in the coastal zone (*b*). Digits stand for month numbers

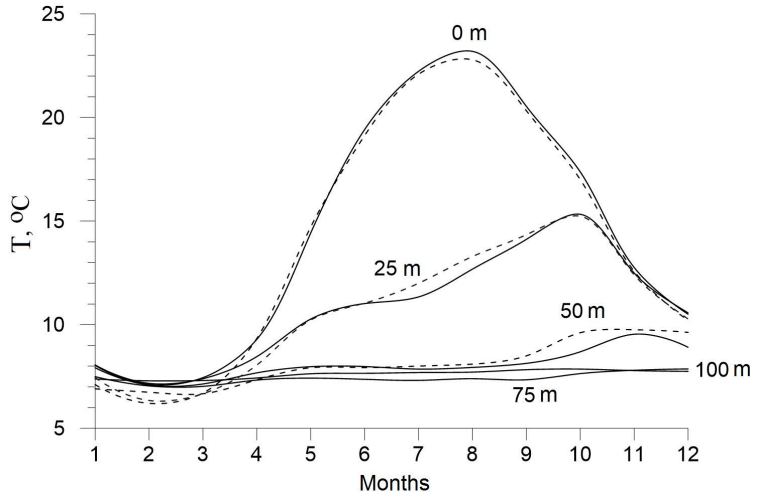

Fig. 4. Climatic seasonal course of water temperature in the Western Crimea shelf area at different depths. Dashed lines denote temperature values in the coastal zone (depth < 50 m), solid lines are those in the outer shelf

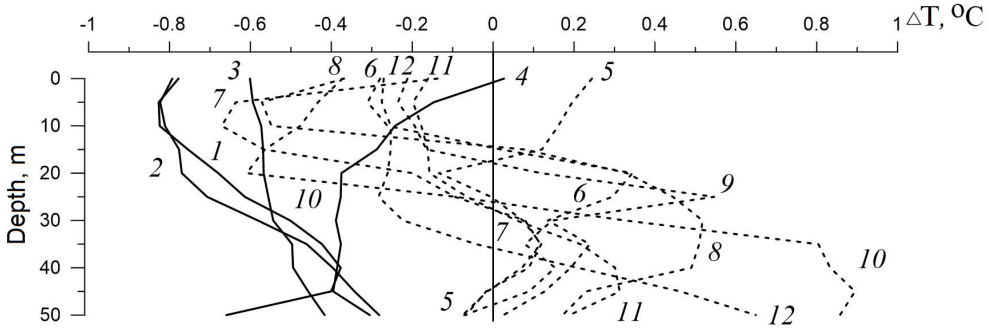

Fig. 5. Differences of climatic monthly temperature between the coastal zone and the Western Crimea outer shelf. Dashed lines denote months when the difference in values changes its sign with depth, solid lines are months without changes. Digits stand for month numbers

(Fig. 5). During the rest of the year, the temperature of coastal waters in the surface layer is generally lower than in the outer shelf part ($\Delta T \leq 0.6$°C) and it is higher in the layer below the thermocline ($\Delta T \leq 0.9$°C) (Fig. 5).

The spatial thermal structure of the area as a whole has a clearly pronounced zonal distribution with cold northern and warm southern parts. With depth, the southern direction of temperature growth changes to the south-eastern direction due to the influence of cold bottom waters of the north-western shelf (Fig. 6).

During the annual cycle, the spatial ratio of warm and cold areas in the temperature field changes (Fig. 7). The greatest deviation from the mean annual distribution in the surface layer is observed in April and May, when the entire coastal zone is on average 0.3–0.4°C warmer than the open part, and in summer, when coastal waters, on the contrary, are 0.2°C colder. This is due to the fact that under the conditions of spring warming and low winds, the coastal zone warms up faster than the open shelf part, and in summer the influence of surges and upwelling events in the coastal zone is most pronounced. From September to March, the thermal field corresponds to the yearly distribution, with the zonal contrast in water temperature being minimal in September.

The geographical position of the Western Crimea shelf between the deep sea and the north-western shelf implies the possibility of advection of cold intermediate layer (CIL) waters from these areas. The results of individual oceanographic measurements showed signs of penetration of the CIL waters into the study area from both northern and southern directions. As for the climatic distribution of water temperature and salinity, it can be concluded that the CIL near the Western

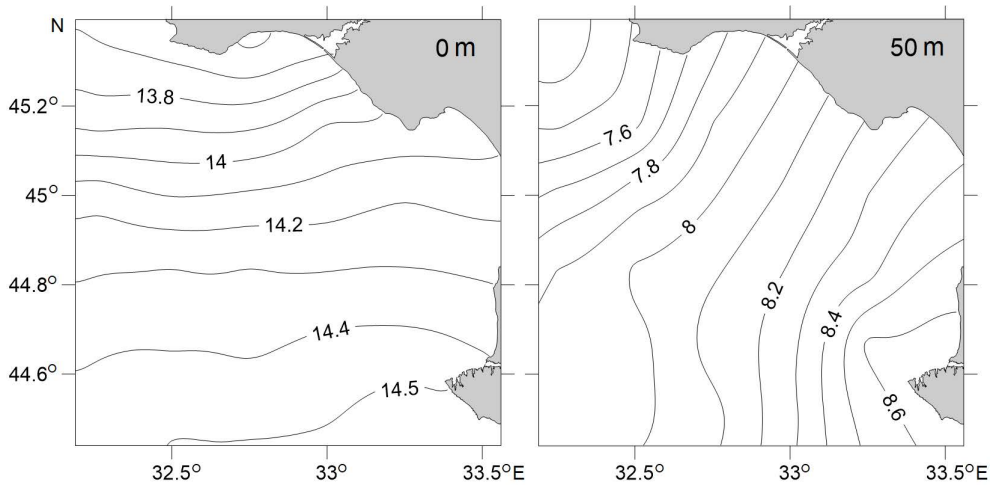

Fig. 6. Climatic yearly water temperature fields in the Western Crimea shelf, °C, at depths of 0 and 50 m

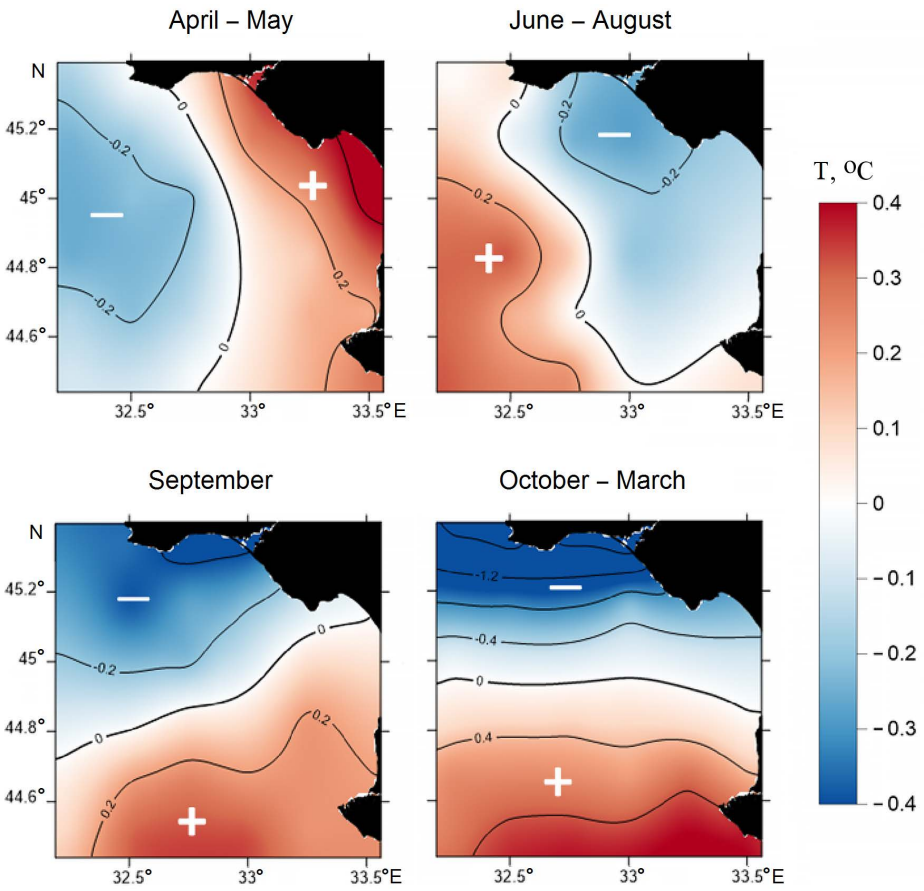

Fig. 7. Generalized types of spatial water temperature distribution in the surface layer of the Western Crimea shelf by deviations from the region area averaged value. Key: "+" – positive anomalies, "–" negative anomalies

Crimea coast is formed mainly on the north-western shelf. Previously, high-resolution winter–spring surveys near the continental slope of the north-western shelf showed that advection of bottom waters into the deep sea occurred mainly in the area between 30° and 32° E. The climatic monthly values of water temperature on the central meridional section of the study area along 32° 45′ E (Fig. 8) show clearly that the sliding of cooled waters towards the open sea also occurs near the Crimean coast.

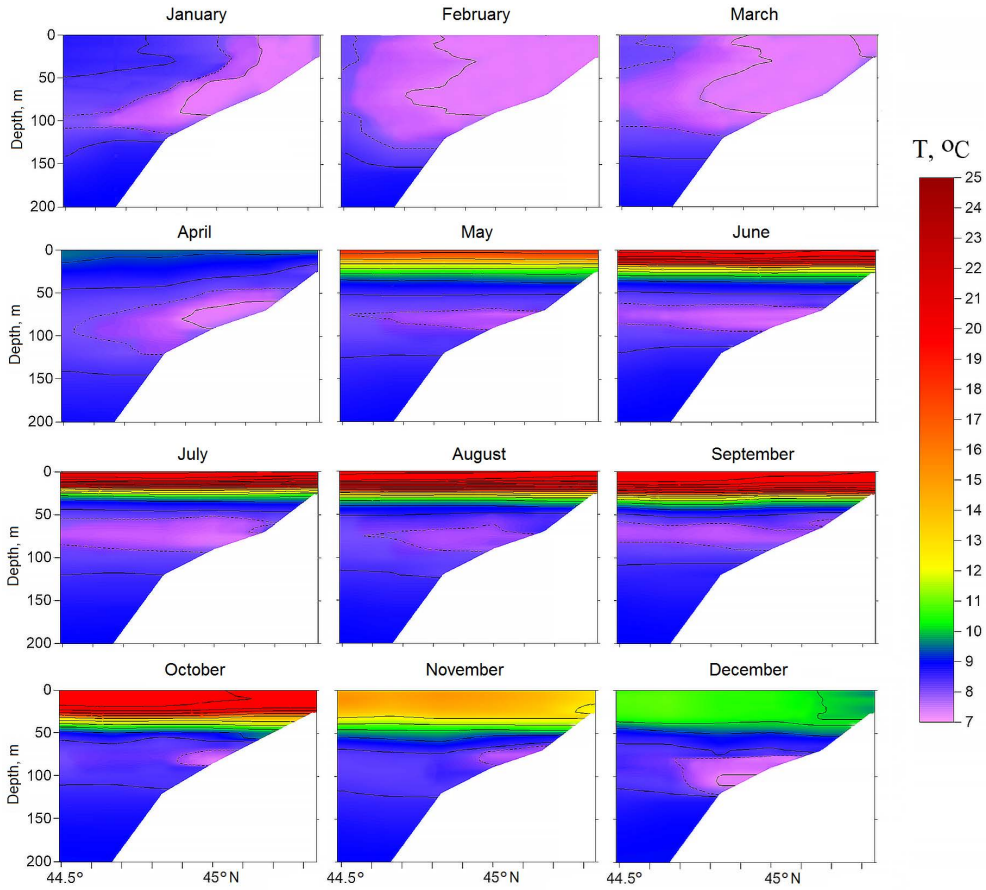

Fig. 8. Climatic monthly water temperature in the Western Crimea shelf along the 32° 45′ E section

Salinity

The annual course of the vertical structure of salinity in the study area (Fig. 9) is conventionally divided into two seasons. From November to May, weak haline stratification in the 0–70 m layer is almost the same as in the deep Black Sea. In June–October, vertical salinity gradients increase and the stratification of the area is intermediate between the north-western shelf with highly stratified waters and the deep sea.

For most of the year, the coastal zone (up to 50 m depth) is more brackish in the entire water column than the rest of the shelf (Fig. 10). From May to September, salinity in the subsurface layer of the coastal part is higher than in the outer part, which is connected with intensification of vertical mixing during upwelling events.

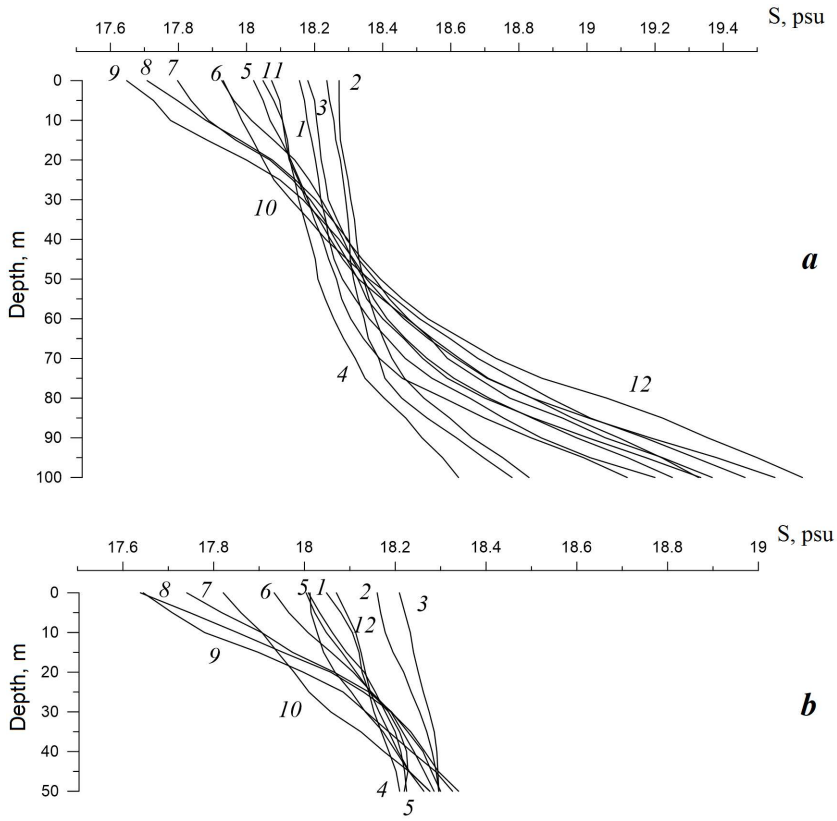

Fig. 9. Climatic monthly vertical salinity profiles in the Western Crimea shelf area: in the outer shelf part (*a*), in the coastal zone (*b*). Digits stand for calendar month numbers

The seasonal course of salinity at different horizons in the study area and in many other areas of the Black Sea differs significantly (Fig. 11). The salinity minimum in the surface layer of this area is shifted to early autumn, whereas in the rest of the Black Sea, the minimum is observed in spring and summer. On the Western Crimea shelf, in the 50–100 m layer, the salinity minimum is reached in April, with its maximum in October, which is also not typical for the sea as a whole. This is largely determined by the seasonal dynamics of the Sevastopol anticyclonic eddy which affects water exchange of the study area with the Rim Current and the north-western shelf.

The spatial haline structure of the area waters (Fig. 12) is characterized by the presence of a saltier tongue coming from the open sea and separating the brackish waters of the north-western shelf and the coastal zone. The spatial orientation of the saline water area does not change much with depth.

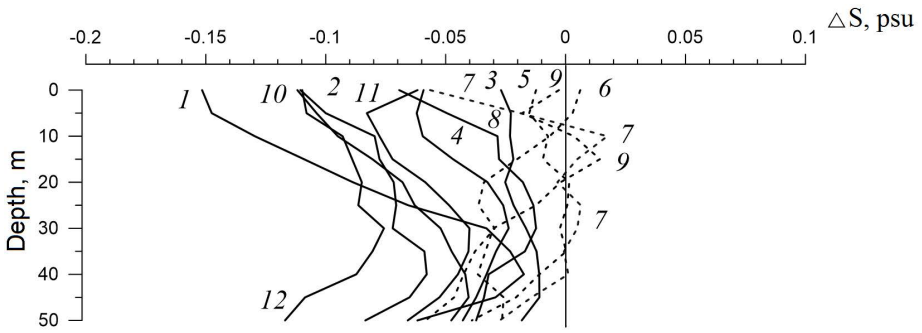

Fig. 10. Differences between climatic monthly salinity values in the coastal zone and the Western Crimea outer shelf. Dashed lines are salinity diagrams for months when the difference in salinity values changes its sign with depth, solid lines are those for months without changes

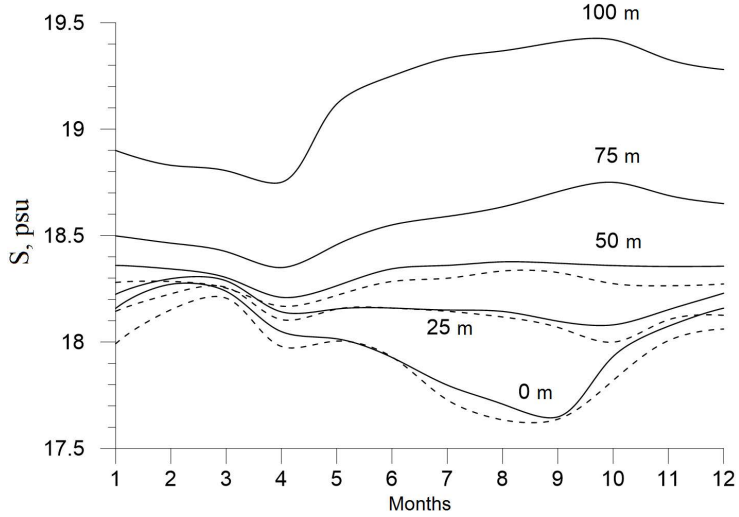

Fig. 11. Climatic seasonal course of salinity in the Western Crimea shelf area at different depths. Dashed lines denote values in the coastal zone (depth < 50 m), solid lines are those in the outer shelf

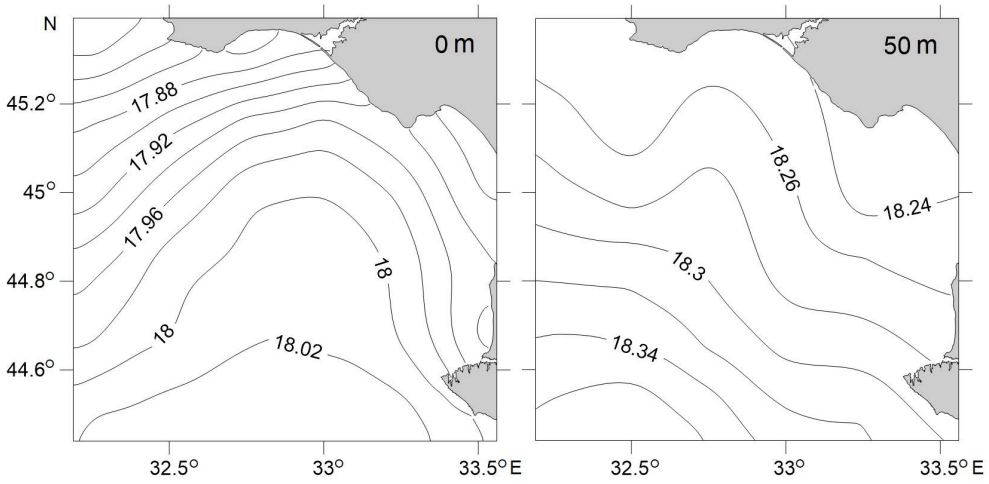

Fig. 12. Climatic yearly salinity fields, psu, in the Western Crimea shelf at depths of 0 and 50 m

The most significant deviations of salinity from the spatial pattern of yearly distribution (Fig. 13) occur in summer when salinity increases in the surface layer of the coastal zone under low water conditions in small rivers of Crimea, surge and upwelling events.

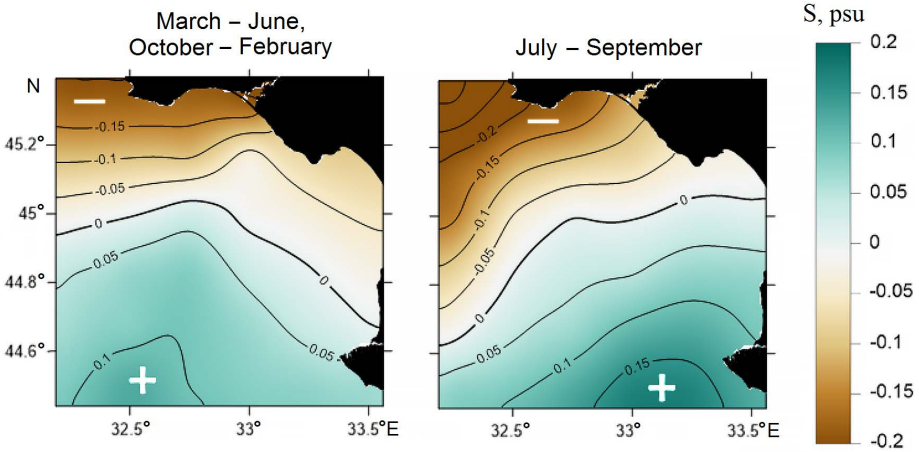

Fig. 13. Generalized types of spatial salinity distribution in the surface layer of the Western Crimea shelf by deviations from the region area averaged value. Key: "+" – positive anomalies, "–" negative anomalies

T,S indices

Monthly T,S curves are qualitatively consistent with the distribution of water masses in most areas of the Black Sea (Fig. 14). Seasonal course of T,S indices (Fig. 15) reflects patterns common to the basin. In the surface layer, during the transition from winter-spring to summer-autumn period, the increase in water temperature is accompanied by a decrease in salinity. In the CIL, seasonal changes are characterized by a joint increase in water temperature and salinity from winter to summer. In the main pycnocline, the seasonal cycle is qualitatively similar to that of the surface layer but with a larger amplitude of salinity fluctuations and a much smaller amplitude of temperature. Characteristic loops on T,S trajectories arising from relative phase shifts between seasonal cycles of temperature and salinity are related to different ratios of contributions of heat, water balance and intensity of vertical mixing of waters.

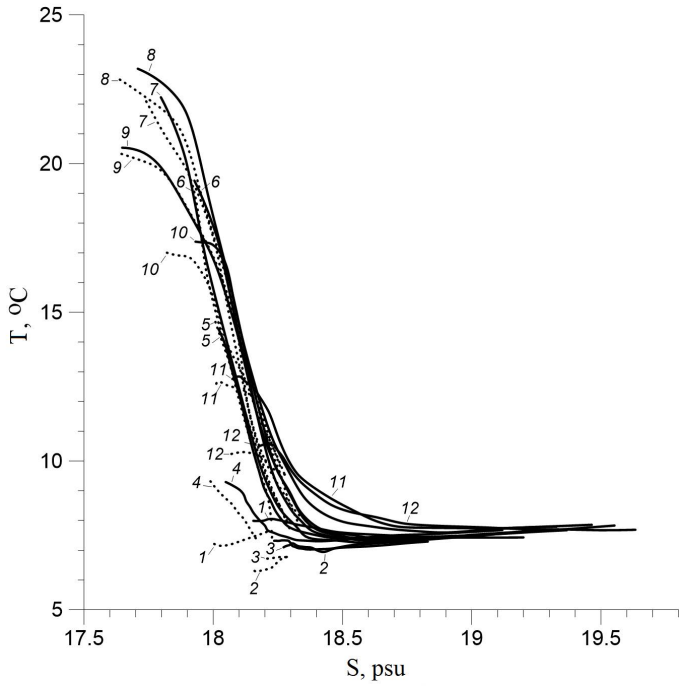

Fig. 14. Climatic monthly T,S curves in the Western Crimea shelf. Dotted lines denote values in the coastal zone (depth < 50 m), solid lines are those in the outer shelf. Digits stand for calendar month numbers

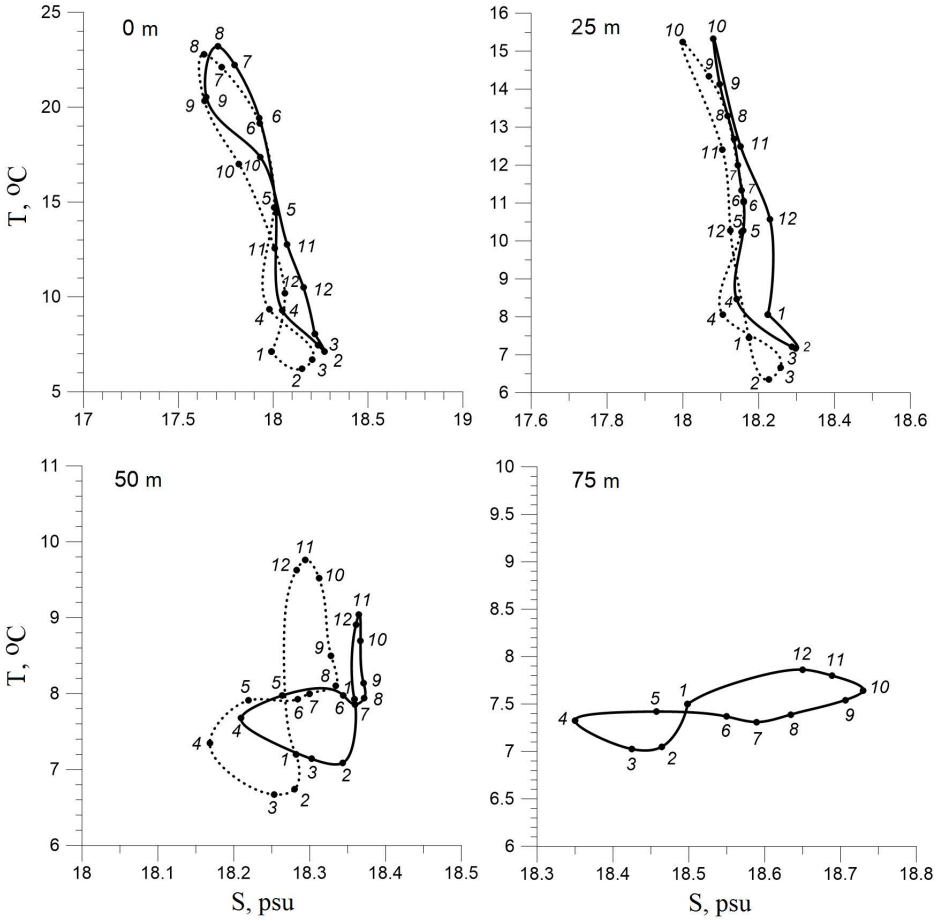

Fig. 15. Climatic seasonal course of T,S indices in the Western Crimea shelf for various depths. Dotted lines denote values in the coastal zone (depth < 50 m), solid lines are those in the outer shelf. Digits stand for calendar month numbers

Conclusion

On the basis of oceanographic observations for 1950–2023, climatic monthly values of temperature and salinity were calculated at the grid 10′ × 15′ and the seasonal variability of the thermohaline structure of the Western Crimean shelf waters was analysed.

In the cold season, the regional spatial thermal structure of the area has a pronounced zonal distribution with cold northern and warm southern parts. During the spring–summer period, the relative location of warm/cold zones changes to the meridional one. The CIL near the Western Crimea coast is formed in winter

on the northwestern shelf. In summer, when the general water circulation weakens, the CIL waters can also penetrate to the study area from the deep sea.

The regional haline structure was characterized by a saltier tongue spreading from the open sea and separating brackish waters of the north-western shelf and coastal waters. In the seasonal course of salinity on the Western Crimea shelf, in contrast to its seasonal course in other areas of the Black Sea, the minimum of salinity in the surface layer was observed in early autumn, which is associated with regional water circulation.

Over the greater part of the year, the coastal zone is colder and less saline than the outer shelf part. The surface layer in the coastal zone under intensive heating and weak winds is warmer than in the outer part of the shelf in April and May and below the seasonal thermocline in the summer–autumn period due to less heat exchange with the CIL. Due to frequent upwelling events in summer, salinity in the subsurface layers of the coastal zone from May to September becomes higher than in the outer shelf part.

In general, in terms of the thermohaline water structure, the Western Crimea shelf is an intermediate zone between the north-western shelf and the deep part of the Black Sea, the water exchange with which depends of the intensity of the Rim Current and the Sevastopol anticyclonic eddy. Regional water masses or sub-types of main Black Sea water masses were not identified in the study area.

References

1. Simonov, A.I. and Altman, E.N., eds., 1991. [*Hydrometeorology and Hydrochemistry of Seas of the USSR. Vol. 4. The Black Sea. Iss. 1. Hydrometeorological Conditions*]. Saint Petersburg: Gidrometeoizdat, 429 p. (in Russian).
2. Blatov, A.S. and Ivanov, V.A., 1992. [*Hydrology and Hydrodynamics of the Black Sea Shelf Zone (on the Example of the South Coast of Crimea*]. Kiev: Naukova Dumka, 244 p. (in Russian).
3. Ivanov, V.A. and Belokopytov, V.N., 2013. *Oceanography of the Black Sea*. Sevastopol: ECOSI-Gidrofizika, 210 p.
4. Ilyin, Yu.P., Repetin, L.N., Belokopytov, V.N., Goryachkin, Yu.N., Diakov, N.N., Kubryakov, A.A. and Stanichny, S.V., 2012. [*Hydrometeorological Conditions of the Ukrainian Seas. Vol. 2. The Black Sea*]. Sevastopol: ECOSI-GIdrofizika, 421 p. (in Russian).
5. Il'in, Yu.P., 1995. Anticyclonic Eddies near the Continental Slope Edge of the North-Western Black Sea: The Formation of Surface Imagery and Satellite IR Observations in Spring Summer Time. In: V. N. Eremeev, ed., 1995. *Investigations of the Shelf Zone of the Azov–Black Sea Basin*. Sevastopol: MGI NAN Ukrainy, pp. 22–30 (in Russian).
6. Il'in, Yu.P. and Belokopytov, V.N., 2005. Seasonal and Interannual Variability of Cold Intermediate Layer Parameters in the Sevastopol Anticyclone Nearby. *Ecological Safety of Coastal and Shelf Zones and Comprehensive Use of Shelf Resources*, 12, pp. 29–41 (in Russian).
7. Belokopytov, V.N., 2019. Seasonal Variability of Vertical Thermohaline Stratification on the Black Sea Shelf of Crimea. *Ecological Safety of Coastal and Shelf Zones of Sea*, (3), pp. 19–24 (in Russian).
8. Lomakin, P.D. and Chepyzhenko, A.I., 2022. The Structure of Fields of Oceanological Quantities in the Upwelling Zone at the Herakleian Peninsula (Crimea) in August 2019. *Ecological Safety of Coastal and Shelf Zones of Sea*, (1), pp. 31–41. https://doi.org/10.22449/2413-5577-2022-1-31-41

9. Lomakin, P.D., Chepyzhenko, A.I. and Chepyzhenko, A.A., 2022. Oceanological Values Fields Structure Around the Northern Coast of Sevastopol Seaside (the Black Sea) in February 2020. *Proceedings of the T.I.Vyazemsky Karadag Scientific Station – Nature Reserve of the Russian Academy of Sciences*. (1), pp. 3–10. https://doi.org/10.21072/eco.2022.21.01 (in Russian).
10. Ryabushko, V.I., Shchurov, S.V., Kovrigina, N.P., Lisitskaya, E.V. and Pospelova, N.V., 2020. Comprehensive Research of the Environmental Status of Coastal Waters of Sevastopol (Western Crimea, Black Sea). *Ecological Safety of Coastal and Shelf Zones of Sea*, (1), pp. 104–119. https://doi.org/10.22449/2413-5577-2020-1-104-119 (in Russian).
11. Aleskerova, A.A., Kubryakov, A.A., Goryachkin, Yu.N., Stanichny, S.V. and Garmashov, A.V., 2019. Distribution of Suspended Matter Off the Western Coast of the Crimea Under Impact of the Strong Winds of Various Directions. *Issledovanie Zemli iz Kosmosa*, (2), pp. 74–88 https://doi.org/10.31857/S0205-96142019274-88 (in Russian).
12. Belokopytov, V.N., Lomakin, P.D., Subbotin, A.A. and Shchurov, S.V., 2002. Background Characteristic and Seasonal Variability of Vertical Stratification of Thermohaline Field near Sevastopol Coast. *Ecological Safety of Coastal and Shelf Zones and Comprehensive Use of Shelf Resources*, 1, pp. 22–28 (in Russian).
13. Tolmazin, D., 1985. Changing Coastal Oceanography of the Black Sea, I, Northwestern Shelf. *Progress in Oceanography*, 15(4), pp. 217–276. https://doi.org/10.1016/0079-6611(85)90039-4
14. Eremeev, V.N., Latun, V.S. and Sovga, E.E., 2001. Influence of Anthropogenic Pollutants and ways of their Transport upon the Ecological Situation in the Northwestern Region of the Black Sea. *Morskoy Gidrofizicheskiy Zhurnal*, (5), pp. 41–55 (in Russian).
15. Grigor'ev, A.V., Ivanov, V.A., Kubryakov, A.I. and Shapiro, N.B., 2001. Anticyclone Eddy of a Ring Type in the Shelf-Slope Zone of the Northwest Part of the Black Sea. *Ecological Safety of Coastal and Shelf Zones and Comprehensive Use of Shelf Resources*, 3, pp. 57–61 (in Russian).
16. Korotaev, G., Oguz, T., Nikiforov, A. and Koblinsky, C., 2003. Seasonal, Interannual, and Mesoscale Variability of the Black Sea Upper Layer Circulation Derived from Altimeter Data. *Journal of Geophysical Research: Oceans*, 108(C4), 3122. https://doi.org/10.1029/2002JC001508
17. Morozov, A.N. and Lemeshko, E.M., 2005. Application Self Contained ADCP to Carry Out Measurements from the Ship Board: Methodical Problems and Physical Results. *Ecological Safety of Coastal and Shelf Zones and Comprehensive Use of Shelf Resources*, (13), pp. 425–432 (in Russian).
18. Poulain, P.-M., Barbanti, R., Motyzhev, S. and Zatsepin, A., 2005. Statistical Description of the Black Sea Near-Surface Circulation Using Drifters in 1999–2003. *Deep-Sea Research I: Oceanographic Research Papers*, 52(12), pp. 2250–2274. https://doi.org/10.1016/j.dsr.2005.08.007
19. Lemeshko, E.M., Morozov, A.N., Stanichnyi, S.V., Mee, L.D. and Shapiro, G.I., 2008. Vertical Structure of the Field of Current Velocities in the Northwest Part of the Black Sea Based on the LADCP Data for May 2004. *Physical Oceanography*, 18(6), pp. 319–331. https://doi.org/10.1007/s11110-009-9029-7
20. Goryachkin, Yu.N., 2008. Near-Bottom Currents in Kalamitskiy Bay. *Ecological Safety of Coastal and Shelf Zones and Comprehensive Use of Shelf Resources*, 17, pp. 258–264 (in Russian).
21. Belokopytov, V.N. and Nikol'sky, N.V., 2015. Stationary Anticyclonic Eddies near the South and West Coasts of Crimea. *Ecological Safety of Coastal and Shelf Zones of Sea*, (1), pp. 47–53 (in Russian).

22. Belokopytov, V.N., 2018. Retrospective Analysis of the Black Sea Thermohaline Fields on the Basis of Empirical Orthogonal Functions. *Physical Oceanography*, 25(5), pp. 380–389. https://doi.org/10.22449/1573-160X-2018-5-380-389

Submitted 26.08.2024; accepted after review 19.09.2024;
revised 25.03.2025; published 30.06.2025

About the authors:

Oksana A. Lukashova, Senior Research Engineer, Marine Hydrophysical Institute of RAS (2 Kapitanskaya St., Sevastopol, 299011, Russian Federation), *luk_ok@mail.ru*

Vladimir N. Belokopytov, Head of Oceanography Department, Marine Hydrophysical Institute of RAS (2 Kapitanskaya St., Sevastopol, 299011, Russian Federation), DSc (Geogr.), **ORCID ID: 0000-0003-4699-9588, ResearcherID: ABA-1230-2020, Scopus Author ID: 6602381894**, *belokopytov.vn@mhi-ras.ru, v.belokopytov@gmail.com*

Contribution of the authors:

Oksana A. Lukashova – literature review, calculations, preparation of graphical materials, analysis and interpretation of the results

Vladimir N. Belokopytov – study tasks statement, formation of the article structure, analysis and interpretation of the results

All the authors have read and approved the final manuscript.

ISSN 2413-5577, Ecological Safety of Coastal and Shelf Zones of Sea, 2025, No. 2, pp. 53–66.

Original paper

Estimation of the Characteristics of the Wind Field Seasonal Variability Near the Southern Coast of Crimea from Measurements with High Temporal Discreteness

A. S. Kuznetsov *, A. V. Garmashov

Marine Hydrophysical Institute of RAS, Sevastopol, Russian Federation
* *e-mail: kuznetsov_as@mhi-ras.ru*

Abstract
The study is aimed to identify the average for the 12-year monitoring period characteristics of the wind field seasonal variability from measurements with high temporal discreteness. This increased the accuracy of wind characteristic meters during synchronous studies of near-water wind and coastal current variations near the Southern Coast of Crimea. The mean annual characteristics of the coastal wind in the near-water layer of the atmosphere and their seasonal variability were identified by analysing the materials of the database of *in situ* measurements made in 2012–2023 during a complex experiment from the stationary oceanographic platform offshore at Cape Kikineiz. The selected wind characteristics near the coast were compared with the known climate wind characteristics in the region. In the seasonal range of spectral characteristics variability, wind fluctuations at periods of seasonal harmonics I–IV and VI were identified. The energy peak of fluctuations at seasonal harmonic VI was statistically significant both in the wind spectra and coastal current. In the other parts of the spectra, significant differences in the energy distributions of seasonal atmospheric and hydrospheric variations were obvious. Synchronous time series of vector characteristics of coastal wind and current variability were processed using identical information technology. In the intra-annual range of wind variability, we revealed the contribution of the monsoon component as well as seasonal fluctuations of the coastal wind directed along the mountain ridge slope. The range of variability of the studied wind characteristics at sea near Cape Kikineiz was obviously consistent with the characteristics of the regional wind field on land, identified at meteorological stations of the Southern Coast of Crimea. The presented results are necessary for comprehensive studies of the interannual variability of the regional wind field in order to assess statistical relationships with certain variability of the coastal current.

Keywords: *in situ* measurements, wind field, seasonal variations, energy spectrum, Southern Coast of Crimea, Black Sea

Acknowledgments: The work was performed under state assignment of MHI RAS on topic FNNN-2024-0016 “Studies of spatial and temporal variability of oceanological processes in the coastal, near-shore and shelf zones of the Black Sea influenced by natural and

anthropogenic factors on the basis of in situ measurements and numerical modelling" and FNNN-2024-0014 "Fundamental studies of interaction processes in the sea–air system that form the physical state variability of the marine environment at various spatial and temporal scales".

For citation: Kuznetsov, A.S. and Garmashov, A.V., 2025. Estimation of the Characteristics of the Wind Field Seasonal Variability Near the Southern Coast of Crimea from Measurements with High Temporal Discreteness. *Ecological Safety of Coastal and Shelf Zones of Sea*, (2), pp. 53–66.

Оценка характеристик сезонной изменчивости поля ветра у Южного берега Крыма по данным измерений с высокой временной дискретностью

А. С. Кузнецов *, А. В. Гармашов

Морской гидрофизический институт РАН, Севастополь, Россия
** e-mail: kuznetsov_as@mhi-ras.ru*

Аннотация

Целью исследования является выделение средних за 12-летний период мониторинга характеристик сезонной изменчивости поля ветра по данным измерений с высокой временной дискретностью, что обеспечило повышение точности измерителей характеристик ветра при синхронных исследованиях колебаний приводного ветра и прибрежного течения у Южного берега Крыма. Среднемноголетние характеристики прибрежного ветра в приводном слое атмосферы и их сезонная изменчивость выделены путем анализа материалов базы данных контактных измерений, выполненных в 2012–2023 гг. при проведении комплексного эксперимента со стационарной океанографической платформы в море у м. Кикинеиз. Выделенные характеристики ветра у побережья сопоставлены с известными климатическими характеристиками ветра в регионе. В сезонном диапазоне изменчивости спектральных характеристик выделены колебания ветра на периодах I–IV и VI сезонных гармоник. Энергетический пик колебаний на VI сезонной гармонике статистически достоверно выражен одновременно в спектрах ветра и прибрежного течения. На других участках спектров очевидны существенные различия в распределении энергии сезонных атмосферных и гидросферных колебаний. Синхронные временны́е ряды векторных характеристик изменчивости прибрежного ветра и течения обработаны в рамках идентичной информационной технологии. Во внутригодовом диапазоне изменчивости ветра выделен вклад муссонной составляющей, а также сезонные колебания прибрежного ветра, направленные вдоль склона горного хребта. Очевидно соответствие диапазона изменчивости исследуемых характеристик ветра в море у м. Кикинеиз и характеристик регионального поля ветра на суше, выделенных на метеостанциях Южного берега Крыма. Представленные результаты необходимы для комплексных исследований межгодовой изменчивости регионального поля ветра в целях оценки статистических связей с определенной изменчивостью прибрежного течения.

Ключевые слова: контактные измерения, поле ветра, сезонные колебания, энергетический спектр, Южный берег Крыма, Черное море

Благодарности: работа выполнена в рамках государственного задания ФГБУН ФИЦ МГИ по темам FNNN-2024-0016 «Исследование пространственно-временной изменчивости океанологических процессов в береговой, прибрежной и шельфовой зонах Черного моря под воздействием природных и антропогенных факторов на основе контактных измерений и математического моделирования» и FNNN-2024-0014 «Фундаментальные исследования процессов взаимодействия в системе океан-атмосфера, формирующих изменчивость физического состояния морской среды на различных пространственно-временных масштабах».

Для цитирования: *Кузнецов А. С., Гармашов А. В.* Оценка характеристик сезонной изменчивости поля ветра у Южного берега Крыма по данным измерений с высокой временной дискретностью // Экологическая безопасность прибрежной и шельфовой зон моря. 2025. № 2. С. 53–66. EDN EYFFWQ.

Introduction

Experimental studies of wind variability in the near-water layer of the atmosphere and its influence on the water circulation of the coastal water area near Cape Kikineiz on the Southern Coast of Crimea (SCC) were initiated in 1929 [1–5] and are ongoing to the present day [6–8]. Concurrently, a sophisticated array of contributions from multi-scale variability to the configuration of the coastal wind field is examined. This involves the conversion of regional baric conditions by the orography of the adjacent mountain massif, the monsoon effect and local winds of thermal origin.

Earlier, based on the analysis of experimental data, the contribution of breeze circulation and slope winds was identified and quantitative estimations of the interseasonal differences in the spectral characteristics of the wind daily variability in the coastal zone of the SCC on land and at sea were presented [6, 7]. The variability of wind conditions near the coast causes rearrangement of the structure of the coastal current [1, 4]. In case of obvious dominance of the contribution of intensive hydrodynamic disturbances formed near the coast, the phenomenon of bimodal modulation of the longshore water flow direction appears in the quasi-stationary flow near the SCC [1, 5], the genesis of which was studied in [7, 8]. The present study investigates a set of multi-scale coastal wind fluctuations [7], which form the wind field in the near-water layer of the atmosphere, on the basis of experimental data.

The aim of the present study is to investigate the 12-year average characteristics of seasonal variability of the wind field in the coastal zone near the SCC as well as to identify regularities and structural features in the energy spectra of seasonal fluctuations of the near-water wind and coastal current near Cape Kikineiz in order to estimate statistical relationships.

Materials and methods of study

In situ measurements of wind field characteristics were carried out on the stationary oceanographic platform of the Black Sea Hydrophysical Subsatellite Polygon (BSHSP) of Marine Hydrophysical Institute (MHI) of RAS in Blue Bay near Cape Kikineiz at a distance of ~500 m from the shore [6, 7]. The region-adapted system of MHI BSHSP hydrometeorological monitoring includes a hardware complex of every-second measurements of wind field characteristics in the sea

by three sets of meters simultaneously installed compactly on the mast of the oceanographic platform at the height of the place 18 m above sea level. Two sets of anemorumbometers M-63 as part of meteorological complex MHI-6503 [9] and a set of wind speed and direction modulus meters SWS as part of the CSCD complex [10] were used. The measurement results were recorded on autonomous data storage devices and in the operational mode. They were also transmitted via radio communication channel from the platform to the onshore working station. The velocity values were adjusted to a standard observation height of 10 m [11] for the conditions of a logarithmic sublayer of the near-water wind. According to the results of [12], the values of the sea surface roughness parameter near the oceanographic platform were determined within the range of 10^{-4}–10^{-3} m. Wind speed correction was performed at an average value of the sea surface roughness parameter equal to 5–10^{-4} m.

Based on the results of instrumental monitoring, annually updated database [1)] of wind characteristics in the near-water layer of the atmosphere near Cape Kikineiz, SCC, was formed. The initial database array generated for the period 2012–2023 contains 105,192 hourly average wind vector values, where each hourly average value is calculated by vector averaging of the hourly wind vector component values. Quality control of wind characteristics measurements is carried out regularly by comparing a set of statistical and spectral indices of certified primary measuring transducers that have passed metrological certification in accordance with the established procedure, which, with a certain redundancy of information, made it possible to exclude the contribution of faulty values and significant systematic errors of measurements from temporal realizations. From the initial array, 4 383 pairs of daily average wind vector components were formed by vector averaging with random error of the velocity modulus measurements not exceeding 0.1 m/s and wind direction 3° [7].

Arrays of vector data of wind characteristics measurements are processed according to the technique developed on the basis of standard methods of mathematical statistics, spectral analysis and digital filtering including centering of vector series. The centering algorithm contains the procedure of vector subtraction of the average vector components from the current values of the vector series components. The spectral analysis of wind circulation variability was performed within the framework of the filter estimation of the full energy spectrum of fluctuations through periodogram smoothing based on the software developed by MHI [6–8]. To minimize the contribution of distortions arising in calculations of the spectral characteristics of the wind field seasonal variability, the contribution of intense fluctuations with periods from one day to three weeks was excluded in the initial vector data array by digital filtering. The structure of wind fluctuations in the specified range of variability was studied in [7].

[1)] Kuznetsov, A.S., Garmashov, A.V. and Zima, V.V., 2023. *Database for Wind Characteristics Monitoring for the Black Sea Coastal Ecotone at Cape Kikineiz of the Southern Coast of Crimea for 2013–2022* [Database]. Moscow. State Registration No. 2023622482 (in Russian).

The analysis of the structure of multi-scale variability of the wind field characteristics presented in [7] made it possible to optimize the order of application of the processing methodology in the formation of the corresponding arrays for the study of the wind field seasonal variability. The monthly averages of the wind field characteristics were used to estimate the 12-year average characteristics of the wind field, from which the spectral characteristics of the seasonal harmonics of wind fluctuations were also calculated [2)].

The regularities of spatial and temporal variability of wind conditions are investigated on the basis of special processing of the generated data sets for the specified 12-year measurement period. For this purpose, the procedure of selective data filtering is applied to the initial time series. The set of parameters of the data sequential filtering (smoothing) is determined by the choice of the range of the wind field variability under study. After selecting the range of variability under study and its corresponding filtering parameters, the energy spectrum and empirical probability density functions of the wind direction distribution calculated after the data filtering procedure are further calculated. Thus, in [7], the daily range of wind variability was studied and its corresponding filtering parameters were selected. After exclusion of intense wind fluctuations with a period of ~1 day from the initial energy spectrum, the direction of ~355° actually disappears in the initial empirical probability density function of wind direction distribution in the total wind contribution. By excluding the contribution of daily wind fluctuations from the time series, the general direction of local winds with a daily fluctuation period was determined. Other ranges of coastal wind variability including the seasonal range are sequentially investigated in the same way. The sequential filtering procedure used earlier in [13] for investigations of large-scale characteristics of the current field is applied in this processing.

Results and discussion

Within the framework of using a non-standard technique for processing vector-averaged series of wind variability, the following results of investigations of the average wind characteristics for a 12-year period of measurements, spectral characteristics of its seasonal variability as well as spatial and temporal structure of fluctuations of the near-water wind field were obtained.

Average for the 12-year period characteristics of wind. The average characteristics of the north-northeasterly wind (~25°) at a speed of ~1.5 m/s are highlighted for the 2012–2023 measurement period and coincide with the estimates obtained earlier in [7]. The indicated average wind characteristics are compared with the known regime (climatic) wind characteristics in the region. It is stated in [3] that northeasterly winds prevail at Cape Kikineiz during the cold period of the year. The characteristics of large-scale variability of the wind field were

[2)] Monin, A.S., Kamenkovich, V.M. and Kort, V.G., 1977. *Variability of the Ocean*. London: John Wiley & Sons Ltd., 241 p.

previously determined by analyzing the materials of standard meteorological observations, archival data and results of expedition studies. The identified estimates of the indicated mean wind characteristics agree with the values of the direction of the climatic wind field in the Black Sea region presented in work [3)] where the prevalence of the northern quarter winds in the SCC during the entire annual cycle is noted. Characteristics of the typical near-water wind field near the northern Black Sea coast obtained by analyzing synoptic maps [4)] as well as results of previously published generalizations [5)-7)] are consistent with the climatic characteristics of the SCC wind field presented in work [3)]. The results obtained by the non-standard methodology differ from the results obtained by the standard approach traditionally used in meteorology. Thus, if the direction of the average for 12-year period of wind measurements corresponds to the courses of the highest climatic wind frequency, the wind speeds are significantly lower than the usual standard estimations for the region. It is well-known that northerly winds make a particularly significant contribution to the climate in the highlands adjacent to the coast, including Babugan-Yayla and Ai-Petri, during the cold season [5)]. According to meteorological observations in Balaklava, Yalta, Gurzuf, Alushta and Sudak, winds of northern direction prevail clearly on the SCC at this time [5)]. During the cold period of the year, the contribution of local winds to the total coastal wind field decreases, which helps to refine the characteristics of the regional wind field. The results of modern calculations of climatic and seasonal characteristics of wind field variability in the Black Sea region obtained on the basis of numerical reanalyses of atmospheric circulation [14–16] demonstrate that winds of northern directions are pronounced near the SCC during the entire annual cycle. The results of multi-scale modelling studies of circulation in the atmospheric boundary layer, including local winds, mesoscale and synoptic processes [14–18], were used earlier for comparison in [6, 7].

Spectral characteristics of wind seasonal variability. In this study, the characteristics of seasonal wind variability are investigated based on the results of statistical and spectral analyses of field data obtained from instrumental monitoring of wind field variability for 2012–2023.

[3)] Prikhotko, G.F., Tkachenko, A.V. and Babichenko, V.N., 1967. [*Climate of Ukraine*]. Leningrad: Gidrometeoizdat, 413 p. (in Russian).

[4)] Chernyakova, A.P., 1965. Typical Wind Fields of the Black Sea. In: MGMO ChAM, 1965. [*Collection of Works of the Basin Hydrometeorological Observatory of the Black and Azov Seas*]. Leningrad: Gidrometeoizdat. Iss. 3, pp. 78–121 (in Russian).

[5)] Penuygalov, A.V., 1930. [*Climate of Crimea: A Record of Climate Zoning*]. Simferopol: Krymgosizdat, 178 p. Materials on Water Sector of Crimea. Iss. 6. (in Russian).

[6)] Zats, V.I., Lukianenko, O.Ya. and Yatsevich, G.V., 1966. [*Hydrometeorological Regime of the Southern Coast of Crimea*]. Leningrad: Gidrometeoizdat, 120 p. (in Russian).

[7)] Logvinova, K.T. and Barabash, M.B., eds., 1982. [*Climate and Dangerous Hydrometeorological Events of Crimea*]. Leningrad: Gidrometeoizdat, 318 p. (in Russian).

As is known, the variability of atmospheric circulation in the Black Sea region is partly connected with the peculiarities of the mechanism of intra-annual development of the monsoon circulation. During the cold period of the year (November–April), local wind speeds near the SCC decrease significantly in the diurnal range of variability compared to the period of intensive breeze circulation (May–October) but at the same time, the intensity of wind fluctuations increases significantly in the range of periods from several days to three weeks [7]. The intensive contribution of multi-scale atmospheric fluctuations distorts constantly the characteristics of the regional wind field during the entire annual cycle. To obtain reliable estimates of the seasonal wind variability, a set of vector-averaged time series was formed, based on which the contribution of intense multi-scale winds was consistently excluded.

The full energy spectrum of seasonal wind fluctuations was calculated from the data of the monthly average series. In the energy density distribution spectrum, reliable energy maxima of wind fluctuations at the annual period and seasonal harmonics are highlighted. It is important to note that, at a certain stage of the spectral processing, the total energy contribution of intense wind fluctuations at periods III and IV of seasonal harmonics is concentrated in the form of a single spectral peak at a period of ~100 days, which is shown in Fig. 1, *a* with a red line.

During the integrated research on the MHI BSHSP stationary oceanographic platform, instrumental measurements of the coastal current characteristics from the surface to the bottom layer are carried out along with monitoring of the wind field characteristics [7, 8]. To compare, Fig. 1, *b* shows average annual full energy spectrum of seasonal fluctuations of surface flow at the hydrological horizon of 5 m. In the current spectrum, reliable energy maxima of fluctuations at the annual (I) period, seasonal harmonics III and VI are highlighted. When comparing synchronously measured characteristics of seasonal wind and current variations, it was found that the spectral peak of variations at seasonal harmonic VI at the period of ~64 days is statistically reliably expressed in the spectrum of wind and coastal current. Other spectral sections revealed structural differences in the energy distribution of atmospheric and hydrospheric fluctuations. The spectral peak of the current variations near seasonal harmonic II is expressed weakly (Fig. 1, *a*) in contrast to the corresponding peak of intense wind fluctuations (Fig. 1, *b*). The energy peak of surface current variations near seasonal harmonic II is weakly pronounced and is highlighted in the area of the fluctuation energy decline with the main annual harmonic. The results of the spectral analysis of the seasonal variability of wind and current make it possible to further estimate statistical relationships and patterns of energy interaction between wind and current in the coastal sea zone.

Regularities of intra-annual variability of the 12-year average wind characteristic. The regularities of variability of the indicated wind characteristic were identified by processing monthly averages of wind field components averaged over a 12-year period of measurements. To minimize the contribution of intensive seasonal fluctuations in the range of periods of seasonal harmonics III–VI, the procedure of vector averaging (smoothing) of initial implementation was performed and

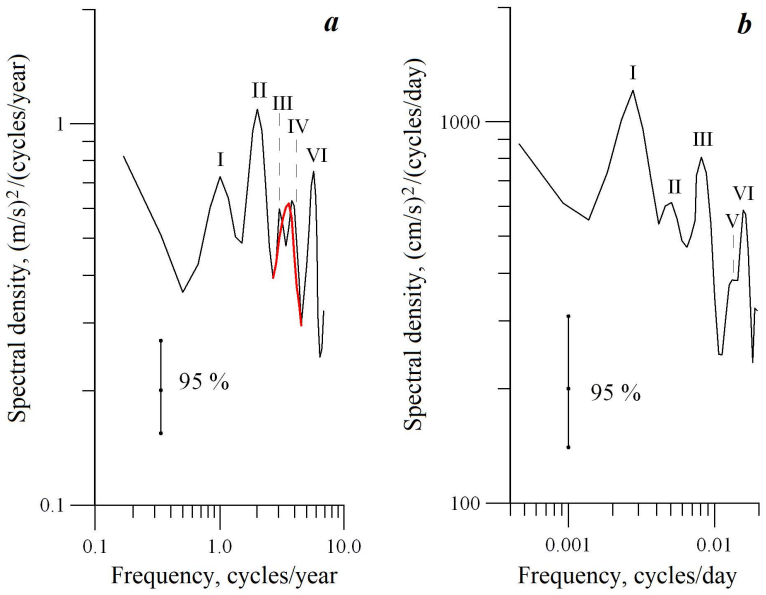

Fig. 1. Average for the 12-year measurement period full energy spectra of seasonal variability of: *a* – wind at the near-water layer of atmosphere with an additional fragment of spectral peak (red line); *b* – current in the near-surface sea layer at corresponding 95% confidence intervals (I–VI are the numbers of seasonal harmonics of fluctuations)

then procedure for centering a smoothed annual average series of monthly wind variability data. The results of processing are presented below. In the process, the monthly mean values of the wind speed and wind direction modulus for each year were sequentially vector-averaged monthly over the entire 12-year measurement cycle. Fig. 2, *a* shows the initial time series of monthly mean values of the wind vector formed in such a way, where maximum values of the monthly average wind speed modulus ~2.5 m/s are identified in October, and minimum values ~0.8 m/s – in June. As it follows from Fig. 2, *a*, the intra-annual variability of mean wind direction is dominated by northerly winds.

Fig. 2, *b* shows seasonal variation of the wind speed and direction modulus when excluding from the initial realization the contribution of intensive wind fluctuations in the range of periods of seasonal harmonics III–VI. The variability of the wind speed modulus time series (Fig. 2, *b*) shows the annual period of fluctuation, where the 12-year average value of the wind speed modulus, equal to ~1.5 m/s, varies within ±0.4 m/s, maximum values of wind speed modulus are

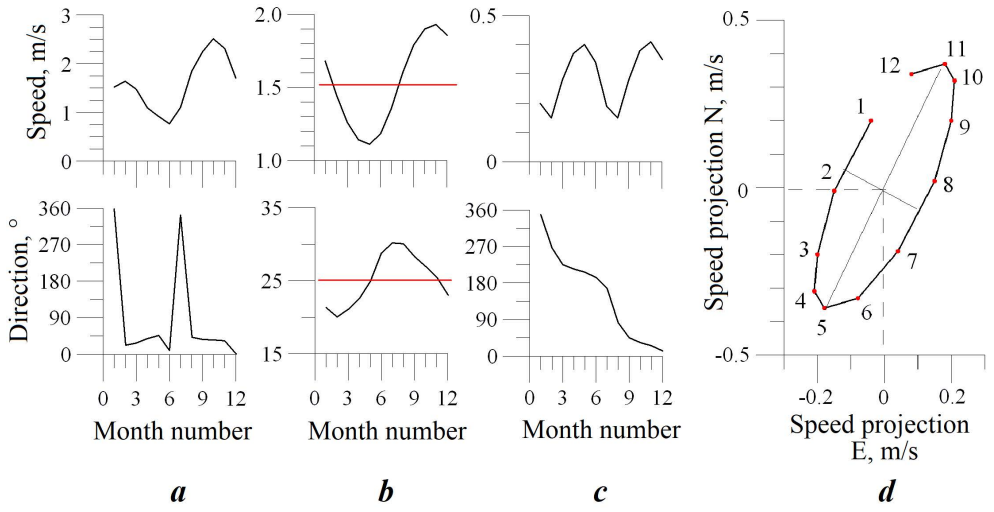

Fig. 2. Average for the 12-year measurement period time sequences of intra-annual variability of monthly mean wind vector components: *a* – original series; *b* – smoothed series (red lines are vector-averaged for 12 years annual values of corresponding vector components); *c* – centered series (seasonal variability of wind speed for each time series – *top* and directions – *bottom*); *d* – hodograph of seasonal variability of centered wind vector (the numerals denote month number)

identified in November, minimum ones – in May. The value of the direction (~25°) of the north-northeasterly wind varies within ±5°. The maximum values of deviations of the wind direction to the east are identified in July – August and to the west – in January – February.

Fig. 2, *c* demonstrates specified time series of variability of mean monthly variations of the modulus of speed and direction of the centered wind vector. In the time series of variability of centered values of the wind speed modulus (Fig. 2, *c*, *top*), the contribution of seasonal harmonic II of the fluctuation is expressed, with the maximum values of the speed modulus of the centered wind vector identified in May and November and the minimum values identified in February and August. The time series of variability of the centered wind vector direction (Fig. 2, *c*, *bottom*) shows the annual cycle of the vector reversal at 360°. The regularities of monthly variability of the centered wind vector are clearly demonstrated by the hodograph plotted in the right-hand orthogonal coordinate system oriented to the north (Fig. 2, *d*). The hodograph is shaped like an ellipse, with its major axis aligned with the mean annual wind direction, and a left-handed reversal of the wind speed modulus during the annual cycle. The maximum value of the modulus of the centered wind vector velocity corresponds to point *11* (November) and the minimum to point *5* (May). In both cases, the north-northeasterly wind direction dominates.

The relevance and physical meaning of *in situ* studies of energy-carrying frequencies of seasonal fluctuations are defined in [19], where it is demonstrated, on the basis of long-term remote satellite measurements of the Black Sea level variability, that the main spectral maxima of sea level fluctuations at periods of seasonal harmonics I and II are caused by corresponding seasonal changes of wind characteristics in the region. The multi-year array of experimental data obtained during the contact monitoring of wind characteristics makes it possible to continue purposefully statistical studies of multi-year spatial and temporal patterns of interannual wind variability in the coastal area of the sea near the SCC.

Regularities of spatial and temporal orientation of seasonal coastal wind fluctuations near the SCC. The total wind field in the region is formed by the interaction of the regional wind with local and local winds. The temporal scales of intense variability of the total wind field in the near-water layer of the atmosphere near Cape Kikineiz are known from the results of spectral analyses of long-term meteorological observations from the stationary oceanographic platform at the Black Sea polygon [6, 7].

The composition of the empirical probability density function of the distribution of coastal wind directions (hereinafter referred to as the empirical function) calculated in ±5° angular segments on the basis of 105,192 hourly averaged data was reliably investigated on the basis of a time series of data on the variability of wind field directions near the coast [1)] (Fig. 3, *a*). In the original empirical function, the contribution of three main wind directions, east-northeasterly, west-southwesterly, and northerly, which have differences in their respective peak probability density values, is evident.

To eliminate distortions introduced by the quasi-stationary average over the 12-year measurement period of the north-northeasterly wind at a speed modulus of 1.5 m/s, the initial series was centered. Fig. 3, *b* shows the results of the centering procedure, where the probability density of the contribution of the winds of east-northeasterly (~75°) and west-southwesterly (~245°) directions has close peaks. Then, following the processing algorithm, the contribution of wind fluctuations at periods 1–3 days to the structure of the empirical function is investigated. Fig. 3, *c* demonstrates the results of this processing stage after digital filtering of the centered time series, during which the contribution of wind fluctuations at periods from 1 to 3 days was excluded. The probability density of the contribution of east-northeasterly and west-southwesterly winds has close peak values.

At the final stage of processing, after removing the contribution of intense wind fluctuations at periods from 4 to 28 days by digital filtering, the contribution of wind fluctuations only at periods of the specified seasonal harmonics is present in the time series. Fig. 3, *d* demonstrates the final empirical function calculated in this process where the value of the integral of the function in the 75 ± 90° range is ~49.6% and in the 245° ± 90° range, it is ~50.4%.

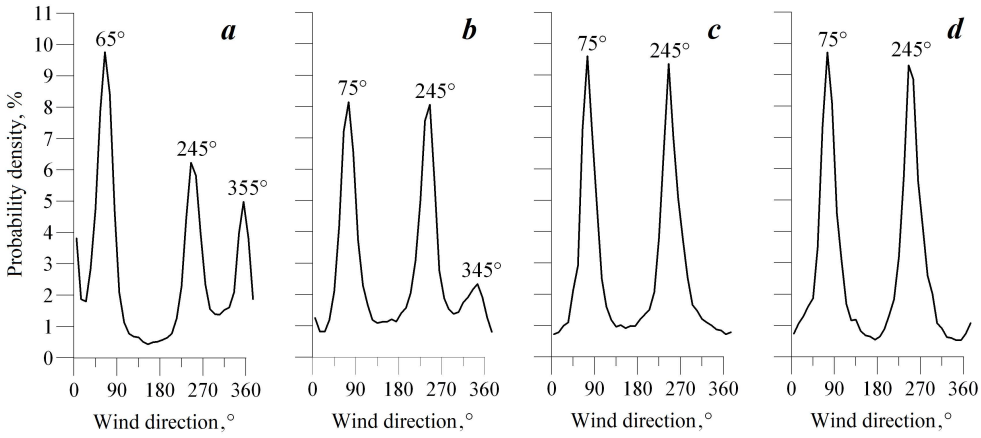

Fig. 3. Empirical probability density functions of the distribution of wind directions in the near-water atmosphere layer calculated for 2012–2023: *a* – from the initial data; *b* – from centered data; *c* – from centered data when excluding the contribution of fluctuations in the range of periods up to three days; *d* – from centered data on the fluctuations of seasonal harmonics

Based on the results of the presented processing, narrowly directed reciprocating wind fluctuations of east-northeasterly and west-southwesterly directions oriented along the southern slope of the Crimean Mountains ridge adjacent to the coast were identified.

It was determined that in the vicinity of Cape Kikineiz, the spatial and temporal configuration of longshore seasonal wind fluctuations was a permanent feature of the near-water layer of the atmosphere. A comparable configuration of longshore transport of air masses in the surface layer of the atmosphere on land was identified at the meteorological stations of the Southern Coast of Crimea and investigated in [6], in which discrepancies attributable to local features of the relief were documented.

Based on the results of the studies of the seasonal variability of the coastal wind near the SCC, it is possible to estimate the connection between the energy maxima of seasonal wind fluctuations and certain physical processes in the Black Sea region. A significant contribution is made by the seasonal variability of the regional wind field, which is related to seasonal changes in the large-scale atmospheric circulation in the European region and the peculiarities of the mechanism of intra-annual development of the monsoon circulation [4]. In [16], on the basis of numerical modelling, the influence of the Crimean Mountains on the wind regime of the region is noted and it is shown that under certain seasonal conditions, the formation of longshore wind is possible and a mesoscale zone of its speed perturbation is temporarily created. According to the presented empirical results of the research, the quasi-stationary longshore air flow exists permanently, varying in the ranges of mesoscale, synoptic and seasonal wind fluctuations. The exception is the range of daily wind fluctuations.

The results obtained are necessary for investigations of statistical relations of interannual variations of the Black Sea coastal current [20] with the corresponding wind fluctuations in the near-water atmospheric boundary layer.

Conclusion

The information technology for long-term complex studies of variability of wind conditions and water circulation in the sea near the coast with synchronous measurements of vector characteristics with high temporal discreteness was developed and applied. According to the results of analysis of data base materials of instrumental monitoring carried out in 2012–2023 in the sea near Cape Kikineiz, the regularities of seasonal variability of the coastal wind in the near-water layer of the atmosphere near the SCC were identified. The empirical regularities of seasonal fluctuations of the wind field highlighted in the present work permit us to draw the following conclusion. The totality of seasonal, synoptic and mesoscale fluctuations of the coastal wind in the near- water layer of the atmosphere has a pronounced orientation of the air flow along the southern slope of the Crimean Mountains ridge adjacent to the coast throughout the year. Intense local winds are oriented mainly along the normal to the mountain slope adjacent to the coast. The new results of studies of wind variability in the near-water layer of the atmosphere are of practical importance for further studies of the contribution of the coastal wind to the formation of the seasonal and interannual variability of the Black Sea coastal current variations. Such studies are necessary for the development and verification of model predictive systems of coastal water dynamics and ecological and economic monitoring of the coastal water area for sustainable social and economic development of the coastal region.

References

1. Ivanov, R.N. and Bogdanova, A.K., 1953. [On Marine Coastal Currents]. In: MHI, 1953. *Trudy MGI AN USSR* [*Proceedings of Marine Hydrophysical Institute, Academy of Sciences of USSR*]. Moscow: Publ. House of AS USSR. Vol. 3, pp. 43–68 (in Russian).
2. Ivanov, R.N., 1957. [Influence of the Coast on the Direction of Wind Surface Current]. In: MHI, 1957. *Trudy MGI AN USSR* [*Proceedings of Marine Hydrophysical Institute, Academy of Sciences of USSR*]. Moscow: Publ. House of AS USSR. Vol. 11, pp. 84–96 (in Russian).
3. Potapova, E.N. and Potapov, N.S., 1959. [Features of Circulation on the Southern Extremity of Crimea]. In: MHI, 1959. *Trudy MGI AN USSR* [*Proceedings of Marine Hydrophysical Institute, Academy of Sciences of USSR*]. Moscow: Publ. House of AS USSR. Vol. 16, pp. 29–43 (in Russian).
4. Koveshnikov, L.A., Ivanov, V.A., Boguslavsky, S.G., Kazakov, S.I. and Kaminsky, S.T., 2001. Problems of Heat and Dynamic Interaction in a Sea – Atmosphere – Land System of the Black Sea Region. *Ecological Safety of Coastal and Shelf Zones and Comprehensive Use of Shelf Resources*, 3, pp. 9–52 (in Russian).

5. Ivanov, V.A. and Belokopytov, V.N., 2013. *Oceanography of the Black Sea*. Sevastopol: EKOSI-Gidrofizika, 210 p.
6. Kuznetsov, A.S., 2023. Spectral Characteristics of Wind Variability in the Coastal Zone of the South Coast of Crimea 1997–2006. *Ecological Safety of Coastal and Shelf Zones of Sea*, (2), pp. 6–20.
7. Kuznetsov, A.S., 2024. Peculiarities of Interseasonal Variability of Alongshore Wind Circulation and Coastal Currents off the Southern Coast of Crimea. *Ecological Safety of Coastal and Shelf Zones of Sea*, (1), pp. 31–44.
8. Kuznetsov, A.S. and Ivashchenko, I.K., 2023. Features of Forming the Alongcoastal Circulation of the Coastal Ecotone Waters nearby the Southern Coast of Crimea. *Physical Oceanography*, 30(2), pp. 171–185.
9. Kuznetsov, A.S. and Zima, V.V., 2019. Development of Observing System of the Black Sea Hydrophysical Polygon in 2001–2015. *Ecological Safety of Coastal and Shelf Zones of Sea*, (4), pp. 62–72. https://doi.org/10.22449/2413-5577-2019-4-62-72 (in Russian).
10. Ivanov, V.A. and Dulov, V.A., eds., 2014. *Monitoring of the Coastal Zone in the Black Sea Experimental Sub-Satellite Testing Area*. Sevastopol: ECOSI-Gidrofizika, 526 p. (in Russian).
11. Thomas, B.R., Kent, E.C. and Swail, V.R., 2005. Methods to Homogenize Wind Speeds from Ships and Buoys. *International Journal of Climatology*, 25(7), pp. 979–995. https://doi.org/10.1002/joc.1176
12. Solov'ev, Y.P. and Ivanov, V.A., 2007. Preliminary Results of Measurements of Atmospheric Turbulence over the Sea. *Physical Oceanography*, 17(3), pp. 154–172. https://doi.org/10.1007/s11110-007-0013-9
13. Ozmidov, R.V., 1964. Some Data on Large-Scale Field Characteristics of Horizontal Velocity Components in the Ocean. *Izvestiya AN SSSR. Seriya Geofizicheskaya*, (11), pp. 1708–1719 (in Russian).
14. Efimov, V.V., Shokurov, M.V. and Barabanov, V.S., 2002. Physical Mechanisms of Wind Circulation Forcing over the Inland Seas. *Izvestiya Atmospheric and Oceanic Physics*, 38(2), pp. 217–227.
15. Efimov, V.V. and Anisimov, A.E., 2011. Climatic Parameters of Wind-Field Variability in the Black Sea Region: Numerical Reanalysis of Regional Atmospheric Circulation. *Izvestiya, Atmospheric and Oceanic Physics*, 47(3), pp. 350–361. https://doi.org/10.1134/S0001433811030030
16. Efimov, V.V. and Komarovskaya, O.I., 2019. Disturbances in the Wind Speed Fields due to the Crimean Mountains. *Physical Oceanography*, 26(2), pp. 123–134. https://doi.org/10.22449/1573-160X-2019-2-123-134
17. Efimov, V.V. and Barabanov, V.S., 2009. Breeze Circulation in the Black-Sea Region. *Physical Oceanography*, 19(5), pp. 289–300. https://doi.org/10.1007/s11110-010-9054-6
18. Efimov, V.V., Barabanov, V.S. and Iarovaya, D.A., 2014. [Mesoscale Processes in the Atmosphere of the Black Sea Region]. In: V. A. Ivanov and V. A. Dulov, eds., 2014. *Monitoring of the Coastal Zone in the Black Sea Experimental Sub-Satellite Testing Area*. Sevastopol: ECOSI-Gidrofizika, pp. 250–271 (in Russian).

19. Korotaev, G.K., Saenko, O.A. and Koblinsky, C.J., 2001. Satellite Altimetry Observations of the Black Sea Level. *Journal of Geophysical Research: Oceans*, 106(C1), pp. 917–933. https://doi.org/10.1029/2000JC900120

20. Kuznetsov, A.S. and Ivashchenko, I.K., 2025. Long-Term Average Annual Spectral Characteristics of the Coastal Current Long-Period Oscillations off the Southern Coast of Crimea. *Physical Oceanography*, 32(1), pp. 32–45.

Submitted 01.10.2024; accepted after review 12.12.2024;
revised 27.03.2025; published 30.06.2025

About the authors:

Alexander S. Kuznetsov, Leading Research Associate, Head of the Shelf Hydrophysics Department, Marine Hydrophysical Institute of RAS (2 Kapitanskaya St., Sevastopol, 299011, Russian Federation), PhD (Tech.), **ORCID ID: 0000-0002-5690-5349; Scopus Author ID: 57198997777**, *kuznetsov_as@mhi-ras.ru*

Anton V. Garmashov, Senior Research Associate, Marine Hydrophysical Institute of RAS (2 Kapitanskaya St., Sevastopol, 299011, Russian Federation), PhD (Geogr.), **Scopus Author ID: 54924806400, ORCID ID: 0000-0003-4412-2483**, *garmashov@mhi-ras.ru*

Contribution of the authors:

Alexander S. Kuznetsov – statement of the study aim and objectives, development of information technology, organisation of and participation in the experiment, processing and analysis of *in situ* data, discussion of the article materials and work results, preparation of the article text

Anton V. Garmashov – organisation of and participation in the experiment, processing and analysis of *in situ* data, discussion of the article materials and work results

All the authors have read and approved the final manuscript.

Original paper

Upwelling in the Black Sea Water Area near Cape Lukull Based on Numerical Modeling and Observational Data

P. D. Lomakin *, Yu. N. Ryabtsev, A. I. Chepyzhenko

Marine Hydrophysical Institute of RAS, Sevastopol, Russian Federation
* *e-mail: p_lomakin@mail.ru*

Abstract
Based on numerical modeling methods (a generalized three-dimensional barotropic linear model of Felsenbaum was used for the case of taking into account Rayleigh friction), the paper considers features of the structure of the current vectors field depending on wind conditions in an upwelling situation in the water area located along the northern coast of the Sevastopol seaside, between Capes Lukull and Tolsty. A two-layer transverse cell of water circulation, typical of upwelling, was identified. The currents were predominantly oriented downwind in the upper layer and in the opposite direction in the bottom layer. It is shown that in the analyzed water area upwelling was caused by northerly, north-easterly, easterly and south-easterly winds. Upwellings caused by the above winds differed in their location and area. Under a north-easterly wind, upwelling was most intense and widespread throughout the water area under consideration. Under a south-easterly wind, upwelling was formed in two small areas: in the bends of the coast, between Capes Margopulo and Lukull and north of Cape Tolsty. The modeling result was compared with data from expeditionary research. Their good agreement under a northerly wind was found.

Keywords: wind, currents, upwelling, numerical modeling, thermohaline structure, cape Lukull, Black Sea

Acknowledgements: The work was performed under state assignment of MHI RAS on topic FNNN-2024-0016 “Studies of spatial and temporal variability of oceanological processes in the coastal, near-shore and shelf zones of the Black Sea influenced by natural and anthropogenic factors on the basis of *in situ* measurements and numerical modelling”.

For citation: Lomakin, P.D., Ryabtsev, Yu.N. and Chepyzhenko, A.I., 2025. Upwelling in the Black Sea Water Area near Cape Lukull Based on Numerical Modeling and Observational Data. *Ecological Safety of Coastal and Shelf Zones of Sea*, (2), pp. 67–79.

Апвеллинг в акватории Черного моря у мыса Лукулл на основе численного моделирования и данных наблюдений

П. Д. Ломакин *, Ю. Н. Рябцев, А. И. Чепыженко

Морской гидрофизический институт РАН, Севастополь, Россия
** e-mail: p_lomakin@mail.ru*

Аннотация
На основе методов численного моделирования (использована обобщенная на случай учета рэлеевского трения трехмерная баротропная линейная модель Фельзенбаума) рассмотрены особенности структуры поля векторов течений в зависимости от ветровых условий в ситуации апвеллинга в акватории, расположенной вдоль северного берега Севастопольского взморья, между м. Лукулл и Толстый. Выявлена типичная для апвеллинга двухслойная поперечная ячейка циркуляции вод. В верхнем слое течения ориентированы преимущественно по ветру, в придонном слое – в обратном направлении. Показано, что в анализируемой акватории апвеллинг вызывают северные, северо-восточные, восточные и юго-восточные ветры. Апвеллинги, обусловленные указанными ветрами, различаются локацией и площадью очага. В условиях северо-восточного ветра апвеллинг наиболее интенсивный и распространен во всей рассматриваемой акватории. При юго-восточном ветре апвеллинг формируется на двух небольших по площади участках – в изгибах берега между м. Маргопуло и Лукулл и севернее м. Толстого. Результат моделирования сопоставлен с данными экспедиционных исследований. Обнаружено их хорошее соответствие при северном ветре.

Ключевые слова: ветер, течения, апвеллинг, численное моделирование, термохалинная структура, мыс Лукулл, Черное море

Благодарности: работа выполнена в рамках государственного задания ФГБУН ФИЦ МГИ по теме FNNN-2024-0016 «Исследование пространственно-временной изменчивости океанологических процессов в береговой, прибрежной и шельфовых зонах Черного моря под воздействием природных и антропогенных факторов на основе контактных измерений и математического моделирования».

Для цитирования: *Ломакин П. Д., Рябцев Ю. Н., Чепыженко А. И.* Апвеллинг в акватории Черного моря у мыса Лукулл на основе численного моделирования и данных наблюдений // Экологическая безопасность прибрежной и шельфовой зон моря. 2025. № 2. С. 67–79. EDN PRIZHP.

Introduction

Upwelling is a typical phenomenon in the oceans and seas. Its types on different spatial and temporal scales are quite well studied, with the results reflected in numerous publications. These include, for example, works [1–6] based on the analysis of experimental contact and satellite data and studies [7, 8] using numerical modeling methods. The results of the study of upwelling are important in terms of application and are widely used in various branches of marine science.

According to [9], surge phenomena (wind upwelling and downwelling, respectively) are typical for Sevastopol bays and open areas of the seaside. Upwelling in the considered small coastal water area is investigated for the first time, it is interesting and significant in fishery terms. According to the results of the Black Sea

fishery monitoring [10], dense accumulations of sprat are formed in this area during upwelling, which are successfully fished by trawlers of medium tonnage.

Objectives of the article are as follows:

– on the basis of numerical modeling, to reveal regularities of the structure of the local current system under upwelling depending on wind conditions in the water area located along the northern coast of the Sevastopol seaside between capes Lukull and Tolsty;

– to estimate the intensity of upwelling;

– to compare the modeling result with data from expeditionary research.

The study area is a coastal zone of about 12 miles along the northern coast of the Sevastopol seaside located between capes Lukull and Tolsty (Fig. 1).

The bold coast is one of the main morphometric features of the water area under consideration, which determines water dynamics. The coastal shallow water area is bounded by a rather pronounced shelf edge.

It is known that in areas with similar bottom relief, upwelling and downwelling are formed both under the influence of winds having a normal component relative to the coastline and under the influence of wind flows directed at an acute angle to the coast.

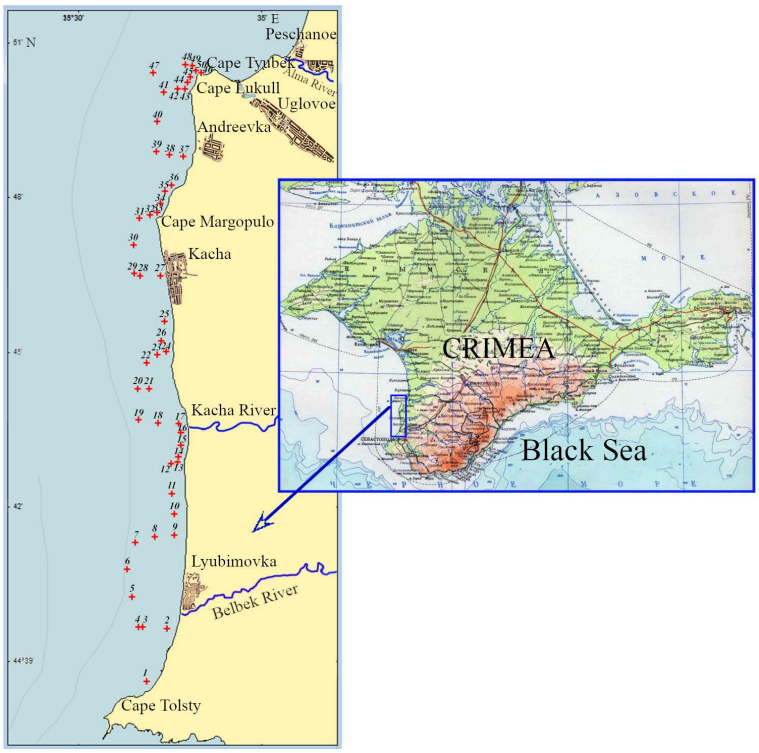

Fig. 1. Geographical location of the study area and survey station map of the survey performed by Marine Hydrophysical Institute in September 2019

Background data and research methods

Problem statement

Wind currents prevail in Sevastopol bays and on the open seaside areas [11, 12]. Therefore, a generalized three-dimensional barotropic linear model [1)] of Felsenbaum was used for the case of taking into account Rayleigh friction to calculate the characteristics of currents [12]. It should be noted that numerical modeling of hydrological processes in such basins is traditionally used by domestic [13, 14] and foreign [15–17] authors to understand the regularities revealed on the basis of *in situ* observation data.

Taking into account that the currents undergo the reorganization on the shelf rather quickly taking into account the wind influence (approximately within a day), we will calculate the average currents in the framework of the steady-state currents theory. The proposed model takes into account the main factors influencing the currents, such as Coriolis force, bottom relief, coast configuration, wind action (direction, intensity and spatial irregularity), bottom and internal friction.

The following equations represent the linear theory of steady-state currents in a homogeneous fluid, taking into account the internal friction proportional to the current velocity

$$-fv = g\varsigma_x + Au_{zz} - ru, \qquad fu = g\varsigma_y + Av_{zz} - rv,$$

$$u_x + v_y + w_z = 0.$$

Here, f is Coriolis parameter; u, v, w are current velocity components; g is gravity acceleration; ς is downgrade; A is kinematic coefficient of vertical viscosity; r is internal friction coefficient.

At the sea surface, which is defined as a current surface, the tangential wind stress is balanced by turbulent friction in the seawater, so that

$$\text{at } z = 0 \qquad Au_z = -\tau_x, \qquad Av_z = -\tau_y, \qquad w = 0,$$

where τ_x, τ_y are components of tangential wind stress related to seawater density.

On the bottom, the condition of adhesion is assumed, on the solid boundaries of the basin (on the coast) – the condition of non-flow, on open liquid boundaries – the condition of free flow.

The solution of the three-dimensional currents problem is reduced to the solution of the two-dimensional problem for the integral current function. The components of the current velocity are calculated using analytical formulae, which makes it possible to carry out calculations on a relatively fine grid and describe the features of coastal and bay currents. The calculation is performed layer-by-layer for eight main directions of moderate winds with a velocity of 7 m/s under real bottom topography conditions. Details of the algorithm and the parameters used are given in work [1)].

[1)] Felsenbaum, A.I., 1960. [*Theoretical Foundations and Methods of Calculating Steady-State Sea Currents*]. Moscow: Izd-vo AN SSSR, 126 p. (in Russian).

Observation data

To confirm the representativity of the results of the numerical experiment, we used the data from the survey conducted by the Marine Hydrophysical Institute (MHI) on 17 September 2019 in a northerly wind. Four other surveys of the Sevastopol seaside area under consideration, the data of which we have at our disposal, were carried out in calm and low-wind weather.

According to the *Wetterzentrale* hydrometeorological center data (available at: http://old.wetterzentrale.de/topkarten/fsreaeur.html), the synoptic situation over the Black Sea during the first and second ten-day periods of September 2019 was determined by the eastern periphery of the Azores High. A moderate northerly wind with an average daily speed of 4–7 m/s was observed over the study water area.

The survey was carried out according to a scheme that included 47 drift stations (Fig. 1). The sampling works were carried out from the board of small-sized vessel *Gladiator*. The investigated depths ranged from 4 to 37 m. The array of initial empirical information was formed with the help of a *Condor* sounding complex [2)]. Temperature, salinity and other parameters of the aquatic environment were measured *in situ* in the probing mode with a depth step of 0.1 m. The accuracy of temperature determination is ±0.01°C, that of salinity – ±0.005 PSU. The ideas about real water circulation under the action of a northerly wind were obtained on the basis of an indirect method – analysis of the structure of temperature and salinity fields.

Results and discussion

As shown by the results of the modeling experiment, upwelling was observed in four of the eight calculation variants corresponding to the northerly, north-easterly, easterly, south-easterly wind directions.

Under these winds, a two-layer transverse circulation cell characteristic of upwelling was revealed, manifested by the outflow of water from the coast to the sea in the upper layer and the compensatory flow in the bottom layer. Upwelling zones (centers) were identified in the calculated field of current vectors in the bottom layer by the position of flows directed along the normal to the coastline (Figs. 2–5).

Let us consider the structure of the local current system for each of the wind directions indicated above.

In the upper water layer, the calculated vector fields had the same property irrespective of the wind direction. The currents were oriented predominantly downwind and had a velocity of 5–25 cm/s (Figs. 2–5).

Northerly wind (Fig. 2). A southward-directed flow along the coast is observed in the upper water layer.

At the bottom in the seaward area, the current is directed north-eastwards. With the approach to the coast, this flow turns clockwise, causing the bottom water

[2)] Available at: http://ecodevice.com.ru/ecodevice-catalogue/multiturbidimeter-kondor [Accessed: 29 April 2024].

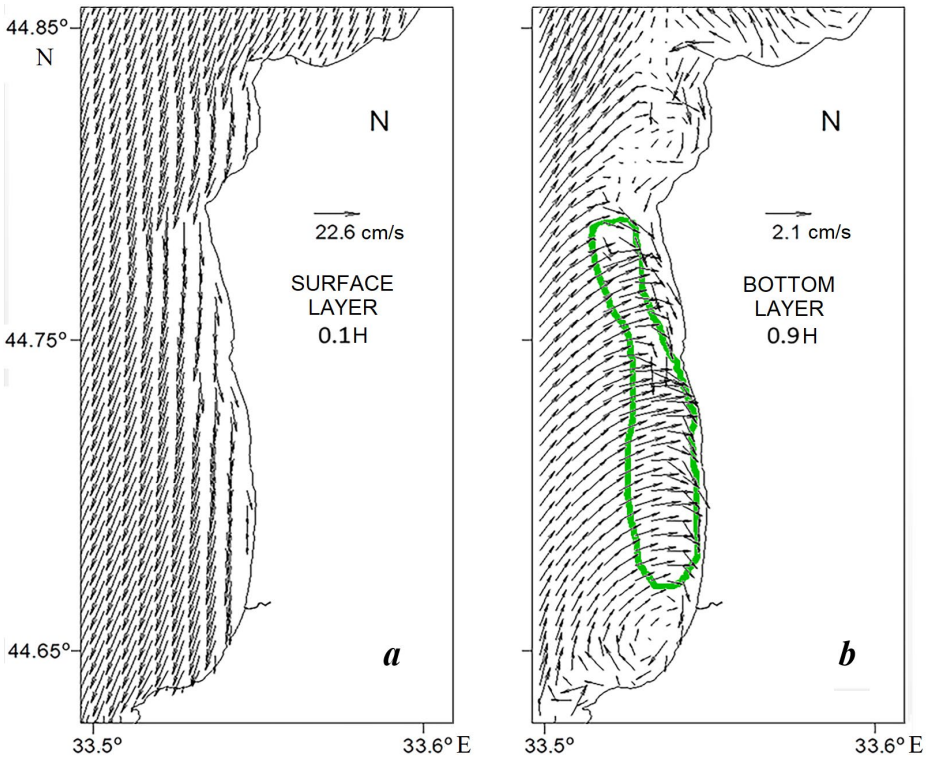

Fig. 2. Currents vectors in the surface (*a*) and bottom (*b*) layers under a northerly wind. The upwelling area is contoured in green

to move to the shallower waters where the longshore jet of the southward current is formed.

An upwelling zone of ~6 square miles (6 miles long and 1 mile wide) is located along a straight stretch of the coastline, between capes Margopulo and Tolsty. Two anticyclonic vortex cells are observed north and south of the upwelling area in the bends of the coastline. One of them is in the coast bend between capes Margopulo and Lukull and the other – to the north of Cape Tolsty (Fig. 2, *b*).

North-easterly wind (Fig. 3). Under this wind in the upper layer in shallow water, the current washes the coastline and is directed south-south-west. As it moves away from the coast, it deflects to the west-south-west (Fig. 3, *a*).

In the bottom layer throughout the entire water area, the current is directed along the normal to the coast, providing maximum transport, uplift and distribution of bottom water in shallower waters. The upwelling zone has a maximum area of ~36 (12 × 3) square miles and is distributed throughout the analyzed water area. Longshore currents jets and vortex cells are not observed (Fig. 3, *b*).

Upwelling is most intense in this wind situation.

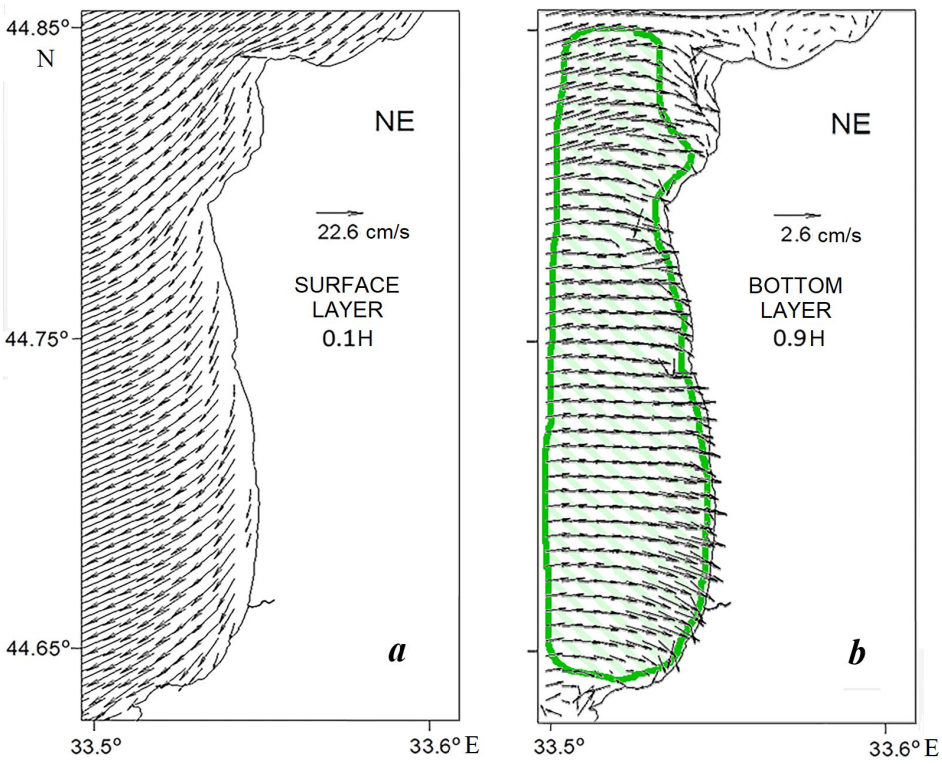

Fig. 3. Currents vectors in the surface (*a*) and bottom (*b*) layers under a north-easterly wind. The upwelling area is contoured in green

Easterly wind (Fig. 4). Under the action of this wind, the current is directed downwind with a slight deflection to the left in the upper water layer.

At the bottom in the seaward area, the current is directed south-eastwards and to the coast in shallow water. Upwelling is not as intense as in the north-easterly wind action situation because the transport of water normal to the coast is concentrated in a narrower coastal strip of ~11 (11 × 1) square miles. No pronounced longshore flow jets and vortex cells are observed (Fig. 4, *b*).

South-easterly wind (Fig. 5). Under this wind, the current follows a north-north-westerly direction in the upper sea layer.

Upwelling is formed in two small areas - in the bends of the coast north of Cape Tolsty and between capes Margopulo and Lukull. Here, the south-easterly wind vector is orientated along the normal to the coastline and two small centers

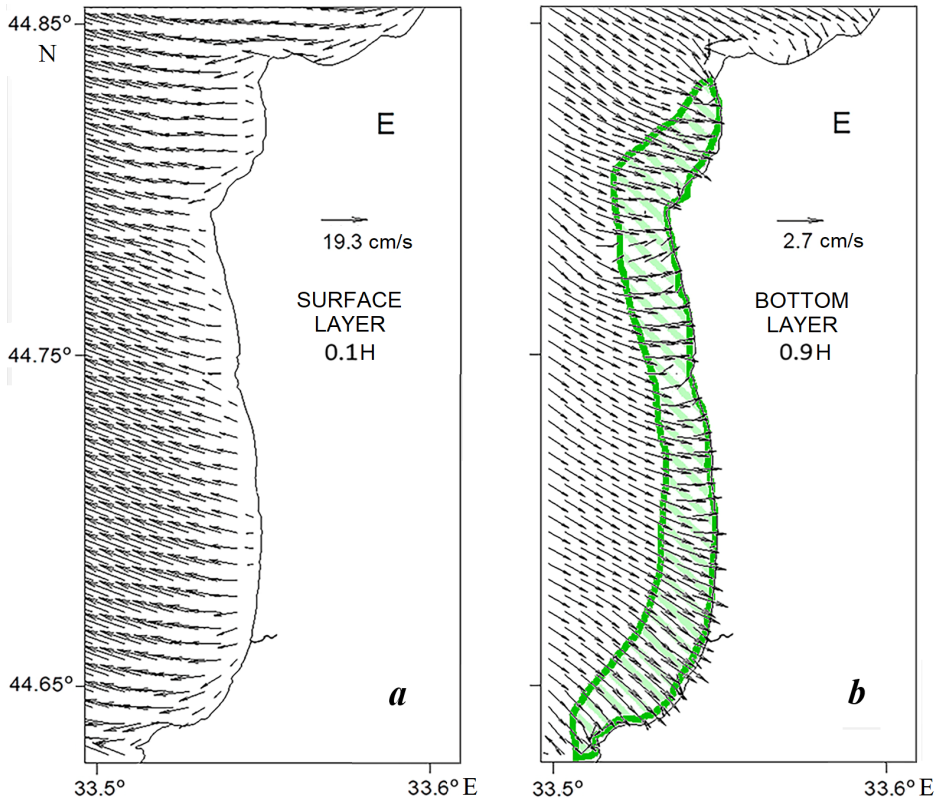

Fig. 4. Currents vectors in the surface (*a*) and bottom (*b*) layers under an easterly wind. The upwelling area is contoured in green

of upwelling develop due to the wind seiche. The area of each of them is estimated to be 2–3 square miles (Fig. 5).

Fig. 6 shows temperature and salinity distribution in the surface sea layer of the study water area under a moderate stable northerly wind. The distribution is based on data from the MHI expedition conducted on 17 September 2019.

Comparison of the elements of the thermohaline structure of waters (Fig. 6) with the result of numerical experiment (see Fig. 2) shows their good agreement.

In the straight-line section between capes Margopulo and Tolsty, a coastal strip of waters with a 0.6–0.8°C lower temperature relative to the ambient background is clearly visible, which could be the result of upwelling.

Local extremes of temperature and salinity were observed in the bend of the coastline to the north of Cape Tolsty, which indicates indirectly the presence of a vortex cell in this area.

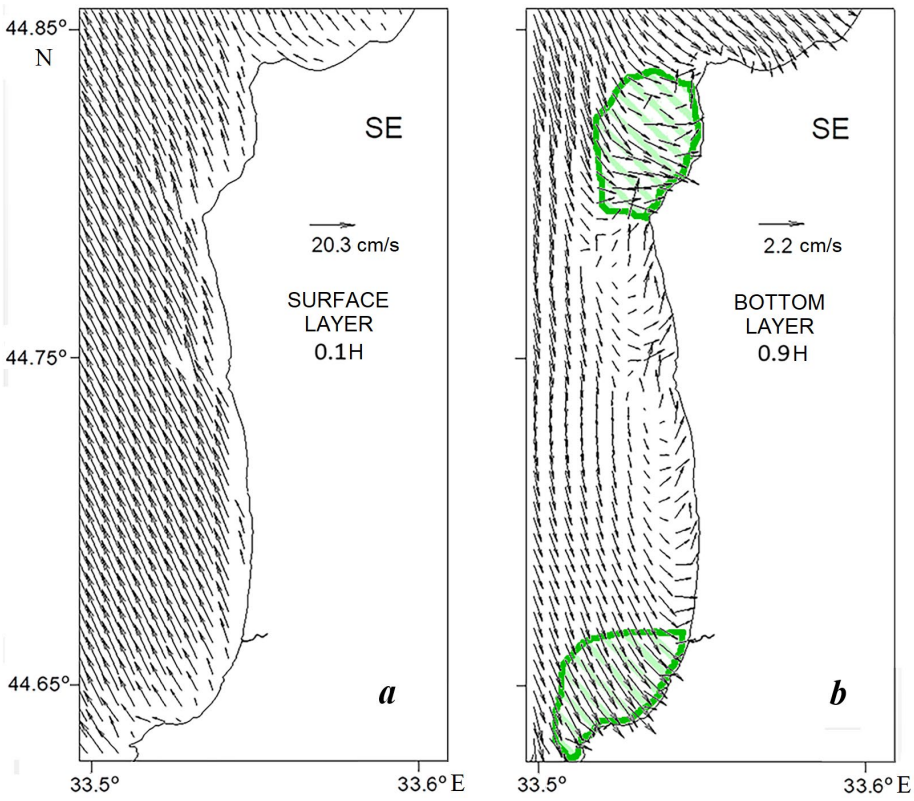

Fig. 5. Currents vectors in the surface (*a*) and bottom (*b*) layers under a south-easterly wind. The upwelling area is contoured in green

The numerical experiment yielded results indicating that wind upwelling was a prevalent phenomenon in the water area of the Sevastopol seaside, observed during a substantial portion of the year. According to the wind rose of the Sevastopol region, the total frequency of upwelling winds identified during the entire year is 49% (Fig. 7).

According to the data of the integrated monitoring of the fishing situation in the Black Sea, in the area of Cape Lukull (including the study area), dense accumulations of sprat (harvested by the fishing fleet) are formed in summer during the development of upwelling. At the same time, the hydrodynamic characteristics and water temperature regime are reliable enough to predict fishing conditions 5–7 days in advance [10].

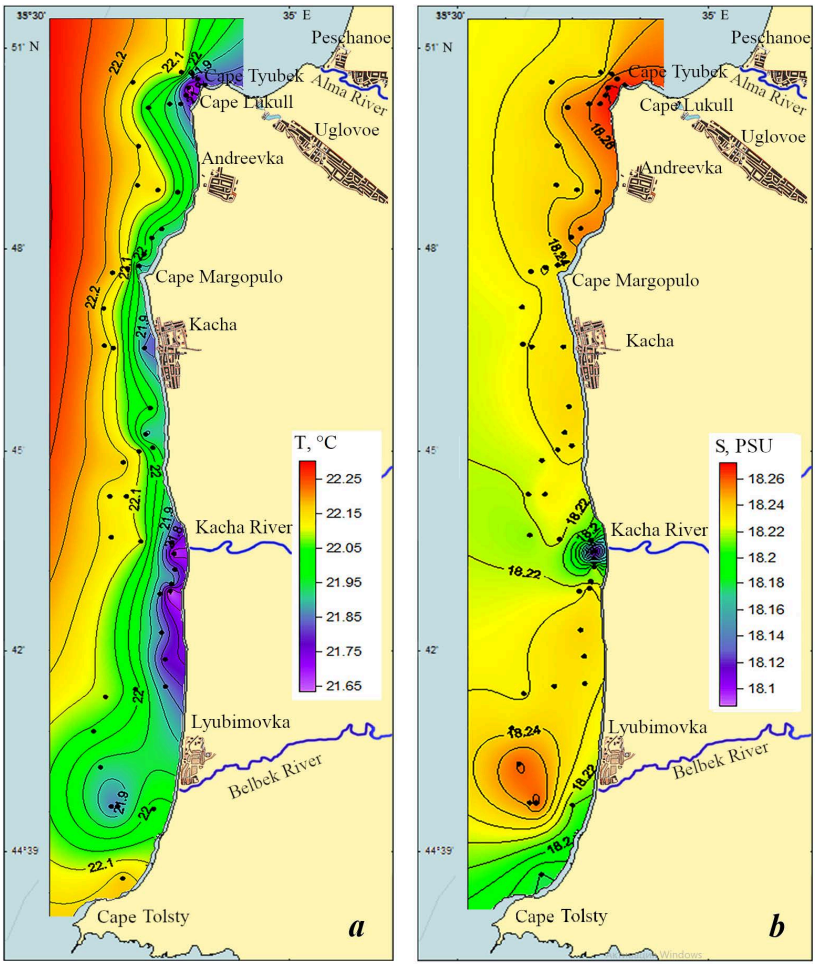

Fig. 6. Distribution of temperature (*a*) and salinity (*b*) in the surface sea layer under a moderate stable northerly wind on 17 September 2019

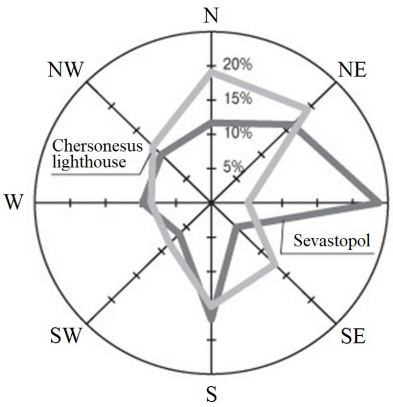

Fig. 7. Wind rose of the Sevastopol region (Adopted from: https://sevastopol.press/2007/05/24/v-kakuju-storonu-veter-duet/)

The results of this study can be used to predict the quality of the fishing situation for sprat in the study area on the basis of wind forecasts. Northerly and south-easterly winds, causing upwelling, create more favourable conditions for fishing compared to winds of other directions.

Conclusion

Based on the numerical modeling, the paper considers peculiarities of upwelling in the coastal waters of the Sevastopol seaside between capes Lukull and Tolsty.

The analysis demonstrates that northerly, north-easterly, easterly and south-easterly winds induce upwelling in the study area. The upwelling caused by these winds varies in terms of location and focus area.

The northerly wind causes upwelling on a straight section of the coastline between capes Margopulo and Tolsty with a center area of 6 square miles. Two anticyclonic vortex cells are formed in the bends of the coast between capes Margopulo and Lukull and to the north of Cape Tolsty.

Under the action of the north-easterly wind, upwelling is the most intense and widespread in the entire water area under consideration. Its area is estimated at 36 square miles.

The easterly wind causes upwelling, well pronounced but less intense compared to the conditions determined by the north-easterly wind. Its center occupies a narrower coastal strip of the whole water area under consideration – 11 square miles.

Under the south-easterly wind, upwelling is formed only in two small areas (2–3 square miles), in the bends of the coast between capes Margopulo and Lukull and to the north of Cape Tolsty.

The modeling experiment with the northern wind was compared with the result of the analysis of the thermohaline field structure based on the materials of the MHI expedition carried out under similar wind conditions. The following results of the study were confirmed during the comparison: an upwelling center was identified in the rectilinear section of the water area under study and a vortex cell was detected in the bend of the coastline to the north of Cape Tolsty.

The analysis demonstrates that wind upwelling is a characteristic phenomenon for the northern part of the Sevastopol seaside, observed during 49% of the entire year.

The results of this study can be used to predict the quality of the fishing situation for sprat in the study area based on wind forecasts. The prevailing winds in the northern and south-eastern sectors, which cause upwelling, create more favourable conditions for fishing when compared to winds from other directions.

REFERENCES

1. Bogdanova, A.K. and Korpachev, L.N., 1959. [Upsurge and Downsurge Circulation and its Role for the Hydrological Regime of the Black Sea]. *Meteorologiya i Gidrologiya*, (4), pp. 26–32 (in Russian).
2. Blatov, A.S. and Ivanov, V.A., 1992. [*Hydrology and Hydrodynamics of the Black Sea Shelf Zone (A Case of the Southern Coast of Crimea)*]. Kiev: Naukova Dumka, 241 p. (in Russian).
3. Ginzburg, A.I., Kostianoy, A.G., Soloviev, D.M. and Stanichny, S.V., 1997. Coastal Upwelling in the Northwestern Part of the Black Sea. *Issledovanie Zemli iz Kosmosa*, (6), pp. 66–72 (in Russian).
4. Borovskaja, R.V., Lomakin, P.D., Panov, B.N. and Spiridonova, E.O., 2008. Structure and Interannual Variability of Characteristics of Inshore Black Sea Upwelling on Basis of Satellite Monitoring Data. *Issledovanie Zemli iz Kosmosa*, (2), pp. 26–36 (in Russian).
5. Csanady, G.T., 1977. Intermittent "Full" Upwelling in Lake Ontario. *Journal of Geophysical Research*, 82(3), pp. 397–419. https://doi.org/10.1029/JC082i003p00397
6. Aleskerova, A.A., Kubryakov, A.A., Goryachkin, Yu.N., Stanichny, S.V. and Garmashov, A.V., 2019. Distribution of Suspended Matter Off the Western Coast of the Crimea Under Impact of the Strong Winds of Various Directions. *Issledovanie Zemli iz Kosmosa*, (2), pp. 74–88. https://doi.org/10.31857/S0205-96142019274-88 (in Russian).
7. Kosnyrev, V.N., Mikhailova, E.N. and Stanichny, S.V., 1997. Upwelling in the Black Sea by the Results of Numerical Experiments and Satellite Data. *Physical Oceanography*, 8(5), pp. 329–340. https://doi.org/10.1007/BF02523759
8. Sur, H.İ., Özsoy, E. and Ünlüata, Ü., 1994. Boundary Current Instabilities, Upwelling, Shelf Mixing and Eutrophication Processes in the Black Sea. *Progress in Oceanography*, 33(4), pp. 249–302. https://doi.org/10.1016/0079-6611(94)90020-5
9. Ivanov, V.A., Ovsyany, E.I., Repetin, L.N., Romanov, A.S. and Ignatyeva, O.G., 2006. *Hydrological and Hydrochemical Regime of the Sebastopol Bay and Its Changing under Influence of Climatic and Anthropogenic Factors*. Sevastopol: MHI, 90 p. (in Russian).
10. Panov, B.N. and Spiridonova, E.O., 2021. Possibilities of Short-Term Forecasting of the Catch of the European Sprat from the Black Sea Stock off the Western Coast of Crimea. *Aquatic Bioresources and Environment*, 4(2), pp 80–88. https://doi.org/10.47921/2619-1024_2021_4_2_80 (in Russian).
11. Mikhailova, E.N., Shapiro, N.B. and Yushchenko, S.A., 2001. Modelling of the Propagation of Passive Impurities in Sevastopol Bays. *Physical Oceanography*, 11(3), pp. 233–247. https://doi.org/10.1007/BF02508870
12. Shapiro, N.B., 2006. Modelling of the Currents on the Seaside Nearby Sevastopol City. *Ecological Safety of Coastal and Shelf Zones and Comprehensive Use of Shelf Resources*, 14, pp. 119–134 (in Russian).
13. Fomin, V.V. and Repetin, L.N., 2005. Numerical Simulation of Wind Currents and Propagation of Impurities in the Balaklava Bay. *Physical Oceanography*, 15(4), pp. 232–246. https://doi.org/10.1007/s11110-005-0045-y
14. Belokopytov, V.N., Kubryakov, A.I. and Pryakhina, S.F., 2019. Modelling of Water Pollution Propagation in the Sevastopol Bay. *Physical Oceanography*, 26(1), pp. 3–12. https://doi.org/10.22449/1573-160X-2019-1-3-12
15. Burchard, H. and Rennau, H., 2008. Comparative Quantification of Physically and Numerically Induced Mixing in Ocean Models. *Ocean Modelling*, 20(3), pp. 293–311. https://doi.org/10.1016/j.ocemod.2007.10.003

16. Hofmeister, R., Beckers, J.-M. and Burchard, H., 2011. Realistic Modeling of the Exceptional Inflows into the Central Baltic Sea in 2003 Using Terrain-Following Coordinates. *Ocean Modelling*, 39(3–4), pp. 233–247. https://doi.org/10.1016/j.ocemod.2011.04.007

17. Fofonova, V., Kärnä, T., Klingbei, K., Androsov, A., Kuznetsov, I., Sidorenko, D., Danilov, S., Burchard, H. and Wiltshire, K.H., 2021. Plume Spreading Test Case for coastal Ocean Models. *Geoscientific Model Development*, 14(11), pp. 6945–6975. https://doi.org/10.5194/gmd-14-6945-2021

Submitted 26.08.2024; accepted after review 17.02.2025;
revised 25.03.2025; published 30.06.2025

About the authors:

Pavel D. Lomakin, Leading Research Associate, Marine Hydrophysical Institute of RAS (2 Kapitanskaya St., Sevastopol, 299011, Russian Federation), DSc (Geogr.), Professor, **ResearcherID: V-7761-2017, Scopus Author ID: 6701439810**, *p_lomakin@mail.ru*

Yuri N. Ryabtsev, Research Associate, Marine Hydrophysical Institute of RAS (2 Kapitanskaya St., Sevastopol, 299011, Russian Federation), **ORCID ID: 0000-0002-9682-9969**, *ruab@mail.ru*

Alexey I. Chepyzhenko, Senior Research Associate, Marine Hydrophysical Institute of RAS (2 Kapitanskaya St., Sevastopol, 299011, Russian Federation), PhD (Tech.), Senior Research Associate, *ecodevice@yandex.ru*

Contribution of the authors:

Pavel D. Lomakin – general task statement, selection and interpretation of field data, general result interpretation, article writing

Yuri N. Ryabtsev – carrying out numerical experiments, modelling results interpretation, general result interpretation

Alexey I. Chepyzhenko – organization and carrying out the expedition, observational data processing and analysis, general result interpretation

All the authors have read and approved the final manuscript.

Original paper

Resonance Properties of Water Areas Based on Mathematical Modelling Results: A Case of Sevastopol Bays (the Black Sea)

Yu. V. Manilyuk *, A. Yu. Belokon, A. V. Bagaev, Yu. Yu. Yurovsky, D. I. Lazorenko

Marine Hydrophysical Institute of RAS, Sevastopol, Russian Federation
* *e-mail: uvmsev@yandex.ru*

Abstract
Within linear approximation of the long-wave theory, the paper uses the hydrodynamic numerical model ADCIRC to study resonance properties of the water areas of the Sevastopol bays: Streletskaya, Kruglaya, Kamyshovaya, and Dvoynaya, which includes Kazachya and Solyonaya bays. The calculations were carried out for the water area of each bay separately based on numerical experiments. At the first stage of modelling, waves in the bays water areas were excited by setting red-noise disturbance at the liquid boundary at the bay entrance. At the second stage, free oscillations were calculated under condition of their free passage at the liquid boundary. The resonance periods of the above bays and spatial distribution of the spectral density of sea-level oscillations in their water areas for individual natural modes were determined using spectral analysis. Most of the resonance periods for the Sevastopol bays were in satisfactory agreement with analytical estimates. The use of realistic bathymetry and shoreline profile data in the modelling allowed obtaining additional resonance periods for all the considered bays, which cannot be obtained with analytical estimates. The spectral composition expansion of the resonance modes due to connection of these bays via their entrances was revealed in Dvoynaya Bay, which includes Kazachya and Solyonaya Bays. The spectral density spatial distribution of the main energy-carrying sea level oscillations in Streletskaya, Kruglaya, Kamyshovaya and Dvoynaya Bays was analysed to show that the spectral density peaked mainly in the bay tops. In Dvoynaya Bay, the spectral density maxima manifested in the eastern or western arms (Kazachya or Solyonaya Bays, respectively) depending on which of the arms their natural periods belonged to. The results obtained here can be used in layout designing of hydraulic structures, development of mariculture, planning of wastewater outlets, etc.

Keywords: seiche oscillations, seiche, Sevastopol bays, ADCIRC model, mathematical modelling

Acknowledgements: The study was funded under grant no. 24-27-20076, https://rscf.ru/project/24-27-20076/ of the Russian Science Foundation and Agreement no. 86 as of 19.06.2024 of the Education and Science Department of the City of Sevastopol.

For citation: Manilyuk, Yu.V., Belokon, A.Yu., Bagaev, A.V., Yurovsky, Yu.Yu. and Lazorenko, D.I., 2025. Resonance Properties of Water Areas Based on Mathematical Modelling Results: A Case of Sevastopol Bays (the Black Sea). *Ecological Safety of Coastal and Shelf Zones of Sea*, (2), pp. 80–98.

Резонансные свойства акваторий севастопольских бухт (Черное море) по результатам математического моделирования

Ю. В. Манилюк*, А. Ю. Белоконь, А. В. Багаев, Ю. Ю. Юровский, Д. И. Лазоренко

Морской гидрофизический институт РАН, Севастополь, Россия
* *e-mail: uvmsev@yandex.ru*

Аннотация
В рамках линейного приближения теории длинных волн на основе гидродинамической численной модели *ADCIRC* исследуются резонансные свойства акваторий севастопольских бухт: Стрелецкой, Круглой, Камышовой, Двойной, включающей в себя б. Казачью и Соленую. Расчеты проведены для акватории каждой бухты отдельно на основе численных экспериментов. На первом этапе моделирования возбуждаются волны в акваториях бухт с помощью задания на жидкой границе, находящейся у входа в бухту, возмущения типа «красный шум». На втором этапе рассчитываются свободные колебания с условием свободного прохождения на жидкой границе. С использованием спектрального анализа установлены резонансные периоды указанных бухт и пространственное распределение спектральной плотности колебаний уровня в их акваториях для отдельных собственных мод. Большинство выделенных резонансных периодов для севастопольских бухт удовлетворительно согласуются с аналитическими оценками. Использование при моделировании данных батиметрии и профиля береговой черты, приближенных к реальным, позволило получить для всех рассмотренных бухт дополнительные резонансные периоды, которые нельзя получить при аналитических оценках. В б. Двойной, включающей в себя б. Казачью и Соленую, выявлено расширение спектрального состава резонансных мод, возникающее из-за связи этих бухт через их входы. Анализ пространственного распределения спектральной плотности основных энергонесущих колебаний уровня в б. Стрелецкой, Круглой, Камышовой, Двойной показал, что максимальные значения спектральной плотности возникают в основном в вершинах бухт. В б. Двойной максимальные значения спектральной плотности проявляются в восточном или западном рукавах (б. Казачья или Соленая соответственно) в зависимости от того, к какому из рукавов относится собственный период. Полученные здесь результаты могут быть использованы при проектировании размещения гидротехнических сооружений, развитии марикультуры, планировании выпусков сточных вод и т. п.

Ключевые слова: сейшевые колебания, сейши, севастопольские бухты, модель *ADCIRC*, математическое моделирование

Благодарности: исследование выполнено за счет гранта Российского научного фонда № 24-27-20076, https://rscf.ru/project/24-27-20076/ и Соглашения с Департаментом образования и науки г. Севастополя № 86 от 19.06.2024 г.

Для цитирования: Резонансные свойства акваторий севастопольских бухт (Черное море) по результатам математического моделирования / Ю. В. Манилюк [и др.] // Экологическая безопасность прибрежной и шельфовой зон моря. 2025. № 2. С. 80–98. EDN SNXXDY.

Introduction

The city of Sevastopol is located mainly within the Heraclean Peninsula and its shoreline is indented with many bays and capes. They form a system consisting of main Sevastopol Bay and several smaller adjacent bays. Seiches, i.e. standing water mass oscillations, are often observed in such water bodies. Unlike seiches in completely enclosed basins, they are excited by the penetration of long waves from the open sea through the liquid boundary, with wave energy mainly being lost through radiation at the bay entrance [1]. In contrast to enclosed water bodies, bays also generate the Helmholtz mode (zero mode). This mode usually dominates all other types of natural oscillations and determines the general character of motions in the water area [2, 3]. The danger of seiches in bays is that they can cause intense periodic currents that threaten coastal infrastructure and ships [4]. It is also known that adjacent bays can interact by exchanging energy across their open boundaries, resulting in the penetration of natural modes of one bay into another [5, 6]. The Sevastopol bays form a system of interconnected oscillators, resulting in an expansion of the seiche mode composition in each bay.

Periods of seiche oscillations are determined by geometrical parameters of the water area, such as depth, shoreline outlines and bathymetry. In the Black Sea, it is known that seiche periods in bays and gulfs range from several minutes to two hours, with periods of 5–10 min occurring in all of them. Level oscillations with periods of 2–3 min can be caused by the transformation of long waves in the coastal zone or by sharp gusts of wind in one direction. Oscillations with periods of 15–20 min can be caused by sharp changes in atmospheric pressure as well as changes in wind direction and speed. Seiches of this type most often appear at the passage of cyclones, especially in the peripheral zone, where wind intensification occurs [7]. At the same time, level oscillations with a period of up to 10 min are the most common. Of the seiches with a longer period on the Crimean coast, the most frequent are those with a period of 30–50 min [7]. Analysis of short-term measurements taken with an ADCP probe during expeditions by Marine Hydrophysical Institute in 2008 and 2014 revealed that current oscillations occurred at the entrance to Sevastopol Bay with a period of ~60 min [8].

In addition to seiches, tidal level oscillations inherent to the Black Sea appear in the Sevastopol bays as a background. In [9], devoted to the study of the Black Sea tides, it is indicated that the main lunar semidiurnal component (12.42 h) and the gravitational lunar-solar diurnal component (23.93 h) are the most intense on the Crimean coast. The intensity values of these tidal modes are close to each other, which agrees well with the data from [10].

At present, seiche oscillations in Sevastopol bays remain poorly studied. Data of *in situ* observations are only available for Sevastopol and Kruglaya bays. Sea level oscillations in Sevastopol Bay were recorded using a mareograph located at the marine hydrometeorological station on Cape Pavlovsky [10]. During the processing of the results of *in situ* observations, the periods corresponding to the semi-diurnal and diurnal components of the tide as well as with values of 0.9, 1.25, and 2.5 h were identified. The oscillation with a period of 0.9 h is the Helmholtz mode of Sevastopol Bay. In Kruglaya Bay, data were obtained relatively recently (in 2023), with level measurements using an ultrasonic sensor and resonance periods of local seiches identified on the basis of spectral analysis [11]. Among them, the most intense Helmholtz mode of Kruglaya Bay with a period of 13.7 min was identified.

The establishment of physical regularities of level oscillations in a system of connected bays, such as the Sevastopol bays, is possible through mathematical modelling. Several studies [1, 6, 11, 12] have investigated seiche oscillations in Sevastopol bays using numerical modelling. In [6], the mutual influence of Sevastopol and Karantinnaya bays on each other due to the exchange of oscillation energy through their entrances was investigated. The study showed that the intensity of the natural modes of Sevastopolskaya Bay could exceed that of Karantinnaya Bay when they penetrated into the latter. In [1], the resonance periods of the main Sevastopol bays and the influence of the duration of the initial disturbance on seiche generation in them were studied. In [12], different modes of seiche oscillations in Sevastopol Bay were studied in the context of disturbances with periods of 2.5, 2.9 and 6.2 min, which correspond to the natural modes of the bay with different spatial structures. The periods of the fundamental modes of the Sevastopol (50 min) and Karantinnaya (9.25 min) bays were determined based on the numerical solution of the problem for natural values.

Nevertheless, information on the periods and spatial structure of natural level oscillations in all Sevastopol bays remains insufficient. Therefore, it is necessary to develop a comprehensive understanding of long-wave oscillations in the Sevastopol bays and determine the resonance (natural) period values of the Sevastopol bays system and its individual elements within the high-frequency spectrum (hours – minutes).

The purpose of this study is to analyse the resonance response of sea levels in the Sevastopol bays: Streletskaya, Kruglaya, Kamyshovaya, Kazachya and Solyonaya, in response to disturbances from the open sea, and to determine their natural periods. Investigating the resonance properties of each bay separately made it possible to study the mode composition of seiches in detail. Understanding the resonance properties of each bay in the system will enable more accurate interpretation of modelling and measurement results for the entire system.

Materials and methods of study

A detailed study of seiche oscillations in Sevastopol bays was conducted using bathymetric data from digitised nautical charts. Fig. 1 shows the bathymetry of the Sevastopol coastal zone and its bay system.

Numerical modelling was carried out separately for each of the studied bays: Streletskaya, Kruglaya, Kamyshovaya, Kazachya and Solenaya. Fig. 2 shows the bathymetry of these bays. Sea level oscillations were calculated at points *1–23* (Fig. 2).

Streletskaya Bay (Fig. 2, *a*) is located 3 km southwest of the southern breakwater of Sevastopol Bay and extends 2 km inland. To the west of Streletskaya Bay, Kruglaya Bay (Fig. 2, *b*), almost circular in shape, is found. This bay is shallow with a sandy bottom. Winding Kamyshovaya Bay (Fig. 2, *c*), about 2.5 km long, is separated by two protective breakwaters limiting its entrance. Kazachya and Solyonaya bays (Fig. 2, *d*) together form Dvoynaya Bay, which is one of the most complex bays in the Sevastopol bays system. It is located 15 km west of the Sevastopol city centre, between Kamyshovaya Bay and Cape Chersonese. Kazachya Bay is approximately 600 m longer than Solyonaya Bay.

Numerical hydrodynamic Advanced Circulation Model for Shelves, Coasts, and Estuaries (ADCIRC) was used for calculations [1), 2)]. A variant of the model [14] based on depth-averaged equations of motion was used in this case

$$\frac{\partial U}{\partial t}+U\frac{\partial U}{\partial x}+V\frac{\partial U}{\partial y}=-g\frac{\partial \eta}{\partial x}-C_d\frac{U\sqrt{U^2+V^2}}{H}+A_h\frac{\Delta q_x}{H}, \quad (1)$$

$$\frac{\partial V}{\partial t}+U\frac{\partial V}{\partial x}+V\frac{\partial V}{\partial y}=-g\frac{\partial \eta}{\partial y}-C_d\frac{V\sqrt{U^2+V^2}}{H}+A_h\frac{\Delta q_y}{H}, \quad (2)$$

$$\frac{\partial \eta}{\partial t}+\frac{\partial q_x}{\partial x}+\frac{\partial q_y}{\partial y}=0. \quad (3)$$

Here, U, V are depth-averaged components of the velocity vector along axes x and y, respectively; η is basin water level; $H = h + \eta$ is dynamic depth; C_d is bottom friction coefficient; Δ is Laplace operator in spatial variables; A_h is horizontal turbulent viscosity coefficient; $q_x = UH$, $q_y = VH$ are components of the vector of total fluxes.

---

1) *Luettich R. A., Westerink J. J., Scheffner N. W.* ADCIRC: An Advanced Three-dimensional Circulation Model for Shelves Coasts and Estuaries. Report 1: Theory and Methodology of ADCIRC-2DDI and ADCIRC-3DL. Vicksburg, MS : U.S. Army Engineers Waterways Experiment Station, 1992. 137 p. (Dredging Research Program Technical Report DRP-92-6).

2) *Luettich R. A., Westerink J. J.* Formulation and Numerical Implementation of the 2D/3D ADCIRC. 2004. URL: https://adcirc.org/wp-content/uploads/sites/2255/2018/11/adcirc_theory_2004_12_08.pdf (дата обращения: 2.05.2025).

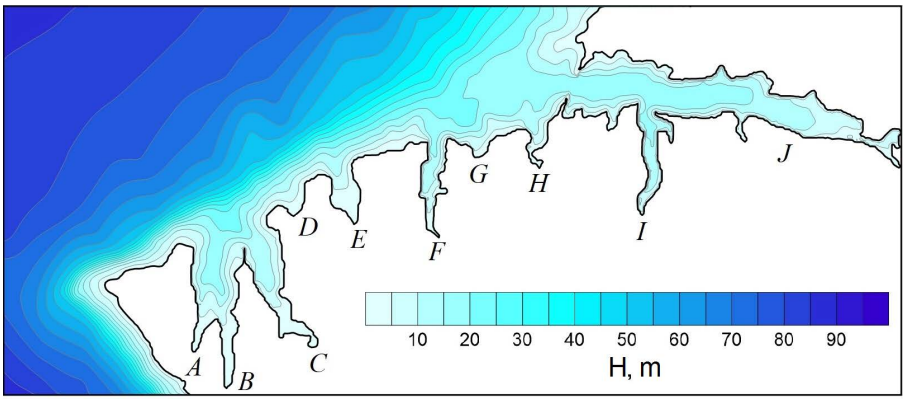

Fig. 1. Bathymetry of the Sevastopol coastal zone. Notations: *A* – Solyonaya Bay, *B* – Kazachya Bay (these two bays constitute Dvoynaya Bay), *C* – Kamyshovaya Bay, *D* – Abramova Bay, *E* – Kruglaya Bay, *F* – Streletskaya Bay, *G* – Pesochnaya Bay, *H* – Karantinnaya Bay, *I* – Yuzhnaya Bay, *J* – Sevastopol Bay

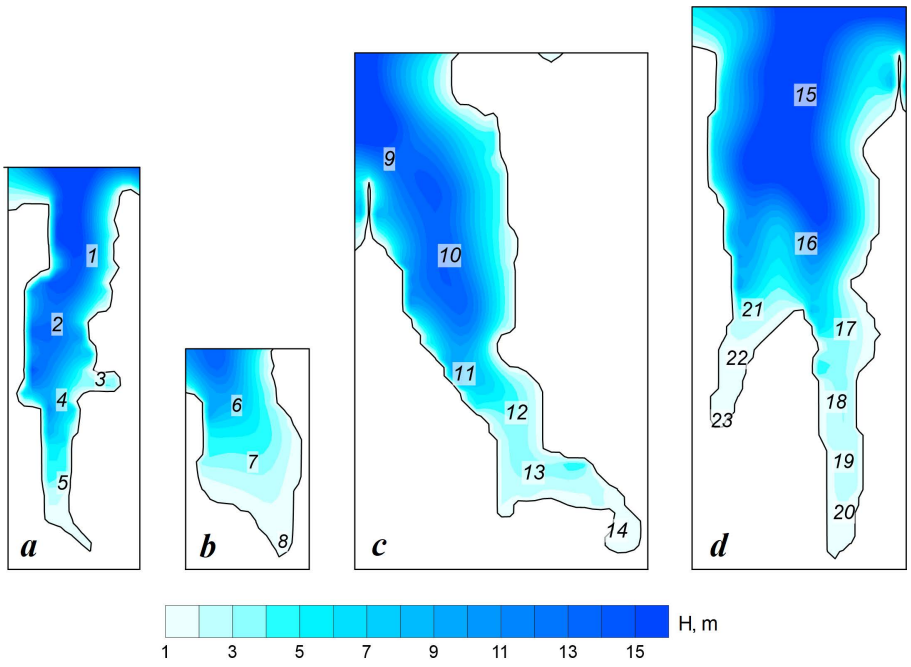

Fig. 2. Bathymetry of Sevastopol bays: *a* – Streletskaya; *b* – Kruglaya; *c* – Kamyshovaya; *d* – Dvoynaya. Numbers *1–23* stand for virtual mareographs (stations)

The numerical algorithm of the ADCIRC model is based on the finite element method using triangular elements and linear basis functions. To reduce computational noise during numerical integration of the system, the continuity equation is represented as so-called Generalized Wave Continuity Equation (GWCE)

$$\frac{\partial G}{\partial t} + \tau_0 G = 0,$$

where $G \equiv \partial\eta / \partial t + \partial q_x / \partial x + \partial q_y / \partial y$; τ_0 is non-negative parameter affecting the phase characteristics and stability of the numerical algorithm. After some identical transformations, the GWCE takes the following form

$$\frac{\partial^2 \eta}{\partial^2 t} + \tau_0 \frac{\partial \eta}{\partial t} + \frac{\partial J_x}{\partial x} + \frac{\partial J_y}{\partial y} = 0,$$

where

$$J_x = -q_x \frac{\partial U}{\partial x} - q_y \frac{\partial U}{\partial y} - \frac{g}{2}\frac{\partial \eta^2}{\partial x} - C_d \frac{U\sqrt{U^2+V^2}}{H} + A_h \frac{\Delta q_x}{H} + \tau_0 q_x + U\frac{\partial \eta}{\partial t} - gH\frac{\partial \eta}{\partial x},$$

$$J_y = -q_x \frac{\partial V}{\partial x} - q_y \frac{\partial V}{\partial y} - \frac{g}{2}\frac{\partial \eta^2}{\partial y} - C_d \frac{U\sqrt{U^2+V^2}}{H} + A_h \frac{\Delta q_y}{H} + \tau_0 q_y + V\frac{\partial \eta}{\partial t} - gH\frac{\partial \eta}{\partial y}.$$

The GWCE-based numerical algorithm suppresses short-wavelength noise effectively when solving the system of equations, without the need for artificial viscosity or distortion of the long-wavelength portion of the spectrum.

The quasi-linear version of the ADCIRC model was used, taking into account bottom friction, because it was assumed that the contribution of nonlinear terms in equations (1)–(3) could be neglected. The Coriolis force was not taken into account due to its weak influence on the scale of Sevastopol bays. Horizontal turbulent viscosity was also not taken into account, so turbulent viscosity coefficient A_h was assumed to be equal to zero; parameter τ_0 was 0.005. Bottom friction coefficient $C_d = C_0\left[1+\left(H_b / H\right)^{\alpha}\right]^{\beta/\alpha}$, where C_0 is minimum value C_d; $\alpha = 10$ is dimensionless parameter that determines the rate of bottom friction growth when the depth is greater or less than the depth of wave breaking $H_b = 1$ m; $\beta = 1/3$ is dimensionless parameter that determines how bottom friction increases with decreasing basin depth.

Numerical modelling was carried out on unstructured computational grids, which numbered from ~4,000 to ~12,200 finite elements for different bays. The grid step ranged from 20 to 100 m. The time integration step was $\Delta t = 0.025$ s.

Waves in the bays water areas were excited by setting red-noise disturbance [15] at the liquid boundary of each bay under consideration.

The boundary condition on the liquid boundary has the following form

$$\zeta_b = \begin{cases} \zeta_p, & t \le t_p \\ 0, & t > t_p \end{cases}, \quad (4)$$

where $\zeta_p(x,y,t)$ is a random function with red-noise spectrum; t_p is pumping time.

The numerical experiment consisted of a 6 h pumping phase and a 6 h free oscillations phase. During the pumping stage, wave disturbances were generated at the liquid boundary of the computational domain due to condition (4). Using disturbances in the form of red-noise suppressed the high-frequency components and enabled the response of the bay system to be considered in the long-wave spectrum. During the free oscillations stage, the initial conditions were formed based on the results of calculations carried out in the previous stage. A free passage condition was set on the liquid boundary of the computational domain. Spectral analysis of the series of level deviations calculated in the free oscillation mode was used to identify the periods of modes with the highest intensity.

Modelling results and discussion

Numerical experiments were conducted to calculate the level oscillations at stations 1–23, which are located within the design area of each of the studied bays. Fig. 3 shows the calculated marigrams for the regime of free level oscillations.

The most intense seiche oscillations occur in Kamyshovaya (Fig. 3, *c*), Kazachya (Fig. 3, *d*) and Solyonaya (Fig. 3, *e*) bays. Additionally, damping of seiches in these bays is slower (within 2 h) than in Streletskaya and Kruglaya bays (Fig. 3, *a*, *b*) where water oscillations damping lasts ~45 min. It should be noted that Solenaya and Kazachya bays are part of Dvoynaya Bay (see Fig. 2, *d*), which results in higher intensity of seiches in more extended Kazachya Bay compared to Solyonaya Bay. This is consistent with the findings reported in [16], where a branched bay model with the characteristic dimensions, mean depth and configuration of Dvoynaya Bay was examined. The paper demonstrates that asymmetry results in a reduction in the intensity of oscillations in the relatively short bay, as well as in their significant amplitudes in the longer bay, and an expansion of the mode composition of seiche oscillations in both bays.

To determine the periods of seiche oscillation in the bays, the calculated marigrams were subjected to spectral analysis using scripts developed by Gert Klopman and *Delft Hydraulics* [3)]. The energy spectra of the oscillations of sea level $E(f)$ were obtained using the Fourier transform. The *ESD* spectral energy density in range of oscillations $[f_a; f_b]$ was calculated as

$$ESD = \int_{f_a}^{f_b} |E(f)|^2 df \ . \quad (5)$$

[3)] *Winde H. P.* Wave height from pressure measurements. 2012. 49 p. Available at: https://repository.tudelft.nl/record/uuid:e3b07efd-1ce9-4fd1-b051-c794c72959ca [Accessed: 12 December 2024].

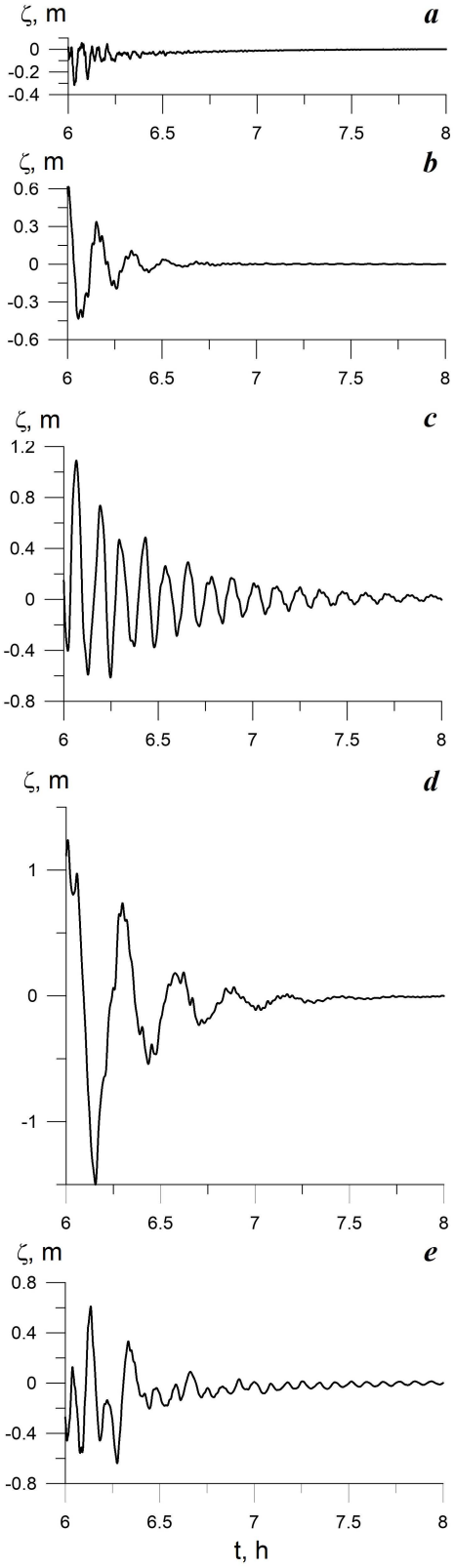

Fig. 4 shows the energy spectra of the oscillations of sea level $E(f)$ in the tops of the Sevastopol bays. It can be seen that modes with periods 1.1, 1.6, 2.8, 1.4 min are dominant in Streletskaya Bay (Fig. 4, *a*). In Kruglaya Bay, the main peaks are noted at periods 4.6, 10.6, 1.7, 2.7 min (Fig. 4, *b*). Modes with periods 7.1, 1.5, 3.6, 4.5, 2.1 min prevail in Kamyshovaya Bay (Fig. 4, *c*). In fact, Kazachya and Solyonaya bays are interconnected, as a result of which the mode composition of their seiches expands due to their mutual influence. The main peaks occur at periods 17.1, 2.7, 3.3, 1.6, 6.7 min in Kazachya Bay and at periods 5.1, 17.1, 9.5, 6.7, 3.3, 2.0, 2.5 min in Solyonaya Bay. Therefore, three similar peaks at periods 17.1, 3.3, 6.7 min can be seen in both bays.

Table shows the periods determined for the resonance oscillation modes of the bay tops, ordered by decreasing oscillation energy. Also given here are the periods of natural sea level oscillations in the Sevastopol bays calculated in [1] using formulas for a stationary-depth basin and a parabolic-bottom basin (these values are given in brackets) from [17]. As can be seen from Table, the values obtained in most periods in the present study coincide with the values of the periods determined analytically in [1] or close to them.

Fig. 3. Marigrams calculated for the free oscillations mode in Sevastopol bays: *a* – Streletskaya (St. *5*); *b* – Kruglaya (St. *8*); *c* – Kamyshovaya (St. *14*); *d* – Kazachya (St. *20*); *e* – Solyonaya (St. *23*)

The absence of certain values and the emergence of new ones in our results are related to complex, non-rectangular shapes of the bays and their bathymetry peculiarities. Thus, in Streletskaya Bay, all of the previously identified periods were detected, except for the 13.5 min period corresponding to the Helmholtz mode of this bay. This appears to be connected with the impact of red-noise disturbance. In Kruglaya Bay, new modes with periods of 4.6, 1.9, 1.6 min appear. The present studies revealed a mode with a 12.9 min period in Kamyshovaya Bay while analytical estimates indicated a maximum period of 19.8 min. As for Kazachya and Solyonaya bays, which together form Dvoynaya Bay, almost all of the periods identified through analysis were detected in these bays. At the same time, the mode composition of sea level oscillations is significantly expanded due to the bays being connected to each other via entrances. The period values calculated for Kazachya (6.7, 2.5, 2.0 min) and Solyonaya (6.7, 3.3, 2.0, 2.5, 2.7 min) bays also agree well with the values obtained in [16] for the model bay, which has the same configuration and average depth as Dvoynaya Bay. At the same time, the present studies revealed a wider range of periods for these bays.

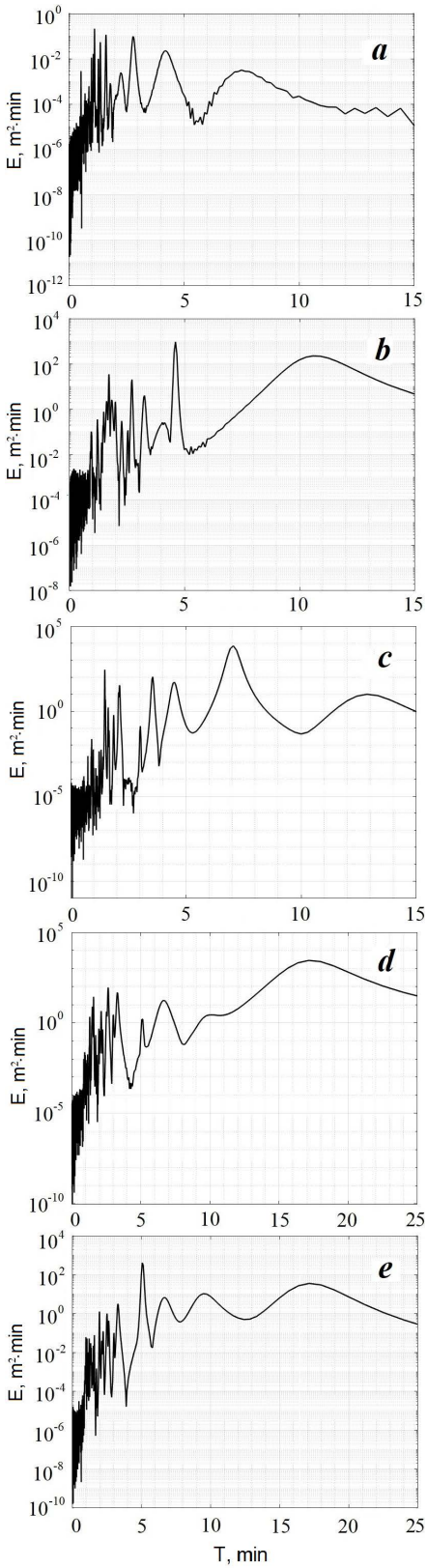

Fig. 4. Energy spectra of sea level oscillations resulting from red-noise disturbance in Sevastopol bays: *a* – Streletskaya (St. *5*); *b* – Kruglaya (St. *8*); *c* – Kamyshovaya (St. *14*); *d* – Kazachya (St. *20*); *e* – Solyonaya (St. *23*)

Periods of natural oscillations in Sevastopol bays, min, for a stationary-depth basin and a parabolic-bottom basin

Bay (station)	Mathematically modelled periods, min	Periods from analytical estimation, min [1]
Streletskaya Bay (St. *5*)	**1.3** **1.6** **2.8** **1.4** **4.2**	13.5 4.5 (**4.3**) **2.7 (2.7)** **1.9** (2.0) **1.3** **1.2**
Kruglaya Bay (St. *8*)	4.6 **2.7** **10.6** **1.7** **3.3** 1.9 1.6 **2.0** **1.5**	**10.2** 3.4 (**2.7**) 2.0 (**1.7**) **1.5** (1.3) **3.0** **2.3**
Kamyshovaya Bay (St. *14*)	**7.1** **1.5** **3.6** 4.5 **2.1** 12.9	19.8 **6.7** (6.0) 4.0 (**3.8**) **2.8 (2.8)** **1.5** 1.4
Kazachya Bay (eastern arm of Dvoynaya Bay) (St. *20*)	**5.1** **17.1** 6.7 2.7 3.3 1.6 **1.5** 2.1 2.5 **3.0** 10.0 1.3 2.0 **2.2**	**15.2** **5.1** **3.0** **2.2** **1.2**

Continued

Bay (station)	Mathematically modelled periods, min	Periods from analytical estimation, min [1]
Solyonaya Bay (western arm of Dvoynaya Bay) (St. *23*)	5.1 17.1 **2.0** **9.5** 6.7 **3.3** 2.5 2.7 2.2 3.0 **1.6**	**9.6** **3.2** **1.9** **1.4** 1.3 1.2

N o t e . Values for the basin with parabolic bottom profile are given in brackets. Periods with good agreement are highlighted in bold. The periods in Kazachya and Solyonaya Bays, resulting from their interaction, are underlined.

Figs. 5–8 demonstrate spatial distribution of the spectral energy density per unit time of the main energy-carrying level oscillations in Streletskaya, Kruglaya, Kamyshovaya, Dvoynaya bays calculated according to formula (5). For Streltskaya Bay (Fig. 5), the maximum values of the spectral energy density of seiche level oscillations are observed near the eastern coast of the bay and in its top (stations *3* and *5*). In Kruglaya Bay (Fig. 6), most of the energy of seiche oscillations is concentrated in its top (station *8*). Fig. 7 shows spatial distribution of spectral density of energy in Kamyshovaya Bay, from where we can see that the most intense oscillations are characteristic of the narrow part of the bay near its top (stations *12–14*). The most complex energy picture was obtained in the case of Dvoynaya Bay (Fig. 8). It can be seen that the resonance properties of the bay, which consists of two arms, are manifested in the intensification of level oscillations in both eastern arm (Kazachya Bay) and western arm (Solyonaya Bay). According to analytical estimates (Table), modes 5.1, 17.1 and 2.7 min are natural periods of Kazachya Bay (eastern arm of Dvoynaya Bay), therefore, the maximum values of the spectral energy density for these periods are noted in this bay (Fig. 8, *a*, *b*, *d*). According to the calculations, the mode with a 6.7 min period was also noticeably pronounced in Kazachya Bay (Fig. 8, *c*). The highest values of spectral energy

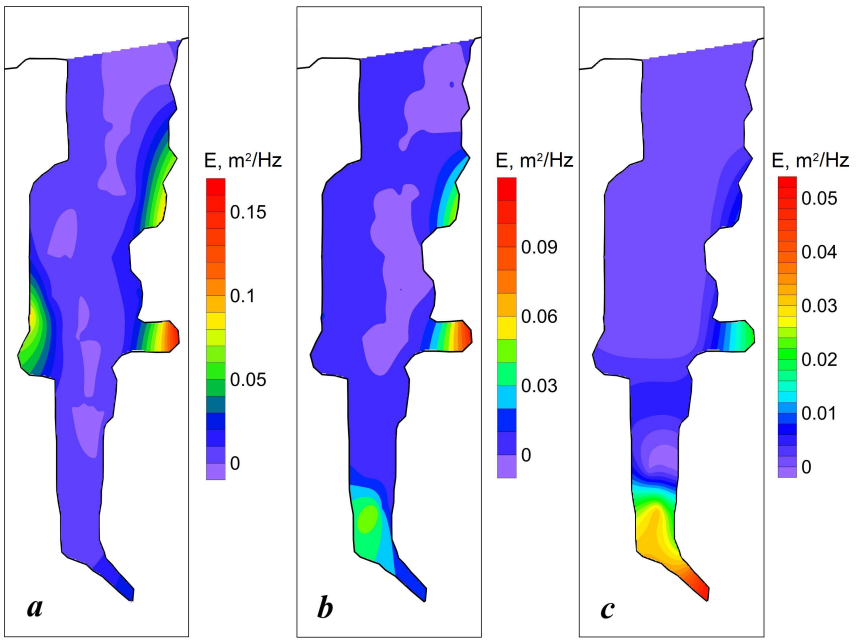

Fig. 5. Spatial distribution of spectral density of main energy-carrying level oscillations in Streletskaya Bay for a period T of 1.3 min (*a*), 1.6 min (*b*), 2.8 min (*c*)

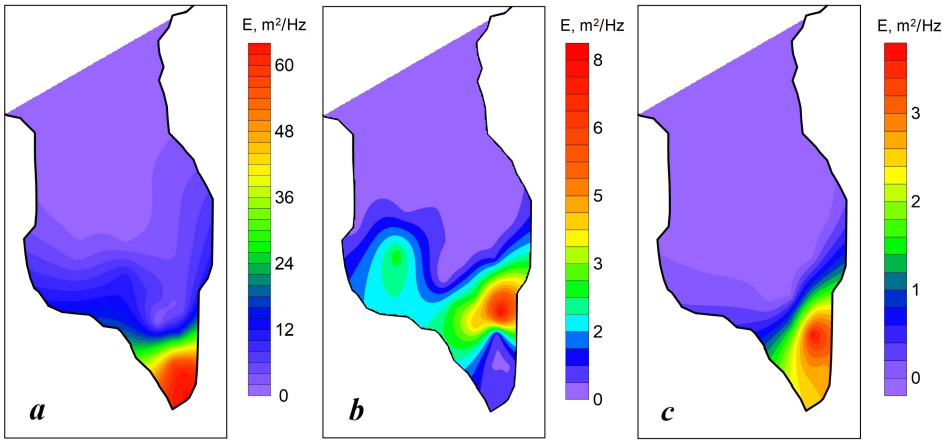

Fig. 6. Spatial distribution of spectral density of main energy-carrying level oscillations in Kruglaya Bay for a period T of 4.6 min (*a*), 2.7 min (*b*), 10.6 min (*c*)

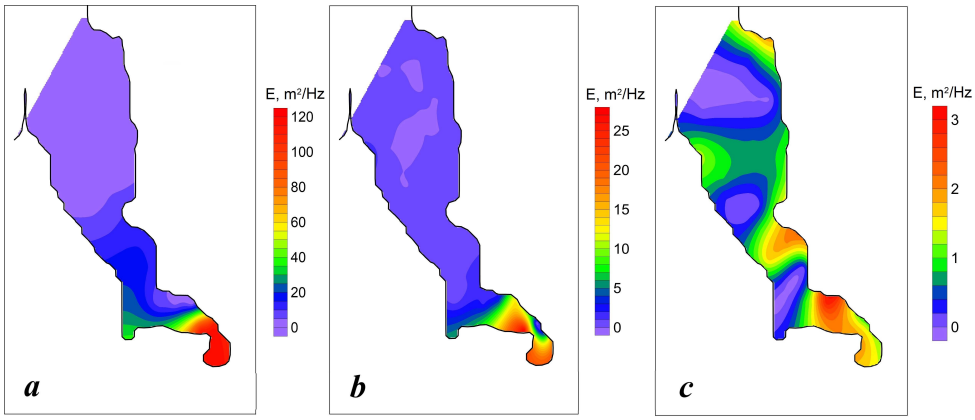

Fig. 7. Spatial distribution of spectral density of main energy-carrying level oscillations in Kamyshovaya Bay for a period T of 7.1 min (*a*), 1.5 min (*b*), 3.6 min (*c*)

density were obtained for 2.0 and 9.5 min periods in Solyonaya Bay, as these are its natural periods (Solyonaya Bay is the western arm of Dvoynaya Bay) (Fig. 8, *e*, *f*).

Analysis of the calculation results showed that Kazachya Bay (Fig. 8), with spectral density of over 150 m^2/Hz for a 5.1 min period, and Kamyshovaya Bay, with ~120 m^2/Hz for a 7.1 min period, had the highest values of spectral energy density of level oscillations. In Kruglaya Bay, maximum spectral energy density was ~65 m^2/Hz for a 4.6 min period. The lowest values of spectral energy density were observed in Streletskaya Bay (~0.15 m^2/Hz for a 1.3 min period).

Fig. 9 demonstrates the spatial distribution of relative (reduced to maximum values) amplitudes of sea level seiche oscillations in the bays. As can be seen, the largest amplitude values occur mainly in the tops of the bays, with the exception of Streletskaya Bay where the transverse mode dominates.

The spatial distribution of the amplitude and spectral density of level oscillations, as shown in Figs. 5–9, can be useful in identifying local zones where significant level rises caused by seiches are possible. This information is important for ensuring the safety of bay coastal infrastructure, such as ports.

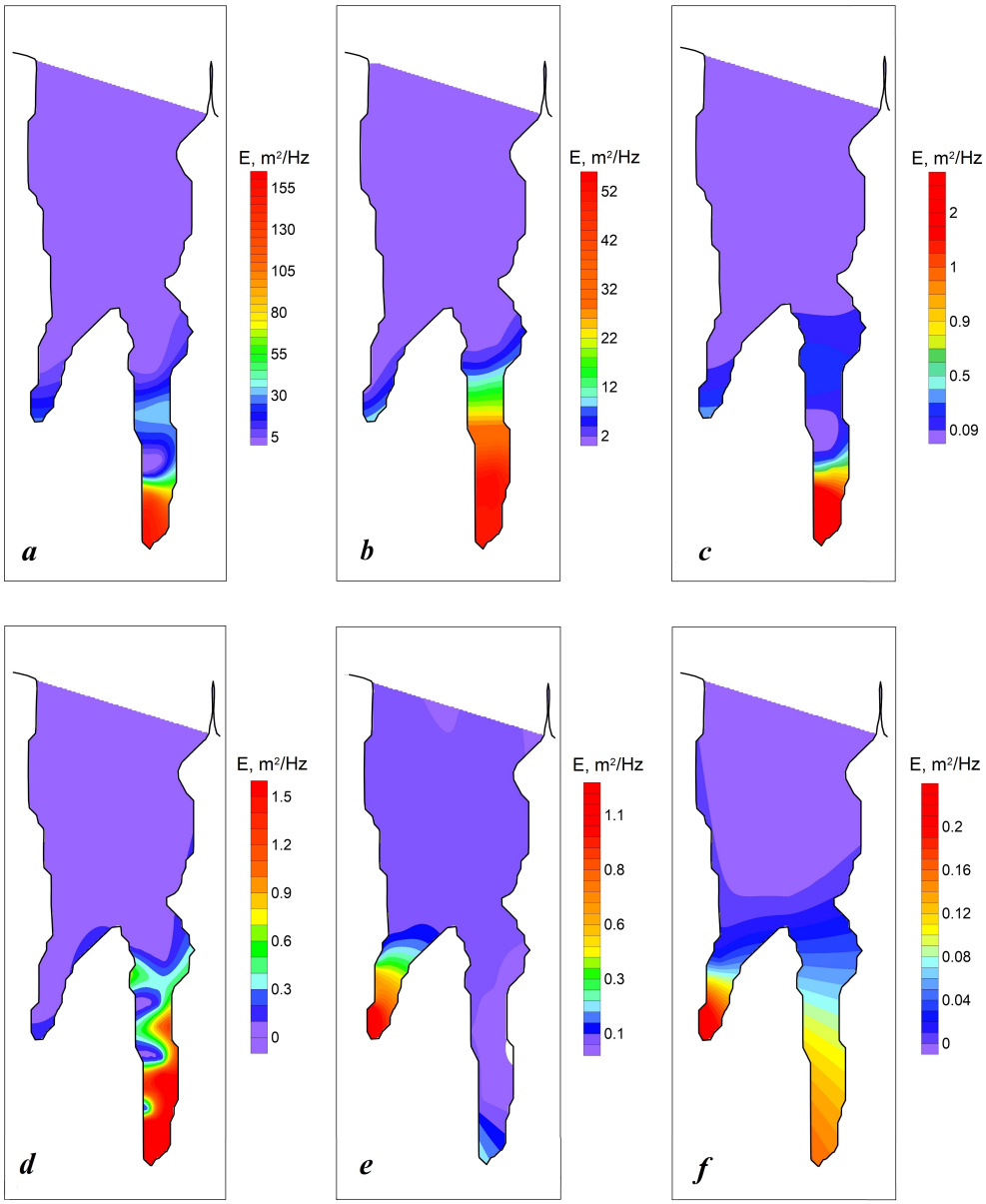

Fig. 8. Spatial distribution of spectral density of main energy-carrying level oscillations in Dvoynaya Bay for a period T of 5.1 min (*a*), 17.1 min (*b*), 6.7 min (*c*), 2.7 min (*d*), 2.0 min (*e*), 9.5 min (*f*)

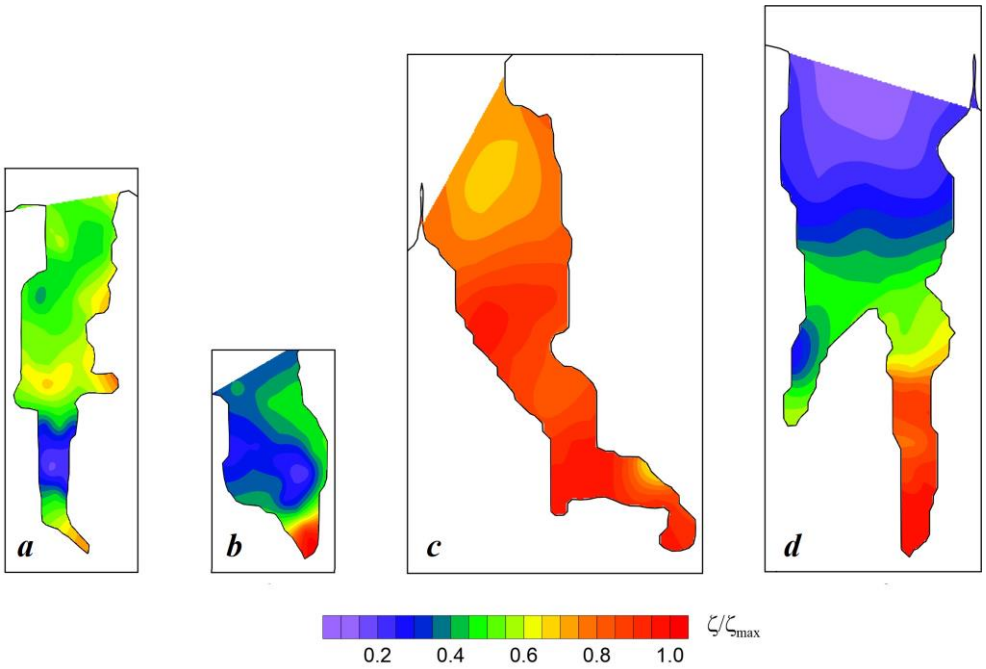

Fig. 9. Spatial distribution of relative amplitudes of level seiche oscillations in Sevastopol bays: *a* – Streletskaya; *b* – Kruglaya; *c* – Kamyshovaya; *d* – Dvoynaya

Conclusion

The hydrodynamic numerical model ADCIRC was used to study resonance properties of the water areas of the Sevastopol bays: Streletskaya, Kruglaya, Kamyshovaya, and Dvoynaya, which includes Kazachya and Solyonaya bays. Analytical estimates were used to control the resonance period values. The following conclusions can be drawn based on the analysis of the results of the calculations performed. The calculations were carried out for the water area of each bay separately. Waves in the bays water areas were excited by setting red-noise disturbance. The resonance periods of the above bays and spatial distribution of the spectral density of sea-level oscillations in their water areas were determined.

Most of the resonance periods identified for the Sevastopol bays are in satisfactory agreement with the analytical estimates of these periods. In Streletskaya Bay, however, it was not possible to excite the Helmholtz mode (the period of which, according to analytical estimates, is approximately 13.5 min) by setting red-noise disturbance. The period of the senior resonance mode of Kamyshovaya Bay was 12.9 min, which differs significantly from the analytical assessment of 19.8 min. This is because the bay water area has a complex spatial structure and two protective breakwaters built at its entrance.

The use of realistic bathymetry and shoreline profile data in the modelling allowed obtaining additional resonance periods for all the considered bays, which cannot be obtained with analytical estimates.

The spectral composition expansion of the resonance modes due to connection of these bays via their entrances was revealed in Dvoynaya Bay, which includes Kazachya and Solyonaya Bays.

The spectral density spatial distribution of the main energy-carrying sea level oscillations in Streletskaya, Kruglaya, Kamyshovaya and Dvoynaya Bays was analysed to show that the spectral density peaked mainly in the bay tops. In Dvoynaya Bay, the spectral density maxima manifested in the eastern or western arms (Kazachya or Solyonaya bays, respectively) depending on which of the arms their natural periods belonged to.

To clarify the resonance properties of the Sevastopol bays, *in situ* observations of the bay system are required.

The results of the study can be used in layout designing of hydraulic structures, development of mariculture, planning of wastewater outlets, etc.

References

1. Manilyuk, Y.V., Lazorenko, D.I. and Fomin, V.V., 2021. Seiche Oscillations in the System of Sevastopol Bays. *Water Resources,* 48(5), pp. 726–736. https://doi.org/10.1134/S0097807821050122
2. Rabinovich, A.B., 1993. *Long Gravitational Waves in the Ocean: Capture, Resonance, and Radiation*. Saint Petersburg: Gidrometeoizdat, 326 p. (in Russian).
3. Alekseev, D.V., Manilyuk, Yu.V. and Sannikov, V.F., 2017. [Seiche Currents in an Open-Entry Basin]. In: S. O. Papkov, ed., 2017. *Applied Problems of Mathematics. Materials XXV of International Scientific and Technical Conference (Sebastopol, September 18–22, 2017)*. Sevastopol, pp. 109–115 (in Russian).
4. Dotsenko, S.F. and Ivanov, V.A., 2010. [*The Azov-Black Sea Region Nature Catastrophes*]. Sevastopol: ECOSI-Gidrofizika, 174 p. (in Russian).
5. Liu, P.L.-F., Monserrat, S., Marcos, M. and Rabinovich, A.B., 2003. Coupling Between Two Inlets: Observation and Modeling. *Journal of Geophysical Research: Oceans*, 108(C3), 3069. https://doi.org/10.1029/2002JC001478
6. Manilyuk, Yu.V., Lazorenko, D.I. and Fomin, V.V., 2020. Investigation of Seiche Oscillations in the Adjacent Bays by the Example of the Sevastopol and the Quarantine Bays. *Physical Oceanography*, 27(3), pp. 242–256. https://doi.org/10.22449/1573-160X-2020-3-242-256
7. Fomicheva, L.A., Rabinovich, A.B. and Demidov, A.N., 1991. [Sea Level]. In: E. N. Altman and A. I. Simonov, eds., 1991. *Hydrometeorology and Hydrochemistry of Seas in the USSR. Vol. IV. Black Sea. Issue 1. Hydrometeorological Conditions*. Leningrad: Gidrometeoizdat, pp. 329–354 (in Russian).
8. Morozov, A.N., Lemeshko, E.M., Shutov, S.A. and Zima, V.V., 2012. Currents in the Sevastopol bay from ADCP-observations (June, 2008). *Morskoy Gidrofizicheskiy Zhurnal*, (3), pp. 31–43 (in Russian).
9. Medvedev, I.P., 2018. Tides in the Black Sea: Observations and Numerical Modelling. *Pure and Applied Geophysics*, 175(6), pp. 1951–1969. https://doi.org/10.1007/s00024-018-1878-x
10. Goriachkin, Yu.N., Ivanov, V.A., Repetin, L.N. and Khmara, T.V., 2002. [Seiches in Sevastopol Bay]. In: UHMI, 2002. *Trudy UkrNIGMI = Proceedings of UHMI*. Kiev: UHMI. Vol. 250, pp. 342–353 (in Russian).

11. Manilyuk, Yu.V., Fomin, V.V., Yurovsky, Yu.Yu. and Bagaev, A.V., 2024. Sea Level Oscillations Spectra of a Shallow Coastal Bay: Cost-Effective Measurements and Numerical Modelling in Kruglaya Bay. *Regional Studies in Marine Science*, 69, 103326. https://doi.org/10.1016/j.rsma.2023.103326
12. Manilyuk, Yu.V., Lazorenko, D.I., Fomin, V.V. and Alekseev, D.V., 2023. Study of Seiche Oscillation Regimes in Sevastopol Bay. *Oceanology*, 63(6), pp. 796–805. https://doi.org/10.1134/s0001437023060115
13. Balinec, N.A. and Khmara, T.V., 2006. Phenomena of Harbor Seiches in the Sevastopol Bays. *Ecological Safety of Coastal and Shelf Zones and Comprehensive Use of Shelf Resources*, 14, pp. 204–208 (in Russian).
14. Fomin, V.V., Lazorenko, D.I. and Ivancha, E.V., 2017. Numerical Simulation of Seiches in the Balaklava Bay. *Ecological Safety of Coastal and Shelf Zones of Sea*, (3), pp. 32–39 (in Russian).
15. Rabinovich, A.B., Monserrat, S. and Fain, I.V., 1999. Numerical Modeling of Extreme Seiche Oscillations in the Region of the Balearic Islands. *Oceanology*, 39(1), pp. 12–19.
16. Belokon, A.Y. and Lazorenko, D.I., 2024. Energy Spectra of Sea Level Fluctuations During Propagation Long Waves in Branched Bays. In: V. Karev, ed., 2024. *Proceedings of the 9th International Conference on Physical and Mathematical Modelling of Earth and Environmental Processes 2023*. Springer Proceedings in Earth and Environmental Sciences. Cham: Springer, pp. 471–484. https://doi.org/10.1007/978-3-031-54589-4_49
17. Ivanov, V.A., Manilyuk, Yu.V., Sannikov, V.F., 2018. Seiches in a Basin with an Open Entrance. *Journal of Applied Mechanics and Technical Physics*, 59(4), pp. 594–600. https://doi.org/10.1134/S0021894418040041

Submitted 18.09.2024; accepted after review 23.12.2024;
revised 25.03.2025; published 30.06.2025

About the authors:

Yuri V. Manilyuk, Research Associate, Wave Theory Department, Marine Hydrophysical Institute of RAS (2 Kapitanskaya St., Sevastopol, 299011, Russian Federation), PhD (Phys.-Math.), **ORCID ID: 0000-0002-5752-7562, ResearcherID: P-6662-2017, Scopus Author ID: 6602563261**, *uvmsev@yandex.ru*

Aleksandra Yu. Belokon, Senior Research Associate, Department of Computational Technologies and Computational Modeling, Marine Hydrophysical Institute of RAS (2 Kapitanskaya St., Sevastopol, 299011, Russian Federation), PhD (Phys.-Math.), **ORCID ID: 0000-0002-1299-0983, ResearcherID: M-6839-2018**, *a.bazykina@mhi-ras.ru*

Andrei V. Bagaev, Leading Research Associate, Marine Hydrophysical Institute of RAS (2 Kapitanskaya St., 299011, Sevastopol, Russian Federation), PhD (Phys.-Math.), **ORCID ID: 0000-0003-4018-7642, ResearcherID: K-5373-2016**, *a.bagaev1984@mhi-ras.ru*

Yury Yu. Yurovsky, Leading Research Associate, Head of the Applied Marine Physics Laboratory, Marine Hydrophysical Institute of RAS (2 Kapitanskaya St., Sevastopol, 299011, Russian Federation), PhD (Phys.-Math.), **Scopus Author ID: 24377122700, ORCID ID: 0000-0002-9995-3965, ResearcherID: F-8907-2014**, *y.yurovsky@mhi-ras.ru*

Dmitry I. Lazorenko, Research Associate, Marine Hydrophysical Institute of RAS (2 Kapitanskaya St., Sevastopol, 299011, Russian Federation), PhD (Tech.), **ORCID ID: 0000-0001-7524-565X, ResearcherID: J-1925-2015**, *d.lazorenko.dntmm@gmail.com*

Contribution of the authors:

Yuri V. Manilyuk – statement of the problem, review of literature on the research problem, description of the research results, implementation of numerical experiments, analysis of the modeling results, writing the text of the article

Aleksandra Yu. Belokon – review of literature on the research problem, processing and description of the results of mathematical modeling, writing the text of the article, preparing graphic materials

Andrei V. Bagaev – processing and analysis of modeling results, preparation of the text of the article

Yury Yu. Yurovsky – processing and analysis of modeling results, preparation of the text of the article

Dmitry I. Lazorenko – preparation of input parameters for mathematical modeling, performing numerical experiments

All the authors have read and approved the final manuscript.

Original paper

Assessment and Characterization of Microplastics in Aquatic Environments near Pekalongan (Indonesia)

S. Widada [1], Kunarso [1], E. Indrayanti [1], R. Widiaratih [1], A. Ismanto [1], M. Zainuri [1, 3] *, T. Hadibarata [2], M. A. Anindita [1], T. Tristanova [1], M. S. Jihadi [1, 3]

[1] *Department of Oceanography, Faculty of Fisheries and Marine Science, Diponegoro University, Semarang, Indonesia*
[2] *Environmental Engineering Program, Faculty of Engineering and Science, Curtin University Malaysia, Miri, Malaysia*
[3] *Center for Coastal Rehabilitation and Disaster Mitigation Studies, Diponegoro University Jl. Prof. Soedarto SH., Tembalang, Semarang, Central Java, Indonesia*
* *e-mail: muhammadzainuri@lecturer.undip.ac.id*

Abstract
The occurrence of microplastics in the marine environment and their impact on the environment, biodiversity, and human life is concerning. Pekalongan is an industrial city with various anthropogenic activities such as fisheries, aquaculture, household, and most notably the batik textile industry. This research was carried out to determine the spatial distribution and characteristics of microplastics in the water and sediment of the Pekalongan coastal area. Water samples were collected at 10 stations (at 5 of them sediments were sampled as well) in the Sengkarang River estuary and its surroundings. Microplastics were identified using the optical microscopy method, followed by Fourier transform infrared spectroscopy (FTIR) testing to determine the polymer of microplastics. Microplastics were characterized using a Motic SMZ-161 microscope, then photographed using a Moticam A5 and counted based on each characteristic. In this study, we found polymers such as polystyrene, polyethylene, polyamide, and polyester. The abundance of microplastics in seawater was 214.4 particles/L and 300 particles/kg in suspended sediments. The microplastics types included fibers, fragments, films, and pellets of various colors and sizes. The dominant microplastic type in seawater and sediments was fiber (44%, 44%), followed by fragments (28%, 25%), foam (15%, 13%), and pellets (7%, 16%). White was the dominant color in seawater (54%) and sediments (53%), blue (21%, 18%), and red (15%, 17%), while yellow, green, and black were also found in small portions. The size of microplastics ranged from 1 μm to 10 mm, and the dominant size range was in the 50–250 μm group. The highest concentration of microplastics in the seawater was found in site *B5* with a concentration of 360 particles/L, while the highest concentration of microplastics in sediments was found in site B4 (389 particles/kg). Site *B5* is located in the midwater area but still close to the estuary, where the pollution from the surrounding areas flows to the location. Site *B4* is in the littoral-intertidal zone where the water is affected by tides and is prime location for sedimentation to occur.

Keywords: microplastics, Pekalongan, North Java Coast, estuary, pollution

Acknowledgments: This work was supported by the Research for International Publications program managed by the Universitas Diponegoro, and that fund was sourced other than APBN UNDIP Number 609-64/UN7.D2/PP/VIII/2023. Collaboration from Curtin University Malaysia is highly appreciated.

For citation: Widada, S., Kunarso, Indrayanti, E., Widiaratih, R., Ismanto, A., Zainuri, M., Hadibarata, T., Anindita, M.A., Tristanova, T. and Jihadi, M.S., 2025. Assessment and Characterization of Microplastics in Aquatic Environments near Pekalongan (Indonesia). *Ecological Safety of Coastal and Shelf Zones of Sea*, (2), pp. 99–117.

Оценка и характеристики микропластика в водной среде в районе Пекалонгана (Индонезия)

С. Видада [1], Кунарсо [1], Э. Индраянти [1], Р. Видиарати [1], А. Исманто [1], М. Зайнури [1, 3] *, Т. Хадибарата [2], М. А. Аниндита [1], Т. Тристанова [1], М. Ш. Джихади [1, 3]

[1] *Department of Oceanography, Faculty of Fisheries and Marine Science, Diponegoro University, Semarang, Индонезия*
[2] *Environmental Engineering Program, Faculty of Engineering and Science, Curtin University Malaysia, Miri, Малайзия*
[3] *Center for Coastal Rehabilitation and Disaster Mitigation Studies, Diponegoro University Jl. Prof. Soedarto SH., Tembalang, Semarang, Central Java, Индонезия*
* *e-mail: muhammadzainuri@lecturer.undip.ac.id*

Аннотация

Присутствие микропластика в морской среде и его воздействие на окружающую среду, биоразнообразие и жизнь человека вызывают обеспокоенность. Пекалонган – промышленный город, в котором ведется разнообразная хозяйственная деятельность, например рыболовство, аквакультура, домашнее хозяйство и особенно текстильная промышленность (производство батика). Цель исследования – определить пространственное распределение и характеристики микропластика в воде и донных отложениях прибрежной зоны Пекалонгана. Пробы воды были отобраны на 10 станциях; на пяти из них также взяты пробы донных отложений. Район отбора проб охватывал устье реки Сенгкаранг и прилегающие территории. Микропластик идентифицировали методом оптической микроскопии, а полимерный состав определяли методом инфракрасной спектроскопии с преобразованием Фурье (*FTIR*). Микропластик характеризовали с помощью микроскопа *Motic SMZ*-161, затем фотографировали на камеру *Moticam A*5 и подсчитывали по каждой категории. В ходе исследования были идентифицированы полимеры: полистирол, полиэтилен, полиамид и полиэстер. Концентрация микропластика составила 214.4 част/л в морской воде и 300 част/кг в донных отложениях. Выделены следующие типы частиц: волокна, фрагменты, пленки и гранулы различных цветов и размеров. Во всех средах преобладали волокна (44 в воде и 44 % в отложениях), за ними следовали фрагменты (28 и 25 % соответственно), вспененный материал (15 и 13%) и гранулы (7 и 16 %). Наиболее распространенным был белый цвет пластика (54 в воде, 53 % в отложениях), затем синий (21 и 18 %) и красный (15 и 17 %). Желтый, зеленый и черный цвета встречались реже. Размер частиц варьировался от 1 мкм до 10 мм, при этом наиболее частым был диапазон 50–250 мкм. Максимальная концентрация микропластика в морской воде зафиксирована на ст. *B1* (360 част/л), а в донных отложениях – на ст. *B4*. Это объясняется расположением станции *B1* на реке вблизи насосной станции, куда поступают загрязнения с прилегающих территорий. Станция *B4* находится в литоральной зоне, подверженной влиянию приливно-отливных течений, что способствует интенсивному накоплению отложений.

Ключевые слова: микропластик, Пекалонган, северное побережье Явы, эстуарий, загрязнение

Благодарности: работа выполнена в рамках программы Research for International Publications Университета Дипонегоро и финансировалась из источников, не являющихся APBN UNDIP № 609-64/UN7.D2/PP/VIII/2023. Авторы высоко ценят сотрудничество с Университетом Кертина, Малайзия.

Для цитирования: Assessment and Characterization of Microplastics in Aquatic Environments of Pekalongan Waters / S. Widada [et al.] // Экологическая безопасность прибрежной и шельфовой зон моря. 2025. № 2. С. 99–117. EDN VHKNLA.

Introduction

Waste has been dumped into the ocean for centuries, but recently the composition of marine debris has drastically changed. Most garbage used to be composed of organic biodegradable items some decades ago. Synthetic materials including plastics, are now prevalent in solid waste. Plastic is one of the major non-organic waste segments in our daily output of municipal solid waste production [1]. Bottles of plastic, ropes, tarpaulins, and synthetic fishing lines float freely, decay slowly, and break into smaller pieces [2]. As the characteristics of microplastic is buoyant and durable, they accumulate on beaches, ocean eddies, and enclosed or semi-enclosed seas where surface water is held for extended periods [3]. Plastic is highly buoyant; thus, it can be carried out for thousands of miles by currents and dispersed across the marine environment, which can be detrimental to marine ecosystems [4–6].

Microplastics are solid particles of polymer with regular or irregular shape and size between 1 μm and 5 mm. Plastic breaks down into finer particles [7–9]. Microplastics made up approximately 92% of the 5.25 trillion plastic particles present at global scale in the ocean [10–12]. Research on microplastics in the Java Sea was first conducted by Purba et al. in 2016 [13] with results of 0.2 mg/L microplastics detected in Java Sea water. Various human activities on land, coastal, and marine areas are the main sources of microplastics present in the Java Sea waters. It is believed that around 75–95% of plastic waste in the marine environment comes from land-based sources, and the remaining 5–25% comes from the ocean [14] like unintentional loss or illegal disposal during offshore drilling or fishing [10]. Because microplastics can be consumed by marine life, and eventually kill them, their effects on the marine biota are concerning [15]. Microplastics can also potentially reduce aquaculture's economic benefits by causing oxidative stress in aquaculture products, altering their behaviour, growth, and reproduction, and even causing them to die [16].

Pekalongan is a coastal industrial and tourist city covering 45.25 km^2 and has population of 315,997 people. The city has various anthropogenic activities including 364 companies that process fish, with ponds and cultivation areas cover 331,292 ha; 634 batik industries, and up to 75 medium- to large-sized companies that make food, textiles, plastics, and shipyard activities (BPS Pekalongan, 2022). Due to this, the garbage produced in Pekalongan City each day approaches 140 tons, or 0.46 kg per resident (Pekalongan City, 2023). The city of Pekalongan's industries use plastic materials in their operations and output. A hazardous consequence of microplastics in sediments and waterways is the disturbance of the ecosystem's biotic and abiotic water ecology [17, 18]. This research was carried out to determine

the spatial distribution and also to identify the abundance, shape, size, color, and polymer type of microplastics in water and suspended sediment samples in Pekalongan waters.

Materials and Methods

The research location was in Pekalongan Waters, Central Java, in the Sengkarang River estuarine area and the surrounding waters. The purposive field sampling method was used to determine 10 sampling sites for microplastics in seawater and 5 sampling sites for sediment samples (sites *B1–B4*, and *B9*), as shown in Fig. 1. The sites were defined as such to represent the coastal environment, both on the seaward, estuary, and riverine areas.

Collection of samples was conducted during the dry season with three replications. The upstream and downstream areas of the Sengkarang River are located within residential areas, textile industries, tourist attractions, fishing grounds, and wastewater treatment plants.

During the collection of samples, half of the 108 μm plankton net was dipped into the surface. The volume of filtered water taken was 10 m^3 (the collected water discharge was calculated using a flow meter). The sediment samples were taken using a grab sampler at each location sites with a total sample of 400 grams.

Water samples were filtered using a vacuum pump and then mixed with 30% Fe (II) solution and H_2O_2 to remove organic matter that was still contained in the sample. The density of the microplastic in the water samples was increased by using NaCl. Each sediment sample was extracted through the process of density separation method using $ZnCl_2$ solution (1.6 $g \cdot L^{-1}$), and the sediment-salt mixture solution was mixed with a spatula [19], HCl was used to remove organic matter that was still contained. The method of testing water and sediment samples refers to the National Oceanic and Atmospheric Administration (NOAA) method with minor adjustments [1)].

Multiple measures were implemented to minimize the possibility of microplastics contamination during the microplastics analysis procedure. Sampling equipment and glassware were rinsed with purified water several times and were dried before use. There were no plastic consumables used in the process of sample collection and extraction. The filters, laboratory consumables, and the solvent were always covered with aluminium foil during the sample extraction procedure. Latex gloves and cotton laboratory coats were used during the microplastics sampling and extraction process. Sample separation was performed by filtration using 0.45 μm cellulose filter membranes. The filter paper was observed under a microscope using the sweeping method to see each type of microplastic. Microplastics were identified using the optical microscopy method [20]. Optical microscopy was the first method of characterization used to observe microplastics [21], followed by Fourier Transform Infrared Spectroscopy (FTIR) testing to determine the polymer of microplastics [22]. Polymer identification was done by dissolving microplastics that is already filtered, and then the solution is pipetted and placed under the FTIR.

---

1) Masura, J., Baker, J., Foster, G., Arthur, C. and Herring, C., 2015. *Laboratory Methods for the Analysis of Microplastics in the Marine Environment: Recommendations for Quantifying Synthetic Particles in Waters and Sediments*. Silver Spring, MD, USA: NOAA, (NOAA Technical Memorandum NOS-OR&R-48).

Microplastic shape, size, and color identification was performed using a Motic SMZ-161 microscope. After that, the microplastics found were photographed using a Moticam A5 and counted based on each characteristic. Statistical data analysis was conducted on the type, size, color, number, and abundance of microplastics. The results of data analysis will be displayed in graphical form for each sample. The distribution of microplastics was visualized in the spatial map.

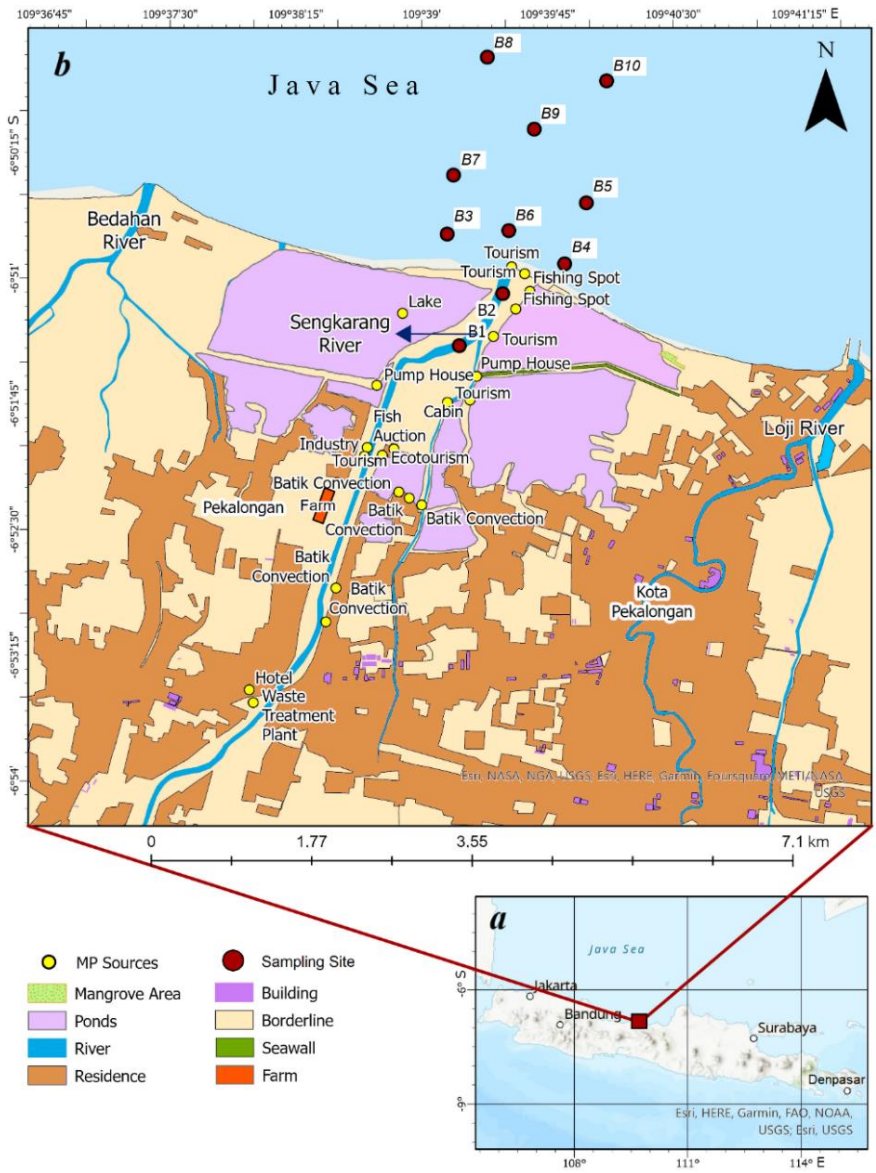

Fig. 1. Map of Java Island, the red square denotes the area of interest (*a*), the enlarged image of the area of interest (*b*)

Results

The spatial abundance of microplastics in seawater and sediment in Pekalongan waters is shown in Fig. 2. The average abundance of MPs in seawater was 214.4 particles/L and 300 particles/kg in suspended sediment. Site *B1* was located in the Sengkarang River, close to the pump house, tourist area, fish auction, and ponds. Site *B2* is located in the Sengkarang estuarine area, close to the beach and fishing grounds. The littoral or intertidal area is represented by sites *B3*, *B4* (close to the mangrove area), and *B6*. Sites *B5* and *B7*, were in the middle water area, and sites B8, *B9* and *B10* were in deep water quite far from anthropogenic activities other than marine fishing (Table 1). The abundance of microplastics in seawater and sediment has significant differences. The abundance of MPs in sediments had higher numbers.

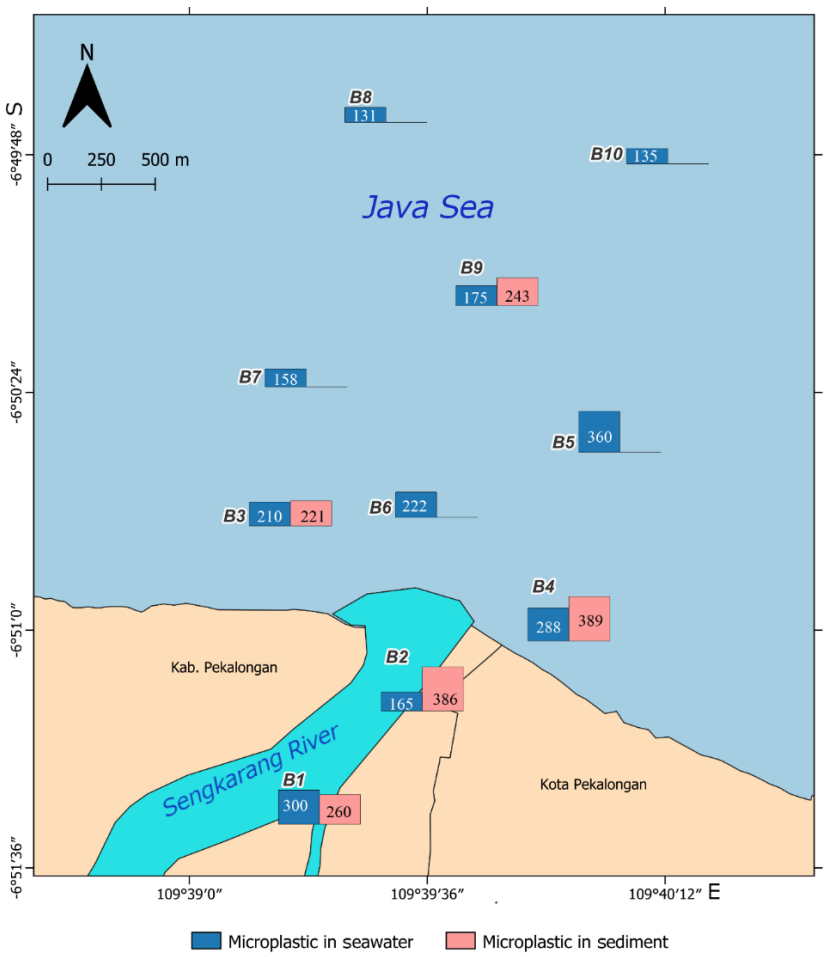

Fig. 2. Microplastics abundance in water, particle/L, and sediments, particle/kg

Table 1. Abundance of microplastics in seawater, particles/L, and sediments, particles/kg, at different sampling sites

Site	Abundance of microplastics		Description of sampling location
	in seawater	in sediments	
B1	300	260	Sengkarang River area, near pump house, tourism area, fish auction, ponds
B2	165	386	Mouth or estuarine of Sengkarang River, tourism area, fishing spot area /
B3	210	221	Near coastal area
B4	280	389	Near coastal area, mangrove area
B5	360	–	Midwater water area
B6	220	–	Near coastal area
B7	158	–	Midwater area
B8	175	–	Open water
B9	131	243	Open water
B10	135	–	Open water

In this research, the types of microplastics shown in Fig. 3, *a* were found. Fiber types were most prevalent in seawater samples (44%) and sediment samples (44%). The second most prevalent type found in Pekalongan waters was the fragment type, which constituted 28% of seawater samples and 25% of sediment samples. In the samples, 15% of foam types were found in seawater samples and 13% in sediments. The pellet type in seawater amounted to 7%, and in sediment it amounted to 16%.

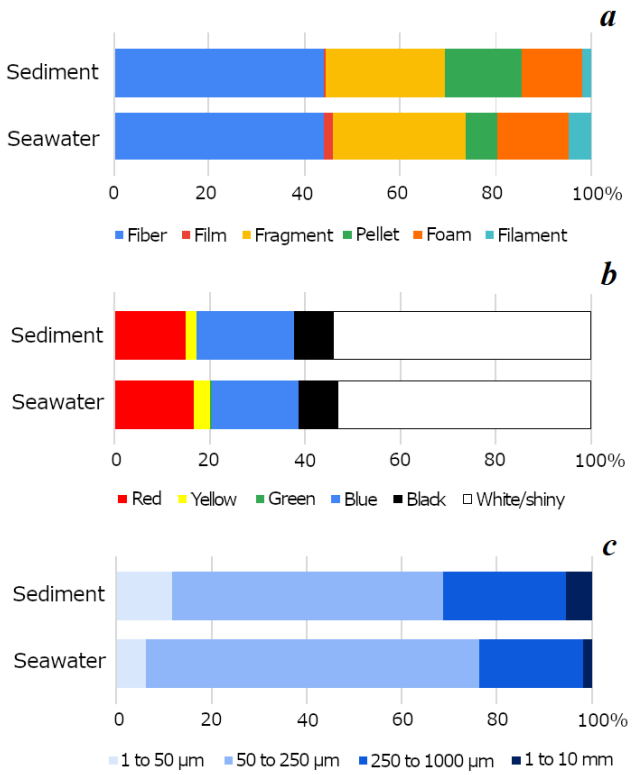

Fig. 3. Percentage of microplastics types (*a*), colors (*b*), and size (*c*) in seawater near Pekalongan

Figure 3, *b* shows the percentage of microplastic color in seawater and sediment samples. The MPs color in seawater and sediment was dominated by white/shiny at 54% in seawater samples and 53% in sediment samples. The second most common color was blue at 21% in water samples and 18% in sediment samples, followed by red at 15% in water samples and 17% in sediment samples. In this study, yellow and black MPs were also found, as well as green ones. The size distribution of microplastics is depicted in Fig. 3, *c*, where size groups include 1–50 µm, 50–250 µm, 250–1000 µm, and 1–10 mm. Microplastics between 50 and 250 µm dominated the samples with 57% in seawater and 70% in sediment. Followed by the 250–1000 µm size group, with 26 % in seawater samples and 22% in sediment samples. The 1–50 µm size was only found in 12% of all seawater samples and 6% of all sediment samples. Microplastics with sizes 1–10 mm were rarely found, only 6% of the total seawater MP and 6% of the total sediment MP. Figure 4 is a bar graph displaying the color and size distribution at each station in Pekalongan waters.

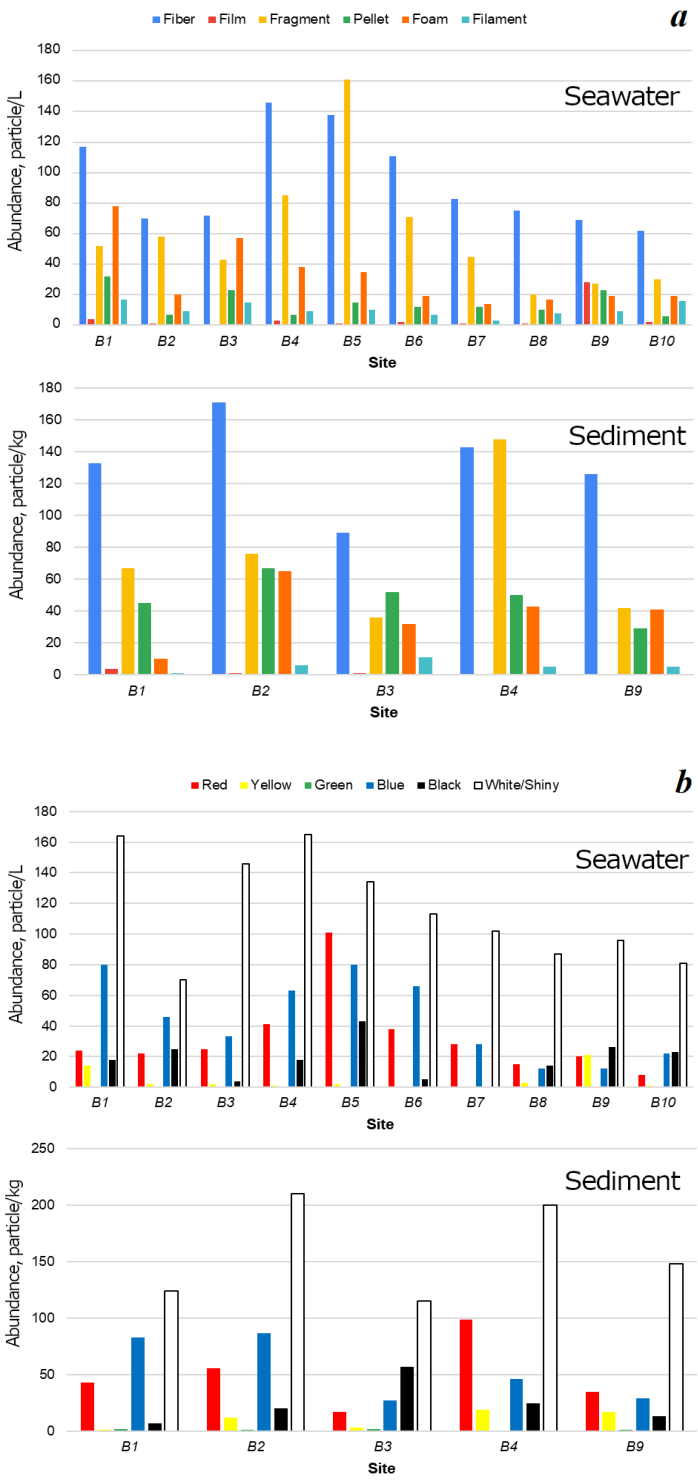

F i g . 4 . Distribution chart of microplastics by types (*a*), colors (*b*), and size (*c*) in each site

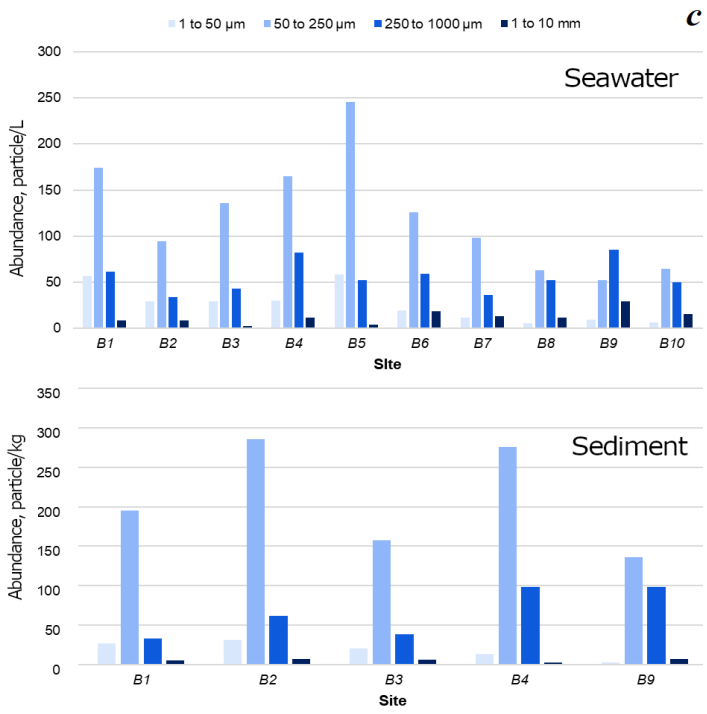

Continued Fig. 4 / Продолжение Рис. 4

Discussion

The presence of MPs in the water and sediments in Fig. 2 related to the texture of the sediment which affects their ability to capture microplastics. The softer the sediment texture, the better its ability to capture microplastics [23]. Based on the research conducted by Yuanita et al. in 2022 [24], the type of sediment in coastal Pekalongan is non-cohesive sediment dominated by sand. This may affect the number of microplastic particles in Pekalongan sediments. In addition to certain accumulation zones in the high seas, marine debris is often more prevalent in shallow coastal areas [25]. This theory is consistent with the present study, where areas close to anthropogenic activities such as rivers, estuaries and coasts had higher abundance compared to central and deep-water areas. Coastal areas sampled both offshore and nearshore by Montoto et al. in 2020 [26] also showed this difference.

The MPs fibers shown in Fig. 3, *a*, are usually ascribed to terrestrial sources, such as river flow and urban runoff [27]. These fiber microplastics are most likely detached from clothing and fabrics through washing or from fishing lines and ropes used in nearby shipping and fishing operations [28]. While the fragment type present in Fig. 3, *a* were mainly generated by fragmentation of plastic products containing hard plastic polymers, such as packaging (beverage bottles and plastic container) [29]. Microplastics in the form of foam are widely used as packaging materials (food containers) and transportation packaging [30]. In addition, the pellet form had less quantity compared to other groups of microplastic forms. Typically, pellets come from the direct discharge of primary microplastics from manufactured plastic waste and residential waste products used for personal care [31].

The results of ATR-FTIR analysis for Pekalongan waters were similar to the research results by Ismanto et al. (2023) [32] that found polystyrene, polyester, and polyamide in the stream area up to the estuary of the Loji River in Pekalongan. In the present study, the same polymers, polystyrene (PS), polyethlene (PE), polyamide (PA), and polyester (PES) were found. Polyester is the dominant polymer, which is commonly used in textile and product packaging industries [33]. Indications of waste from anthropogenic activities are supported by the dominance of fibers and fragments (secondary microplastics) compared to pellets (primary microplastics) [34]. Density also influences the abundance of MPs as it determines how widely they are distributed throughout the water column [35]. The density of polystyrene foam (PS) 0.01–0.05 g/cm^3 was used as a reference. This polymer is expected to float on the surface of water because its density is lower than that of seawater (1.0267 g/cm^3). However, being denser than water, some polymers, such as solid PS (1.04–1.50 g/cm^3), tend to sink slower in the water column [36].

Previous research on microplastics in marine waters and estuaries in Indonesia is shown in Table 2. The abundance of MPs particles in seawaters and sediments in each region varies significantly. The abundance of microplastics in Pekalongan is higher than in several cases, such as Tambak Lorok, Semarang, Indonesia [37], Jakarta Bay, Indonesia [38], and Trengganu Estuary, Malaysia [39]. Several factors cause the large abundance of microplastics in Pekalongan, namely the anthropogenic waste, small scale industries, and textile industries. Cases with high amounts of microplastics use a mobile water pump with an additional mesh net filter [39]. This method produces an abundance of microplastics comparatively higher than the manual sampling method using a net [34, 40, 41]. Variations in microplastic abundance are greatly affected by the level of pollution, sampling location, and water hydrodynamics in each study area.

Table 2. Previous microplastics research used for comparison

Location	Sample	Methods	Identification tool	Abundance	Ref.
Banten Bay, Indonesia	Sediment	Smith-McIntyre grabs	Nikon Eclipse E600 stereo microscope	267 ± 98 particles/kg	[42]
Tambak Lorok, Semarang, Indonesia	Water and sediment	Gravity corer	Microscope Olympus MD 50	7–111 particles/10 mL seawater and 8–49 particles/g sediment	[37]

Continued Table 2

Location	Sample	Methods	Identification tool	Abundance	Ref.
Bintan Water, Indonesia	Water	Neuston net	Hirox Digital Microscope KH-8700	0.45 pieces per m^3	[40]
Jakarta Bay, Indonesia	Surface Water	Round net	Nikon SMZ 745T stereo microscope	9.729 to 89.164 nm^{-3}, with an average of 48.179 ± 21.960 nm^{-3}	[38]
Lampung and Sumbawa, Indonesia	Sediment and sandfish	Van Veen grab & local fishers	Nikon Eclipse Ni–U microscope	72.64 ± 25.28 particles/kg (sediments) 2.01 ± 1.59 particles /individual (fish)	[43]
Brantas Water, Indonesia	*Gambusia affinis*	Random sampling	Olympus CX-23 Lighting System	Downstream (209.18 ± 48.85 particles/g) upstream (24.44 ± 0.14 particles/g)	[44]
Ciliwung Estuary, Indonesia	Water and *Aplocheilus* sp.	Manta trawl net & randomly collected	Nikon DF-12 stereo microscope	River flow (9.37 ± 1.37 particles/m^3), coastal waters (8.48 ± 9.43 particles/m^3), and in 75% samples of *Aplocheilus* sp. (1.97 particles/individual)	[41]

End of Table 2

Location	Sample	Methods	Identification tool	Abundance	Ref.
Benoa Bay, Bali, Indonesia	Surface water	Mini manta trawl net equipped with flow-meter	Stereo microscope Nikon Eclipse Ni-U	1.41–1.88 particles/m^3	[34]
Trengganu Estuary, Malaysia	Seawater & zoo-plankton	Mobile water pump & 2000 μm mesh net filter	Olympus SZX7, Olympus CX21	545.8 particles/m^3	[39]
Yellow Sea, China	Surface water	Manta trawl net	Stereo microscope M205FA	0.63 ± 0.57 particles/m^3	[45]
Northern Indian Ocean	Surface water	Manta net	Nikon SMA800N	Pre-monsoon 15,200 ± 7999 no./km^2, monsoon 18,223 ± 14,725 no./km^2 and post monsoon 72,381 ± 77,692 no./km^2	[46]

Conclusion

The assessment and characterization of microplastics in the waters around Pekalongan showed that both seawater and sediment samples were polluted with microplastics. The average microplastics abundances were 214.4 particles/m³ in seawater and 300.0 particles/kg in suspended sediments. The highest concentration of microplastics in the seawater was found in site *B5* with a concentration of 360 particles/L, while the highest concentration of microplastics in sediments was found in site *B4* (389 particles/kg). Site *B5* is located in the located in the mid-water area but still close to the estuary, where the pollution from the surrounding areas flows to the location. Site *B4* is in the littoral-intertidal zone where the water is affected by tides and is prime location for sedimentation to occur.

Four main types of microplastics were identified: fibers (44% both in water and sediments), fragments (28% in water and 25% in sediments), foam (15% in water and 13% in sediments), and pellets (7% in water and 16% in sediments). The prevalent fibers are likely to have detached from clothing and fabric or fishing lines and ropes, while the fragments primarily come from the degradation of hard plastic products (bottles, containers).

The dominant color was white, accounting for 54% in water and 53% in sediments. The most widespread size range was 50–250 μm (57 and 70% in water and sediments, respectively).

The detection of various polymers (polystyrene, polyethylene, polyamide and polyester) suggests that the microplastics originate from diverse anthropogenic activities, including urban runoff, fisheries, batik industries.

The existence of widely distributed microplastics in the environment is the reason for the concern about water quality, ecosystems, and human health. Fourteen million tons of microplastics are estimated to be accumulated in the bottom of the ocean [47]. Aquatic biotas, ranging from plankton to large marine mammals, are likely to ingest microplastics. Humans are being exposed to microplastics through the ingestion of contaminated seafood and other foods and beverages, or through the inhalation of airborne microplastics. Along with increasing scientific understanding of the risks caused by plastic pollution and greater policy attention to reduce these risks, multiple governments are now looking at ways to address the emission of microplastics into the environment.

In response to growing concerns over the risks related to plastic pollution, Indonesia has introduced measures to reduce plastic widespread into the environment, mainly through better waste management policies, a ban on single-use plastics that are often discarded carelessly, and restrictions on the manufacture and distribution of personal care products and cosmetics which contain microplastics. Indonesia has carried out a priority program to improve waste management in several tourist locations, including marine national parks, to prevent and collect plastic waste in the sea for recycling, as well as address the issue of the impact of plastic waste and microplastics. In 2017, monitoring and surveys of plastic waste in the sea were carried out, using UNEP and NOAA guidelines in 18 coastal areas in 18 cities/districts, from 25 priority cities/districts, and will continue in the following years. As with the waste management target following Presidential Regulation Number 97 of 2017, namely reducing waste from the source by 30% and waste handling by 70% by 2025, Indonesia is adapting its commitment at the international

level, with a target of reducing marine waste by 70% by 2025 (KLHK (Ministry of Environment and Forestry) press release, 2018). Mitigation efforts from residents can be done through the 6 R movement: Reduce, Reuse, Recycle, Repair, Refuse, Rethink [48], separating the types of waste from the beginning, encouraging the role of government through education and regulation, research and technology support and increase the comfort of the local civilian and visitors so that the function of Pekalongan waters remains sustainable.

References

1. Kibria, M.G., Masuk, N.I., Safayet, R., Nguyen, H.Q. and Mourshed, M. 2023. Plastic Waste: Challenges and Opportunities to Mitigate Pollution and Effective Management. *International Journal of Environmental Research*, 17, 20. https://doi.org/10.1007/s41742-023-00507-z
2. Chamas, A., Moon, H., Zheng, J., Qiu, Y., Tabassum, T., Jang, J.H., Abu-Omar, M., Scott, S.L. and Suh, S., 2020. Degradation Rates of Plastics in the Environment. *ACS Sustainable Chemistry and Engineering*, 8(9), pp. 3494–3511. https://doi.org/10.1021/acssuschemeng.9b06635
3. Lassen, C., Hansen, S.F., Magnusson, K., Hartmann, N.B., Rehne Jensen, P., Nielsen, T.G. and Brinch, A., 2015. *Microplastics: occurrence, effects and sources of releases to the environment in Denmark*. Danish Environmental Protection Agency, 207 p. Available at: https://backend.orbit.dtu.dk/ws/portalfiles/portal/118180844/Lassen_et_al._2015.pdf [Accessed: 28 May 2025].
4. Jambeck, J.R., Geyer, R., Wilcox, C., Siegler, T.R., Perryman, M., Andrady, A., Narayan, R. and Law, K.L., 2015. Plastic Waste Inputs from Land into the Ocean. *Science*, 347(6223), pp. 768–771. https://doi.org/10.1126/science.1260352
5. Nchimbi, A.A., Shilla, D.A., Kosore, C.M., Shilla, D.J., Shashoua, Y. and Khan, F.R., 2022. Microplastics in Marine Beach and Seabed Sediments along the Coasts of Dar es Salaam and Zanzibar in Tanzania. *Marine Pollution Bulletin*, 185, 114305. https://doi.org/10.1016/j.marpolbul.2022.114305
6. Sheavly, S. and Register, K., 2007. Marine Debris and Plastics: Environmental Concerns, Sources, Impacts and Solutions. *Journal of Polymers and the Environment*, 15, pp. 301–305. https://doi.org/10.1007/s10924-007-0074-3
7. McEachern, K., Alegria, H., Kalagher, A.L., Hansen, C., Morrison, S. and Hastings, D., 2019. Microplastics in Tampa Bay, Florida: Abundance and Variability in Estuarine Waters and Sediments. *Marine Pollution Bulletin*, 148, pp. 97–106. https://doi.org/10.1016/j.marpolbul.2019.07.068
8. Park, H. and Park, B., 2021. Review of Microplastic Distribution, Toxicity, Analysis Methods, and Removal Technologies. *Water*, 13(19), 2736. https://doi.org/10.3390/w13192736
9. Wulandari, S.Y., Radjasa, O.K., Bambang, Y., Aris, I., Muslim, M., Jarot, M., Siagian, H. and Siti, M., 2021. Microplastics Model Distribution in Semarang Waters. *Research Journal of Chemistry and Environment*, 25(1), pp. 109–120. Available at: https://www.researchgate.net/publication/348379282 [Accessed: 28 May 2025].
10. Coyle, R., Hardiman, G. and Driscoll, K.O., 2020. Microplastics in the Marine Environment: A Review of their Sources, Distribution Processes, Uptake and Exchange in Ecosystems. *Case Studies in Chemical and Environmental Engineering*, 2, 100010. https://doi.org/10.1016/j.cscee.2020.100010
11. Auta, H.S., Emenike, C.U. and Fauziah, S.H., 2017. Distribution and Importance of Microplastics in the Marine Environment: a Review of the Sources, Fates, Effects and Potential Solutions. *Environment International*, 102, pp. 165–176. https://doi.org/10.1016/j.envint.2017.02.013

12. Eriksen, M., Lebreton, L.C.M., Carson, H.S., Thiel, M., Moore, C.J., Borerro, J.C., Galgani, F., Ryan, P.G. and Reisser, J., 2014. Plastic Pollution in the World's Oceans: More than 5 Trillion Plastic Pieces Weighing over 250,000 Tons Afloat at Sea. *PLoS One*, 9(12), e111913. https://doi.org/10.1371/journal.pone.0111913

13. Pangestu, I.F., Purba, N.P. and Syamsudin, M.L., 2016. Microplastic Condition in Indramayu Waters, West Java. In: E. Afrianto [et al.], eds., 2016. *Proceedings of the National Seminar on Fisheries and Maritime Affairs: Technology, Law and Policy Synergy on Fisheries and Marine Sciences Toward Food Sovereignty in AEC (Bandung, Indonesia)*. 382.

14. Duis, K. and Coors, A., 2016. Microplastics in the Aquatic and Terrestrial Environment: Sources (with a Specific Focus on Personal Care Products), Fate and Effects. *Environmental Sciences Europe*, 28, 2. https://doi.org/10.1186/s12302-015-0069-y

15. Chatterjee, S. and Sharma, S., 2019. Microplastics in our Oceans and Marine Health. *Field Actions Science Reports*, (19), pp. 54–61. Available at: https://journals.openedition.org/factsreports/5257 [Accessed: 28 May 2025].

16. Wu, H., Hou, J. and Wang, X., 2023. A Review of Microplastic Pollution in Aquaculture: Sources, Effects, Removal Strategies and Prospects. *Ecotoxicology and Environmental Safety*, 252, 114567. https://doi.org/10.1016/j.ecoenv.2023.114567

17. Yap, H.S., Shukor, M.Y. and Yasid. N.A., 2022. The Microplastics Occurrence and Toxic Effects in Marine Environment. *Journal of Environmental Microbiology and Toxicology*, 10(2), pp. 1–6. https://doi.org/10.54987/jemat.v10i2.733

18. Bhuyan, M.S., 2022. Effects of Microplastics on Fish and in Human Health. *Frontiers in Environmental Science*, 10, pp. 1–17. https://doi.org/10.3389/fenvs.2022.827289

19. Nahian, S.A., Rakib, M.R.J., Kumar, R., Haider, S.M.B., Sharma, P. and Idris, A.M., 2023. Distribution, Characteristics, and Risk Assessments Analysis of Microplastics in Shore Sediments and Surface Water of Moheshkhali Channel of Bay of Bengal, Bangladesh. *Science of the Total Environment*, 855, 158892. https://doi.org/10.1016/j.scitotenv.2022.158892

20. Sierra, I., Chialanza, M.R., Faccio, R., Carrizo, D., Fornaro, L. and Pérez-Parada, A., 2019. Identification of Microplastics in Wastewater Samples by Means of Polarized Light Optical Microscopy. *Environmental Science and Pollution Research*, 27, pp. 7409–7419. https://doi.org/10.1007/s11356-019-07011-y

21. Wang, Z.M., Wagner, J., Ghosal, S., Bedi, G. and Wall, S., 2017. SEM/EDS and Optical Microscopy Analyses of Microplastics in Ocean Trawl and Fish Guts. *Science of the Total Environment*, 603–604, pp. 616–626. https://doi.org/10.1016/j.scitotenv.2017.06.047

22. Kalaronis, D., Ainali, N.M., Evgenidou, E., Kyzas, G.Z., Yang, X., Bikiaris, D.N. and Lambropoulou, D.A., 2022. Microscopic Techniques as Means for the Determination of Microplastics and Nanoplastics in the Aquatic Environment: A Concise Review. *Green Analytical Chemistry*, 3, 100036. https://doi.org/10.1016/j.greeac.2022.100036

23. Watters, D.L., Yoklavich, M.M., Love, M.S. and Schroeder, D.M., 2010. Assessing Marine Debris in Deep Seafloor Habitats Off California. *Marine Pollution Bulletin*, 60(1), pp. 131–138. https://doi.org/10.1016/j.marpolbul.2009.08.019

24. Yola, Yuanita, N., Kurniawan, A., Nugroho, E.O., Martin, R.J., Muhammad, I.F., Wijaya, F.S. and Fauzi, N., 2022. Coastal Protection System Design at the Indonesian Mangrove Center in Pekalongan, Central Java–Indonesia. In: IOP, 2022. *IOP Conference Series: Earth and Environmental Science. The Fourth International Conference on Sustainable Infrastructure and Built Environment 08/03/2022–09/03/2022 Online. ITB, Bandung, Indonesia*. IOP Publishing. Vol. 1065, iss. 1, 012062. https://doi.org/10.1088/1755-1315/1065/1/012062

25. Katsanevakis, S., 2008. Marine Debris, a Growing Problem: Sources, Distribution, Composition, and Impacts. In: T. N. Hofer, ed., 2008. *Marine Pollution: New Research*. New York: Nova Science Publishers, pp. 53–100.

26. Montoto-Martínez, T., Hernández-Brito, J.J. and Gelado-Caballero, M.D., 2020. Pump-Underway Ship Intake: An Unexploited Opportunity for Marine Strategy Framework Directive (MSFD) Microplastic Monitoring Needs on Coastal and Oceanic Waters. *PLoS ONE*, 15(5), e0232744. https://doi.org/10.1371/journal.pone.0232744

27. Qu, J., Wu, P., Pan, G., Li, J. and Jin, H., 2022. Microplastics in Seawater, Sediment, and Organisms from Hangzhou Bay. *Marine Pollution Bulletin*, 181, 113940. https://doi.org/10.1016/j.marpolbul.2022.113940

28. Tien, C., Wang, Z. and Chen, C.S., 2020. Microplastics in Water, Sediment and Fish from the Fengshan River System: Relationship to Aquatic Factors and Accumulation of Polycyclic Aromatic Hydrocarbons by Fish. *Environmental Pollution*, 265, part B, 114962. https://doi.org/10.1016/j.envpol.2020.114962

29. Shim, W.J., Hong, S.H. and Eo, S., 2018. Chapter 1 – Marine Microplastics: Abundance, Distribution, and Composition. In: E. Y. Zeng, ed., 2018. *Microplastic Contamination in Aquatic Environments*. Elsevier, pp. 1–26. http://dx.doi.org/10.1016/B978-0-12-813747-5.00001-1

30. Wang, T., Zou, X., Li, B., Yao, Y., Zang, Z., Li, Y., Yu, W. and Wang, W., 2019. Preliminary Study of the Source Apportionment and Diversity of Microplastics: Taking Floating Microplastics in the South China Sea as an Example. *Environmental Pollution*, 245, pp. 965–974. https://doi.org/10.1016/j.envpol.2018.10.110

31. Di, M. and Wang, J., 2018. Microplastics in Surface Waters and Sediments of the Three Gorges Reservoir, China. *Science of the Total Environment*, 616–617, pp. 1620–1627. https://doi.org/10.1016/j.scitotenv.2017.10.150

32. Ismanto, A., Hadibarata, T., Kristanti, R.A., Sugianto, D.N., Widada, S., Atmodjo, W., Satriadi, A., Anindita, M.A., Al-Mohaimeed, A.M. and Abbasi, A.M., 2023. A Novel Report on the Occurrence of Microplastics in Pekalongan River Estuary, Java Island, Indonesia. *Marine Pollution Bulletin*, 196, 115563. https://doi.org/10.1016/j.marpolbul.2023.115563

33. Avio, C.G., Gorbi, S. and Regoli, F., 2017. Plastics and Microplastics in the Oceans: from Emerging Pollutants to Emerged Threat. *Marine Environmental Research*, 128, pp. 2–11. https://doi.org/10.1016/j.marenvres.2016.05.012

34. Suteja, Y., Atmadipoera, A.S., Riani, E., Nurjaya, I.W., Nugroho, D. and Cordova, M.R., 2021. Spatial and Temporal Distribution of Microplastic in Surface Water of Tropical Estuary: Case Study in Benoa Bay, Bali, Indonesia. *Marine Pollution Bulletin*, 163, 111979. https://doi.org/10.1016/j.marpolbul.2021.111979

35. Flores-Ocampo, I.Z. and Armstrong-Altahatrin, J.S., 2023. Abundance and Composition of Microplastics in Tampico Beach Sediments, Tamaulipas State, Southern Gulf of Mexico. *Marine Pollution Bulletin*, 191, 114891. https://doi.org/10.1016/j.marpolbul.2023.114891

36. Crawford, C.B. and Quinn, B., 2016. *Microplastic Pollutants*. Elsevier Science, 336 p.

37. Khoironi, A., Hadiyanto, H., Anggoro, S. and Sudarno, S., 2020. Evaluation of Polypropylene Plastic Degradation and Microplastic Identification in Sediments at Tambak Lorok Coastal Area, Semarang, Indonesia. *Marine Pollution Bulletin*, 151, 110868. https://doi.org/10.1016/j.marpolbul.2019.110868

38. Purwiyanto, A.I.S., Prartono, T., Riani, E., Naulita, Y., Cordova, M.R., and Koropitan, A.F., 2022. The Deposition of Atmospheric Microplastics in Jakarta-Indonesia: The Coastal Urban Area. *Marine Pollution Bulletin*, 174, 113195. https://doi.org/10.1016/j.marpolbul.2021.113195

39. Taha, Z.D., Amin, R.M., Anuar, S.T., Nasser, A.A.A. and Sohaimi, E.S., 2021. Microplastics in Seawater and Zooplankton: A Case Study from Terengganu Estuary and Offshore Waters, Malaysia. *Science of the Total Environment*, 786, 147466. https://doi.org/10.1016/j.scitotenv.2021.147466

40. Syakti, A.D., Hidayati, N.V., Jaya, Y.V., Siregar, S.H., Yude, R., Suhendy, Asia, L., Wong-Wah-Chung, P. and Doumenq, P., 2018. Simultaneous Grading of Microplastic Size Sampling in the Small Islands of Bintan Water, Indonesia. *Marine Pollution Bulletin*, 137, pp. 593–600. https://doi.org/10.1016/j.marpolbul.2018.11.005

41. Cordova, M.R., Riani, E. and Shiomoto, A., 2020. Microplastics Ingestion by Blue Panchax Fish (Aplocheilus sp.) from Ciliwung Estuary, Jakarta, Indonesia. *Marine Pollution Bulletin*, 161, 111763. https://doi.org/10.1016/j.marpolbul.2020.111763

42. Falahudin, D., Cordova, M.R., Sun, X., Yogaswara, D., Wulandari, I., Hindarti, D. and Arifin, Z., 2020. The First Occurrence, Spatial Distribution and Characteristics of Microplastic Particles in Sediments from Banten Bay, Indonesia. *Science of the Total Environment*, 705, 135304. https://doi.org/10.1016/j.scitotenv.2019.135304

43. Riani, E. and Cordova, M.R., 2022. Microplastic Ingestion by the Sandfish Holothuria scabra in Lampung and Sumbawa, Indonesia. *Marine Pollution Bulletin*, 175, 113134. https://doi.org/10.1016/j.marpolbul.2021.113134

44. Buwono, N.R., Risjani, Y. and Soegianto, A., 2021. Distribution of Microplastic in Relation to Water Quality Parameters in the Brantas River, East Java, Indonesia. *Environmental Technology and Innovation*, 24, 101915. https://doi.org/10.1016/j.eti.2021.101915

45. Zhang, W., Zhang, S., Qu, L., Ju, M., Huo, C. and Wang, J., 2023. Seasonal Distribution of Microplastics in the Surface Waters of the Yellow Sea, China. *Marine Pollution Bulletin*, 193, 115051. https://doi.org/10.1016/j.marpolbul.2023.115051

46. Janakiram, R., Keerthivasan, R., Janani, R., Ramasundaram, S., Martin, M.V., Venkatesan, R., Ramana Murthy, M.V., and Sudhakar, T., 2023. Seasonal Distribution of Microplastics in Surface Waters of the Northern Indian Ocean. *Marine Pollution Bulletin*, 190, 114838. https://doi.org/10.1016/j.marpolbul.2023.114838

47. Barrett, J., Chase, Z., Zhang, J., Holl, M.M.B., Willis, K., Williams, A., Hardesty, B.D. and Wilcox, C., 2020. Microplastic Pollution in Deep-Sea Sediments from the Great Australian Bight. *Frontiers in Marine Science*, 7, 576170. https://doi.org/10.3389/fmars.2020.576170

48. Muhsin, Ahmad, S.W., Yanti, N.A., Mukhsar and Safitri, A.N., 2021. Distribution and Mitigation Efforts for Microplastic Pollution in Kendari Bay as the Mainstay Coastal Tourism Area of Southeast Sulawesi. *Journal of Physics: Conference Series 2021*, 1899, 012012. https://doi.org/10.1088/1742-6596/1899/1/012012

Submitted 11.08.2024; accepted after review 03.10.2024;
revised 25.03.2025; published 31.03.2025

About the authors:

Sugeng Widada, Lecturer, Department of Oceanography, Faculty of Fisheries and Marine Science, Diponegoro University (Jl. Prof. Jacub Rais, Tembalang, Semarang, 50275, Indonesia), DSc (Marine Science)

Kunarso, Lecturer, Department of Oceanography, Faculty of Fisheries and Marine Science, Diponegoro University (Jl. Prof. Jacub Rais, Tembalang, Semarang, 50275, Indonesia), DSc (Marine Science)

Elis Indrayanti, Lecturer, Department of Oceanography, Faculty of Fisheries and Marine Science, Diponegoro University (Jl. Prof. Jacub Rais, Tembalang, Semarang, 50275, Indonesia), DSc (Marine Science)

Rikha Widiaratih, Lecturer, Department of Oceanography, Faculty of Fisheries and Marine Science, Diponegoro University (Jl. Prof. Jacub Rais, Tembalang, Semarang, 50275, Indonesia), DSc (Marine Science)

Aris Ismanto, Lecturer, Department of Oceanography, Faculty of Fisheries and Marine Science, Diponegoro University (Jl. Prof. Jacub Rais, Tembalang, Semarang, 50275, Indonesia), DSc (Marine Science)

Muhammad Zainuri, Professor, Department of Oceanography, Faculty of Fisheries and Marine Science, Diponegoro University (Jl. Prof. Jacub Rais, Tembalang, Semarang, 50275, Indonesia), Center for Coastal Rehabilitation and Disaster Mitigation Studies (CoREM) (Jl. Prof. Soedarto, Tembalang, Kec. Tembalang, Kota Semarang, 50275, Jawa Tengah), DEA (Biol.), **Scopus Author ID: 57188871982**, **ORCID ID: 0000-0001-8131-8448**, *muhammadzainuri@lecturer.undip.ac.id*

Tony Hadibarata, Professor, Environmental Engineering Program, Faculty of Engineering and Science, Curtin University Malaysia (CDT 250, Miri, Malaysia), PhD (Env Eng)

Malya Asoka Anindita, Research Assistant**,** Postgraduate study of Marine Science (Master), Faculty of Fisheries and Marine Science, Diponegoro University (Jl. Prof. Jacub Rais, Tembalang, Semarang, 50275, Indonesia), BSc (Oceanography)

Tanya Tristanova, Research Assistant, Postgraduate study of Marine Science (Master), Faculty of Fisheries and Marine Science, Diponegoro University (Jl. Prof. Jacub Rais, Tembalang, Semarang, 50275, Indonesia), BSc (Oceanography)

Muhammad Shulhan Jihadi, Research Assistant, Postgraduate study of Marine Science (Master), Faculty of Fisheries and Marine Science, Diponegoro University (Jl. Prof. Jacub Rais, Tembalang, Semarang, Indonesia, 50275), Center for Coastal Rehabilitation and Disaster Mitigation Studies (CoREM) (Jl. Prof. Soedarto, Tembalang, Kec. Tembalang, Kota Semarang, 50275, Jawa Tengah), BSc (Oceanography), **ORCID ID: 0009-0003-7193-7298,** *mail.shulhanj@gmail.com*

Contribution of the authors:

Sugeng Widada – lead researcher, supervisor, marine sedimentation and geology expert

Kunarso – supervisor, marine productivity and water quality

Elis Indrayanti – researcher, marine and coastal ecology

Rikha Widiaratih – researcher, physical oceanography, ocean modelling, and microplastics

Aris Ismanto – researcher, physical oceanography, ocean modelling, and microplastics

Muhammad Zainuri – lead researcher, supervisor, manuscript writing, conceptualization

Tony Hadibarata – researcher, environmental health, laboratory analysis, microplastics

Malya Asoka Anindita – researcher, manuscript writing, field data collection, laboratory analysis, Geographic Information System (GIS)

Tanya Tristanova – researcher, manuscript writing, field data collection, laboratory analysis

Muhammad Shulhan Jihadi – researcher, manuscript writing, field data collection, Geographic Information System (GIS)

All the authors have read and approved the final manuscript.

ISSN 2413-5577, Ecological Safety of Coastal and Shelf Zones of Sea, 2025, No. 2, pp. 118–134.

Original paper

Ecological State of Waters of the Sevastopol Seashore (Western Crimea) and its Influence on the Dynamics of Plankton Communities

N. V. Pospelova *, S. V. Shchurov, N. P. Kovrigina, E. V. Lisitskaya, O. A. Troshchenko

A. O. Kovalevsky Institute of Biology of the Southern Seas of Russian Academy of Sciences, Sevastopol, Russian Federation

* *e-mail: nvpospelova@ibss-ras.ru*

Abstract

The Sevastopol seashore is influenced by a variety of anthropogenic and natural factors, which can be particularly pronounced in enclosed bays. The objective of this study is to analyse the spatial and temporal variability of hydrological and hydrochemical parameters and the modern state of plankton communities of the Sevastopol seashore. The variability of hydrochemical indicators of water, phytoplankton and meroplankton was studied in 2020–2022 in Kamyshovaya, Kazachya, Kruglaya, Streletskaya, Sevastopol and Karantinnaya Bays. The hydrochemical parameters (salinity, biochemical oxygen demand over five days (BOD_5), permanganate index, silicon content, mineral and organic forms of nitrogen and phosphorus) were determined according to generally accepted methods. The Redfield stoichiometric ratios were applied in order to ascertain the limiting nutrient factor. The species composition, abundance and biomass of phytoplankton and meroplankton were determined. In comparison to data collected 20 years ago, an increase in surface water pollution (BOD_5 and permanganate index exceeding maximum permissible values) was observed on the seashore of Sevastopol. Biogenic elements (nitrogen, phosphorus, and silicon compounds) varied widely. The study found that that limiting factor for phytoplankton vegetation was nitrogen in spring, silicon in summer, and phosphorus in summer and autumn. No phytoplankton blooms were recorded during the study period. Mass development of diatoms and coccolithophores was observed in spring. In summer and autumn, the abundance and biomass of planktonic microalgae decreased to minimum values. Relative synchrony of seasonal dynamics of meroplankton density was observed: in all Sevastopol bays minimum values were registered in the cold period of the year, whereas maximum values were recorded in the warm period when the water warmed up above 14.5°C. Comparative analyses and quantitative assessments of plankton dynamics in bays, differing in hydrological and hydrochemical environmental parameters, can contribute to the assessment of the functional response of Black Sea coastal ecosystems to anthropogenic and natural factors.

Keywords: phytoplankton, meroplankton, nutrients, biochemical oxygen demand over five days, BOD_5, Black Sea

Acknowledgments: This work was carried out under state assignment of the A.O. Kovalevsky Institute of Biology of the Southern Seas of RAS (124022400152-1).

For citation: Pospelova, N.V., Shchurov, S.V., Kovrigina, N.P., Lisitskaya, E.V. and Troshchenko, O.A., 2025. Ecological State of Waters of the Sevastopol Seashore (Western Crimea) and its Influence on the Dynamics of Plankton Communities. *Ecological Safety of Coastal and Shelf Zones of Sea*, (2), pp. 118–134.

Экологическое состояние вод Севастопольского взморья (Западный Крым) и его влияние на динамику планктонных сообществ

Н. В. Поспелова *, С. В. Щуров, Н. П. Ковригина, Е. В. Лисицкая, О. А. Трощенко

Институт биологии южных морей имени А.О. Ковалевского РАН, Севастополь, Россия

* *e-mail: nvpospelova@ibss-ras.ru*

Аннотация

Севастопольское взморье испытывает постоянное воздействие антропогенных и природных факторов, которое может усиливаться в закрытых бухтах. Цель работы – проанализировать пространственно-временну́ю изменчивость гидролого-гидрохимических параметров и состояние планктонных сообществ Севастопольского взморья в современный период. Исследования изменчивости гидрохимических показателей вод, фитопланктона и мезопланктона проведены в 2020–2022 гг. в бухтах Камышовой, Казачьей, Круглой, Стрелецкой, Севастопольской и Карантинной. Гидрохимические показатели (соленость, биохимическое потребление кислорода за пять суток ($БПК_5$), перманганатная окисляемость, содержание кремния, минеральных и органических форм азота и фосфора) определяли по общепринятым методикам. Для определения лимитирующего биогенного фактора использовали стехиометрические соотношения Редфилда. Определяли видовой состав, численность и биомассу фитопланктона и мезопланктона. За 20 лет на взморье Севастополя отмечено повышение уровня загрязнения поверхностных вод ($БПК_5$ и окисляемость превышали предельно допустимые значения). Биогенные элементы (соединения азота, фосфора, кремния) изменялись в широких пределах. Лимитирующим фактором для развития фитопланктона в весенний период был азот, летом – кремний, летом и осенью – фосфор. За период исследования не зафиксировано случаев «цветения» фитопланктона. Массовое развитие диатомовых водорослей и кокколитофорид отмечено в весенний период. Летом и осенью численность и биомасса планктонных микроводорослей снижались до минимальных значений. Отмечена относительная синхронность сезонной динамики плотности мезопланктона: во всех бухтах Севастополя минимальные значения зарегистрированы в холодный период года, максимальные – в теплый период при прогреве воды выше 14.5 °С. Сравнительный анализ и количественные оценки динамики планктона в бухтах, различающихся по гидрологическим и гидрохимическим параметрам среды, могут внести вклад в оценку функциональной реакции прибрежных экосистем Черного моря на антропогенные и природные факторы.

Ключевые слова: фитопланктон, мезопланктон, биогенные элементы, биохимическое потребление кислорода, $БПК_5$, Черное море

Благодарности: работа выполнена по теме государственного задания ФИЦ ИнБЮМ (№ 124022400152-1).

Для цитирования: Экологическое состояние вод Севастопольского взморья (Западный Крым) и его влияние на динамику планктонных сообществ / Н. В. Поспелова [и др.] // Экологическая безопасность прибрежной и шельфовой зон моря. 2025. № 2. С. 118–134. EDN JDOMVD.

Introduction

The basis of pelagic food chains in aquatic systems is phytoplankton, with its dynamics of abundance, species diversity and productivity influenced by various environmental factors. In this regard, structural and functional parameters of phytoplankton can serve as indicators of changes in bay ecosystems. One of the links of the food chain in the pelagial ecosystem is meroplankton (pelagic larvae of bottom-dwelling invertebrates). On the one hand, larvae consume a large amount of phytoplankton, and on the other hand, they themselves are part of the food of many marine invertebrates and fish. At the same time, the representatives of meroplankton are most vulnerable to the impact of various toxicants and domestic sewage [1].

The Sevastopol seashore is considerably influenced by a variety of anthropogenic factors which can be particularly pronounced in enclosed bays [2, 3]. The bays have different configuration, size and depth. Most of them are elongated and run deep into the shore (Sevastopol, Karantinnaya, Streletskaya, Kamyshovaya and Kazachya bays), except for Kruglaya Bay [4]. The formation of the hydrochemical regime of the Sevastopol seashore is influenced by river and storm water runoff as well as domestic sewage with a high content of mineral nitrogen, which exceeds the content of phosphorus compounds by one to three orders of magnitude and is a determinant in the eutrophication of water bodies [2]. The impact of river runoff and anthropogenic pollution increases from west to east. The most unfavourable location is Karantinnaya Bay while Kazachya Bay is the least unfavourable. Simultaneously, research conducted in certain bays of the Sevastopol seashore in recent years has revealed the emergence of novel anthropogenic pollution hotspots and a substantial increase in the concentration of total suspended solids, dissolved organic matter and petroleum hydrocarbons. These concentrations exceeded the maximum permissible concentration (MPC) frequently [5–7].

The objective of this study is to analyse the spatial and temporal variability of hydrological and hydrochemical parameters and the state of plankton communities of the Sevastopol seashore according to the data obtained in 2020–2022.

Materials and methods

The study was conducted from October 2020 to November 2022. Six one-day surveys were carried out in spring (May 2021), summer (July 2021, August 2022) and autumn (October 2020, November 2021 and 2022). Samples were taken at the traverse of Kamyshovaya (station *1*), Kazachya (station *2*), Kruglaya (station *1*), Streletskaya (station *4*), Karantinnaya (station *6*) and Sevastopol (station *7*) bays as well as at a station in the open part of the seashore (station *5*) 2 km offshore (Fig. 1). The depth in the study area was mainly 12–20 m, except for the control station (station *5*), where it reached 50 m.

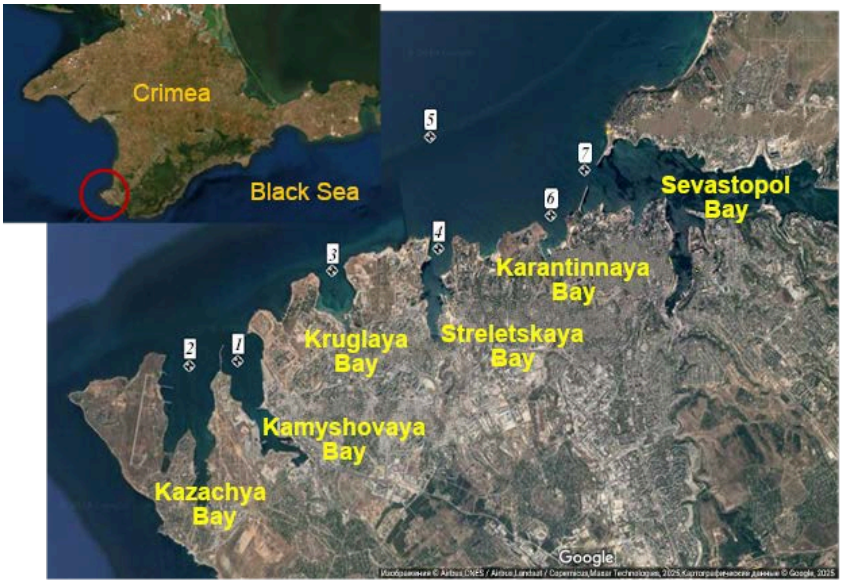

Fig. 1. A map-scheme of the study area (*1–7* are station numbers). Adopted from Google Maps (URL: https://www.google.ru/maps)

Samples were taken in the surface and bottom layers using a BM-48M bathometer. Salinity (a GM-65 electrosalinometer with regular calibration by titration with $AgNO_3$ solution), biochemical oxygen demand over five days (BOD_5), permanganate index in alkaline medium, silicon content as well as content of mineral and organic forms of nitrogen and phosphorus were determined according to generally accepted methods [1), 2)]. The Redfield stoichiometric ratios (PR_{at}) [3)] were used in order to ascertain the limiting nutrient factor, which had the following form for known concentrations of inorganic compounds of nitrogen, phosphorus and silicon:

$$PR_{at}\,(N/P) = 1.53\,(1.35\,NO_2 + NO_3 + 3.44\,NH_4)\,/\,PO_4,$$

$$PR_{at}\,(Si/N) = SiO_4\,/\,(1.47\,(1.37\,NO_2 + NO_3 + 3.77\,NH_4)),$$

$$PR_{at}\,(Si/P) = 1.03\,SiO_4/PO_4.$$

---

1) Guideline Documents РД 52.24.420-2019; РД 52.24.383-2018; РД 52.24.380-2017; РД52.24.381-2017; РД 52.24.382-2019; РД 52.24.432-2018; РД 52.10.805-2013; РД 52.24.387-2019 (in Russian).

2) *On the Approval of Water Quality Standards for Water Bodies of Commercial Fishing Importance, Including Standards for Maximum Permissible Concentrations of Harmful Substances in the Waters of Water Bodies of Commercial Fishing Importance*: Order of the Ministry of Agriculture of Russia dated December 13, 2016, No. 552 (in Russian).

3) Redfield, A.C., Ketchum, B.H. and Richards, F.A., 1963. The Influence of Organisms on the Composition of Sea-Water. In: N. M. Hill, ed., 1963. *The Sea: Ideas and Observations on Progress in the Study of the Seas*. New York: Wiley Interscience, Vol. 2, pp. 26–77.

To determine the species composition, abundance and biomass of phytoplankton, samples (V = 2.0 L) were collected from the upper layer of seawater (0–1 m). Seawater was filtered through nuclear-track membranes with a pore diameter of 1 μm (JINR, Dubna) on a reverse filtration unit. Then, it was concentrated to a volume of 40–50 mL and fixed with Utermel solution. The identification of microalgae species was conducted using a light microscope at magnifications of 200× and 400× (Olympus BX43) with the help of identifiers [4), 5)]. Phytoplankton abundance and biomass were calculated using the Gloria software developed at the IBSS [8]. Taxonomic names are given according to the AlgaeBase (available at: https://www.algaebase.org) and World Register of Marine Species (available at: https://www.marinespecies.org) databases.

Sampling of meroplankton during the study period was carried out at coastal stations with a depth of up to 13 m. The material was collected with a Juday net with an inlet diameter of 36 cm and a silk bolting cloth mesh size of 135 μm. The water layer 0–10 m from bottom to surface was considered under study. Live material was processed by total counting of larvae in a Bogorov type chamber under an MBS-9 binocular; a MIKMED-5 light microscope was used to clarify the species affiliation of larvae [3].

A total of 96 samples for hydrological and hydrochemical analysis and 23 phyto- and meroplankton samples each were processed and analysed.

Mathematical and statistical calculations were performed in Excel 2016. Estimates of minimum, maximum, mean values and standard deviations were obtained.

Results

Spatial and temporal distribution of thermohaline and hydrochemical parameters

Temperature and salinity. Surface layer temperature varied from 14.4 (May) to 26.1°C (August) decreasing to 13.1°C as a result of autumn cooling (November). During the period of thermocline formation (May–August), water stratification was observed: the maximum temperature difference between the surface and bottom layers at the control station reached 16.2°C while at the shallow station (Kamyshovaya Bay), stratification was minimal, with the temperature difference not exceeding 0.9°C. During the autumn months, convective mixing resulted in vertical equilibrium of temperatures.

The spatial structure of the surface layer thermohaline fields was characterised by insignificant gradients. It was demonstrated that the range of variability of sea water surface layer temperature was 0.3–1.4°C and that of salinity – 0.08–0.21 PSU. It is important to note the elevated salinity levels observed at the control station

---

[4)] Proshkina-Lavrenko, A.I., 1955. [*Diatom Algae of the Black Sea Plankton*]. Moscow, Leningrad: Izd. AN SSSR, 224 p. (in Russian).

[5)] Tomas, C.R., ed., 1993. *Marine Phytoplankton: A Guide to Naked Flagellates and Coccolithophorids*. Academic Press, 263 p.

in comparison to the bays. Extremely low salinity values were recorded in November 2021 (17.63–17.84 PSU). During the periods of other surveys, the surface layer salinity values varied in the range of 18.02–18.54 PSU. Salinity increased from the surface to the bottom, the maximum difference in salinity values was recorded in the 0–50 m layer (0.42 PSU on 17.11.2021 and 0.33 PSU on 09.07.2021).

BOD_5 and permanganate index. BOD_5 values varied over a wide range of 0.57–3.87 mg/dm^3 (Table). Values close to water quality standards for water bodies of fishery significance and exceeding them ($\geq$2.1 mg/dm^3) were observed in spring (Kamyshovaya, Kruglaya, Karantinnaya, Sevastopol bays) and during summer surveys (Kamyshovaya, Kazachya, Kruglaya, Streletskaya bays). Furthermore, autumn BOD_5 values did not exceed the normative values at all stations, except for the survey in autumn 2021 at the station in Kamyshovaya Bay (3.84 mg/dm^3).

Permanganate index varied from 1.62 to 5.49 mgO/dm^3 during the period under consideration (Table). Exceedance of this index standard (> 4.0 mgO/dm^3) was observed in all bays and in different seasons of the year. Mean values of permanganate for the observation period in the bays were below the water quality standards.

Nutrients. Nitrite nitrogen concentration (NO_2) was low and did not exceed 3.5 μg/dm^3 in the surface layer (Table) and 4.6 μg/dm^3 in the near-bottom one (Streletskaya Bay). Nitrate concentration in the surface layer varied from 4.6 (May 2021, Sevastopol Bay) to 267.5 μg/dm^3 (August 2022, Karantinnaya Bay). The near-bottom layer demonstrated the nitrate concentration variation from 3.8 to 86.8 μg/dm^3 (August 2022). Mean values of nitrate in the surface layer varied in the bays from 12.7 in Kruglaya Bay to 58.1 μg/dm^3 in Karantinnaya Bay. Of note is the August 2022 survey when high nitrate values were recorded at all stations and reached 267.5 μg/dm^3 in the Karantinnaya Bay surface layer. Elevated concentration values in the same survey were also recorded in the bottom layer (39–59 μg/dm^3) while the maximum (86.8 μg/dm^3) was observed at the control station near the bottom. Ammonium nitrogen concentration on the Sevastopol seashore was low and ranged from 0.6 μg/dm^3 (Kruglaya Bay, May 2021) to 32.4 μg/dm^3 (Kamyshovaya Bay, August 2022). August 2022 was characterised by NH_4 increased concentration at all stations. Organic nitrogen concentration (N_{org}) varied over a wide range: from 331 μg/dm^3 in May 2020 to 1375 μg/dm^3 in Streletskaya Bay in August 2022 (Table). High N_{org} concentration values were recorded also in Kruglaya, Kazachya and Kamyshovaya bays.

Mineral phosphorus (PO_4) concentration varied from 1.1 to 15.9 μg/dm^3. Minimum content was observed in autumn 2022 at the control station, maximum – in spring 2021 in Kamyshovaya Bay (Table). The mean value of PO_4 in the Sevastopol seashore water area for 2020–2022 is 6.3 μg/dm^3. Organic phosphorus (P_{org}) content varied from 3.7 to 34.9 μg/dm^3. Maximum values were recorded in summer in Kazachya Bay. Mean values of P_{org} for all the period under study varied from 15.3 to 22.1 μg/dm^3. In general, P_{org} concentration values were low and uniform. No seasonal variability was recorded.

Hydrochemical parameters in the surface layer of the water area under study (2020–2022)

Bays	Value	BOD_5, mg/dm^3	PI, mgO/dm^3	Content, μg/dm^3						
				NO_2	NO_3	NH_4	N_{org}	PO_4	P_{org}	Si
Kazachya	mean	1.63	3.23	0.9	24.3	8.7	696	4.0	17.8	44.5
	min	0.70	1.75	0.4	4.7	2.1	378	1.4	3.7	12.4
	max	**2.72***	**4.37**	1.3	90.3	15.0	1131	12.3	34.9	72.6
Kamyshovaya	mean	**2.61**	3.92	1.3	24.6	13.5	645	6.5	21.0	60.3
	min	1.31	2.30	0.9	5.3	1.7	331	2.4	5.0	14.8
	max	**3.87**	**5.49**	1.6	70.4	32.4	1188	15.9	26.7	98.6
Kruglaya	mean	1.40	3.24	0.8	12.7	8.2	645	3.7	17.6	40.0
	min	0.57	2.01	0.1	5.4	0.6	372	1.4	4.3	17.9
	max	**2.23**	**4.11**	1.2	44.5	17.4	1235	10.9	26.4	63.7
Streletskaya	mean	1.38	3.37	1.4	24.2	8.6	660	3.9	19.2	81.2
	min	0.60	1.98	0.7	5.1	1.8	412	1.1	4.1	23.8
	max	**2.21**	**4.50**	2.1	40.9	19.1	1375	10.5	33.4	118.1
Karantinnaya	mean	1.43	3.22	1.4	58.1	8.8	545	5.1	17.1	64.8
	min	0.66	1.62	0.8	6.5	1.9	411	1.8	4.6	15.1
	max	**2.72**	**4.73**	3.5	267.5	17.8	824	11.5	27.3	152.4
Sevastopol	mean	1.45	3.51	1.7	14.1	8.7	670	6.3	22.1	47.4
	min	1.10	2.39	1.2	4.6	2.6	459	3.5	15.0	19.8
	max	**2.32**	**4.63**	2.3	22.2	12.9	838	11.2	34.2	75.0
Control	mean	1.50	3.89	0.8	14.3	7.7	618	4.2	22.8	31.0
	min	1.26	3.28	0.5	6.5	2.2	370	1.8	14.2	14.3
	max	**2.02**	**4.42**	1.0	29.1	13.6	801	9.5	29.1	58.7

Note: values exceeding maximum permissible concentrations (MPC) [2)] and limits for water quality of fisheries [2)] are given in bold. PI – permanganate index. MPC of NO_2 – 20 μg/dm^3, NO_3 – 9,000 μg/dm^3, NH_4 – 390 μg/dm^3. BOD_5 limit value – under 2.1 μg/dm^3, PI limit value – 4.0 μg/dm^3.

Silicon (Si) content was characterised by great variability. Thus, Si concentration in the surface layer varied from 12.4 μg/dm^3 (July 2021) in Kazachya Bay to 152.4 μg/dm^3 (August 2022) in Karantinnaya Bay (Table). High Si concentrations were recorded in all bays in August 2022 in the surface (64–152 μg/dm^3) and near-bottom layers (100–153 μg/dm^3). No silicon concentration seasonal variability was recorded.

Ratio of nutrients

Fig. 2 shows the results of calculations of the Redfield ratio (PR_{at}) for nitrogen, phosphorus and silicon to determine the limiting factor for phytoplankton. A wide range of relative N/P values was observed – from 1 to 53. The minimum values were observed in spring (1–3), indicating significant nitrogen limitation. The ratio was close to the classical Redfield ratio in summer (except for Kazachya and Karantinnaya bays), autumn 2020 in Karantinnaya and Sevastopol bays and autumn 2021 in Kamyshovaya Bay. In other cases, the ratio of N/P values exceeded 16 which corresponded to phosphorus-induced limitation.

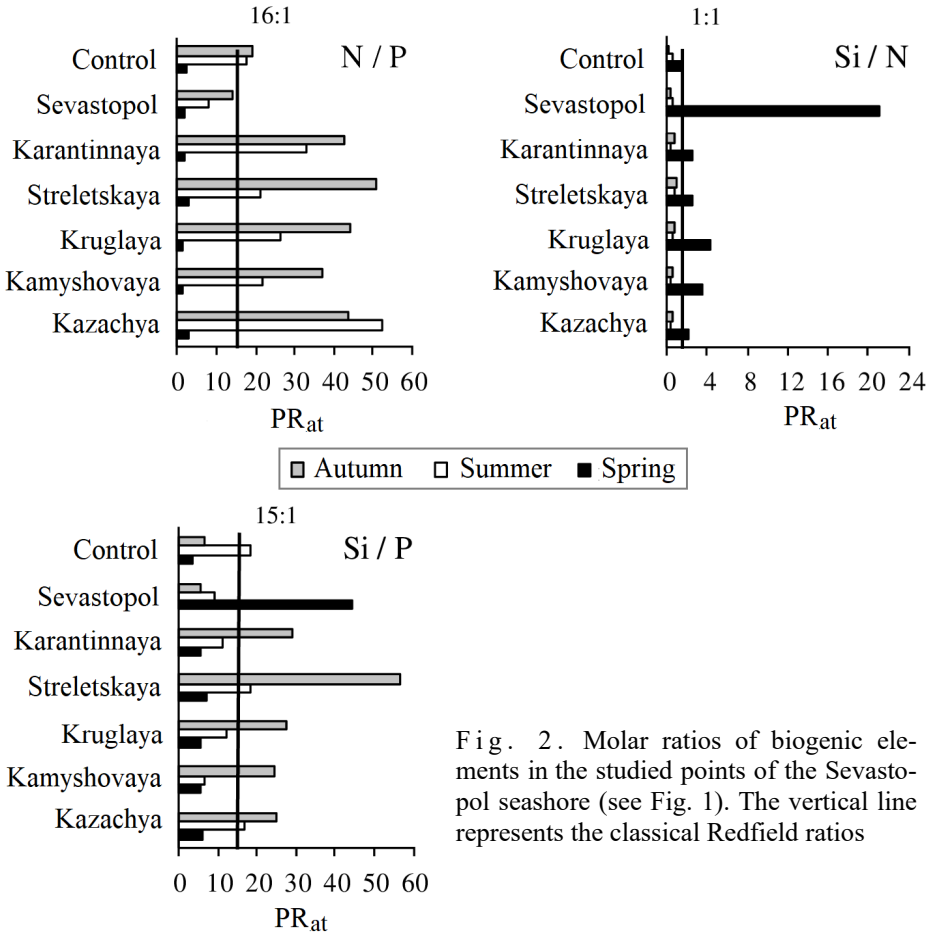

Fig. 2. Molar ratios of biogenic elements in the studied points of the Sevastopol seashore (see Fig. 1). The vertical line represents the classical Redfield ratios

The Si/N ratio varied from 0.2 to 21. The Si/N value greater than one was recorded in spring and also in autumn 2020 in Streletskaya Bay. The Si/P ratio varied from 3 to 56. In autumn 2020 and 2021 this ratio exceeded the classical values. In spring and summer, lower values of the Si/P ratio were observed.

Taking the ratio of all three elements (N/Si/P) into account, the values close to the classical Redfield ratio were observed only in autumn 2020 in Karantinnaya Bay (18/17/1). Significant deviations were noted at other times.

Phytoplankton: dynamics of taxonomic composition and density

A total of 75 species of microalgae were recorded in phytoplankton samples, 35 of which belong to diatoms and 32 to dinophytes. The remaining species belong to such phyla as Haptophyta, Euglenozoa, Ochrophyta, Cercozoa. The maximum values of phytoplankton abundance and biomass in all bays were observed in spring (Fig. 3). The exception was the autumn period of 2020 in Sevastopol Bay, when the biomass of planktonic microalgae exceeded 400 mg·L^{-1}, with low abundance of phytoplankton. Phytoplankton abundance was also low during summer and autumn 2021.

The spatial and temporal variability of the abundance of the main phytoplankton groups indicates high variability of the community composition. In autumn 2020 and 2021, diatoms were absolutely dominant in terms of both abundance (75–100%) and biomass (64–100%). In spring, diatoms and coccolithophores dominated in abundance (98–99%) in Kamyshovaya, Kruglaya and Sevastopol bays and in biomass – at all stations. In summer, diatoms dominated in abundance (52–80%), but were inferior to dinoflagellates (57–91%) in biomass. In autumn 2020 at all stations, large-celled diatom alga *Proboscia alata* was the main contributor (57–97%) to total abundance and biomass, while in autumn 2021, it was *Pseudosolenia calcar-avis* (87–99%). Coccolithophore *Emiliania huxleyi*

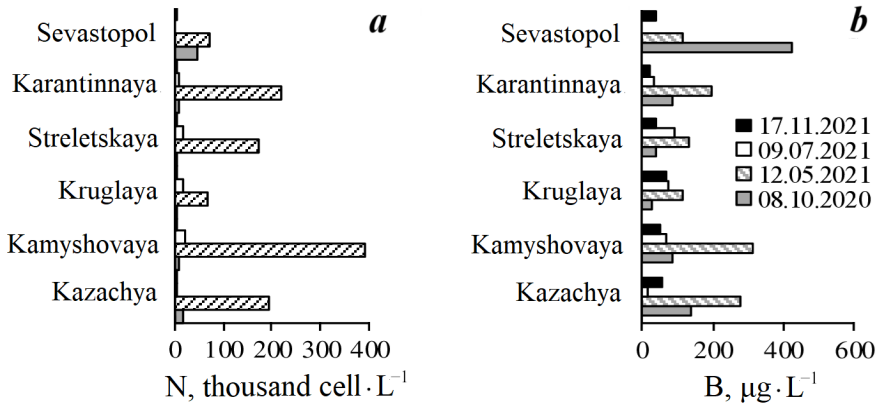

F i g . 3 . The total abundance *N* (*a*) and biomass *B* (*b*) of phytoplankton in Sevastopol bays (see Fig. 1)

dominated almost at all stations in May 2021 (37–58% of total abundance), and in Kamyshovaya Bay, diatoms *Pseudo-nitzschia calliantha* and *Chaetoceros wighamii* made a significant contribution to abundance (23 and 45% of the total number, respectively) along with coccolithophores.

P. alata formed the basis of biomass (40–58% of the total biomass) of spring phytoplankton in all bays. In summer, dinophytes of genus *Prorocentrum* gave peak abundance in Kazachya and Streletskaya bays. In Kamyshovaya Bay, diatoms *Chaetoceros tortissimus*, *Leptocylindrus danicus* and *P. alata* accounted for more than 68% of the total abundance, while diatoms *P. calliantha* and *P. alata* dominated in Kruglaya Bay (more than 50% of the total abundance). The basis of biomass was formed by large-celled diatom *P. alata* and dinoflagellates of genus *Prorocentrum*.

Meroplankton: dynamics of taxonomic composition and density

During the study period, larvae of 41 species of benthic invertebrates belonging to the following taxa were identified in plankton: type Annelida, class Polychaeta – 16 species; type Mollusca, classes Bivalvia – 7, Gastropoda – 9 species; type Arthropoda, subtype Crustacea: infraclass Cirripedia – 2 species and order Decapoda – 7 species. Planulae Coelenterata (Type Cnidaria), larvae Kamptozoa (Type Entoprocta) and Bryozoa (Type Bryozoa) not identified to species, were encountered sporadically.

The minimum number of larvae of benthic invertebrates was recorded in the cold period of the year in the whole water area of the Sevastopol seashore. In November 2021 the total density of meroplankton did not exceed 29 ind./m^3 (Fig. 4). Veliconchae of such bivalves as mussel *Mytilus galloprovincialis* Lamarck, 1819 and surf clam *Spisula subtruncata* (Da Costa, 1778), gastropod veligers not identified to species, polychaete larvae (*Spio decorata* Bobretzky, 1870) and barnacle nauplii *Amphibalanus improvisus* (Darwin, 1854) were found in the plankton.

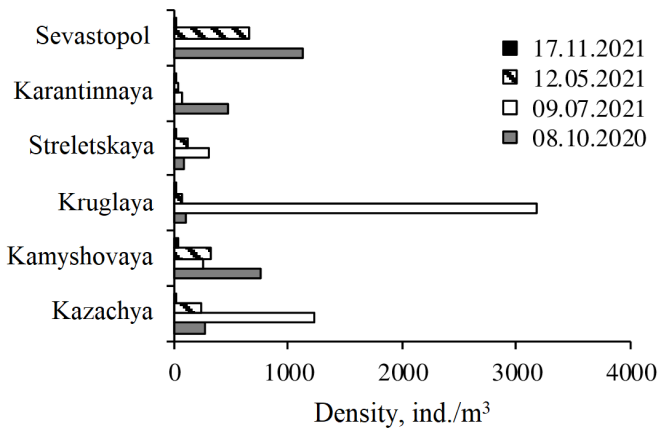

Fig. 4. Dynamics of meroplankton density in Sevastopol bays (see Fig. 1)

A substantial increase in the number of larvae in the plankton was observed during the warm period of the year when a multitude of species of benthic invertebrates commenced their reproductive cycle. In May, the maximum plankton density (661 ind./m^3) was recorded in Sevastopol Bay, it reached 322 ind./m^3 in Kamyshovaya Bay and ranged from 26 ind./m^3 (in Karantinnaya Bay) to 227 ind./m^3 (in Kazachya Bay) in other areas (Fig. 4).

The species composition of meroplankton underwent an increase in diversity. Among mollusks, with the exception of mussel larvae, veliconchae of the bivalve mollusks of family Cardiidae, gastropod veligers of family Rissoidae were observed to occur in the plankton. The density of mussel larvae was low – up to 15 ind./m^3, while that of veligers Gastropoda reached 147 ind./m^3 (in Kamyshovaya Bay). Larvae of polychaetes *Harmothoe reticulata* (Claparède, 1870), *Pholoe inornata* Johnston, 1839, *Polydora cornuta* Bosc, 1802, *Alitta succinea* (Leuckart, 1847) and larvae of family Nereididae not identified to species appeared in the plankton. Larvae Decapoda (*Hippolyte leptocerus* (Heller, 1863), *Upogebia pusilla* (Petagna, 1792)) were recorded sporadically. In terms of abundance, all bays were dominated by larvae of barnacle *A. improvisus,* from their maximum of 597 ind./m^3 (in Sevastopol Bay) to 227 ind./m^3 (in Kazachya Bay).

In July, the maximum meroplankton density (3180 ind./m^3) was recorded in Kruglaya Bay. It was stipulated by high density of gastropods larvae (2173 ind./m^3). Veligers of bittium (*Bittium reticulatum* (Da Costa, 1778)) and representatives of family Rissoidae dominated in the plankton. With their density not exceeding 135 ind./m^3 in other bays, it reached 373 ind./m^3 in Kazachya Bay only. During this period, an increase in the density of barnacle larvae was also noted in all bays but the plankton was dominated by nauplii of another species, *Verruca spengleri* Darwin, 1854.

In October, Sevastopol and Kamyshovaya bays showed higher meroplankton density values – up to 1126 and 756 ind./m^3, respectively (Fig. 4). At the same time, the number of larvae in other bays ranged from 91 ind./m^3 (in Streletskaya Bay) to 463 ind./m^3 (in Karantinnaya Bay). In terms of abundance, veligers of gastropods (*Retusa truncatula* (Bruguière, 1792), *Caecum trachea* (Montagu, 1803), *Limapontia capitata* (O. F. Müller, 1774), *Rissoa parva* (Da Costa, 1778), *Rissoa* sp.) dominated. Their maximum total density (235 ind./m^3) was recorded in Kamyshovaya Bay. That period was also characterised by the increased number of mussel *M. galloprovincialis* larvae in the stage of ocellated veliconcha. Their density was 110 ind./m^3 in Kamyshovaya Bay and ranged from 9 to 62 ind./m^3 in other areas under study. The density of polychaete larvae did not exceed 29 ind./m^3. *Lysidice ninetta* Aud. et H. M. Edw., 1833 *Magelona rosea* Moore, 1907, *Malacoceros fuliginosus* (Claparède, 1870) and *Prionospio* sp. and *Phyllodoce* sp. not identified to species were observed. Barnacle nauplii *A. improvisus* (up to 782 ind./m^3) dominated in Sevastopol Bay. Larvae of decapods (*Clibanarius erythropus* (Latreille, 1818), *Pisidia longimana* (Risso, 1816), *Xantho poressa* (Olivi, 1792), *Pachygrapsus marmoratus* (Fabricius, 1787), *Athanas nitescens* (Leach, 1813) were recorded in the plankton in October but their total density did not exceed 30 ind./m^3 (Karantinnaya Bay).

The meroplankton density dynamics in all bays exhibited a high degree of synchrony. Minimum values, with a maximum of 29 ind./m^3, were observed to be characteristic of the cold period of the year when the water temperature was recorded at 14.5°C (in November). An increase in density was noted with the onset of water warming in May, July and October. In terms of abundance, the meroplankton showed the domination of barnacle nauplii *Amphibalanus improvisus*: during the cold period of the year, they occurred sporadically and dominated the plankton in May and October, which then influenced the total meroplankton density values. The maximum number of barnacle larvae was recorded in Sevastopol and Kamyshovaya bays.

Discussion

A comparison of the hydrological and hydrochemical data obtained from one station scheme in 2001–2005 and 2020–2022 is of interest [2]. In 2020–2022, an increase of salinity in the surface layer in the water area was noted. In 2001–2005, mean salinity values ranged from 17.70 to 17.94 PSU [2] while in 2020–2022, salinity values reached 18.54 PSU. The trend of salinity increase in the Sevastopol coastal area in recent years has also been indicated by other authors [3, 9]. A positive salinity trend in the surface layer was found in Karantinnaya Bay from 2001 to 2018 [9]. Studies in the shelf zone of the north-eastern Black Sea also demonstrated a progressive increase in salinity in the upper 200 m layer of the sea from 2010 to 2020 [10]. The authors attribute this primarily to fluctuations in the Black Sea climate regime.

According to the official data provided by the Crimean Service of State Statistics (available at: https://82.rosstat.gov.ru/), the population of the City of Sevastopol has increased by 33% over the last 20 years while the government estimates that the actual increase is over 40%. Urban development has expanded in the coastal zone, with a corresponding increase in the volume of domestic water and the load on sewage treatment plants. In addition, as urbanization increases, the volume of stormwater runoff also increases with the deterioration of its quality [5, 11]. All this results in an increase in the concentration of mineral and organic substances in the coastal water area and affects the level of surface water pollution which we assessed by two indicators – BOD_5 and permanganate index. The first value reflects the pollution of the environment by non-persistent organic matter; the second one indicates the degree of pollution by persistent organic matter. BOD_5 mean values obtained until 2005 on the Sevastopol seashore did not exceed 0.79 mg/dm^3 [2] while in the modern period, BOD_5 values exceeded water quality standards for water bodies of fishery significance in spring (in Kamyshovaya, Kruglaya, Karantinnaya, Sevastopol bays) and in summer (in Kamyshovaya, Kazachya, Kruglaya, Streletskaya bays), which indicates an increase in the degree of pollution of the seashore. This is also confirmed by permanganate index (exceedance of standards was observed in all bays and in different seasons) and nitrogen concentration. It should be noted that nutrient content is influenced by water dynamics, anthropogenic pollution and interactions with biota.

The dynamics of abundance, species diversity and productivity of the phytoplankton community are influenced by a complex of different environmental factors: temperature, light, nutrients, trace elements, pollutants, consumption by other components of food chains, water dynamics, etc. However, it is not possible to isolate the influence of individual factors in natural conditions. The impact of temperature and light on the reproductive capacity of diverse phytoplankton groups is a well-documented phenomenon. In order to gain a more complete understanding of the effects of trace elements and pollutants, experimental work is required. To facilitate a discussion regarding the influence of wind-wave processes, a series of long-term observations must be conducted. Nutrients represented by mineral compounds of nitrogen, phosphorus and silicon constitute the material basis for the creation of primary production in water bodies. The concentration of these substances and their ratio regulate phytoplankton vital activity and ensure biological productivity of aquatic ecosystems as a whole. In this connection, we tried to assess the relationships of nutrients with the development of phytoplankton communities in the studied water areas in different seasons.

No seasonal regularity in the change of nitrate and organic nitrogen concentration was observed, which confirms the influence of anthropogenic pollution as the main source of nitrogen. At the same time, the concentration of nitrate nitrogen required by the phytoplankton varied widely. NH_4^+ maximum concentrations were observed in autumn when the plankton composition was dominated by large-celled diatom algae. The phytoplankton are known to consume NH_4 during photosynthesis, with algae using less energy compared to nitrate assimilation [12]. Absorption of reduced forms of nitrogen, including NH_4^+, depends on the phytoplankton cell size. Small-cell phytoplankton assimilate ammonium nitrogen predominantly while large-cell phytoplankton are the main consumers of nitrates [13]. Mean values of mineral and organic nitrogen concentrations in Kamyshovaya, Kazachya and Kruglaya bays exceeded similar values recorded until 2005 [2].

Maximum phosphate concentrations were observed during the period of phytoplankton mass development with predominance of coccolithophores (spring 2021). The same period was characterised by minimal Redfield ratio PR_{at} (N/P) (1–3), which can indicate nitrogen limitation of the phytoplankton production. Similar data on biogenic elements in the spring period were obtained by A. S. Mikaelyan et al. [14]. The authors noted an interesting peculiarity for the Black Sea: phosphates have a positive effect on the mass development of coccolithophores under nitrogen limitation of primary production. In summer and autumn, we observed phosphorus deficiency in most cases. The importance of mineral phosphorus as the leading factor of chemical limitation of phytoplankton production along with the length of daylight hours and water temperature on the Sevastopol seashore is stated in [15].

The silicon content exhibited significant variability over the 2020–2022 period, with values gradually declining from the peak recorded in spring to lower levels in summer and autumn, attributed to the consumption of this element

by the phytoplankton. It is probable that silicates did not constitute a limiting factor for the phytoplankton growth in spring, when diatom algae were predominant, in conjunction with coccolithophores. The lowest silicon content was observed in summer when the silicon-to-nitrogen ratio was less than 0.5. This period also coincided with the absence of diatoms as the dominant phytoplankton group. The observed deviation from the classical Redfield ratios (Si/N) in summer and autumn in some bays indicates higher consumption of silicates by phytoplankton compared to nitrates.

Excess nitrogen combined with a deficiency of phosphorus, and in some cases silicon, resulted in an unbalanced stoichiometry of dissolved nutrients. This imbalance is reflected in deviations from the classical Redfield ratios (N/Si/P) as well as wide variations in these ratios. The enrichment of the biosphere with nitrogen, the concentration of which in the ocean far exceeds that of phosphorus, is of concern as it can affect coastal ecosystems [16].

No direct influence of nutrients and phytoplankton on the dynamics of meroplankton density was found. The influence of phytoplankton is likely to have a delayed effect. Furthermore, the main influence of the temperature factor on mass reproduction of some meroplankton taxa cannot be excluded. At the same time, taking into account that larvae of bottom invertebrates consume phytoplankton, we can assume the opposite effect. Thus, in July 2021, in Kruglaya Bay, in the context of low phytoplankton abundance, the maximum value of meroplankton density was recorded, which can be associated with the ingestion of phytoplankton by larvae. The density of meroplankton in autumn 2020 and spring 2021 in Kamyshovaya and Sevastopol bays was high due to an increase in the number of larvae of barnacles and bivalves, which is associated with seasonal cycles of their reproduction, and did not depend on hydrochemical parameters. At the same time, a large number of quay walls, breakwaters and other hydro-technical structures in the above-mentioned bays attract larvae of these meroplankton groups as a convenient substrate for settling.

Conclusion

During the period under study, an increase in the level of pollution on the Sevastopol seashore was observed in comparison with the 2001–2005 period. The maximum BOD_5 values in all bays exceeded water quality standards for water bodies of fishery significance. According to this indicator, the bays can be arranged from the most polluted with non-stable organic substances to the less polluted in the following order: Kamyshovaya, Kazachya, Karantinnaya, Sevastopol, Kruglaya, Streletskaya. The maximum permanganate index values in all bays also exceeded quality standards. Nitrate concentration on the Sevastopol seashore increased from spring to summer and decreased by autumn. The average values of mineral and organic nitrogen concentrations in Kamyshovaya, Kazachya and Kruglaya bays exceeded similar values recorded until 2005. The minimum concentration of nitrates was recorded in Kruglaya Bay, the maximum one – in Karantinnaya Bay. Ammonium nitrogen concentrations exhibited seasonal variations, analogous to the fluctuations observed in nitrate levels. The phytoplankton community

composition exhibited significant spatial and temporal variability in the abundance of the main groups. The predominance of large-celled diatom algae was observed in autumn while the spring period was characterised by the dominance of small-celled colonial diatoms and coccolithophore *Emiliania huxleyi*, diatoms dominated in summer in terms of abundance and dinoflagellates – in terms of biomass. Relative synchrony of seasonal dynamics of meroplankton density in Sevastopol bays was noted, with minimum values registered in the cold period of the year and maximum ones in the warm period. The meroplankton community was dominated by barnacle nauplii *Amphibalanus improvisus* which were found to be the most prevalent species in the fouling of hard substrates. The maximum number of larvae of this species was recorded in Sevastopol and Kamyshovaya bays.

The results obtained can be used to assess the functional response of the Black Sea coastal ecosystems to variability of anthropogenic and natural factors.

References

1. Pavlova, E.V. and Lisitskaya, E.V., 2009. State of the Zooplanktonic Communities of the Coastal Waters from the Karadag Reserve (2002–2005). In: A. V. Gaevskaya and A. L. Morozova, eds., 2009. *Karadag – 2009: Collection of Scientific Papers Dedicated to the 95th Anniversary of the Karadag Research Station and 30th Anniversary of the Karadag Nature Reserve of the National Academy of Sciences of Ukraine*. Sevastopol: ECOSI-Gidrofizika, pp. 292–312 (in Russian).
2. Kuftarkova, E.A., Rodionova, N.Yu., Gubanov, V.I. and Bobko, N.I., 2008. Hydrochemical Characteristics of Several Bays of Sevastopol Coast. In: YugNIRO, 2008. *Trudy YUGNIRO = YugNIRO Proceedings*. Kerch: YugNIRO Publishers. Vol. 46, pp. 110–111 (in Russian).
3. Ryabushko, V.I., Shchurov, S.V., Kovrigina, N.P., Lisitskaya, E.V. and Pospelova, N.V., 2020. Comprehensive Research of the Environmental Status of Coastal Waters of Sevastopol (Western Crimea, Black Sea). *Ecological Safety of Coastal and Shelf Zones of Sea*, (1), pp. 104–119. https://doi.org/10.22449/2413-5577-2020-1-104-119 (in Russian).
4. Manilyuk, Y.V., Lazorenko, D.I. and Fomin, V.V., 2021. Seiche Oscillations in the System of Sevastopol Bays. *Water Resources*, 48(5), pp. 726–736. EDN JYJFLJ. https://doi.org/10.1134/S0097807821050122
5. Lomakin, P.D. and Chepyzhenko, A.A., 2019. Hydrophysical Conditions and Characteristics of Water Pollution of the Kazachya Bay (Crimea Region) in September of the Year 2018. *Monitoring Systems of Environment*, (1), pp. 48–54. https://doi.org/10.33075/2220-5861-2019-1-48-54
6. Lomakin, P.D. and Chepyzhenko, A.I., 2019. Estimation of Water Pollution of Streletskaya Bay (Crimea) Associated with Fleet Operation. *Ekspluatatsia Morskogo Transporta*, (3), pp. 131–136. https://doi.org/10.34046/aumsuomt92/20
7. Gruzinov, V.M., Dyakov, N.N., Mezenceva, I.V., Malchenko, Y.A., Zhohova, N.V. and Korshenko, A.N., 2019. Sources of Coastal Water Pollution near Sevastopol. *Oceanology*, 59(4), pp. 523–532. https://doi.org/10.1134/S0001437019040076
8. Lyakh, A.M. and Bryantseva, Yu.V., 2001. Computer's Program for the Calculation of Basic Phytoplankton Parameters. *Ecology of the Sea*, 58, pp. 87–90 (in Russian).

9. Kapranov, S.V., Kovrigina, N.P., Troshchenko, O.A. and Rodionova, N.Y., 2020. Long-Term Variations of Thermohaline and Hydrochemical Characteristics in the Mussel Farm Area in the Coastal Waters off Sevastopol (Black Sea) in 2001–2018. *Continental Shelf Research*, 206, pp. 104–185. https://doi.org/10.1016/j.csr.2020.104185
10. Podymov, O.I., Zatsepin, A.G. and Ocherednik, V.V., 2021. Increase of Temperature and Salinity in the Active Layer of the North-Eastern Black Sea from 2010 to 2020. *Physical Oceanography*, 28(3), pp. 257–265. https://doi.org/10.22449/1573-160X-2021-3-257-265
11. Lomakin, P.D., Chepyzhenko, A.A. and Popov, M.A., 2024. Anthropogenic Changes in the Morphometric Characteristics of Kruglaya Bay (Crimea). *Biodiversity and Sustainable Development*, 9(1), pp. 77–90 (in Russian).
12. Dortch, Q., 1990. The Interaction Between Ammonium and Nitrate Uptake in Phytoplankton. *Marine Ecology Progress Series*, 61, pp. 183–201. https://doi.org/10.3354/meps061183
13. Bhavya, P.S., Kang, J.J., Jang, H.K., Joo, H., Lee, J.H., Park, J.W., Kim, K., Kim, H.C. and Lee, S.H., 2020. The Contribution of Small Phytoplankton Communities to the Total Dissolved Inorganic Nitrogen Assimilation Rates in the East/Japan Sea: An Experimental Evaluation. *Journal of Marine Science and Engineering*, 8(11), 854. https://doi.org/10.3390/jmse8110854
14. Mikaelyan, A.S., Silkin, V.A. and Pautova, L.A., 2011. Coccolithophorids in the Black Sea: Their Interannual and Long-Term Changes. *Oceanology*, 51(1), pp. 39–48. https://doi.org/10.1134/S0001437011010127
15. Egorov, V.N., Popovichev, V.N., Gulin, S.B., Bobko, N.I., Rodionova, N.Y., Tsarina, T.V. and Marchenko, Y.G., 2018. The Influence of Phytoplankton Primary Production on the Cycle of Biogenic Elements in the Coastal Waters off Sevastopol, Black Sea. *Russian Journal of Marine Biology*, 44(3), pp. 240–247. https://doi.org/10.1134/S1063074018030057
16. Sutcu, A. and Kocum, E., 2017. Phytoplankton Stoichiometry Reflects the Variation in Nutrient Concentrations and Ratios in a Nitrogen-Enriched Coastal Lagoon. *Chemistry and Ecology*, 33(5), pp. 464–484. https://doi.org/10.1080/02757540.2017.1316492

Submitted 23.07.2024; accepted after review 5.09.2024;
revised 25.03.2025; published 30.06.2025

About the authors:

Natalya V. Pospelova, Leading Research Associate, A.O. Kovalevsky Institute of Biology of the Southern Seas of RAS (2 Nakhimov Av., Sevastopol, 299011, Russian Federation), Ph.D. (Biol.), **ORCID ID: 0000-0002-3165-2090, Scopus Author ID: 56884605100, ResearcherID: C-7572-2016**, *nv.pospelova@ibss-ras.ru*

Sergey V. Shchurov, Research Associate, A.O. Kovalevsky Institute of Biology of the Southern Seas of RAS (2 Nakhimov Av., Sevastopol, 299011, Russian Federation), **ORCID ID: 0000-0002-8913-2637, Scopus Author ID: 57214992790, ResearcherID: AAC-9044-2022**, *skrimea@mail.ru*

Nelya P. Kovrigina, Senior Research Associate, A.O. Kovalevsky Institute of Biology of the Southern Seas of RAS (2 Nakhimov Av., Sevastopol, 299011, Russian Federation), Ph.D. (Geogr.), **ORCID ID: 0000-0002-6734-8285, Scopus Author ID: 6507114864, ResearcherID: AAC-9395-2022**, *npkovrigina@yandex.ru*

Elena V. Lisitskaya, Senior Research Associate, A.O. Kovalevsky Institute of Biology of the Southern Seas of RAS (2 Nakhimov Av., Sevastopol, 299011, Russian Federation), Ph.D. (Biol.), **ORCID ID: 0000-0002-8219-4616, Scopus Author ID: 6504112143, ResearcherID: T-1970-2017**, *lisitskaya@ibss-ras.ru*

Oleg A. Troshchenko, Research Associate, A.O. Kovalevsky Institute of Biology of the Southern Seas of RAS (2 Nakhimov Av., Sevastopol, 299011, Russian Federation), Ph.D. (Geogr.), **ORCID ID: 0000-0001-5200-9996, Scopus Author ID: 57218589904, ResearcherID: AAC-9364-2022**, *oleg_tr59@mail.ru*

Contribution of the authors:

Natalya V. Pospelova – literature review on the study problem, analysis and interpretation of phytoplankton results, statistical analysis, conclusion drawing

Sergey V. Shchurov – concept development, problem statement, literature review on the study problem, analysis and interpretation of hydrological and hydrochemical results, conclusion drawing

Nelya P. Kovrigina – analysis and interpretation of hydrological and hydrochemical results, conclusion drawing

Elena V. Lisitskaya – literature review on the study problem, analysis and interpretation of meroplankton results, conclusion drawing

Oleg A. Troshchenko – analysis and interpretation of hydrological and hydrochemical results, conclusion drawing

All the authors have read and approved the final manuscript.

ISSN 2413-5577, Ecological Safety of Coastal and Shelf Zones of Sea, 2025, No. 2, pp. 135–148.

Original paper

The Abundance and Distribution of Individual Bacterial Groups in Coastal Waters of the Kamchatka Peninsula

K. M. Zaripova [1] *, E. A. Demidova [2], E. A. Tikhonova [1], N. V. Burdiyan [1], Yu. V. Doroshenko [1], E. D. Basova [3]

[1] *A. O. Kovalevsky Institute of Biology of the Southern Seas of Russian Academy of Sciences, Sevastopol, Russian Federation*
[2] *Moscow Institute of Physics and Technology, Dolgoprudny, Russian Federation*
[3] *Institute of Oil and Gas Problems of the Russian Academy of Sciences, Moscow, Russian Federation*
* *e-mail: zaripova_km@ibss-ras.ru*

Abstract
The paper presents the results of microbiological study in the coastal waters of the northwestern Pacific Ocean and the Sea of Okhotsk, obtained during the expedition of cruise 23/4 of PV *Professor Multanovsky* (August–September 2023) within the Floating University Program. Quantitative characteristics and spatial distribution of bacteria transforming major classes of organic compounds, including petroleum hydrocarbons (diesel fuel), lipids, and phenols, in the surface and bottom layers of the water column were determined. The abundance of heterotrophic bacteria in the surface and bottom layers ranged from 10^3 to 10^5 cells/mL. The abundance of hydrocarbon-oxidizing bacteria ranged from 1 to 10^2 cells/mL in the surface layer and from 1 to 10 cells/mL in the bottom layer. The abundance of lipolytic bacteria varied from 10 to 10^3 cells/mL in both layers. The phenol-oxidizing bacterial group ranged in abundance values from 1 to 10^2 cells/mL in both the surface and bottom layers. The investigated bacterial groups exhibited non-uniform distribution in the coastal waters of the Kamchatka Peninsula. Maximum values are associated with the anthropogenically loaded Avacha Bay, exploited bays, and sites of active river runoff. During the study period, the water temperature of the surface layer ranged from 11.0 to 16.1°C, and the bottom layer ranged from 1.3 to 11.3°C. The pH values in surface water varied from 8.38 to 8.49. The depth at the bottom water sampling stations was from 13.5 to 780 m in the Pacific Ocean and from 26 to 62 m in the Sea of Okhotsk. No significant correlation was found between the abundance of identified microbial groups and the recorded physical and chemical parameters.

Keywords: heterotrophic bacteria, coastal waters, Kamchatka Peninsula, Avacha Bay, Sea of Okhotsk

Acknowledgements: The work was carried out during cruise 23/4 of PV *Professor Multanovsky* as part of the Floating University Program (Agreement no. 075-01593-23-06)

with the support of the Ministry of Science and Higher Education of the Russian Federation. The nutrient media for determining the abundance of indicator groups of bacteria were prepared as part of the IBSS state research assignment “Study of biogeochemical patterns of radioecological and chemoecological processes in the ecosystems of water bodies of the Sea of Azov–Black Sea Basin in comparison with other areas of the World Ocean and individual aquatic ecosystems of their drainage basins to ensure sustainable development in the southern seas of Russia” (No. 124030100127-7).

For citation: Zaripova, K.M., Demidova, E.A., Tikhonova, E.A., Burdiyan, N.V., Doroshenko, Yu.V. and Basova, E.D., 2025. The Abundance and Distribution of Individual Bacterial Groups in Coastal Waters of the Kamchatka Peninsula. *Ecological Safety of Coastal and Shelf Zones of Sea*, (2), pp. 135–148.

Численность и распределение отдельных групп бактерий в воде прибрежной акватории полуострова Камчатка

К. М. Зарипова [1] *, Е. А. Демидова [2], Е. А. Тихонова [1], Н. В. Бурдиян [1], Ю. В. Дорошенко [1], Е. Д. Басова [3]

[1] *Институт биологии южных морей имени А. О. Ковалевского РАН, Севастополь, Россия*

[2] *Московский физико-технический институт, Долгопрудный, Россия*

[3] *ИПНГ РАН «Институт проблем нефти и газа Российской академии наук», Москва, Россия*

* *e-mail: zaripova_km@ibss-ras.ru*

Аннотация

Представлены результаты микробиологических исследований прибрежной акватории северо-западной части Тихого океана и Охотского моря, полученные в ходе экспедиции рейса 23/4 ПС «Профессор Мультановский» (август – сентябрь 2023 г.) в рамках программы «Плавучий университет». Определены количественные характеристики и изучено пространственное распределение бактерий, трансформирующих основные классы органических соединений, включая углеводороды нефти (дизельное топливо), липиды и фенолы в поверхностном и придонном слоях водной толщи. Численность гетеротрофных бактерий в этих слоях варьировала от 10^3 до 10^5 кл/мл. Численность углеводородокисляющих бактерий составляла от 1 до 10^2 кл/мл в поверхностном слое и от 1 до 10 кл/мл − в придонном. Численность липолитических бактерий изменялась от 10 до 10^3 кл/мл в обоих слоях, а фенолокисляющей группы бактерий колебалась от 1 до 10^2 кл/мл. Исследованные группы бактерий распределены в прибрежной акватории п-ова Камчатка неравномерно. Максимальные показатели были зафиксированы в антропогенно нагруженной акватории Авачинской губы, эксплуатируемых бухтах и местах активного речного стока. В рассматриваемый период температура воды поверхностного слоя изменялась от 11.0 до 16.1 °С, придонного слоя – от 1.6 до 11.3 °С. Значения водородного показателя в воде поверхностного горизонта колебались в диапазоне от 8.38 до 8.49. Глубина на станциях отбора придонной воды варьировала от 13.5 до 780 м в Тихом океане и от 26 до 62 м в Охотском море. Значимых корреляционных связей между численностью определяемых групп микроорганизмов и указанными физико-химическими параметрами выявлено не было.

Ключевые слова: гетеротрофные бактерии, прибрежные воды, полуостров Камчатка, Авачинский залив, Охотское море

Благодарности: работы выполнены в рейсе 23/4 ПС «Профессор Мультановский» в рамках научно-образовательной программы «Плавучий университет» (соглашение № 075-01593-23-06) при поддержке Министерства науки и высшего образования РФ, питательные среды для определения численности индикаторных групп бактерий подготовлены в рамках темы госзадания ФГБУН ФИЦ «Институт биологии южных морей имени А. О. Ковалевского РАН (ФИЦ ИнБЮМ) «Изучение биогеохимических закономерностей радиоэкологических и хемоэкологических процессов в экосистемах водоемов Азово-Черноморского бассейна в сравнении с другими акваториями Мирового океана и отдельными водными экосистемами их водосборных бассейнов для обеспечения устойчивого развития на южных морях России» (№ гос. регистрации 124030100127-7).

Для цитирования: Численность и распределение отдельных групп бактерий в воде прибрежной акватории полуострова Камчатка / К. М. Зарипова [и др.] // Экологическая безопасность прибрежной и шельфовой зон моря. 2025. № 2. С. 135–148. EDN VUFBCX.

Introduction

Coastal marine waters represent a contact zone where land and sea pollutant fluxes are mixed. Furthermore, these bodies of water are frequently subject to intensive economic activities. A variety of organic substances are introduced into marine ecosystems, thereby becoming a significant and permanent environmental factor. These substances are then degraded by microorganisms [1]. Hydrocarbons are the most prevalent organic pollutants in ecosystems [2, 3]. Petroleum hydrocarbons and phenols play a substantial role in the contamination of the marine waters surrounding Kamchatka [1)].

When water bodies are polluted, increases in populations of individual bacterial groups are often observed before changes in water chemistry can be detected. Therefore, microbiological methods can be significantly more sensitive than sanitary-chemical ones [4]. Thus, we consider the number of hydrocarbon-oxidizing bacteria (HOB) as indicators of water pollution by hydrocarbons, the number of phenol-oxidizing bacteria (POB) – by phenol, the number of lipolytic bacteria (LLB) – by lipid substances [5]. In consideration of the fact that diesel-fuelled ships are moored in the study area [2)] and that fuel transportation and bunkering of ships are in constant operation [6, 7], one of the common types of hydrocarbon raw materials, namely diesel fuel, was selected as the sole source of carbon and energy for HOB.

Studies aimed at monitoring pollution levels and assessing the quality of natural waters pay special attention to the heterotrophic component of microbial communities. This component plays a key role in the energy balance of aquatic ecosystems and in the self-purification of water bodies.

[1)] Ministry of Natural Resources and Environment of the Kamchatka Krai, 2023. [*A Report on the State of the Environment in the Kamchatka Krai in 2022*]. 418 p. (in Russian).

[2)] Kasperovich, E.V., 2011. [*Technogenic Influence of Marine Vessels on the State of Near-Kamchatka Ecosystems*]. Extended Abstract of PhD Thesis. Petropavlovsk-Kamchatsky, 25 p. (in Russian).

In the coastal waters of East Kamchatka and the Sea of Okhotsk, the microbial indication method was previously used for operational characterisation of the water pollution degree (the number of heterotrophic microorganisms, including some physiological groups such as HOB and POB) in the surface water layer in the area of Avacha Bay, in the coastal water areas of Sakhalin and in the water area of the port of Magadan in 2001 [8]. Furthermore, in 1997–1999, microbiological studies were conducted in Avacha Bay and in the vicinity of the north-eastern coast of Sakhalin Island (as well as in the northern Primorye region and in the Peter the Great Gulf). Heterotrophic microorganisms from the surface and bottom water layers were studied, though within the context of evaluating the ecological status of water bodies subject to elevated levels of heavy metal pollution [9, 10]. In 2004–2006, the abundance of heterotrophic bacteria (HB), *E. coli* bacteria, HOB and LLB was investigated in the coastal waters of southern Sakhalin Island [3)]. In 2015, a study was conducted in Avacha Bay to ascertain the number of saprophytic microorganisms in marine water and other sanitary and microbiological indicators by determining the relevant measurements at six stations in different seasons [11]. In 2021, HOB were studied as indicators of watercourse pollution in the city of Petropavlovsk-Kamchatsky [12]. It can be concluded that studies of the abundance of heterotrophic microorganisms of different ecological and trophic groups were mainly episodic. Furthermore, the studies were localized in Avacha Bay, within the area of coastal waters of the Kamchatka Peninsula, while other areas were insufficiently investigated. The 2022 report on the state of the environment in Kamchatka Krai contains information on marine pollution in only two areas: Avacha Bay and Khalaktyrsky Beach [1)].

The work aims to reveal the peculiarities of the distribution of different bacterial indicator groups in the southeastern and southwestern coastal waters of the Kamchatka Peninsula in summer and autumn period.

Materials and methods

The studies were carried out in the summer and autumn period of 2023 during the cruise of PV *Professor Multanovsky* in the northwestern Pacific Ocean and the Sea of Okhotsk (Fig. 1, Table 1).

Sampling stations are linked to areas of potentially high anthropogenic impact: they are located in bays, in the marine mouths of large rivers and in pre-estuary areas with settlements, agricultural and industrial facilities in their catchment areas (Fig. 1). Thus, stations *1–3* are located in Avacha Bay, including directly at the mouth of the Avacha River, station *4* – in the strait connecting Avacha Bay to the ocean, station *15* – a few kilometres from the bay's outlet. Stations *6–8* are located near Khalaktyrsky Beach – next to the mouth of Nalycheva River where "red tides" were recorded in 2020 [13, 14]; station *12* – near the mouths of the Vakhil and Ostrovnaya rivers; station *24* – in the water area of Vilyuchinskaya Bay

[3)] Repina (Smirnova), M.A., 2009. [*Petroleum- and Hydrocarbon-Oxidizing Microorganisms of Coastal Waters of the Southern Sakhalin Island*]. Extended Abstract of PhD Thesis. Vladivostok: FEFU, 22 p. (in Russian).

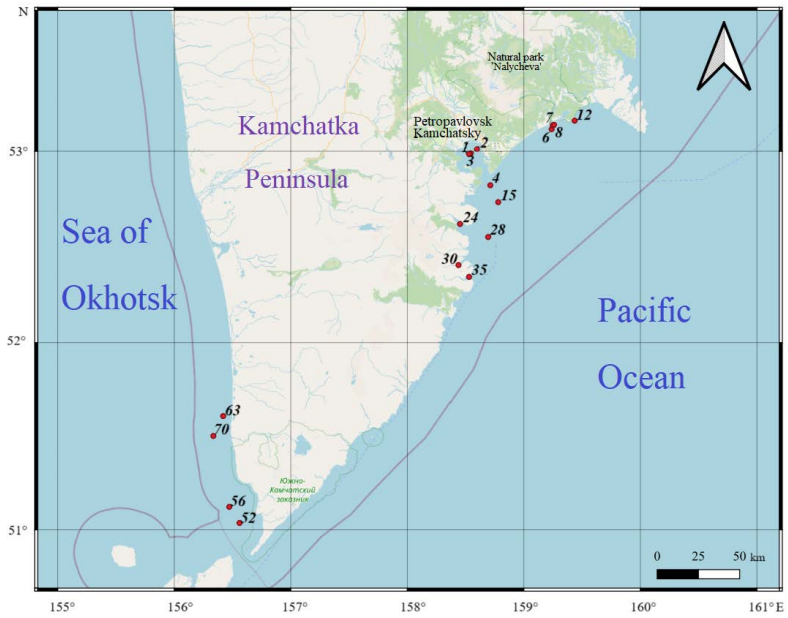

F i g . 1 . Map of sampling points in the coastal zone of the Kamchatka Peninsula, 2023

where the Vilyucha and Zhirovaya rivers flow into; station *30* was carried out in Russkaya Bay; station *35* – in Listvennichnaya Bay where the river of the same name flows into; station *56* – near the mouths of the Lysaya and Krivaya rivers; station *70* – around the mouth of the Ozernaya River near the settlement of Ozernovskiy.

Water samples were taken from the surface layer using a bathometer, while bottom water was taken directly from a box corer.

HB, HOB, LLB, POB abundance was determined in surface and bottom water layers. No inoculation was carried out for samples from the surface layer at station *28*, from the bottom layer at station *7* (and at station *15* for LLB and POB). Bacterial abundance was determined by the method of limiting dilutions using liquid nutrient media. Peptone medium was used for HB [4)], Voroshilova–Dianova medium – for HOB and LLB [15], modified Kalabina medium – for POB [16]. As the sole carbon and energy source, 1% sterile diesel fuel was added to each tube after inoculation for HOB and 1% sterile vegetable oil for LLB. The salinity of seawater was taken into account when preparing the media. The most probable number of microorganisms per unit volume was calculated using the McCredie table based on the method of variation statistics. Samples were processed no later than two hours from the time of collection [5)].

[4)] Mironov, O.G., ed., 1988. [*Biological Aspects of Oil Pollution of the Marine Environment*]. Kiev: Naukova Dumka, 248 p. (in Russian).

[5)] Netrusov, A.I., ed., 2005. [*Practical Course of Microbiology*]. Moscow: Akademiya, 608 p. (in Russian).

Table 1. Numbers, coordinates and depths of sampling stations on cruise 23/4 of PV *Professor Multanovsky*

Station number	Latitude, N	Longitude, E	Depth, m
1	52° 59.53′	158° 32.42′	25.0
2	53° 00.79′	158° 35.61′	22.0
3	52° 59.30′	158° 31.62′	26.0
4	52° 49.63′	158° 42.48′	59.0
6	53° 08.08′	159° 14.30′	15.0
7	53° 08.16′	159° 14.76′	15.0
8	53° 08.34′	159° 15.43′	13.6
12	53° 09.64′	159° 26.02′	24.0
15	52° 44.53′	158° 46.80′	780.0
24	52° 37.52′	158° 26.95′	14.0
28	52° 33.41′	158° 41.42′	119.0
30	52° 24.65′	158° 26.16′	26.0
35	52° 20.94′	158° 31.61′	31.0
52	51° 02.34′	156° 33.73′	33.0
56	51° 07.49′	156° 28.44′	62.0
63	51° 36.75′	156° 25.30′	26.0
70	51° 30.38′	156° 20.24′	57.0

To profile coastal waters as microbial habitat, temperature and salinity in the surface and bottom layers were recorded using a CTD probe (CTD Sea-bird SBE 911plus) and pH values in the surface water layer were determined using a pH meter (FireSting-PRO).

The map of sampling points was constructed in QGIS 3.34.11 software using an OpenStreetMap basemap.

Results and discussion

During the study period, surface water temperature at stations *1–35* in the northwestern Pacific Ocean varied from 11.0 to 15.7°C, bottom water temperature ranged from 1.6 to 11.3°C. Water salinity ranged from 26.8 to 30.8 PSU in the surface layer and from 31.2 to 34.1 PSU in the bottom layer. Bottom water sampling depths ranged from 13.6 to 780 m (Tables 1, 2).

In the Sea of Okhotsk, at sampling stations *52–70*, surface water temperature varied from 7.8 to 12.1°C and bottom water temperature ranged from 3.6 to 6.7°C. Recorded water salinity in the surface layer varied between 31.9 and 32.5 PSU and in the bottom layer between 32.5 and 32.9 PSU. Bottom water sampling depths ranged from 26 to 62 m (Tables 1, 2).

Table 2. Temperature and salinity in the surface and bottom water layers at sampling stations

Station number	Surface layer		Bottom layer	
	t, °C	*S*, PSU	*t*, °C	*S*, PSU
1	14.40	27.48	4.05	31,70
2	14.53	27.97	3.57	31.95
3	14.30	26.83	4.04	31.95
4	11.04	30.43	2.13	32.93
6	15.30	29.66	9.80	31.49
7	14.70	30.03	9.07	31.50
8	15.00	29.54	11.32	31.15
12	15.57	29.66	5.40	32.28
15	15.73	29.86	3.58	34.11
24	13.31	30.50	8.70	31.60
28	14.40	30.80	1.60	33.05
30	12.77	30.18	3.99	32.67
35	13.90	30.16	3.61	32.71
52	7.80	32.55	6.70	32.50
56	10.20	32.46	4.23	32.87
63	12.05	32.01	6.56	32.63
70	11.47	31.87	3.57	32.94

Organic matter-degrading bacteria were detected in all water samples from both layers (Fig. 2). HB abundance in both surface and bottom layers varies from 10^3 to 10^5 cells/mL. No statistically significant differences between the bacterial abundance values in these two layers were observed. Based on the HB abundance we determined, according to state standard GOST 17.1.2.04-77, 75% of water samples from the northwestern Pacific Ocean are classified as oligo- and beta-mesosaprobic waters. Exceptions are samples from the surface layer at stations *8*, *24* and *30* and from the bottom layer at stations *30* and *35*: water from these samples belongs to polysaprobic, i. e. to “dirty” water according to the organic pollution degree. In the Sea of Okhotsk, water samples taken from the surface layer (from the bottom layer at station *52*) are classified as polysaprobic (state standard GOST 17.1.2.04-77) based on the number of heterotrophic microorganisms. High HB abundance indicates water pollution with organic substances and high degree of adaptation of microorganisms to destruction of these substances.

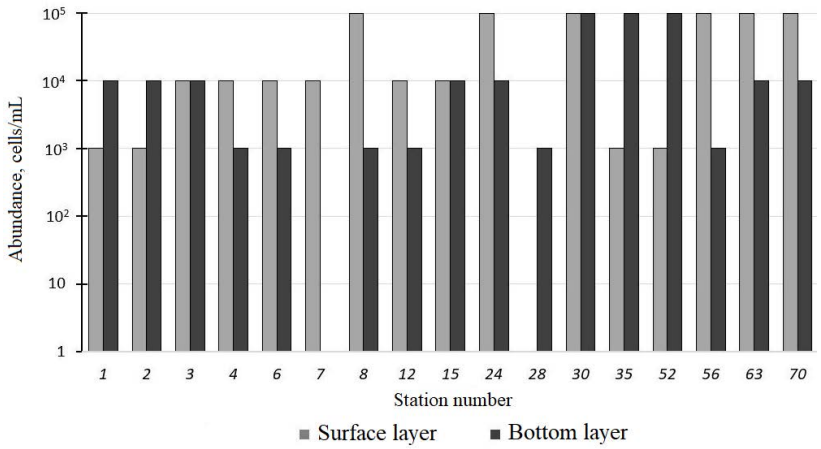

Fig. 2. Abundance of heterotrophic bacteria in the surface and bottom layers of the water column at the studied stations

Station *8* is located near the mouth of the Nalycheva River (the largest catchment area among the rivers of the Avacha group of volcanoes) and probably falls within the high turbidity contour of the river turbidity plume [17]. Higher HB abundance in the surface layer compared to the bottom layer at station 8 can indicate the input of organic matter with river runoff.

Stations 24, 30 and 35 are located in bays with high recreational value, which are often visited by tourists travelling by water transport, resulting in a certain anthropogenic load. Furthermore, these bays contain the mouths of minor rivers, which can serve as a source of organic matter input to the water areas under study.

HOB were isolated in 100% of samples. The abundance of hydrocarbon-oxidizing bacteria in seawater at most stations is 10 cells/mL in samples from the surface layer. The exceptions are station *3* (in Avacha Bay) and station *35* (in Listvennichnaya Bay) on

he Pacific coast of southeastern Kamchatka: at these stations, their abundance reaches 100 cells/mL in the surface layer and 1 cell/mL at stations *15* and *24*. The highest concentrations of dissolved hydrocarbons in Avacha Bay are regularly recorded in areas where ships are moored, ship repair plants and transport enterprises discharge wastewater. At the same time, tidal and surge currents contribute to the spread of petroleum hydrocarbons over the entire water area of the bay [18]. It should be noted that in May 2022, a discharge of oil products was detected near the pier of *Okeanrybflot* JSC (15 tons of oil products fell into the bay). During the spill, high concentrations of petroleum hydrocarbons were observed in the surface layer of the bay (at the level of 22–38 MPC, up to 1.7 mg/L), but six months after the spill clean-up, the content of hydrocarbons in the water in the accident area decreased 2.5 times [18].

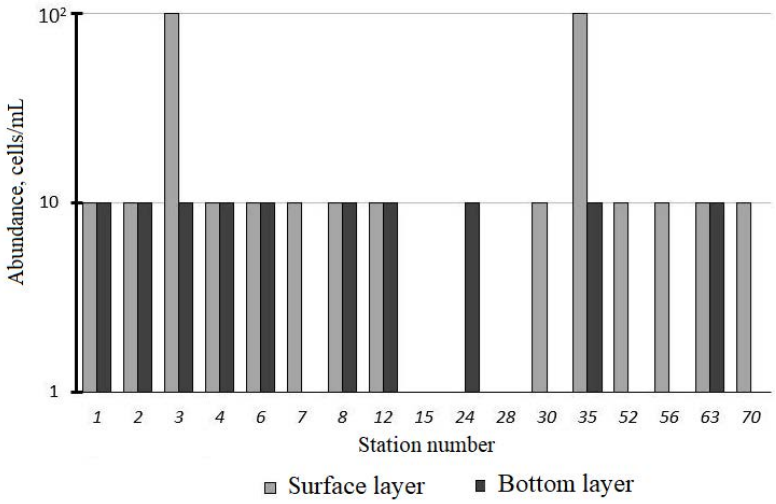

F i g . 3 . Abundance of hydrocarbon-oxidizing bacteria in the surface and bottom layers of the water column at the studied stations

The abundance of HOB in the bottom layer at most stations is also 10 cells/mL but minimum single values were recorded at stations *28*, *30*, *52*, *56* and *70* (Fig. 3).

No statistically significant differences between the bacterial abundance values in the surface and bottom layers of the marine water were recorded.

Oil hydrocarbons and phenols make the greatest contribution to the pollution of near-Kamchatka waters. It is noteworthy that, according to Kamchatka Hydrometeorological Service, the mean content of petroleum products in the water of 22 rivers of the peninsula from 2019 to 2022 decreased more than eight times and in 2022, the exceedance of MPC was approximately two times. In Kamchatka marine coastal waters – in Avacha Bay and in the coastal part of the gulf (Khalaktyrsky Beach area) – the mean content of dissolved petroleum hydrocarbons decreased from about 2 MPC in 2019 to 0.3 MPC in 2022 but in isolated cases, elevated values were observed in Avacha Bay [1)].

POB were isolated in 87.5% of samples from the surface layer. At most stations, their abundance was 10 cells/mL, at stations *7* and *8* (Khalaktyrsky Beach area, at different distances from the mouth of the Nalycheva River) and at station *30* in Russkaya Bay (Fig. 4) it reached 100 cells/mL and at stations *1* and *24* it was 1 cell/mL.

POB were isolated in 93.3% of samples from the bottom layer. At most stations, their abundance was 10 cells/mL, at station *6* (Khalaktyrsky Beach area) and at station *30* in Russkaya Bay (Fig. 4) it reached 100 cells/mL and at stations *3, 52* and *70* it was 1 cell/mL.

No statistically significant differences between the POB abundance in the surface and bottom layers were recorded.

Over the five-year (2018–2022) observation period of Kamchatka Hydrometeorological Service, the mean annual amount of phenols in coastal marine waters

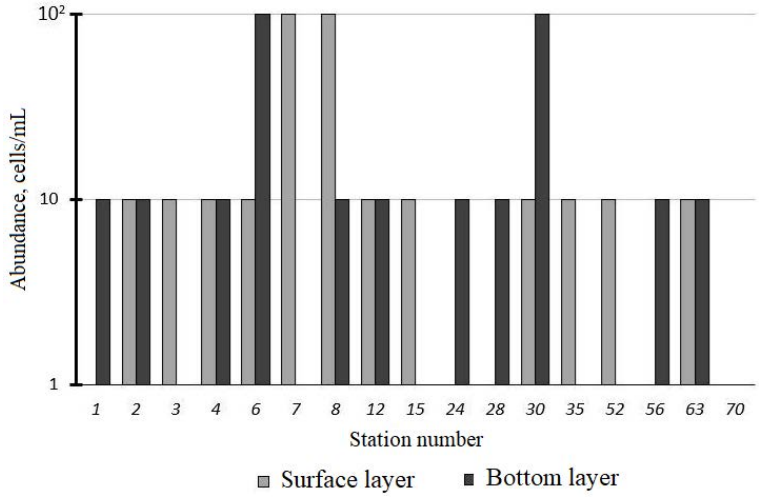

Fig. 4. Abundance of phenol-oxidizing bacteria in the surface and bottom layers of the water column at the studied stations

decreased from 2 to 0.3 MPC. Concurrently, phenol is a principal pollutant contaminating the river network of the peninsula. Its mean content in the river water remained at a level of 5–6 MPC from 2019 to 2022 [1)].

LLB were isolated in 100% of samples. The abundance of bacteria capable of lipid oxidation varied greatly from 1 to 1000 cells/mL in water samples from both surface and bottom layers (Fig. 5).

In the surface layer, the maximum abundance value (1000 cells/mL) was observed at stations *3* и *70*, the minimum one (1 cell/mL) was at station *63*. In the bottom layer, the maximum value (1000 cells/mL) was recorded at station *63*, the minimum one (1 cell/mL) was at station *70*.

No statistically significant differences between the LLB abundance in the surface and bottom layers were recorded. The correlation coefficient between the abundance of HOB and LLB is 0.4 (P = 0.05), which corresponds to a weak positive correlation. It is important to note that lipids can be formed during the process of oil biodegradation.

The abundance of microorganisms in seawater is determined by a number of factors, including temperature, salinity, depth, etc. The data on water temperature obtained during the study correspond to optimal conditions for the development of psychrophilic and psychrotrophic microorganisms. The findings of the study indicate that the values of the water hydrogen index in the designated area are conducive to the existence of HOB [19].

No significant correlations were found between the abundance of the studied microorganism groups and values of such indicators as surface and bottom water temperature, salinity and depth.

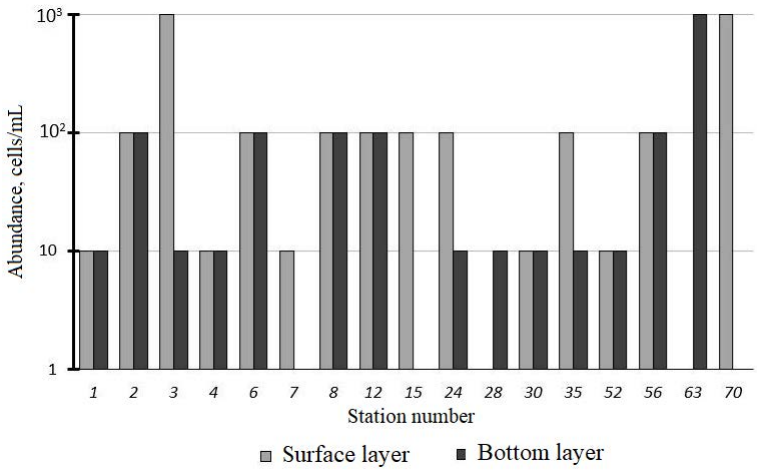

F i g . 5 . Abundance of lipolytic bacteria in the surface and bottom layers of the water column at the studied stations

The obtained HB abundance is comparable to the data for the coastal waters of Sakhalin Island in 2004–2006: the summer range of fluctuations in the average abundance of heterotrophic microorganisms was from $6 \cdot 10^3$ cells/mL (the settlement of Prigorodnoye) to $45 \cdot 10^7$ cells/mL (the port of Korsakov). In summer, the waters of the ports of Kholmsk and Korsakov as well as Lososey Bay corresponded to the category "very dirty" and the waters of the other stations – "dirty". Sakhalin coastal waters represent an area with multiple sources of oil pollution of both anthropogenic and natural origin: in summer, the share of HOB in the total number of heterotrophs here ranged from 60% (the village of Okhotskoye) to 80% (the village of Zolotorybnoye) [3)], which is several times higher than the HOB quantitative characteristics we obtained (see Fig. 3). It is also noted that the values of the absolute abundance of planktonic heterotrophic colony-forming microorganisms were previously studied in water samples collected from Avacha Bay in July 1999: their abundance was from $1.63 \cdot 10^4 \pm 0$ cells/mL in Turpanka Bay to $7.98 \cdot 10^5 \pm 0.83 \cdot 10^5$ cells/mL in Rakovaya Bay [9].

Conclusions

The study characterised the spatial distribution and quantitative characteristics of various organic-oxidising bacteria in the surface and bottom water layers near the southeastern and southwestern coasts of the Kamchatka Peninsula in August–September 2023. The abundance of all investigated groups of bacteria fluctuated within wide limits and was unevenly distributed in the peninsula coastal waters. The maximum values were recorded in the anthropogenically loaded water area of Avacha Bay, in occupied bays and places of active river runoff. Local high abundance of HB indicates both pollution of waters with organic substances and high potential of waters for self-purification.

The studied physiological groups of bacteria exhibited no significant differences in abundance in the surface and bottom layers. No significant correlations were identified between the abundance of bacteria of different groups and such parameters as salinity, temperature and depth.

References

1. Pandolfo, E., Caracciolo, A.B. and Rolando, L., 2023. Recent Advances in Bacterial Degradation of Hydrocarbons. *Water*, 15(2), 375. https://doi.org/10.3390/w15020375
2. Giri, K. and Rai, J.P.N., 2014. Bacterial Metabolism of Petroleum Hydrocarbons. In: M. Ahmad, ed., 2014. *Biotechnology. Vol. 11: Biodegradation and Bioremediation*. Studium Press India Pvt. Ltd., pp. 73–93.
3. Abdullah, S.R.S., Al-Baldawi, I.A., Almansoory, A.F., Purwanti, I.F., Al-Sbani, N.H. and Sharuddin, S.S.N., 2020. Plant-Assisted Remediation of Hydrocarbons in Water and Soil: Application, Mechanisms, Challenges and Opportunities. *Chemosphere*, 247, 125932. https://doi.org/10.1016/j.chemosphere.2020.125932
4. Nemirovskaya, I.A., 2013. *Oil in the Ocean (Pollution and Natural Flow)*. Moscow: Nauchny Mir, 428 p. (in Russian).
5. Mironov, O.G., 2002. Bacterial Transformation of Oil Hydrocarbons in the Coastal Zone of Sea. *Marine Ekological Journal*, 1(1), pp. 56–66. (in Russian).
6. Trudnev, S.Yu. and Nistor, A.S., 2020. The Analysis of Accident Rate of Fishing Fleet Vessels in the Far East. In: O. A. Belov, ed., 2020. [*Technical Operation of Water Transport: Problems and Ways of Development. Proceedings of the Second International Scientific and Technical Conference (23–25 October 2019)*]. Petropavlovsk-Kamchatsky: KamchatGTU, pp. 66–69 (in Russian).
7. Shevtsov, M.N. and Makarova, V.S., 2023. Assessment of Possible Negative Consequences from Accidental Spill of Oil Products on the Sea Area during Cargo Transfer from the Barge Operations. *Bulletin of PNU*, (1), pp. 153–160 (in Russian).
8. Zhuravel, E.V., Bezverbnaya, I.P. and Buzoleva, L.S., 2004. Microbian Indication of Pollution of the Coastal Zone of the Sea of Okhotsk and Avacha Bay. *Russian Journal of Marine Biology*, 30(2), pp. 138–142. (in Russian).
9. Dimitrieva, G.Yu., Bezverbnaya, I.P. and Khristoforova, N.K., 2001. Microbial Indication as Possible Approach for Heavy Metals Monitoring in Far-Eastern Seas. *Izvestia TINRO*, 128(3), pp. 719–736. (in Russian).
10. Dimitrieva, G.Yu. and Bezverbnaya, I.P., 2002. Microbial Indication as Effective Tool for Monitoring of Heavy Metals Pollution of Coastal Sea Waters. *Okeanologiya*, 42(3), pp. 408–415 (in Russian).
11. Sergeenko, N.V. and Ustimenko, E.A., 2016. In: A. V. Gaevskaya, ed., 2016. *Marine Biological Research: Achievements and Perspectives. Proceedings of All-Russian Scientific-Practical Conference with International Participation Dedicated to the 145th Anniversary of Sevastopol Biological Station (Sevastopol, 19–24 September, 2016)*. Sevastopol: EKOSI-Gidrofizika, Vol. 3, pp. 214–217 (in Russian).
12. Koneva, M.N. and Stupnikova, N.A., 2021. Oil-Oxidizing Microorganisms as Indicators of Oil Pollution of Watercourses of Petropavlovsk-Kamchatsky. *International Research Journal,* (7), pp. 23–27 (in Russian).
13. Sanamyan, N.P., Korobok, A.V. and Sanamyan, K.E., 2023. Qualitative Assessment of Algae Harmful Bloom Impact in Autumn 2020 off the Coast of South-Eastern Kamchatka (North-West Pacific) on Shallow-Water Benthic Communities. *Bulletin of Kamchatka State Technical University*, (63), pp. 22–43 (in Russian).

14. The Mysterious Mass Death of Marine Organisms on the Kamchatka Peninsula: A Consequence of a Technogenic Impact on the Environment or a Natural Phenomenon? *Marine Pollution Bulletin*, 166, 112175. https://doi.org/10.1016/j.marpolbul.2021.112175
15. Voroshilova, A.A. and Dianova, E.V., 1952. [Oil-Oxidizing Bacteria – Performance Indices of Oil Biological Oxidation under Natural Conditions]. *Mikrobiologiya*, 21(4), pp. 408–415 (in Russian).
16. Ermolaev, K.K. and Mironov, O.G., 1975. The Role of Phenol Decomposing Microorganisms in Detoxication of Phenol in the Black Sea. *Mikrobiologiya*, 10(5), pp. 928–932 (in Russian).
17. Chalov, S.R., Tsyplenkov, A.S., Shkolny, D.I., Prokopeva, K.N. and Bahareva, E.I., 2022. Overland Runoff and Its Impact on Hydrobiont Mortality in Avachinsky Gulf (Pacific Ocean, Kamchatka). *Proceedings of the Russian Geographical Society*, 154(4), pp. 69–84. https://doi.org/10.31857/S0869607122040048 (in Russian).
18. Rusanova, V.A. and Sedova N.A., 2023. Determining the Content of Oil Products in Water and Bottom Sediments of Avacha Bay in 2022. In: E. G. Lobkov, 2023. [*Natural Resources, Their Current State, Protection, Commercial and Technical Application : Proceedings of the 14th National (All-Russian) Scientific and Practical Conference (21–22 March 2023)*]. Petropavlovsk-Kamchatsky: KamchatGTU, pp. 149–152. https://doi.org/10.24412/cl-35030-2023-1-149-152
19. Chaudhry, G.R., ed., 1994. *Biological Degradation and Bioremediation of Toxic Chemicals*. Oregon: Dioscorides Press, 1994. 515 p.

Submitted 22.05.2024; accepted after review 23.07.2024;
revised 25.03.2025; published 30.06.2025

About the authors:

Ksenia M. Zaripova, Junior Research Associate, A. O. Kovalevsky Institute of Biology of the Southern Seas of RAS (2 Nakhimova Ave., Sevastopol, 299011, Russian Federation), **ORCID ID: 0009-0001-1160-4139, Scopus Author ID: 59173430600, ResearcherID: GWV-4575-2022**, *zaripova_km@ibss-ras.ru*

Ekaterina A. Demidova, Master's Degree Student, Moscow Institute of Physics and Technology (9 Institutskiy Lane, Dolgoprudny, Moscow Region, 141700, Russian Federation), **ORCID ID: 0009-0003-6756-5962, ResearcherID: KIK-8782-2024**, *kated.00000@gmail.com*

Elena A. Tikhonova, Leading Research Associate, A. O. Kovalevsky Institute of Biology of the Southern Seas of RAS (2 Nakhimova Ave., Sevastopol, 299011, Russian Federation), PhD (Biol.), **ORCID ID: 0000-0002-9137-087X, Scopus Author ID: 57208495804, ResearcherID: X-8524-2019**, *tihonoval@mail.ru*

Nataliya V. Burdiyan, Senior Research Associate, A. O. Kovalevsky Institute of Biology of the Southern Seas of RAS (2 Nakhimova Ave., Sevastopol, 299011, Russian Federation), PhD (Biol.), **ORCID ID: 0000-0001-8030-1556, Scopus Author ID: 57208497483, ResearcherID: AAD-1704-2022**, *burdiyan@mail.ru*

Yulia V. Doroshenko, Research Associate, A.O. Kovalevsky Institute of Biology of the Southern Seas of RAS (2 Nakhimova Ave., Sevastopol, 299011, Russian Federation), PhD (Biol.), **ORCID ID: 0000-0003-0498-3369; Scopus Author ID: 57211643141, ResearcherID: AAD-1706-2022**, *julia_doroshenko@mail.ru*

Evgeniya D. Basova, Research Associate, Institute of Oil and Gas Problems of RAS (3 Gubkina St., Moscow, 119333, Russian Federation), **Scopus Author ID: 57206472011, ORCID ID: 0009-0003-4017-2595**, *basovaed@my.msu.ru*

Contribution of the authors:

Ksenia M. Zaripova – writing and preparation of the article, justification of the study and preparation of the literature review, construction of graphical material, sampling, microbiological work to determine the number of indicator bacteria groups, processing and description of the study results, analysis and discussion of the results

Ekaterina A. Demidova – construction of graphical material, preparation of the article, sampling, microbiological work to determine the number of indicator bacteria groups

Elena A. Tikhonova – concept development, aim and objectives statement, discussion of the results, justification of the study, sampling

Nataliya V. Burdiyan – methodology description, discussion of the results, preparation of culture media

Yulia V. Doroshenko – methodology description, discussion of the results, preparation of culture media

Evgeniya D. Basova – sampling, glossary preparation

All the authors have read and approved the final manuscript.

Original paper

Distribution of the Chestnut Goby *Chromogobius quadrivittatus* (Steindachner, 1863) in the Black Sea and the Problem of its Range Expansion

E. P. Karpova [1] *, **E. R. Abliazov** [1, 2]

[1] *A. O. Kovalevsky Institute of Biology of the Southern Seas of Russian Academy of Sciences, Sevastopol, Russian Federation*

[2] *Severtsov Institute of Ecology and Evolution, Russian Academy of Sciences, Moscow, Russian Federation*

* *e-mail: karpova_jey@mail.ru*

Abstract

Under climate change and increasing anthropogenic pressure, rare species with unique ecosystem functions are particularly vulnerable. One of these species is the chestnut goby *Chromogobius quadrivittatus*, whose presence in the Black Sea has long been considered occasional. The study aims to specify the range, abundance and ecological peculiarities of this species. For this purpose, underwater observations and captures were carried out from 2012 to 2022 near the Crimean and the Caucasian coasts using the apnoea diving method, photosurvey and artificial habitat traps. Four stationary habitats of the species were recorded in the mentioned area predominantly in rocky and stony biotopes in shallow waters. The populations showed mosaic distribution and significant inter-annual fluctuations in abundance. Maximum abundance was recorded in 2016–2018 in Kazachya Bay (Sevastopol) and was up to 3 individuals per square metre. No such concentrations of the species have been noted since 2020. It is presumably due to increased abundance of the rock bass *Serranus scriba*. In the Black Sea populations, the size characteristics of fish were close to the maximum known and positive allometry was observed. Fish matured at SL 45.5 mm, and the male-to-female ratio in the sample was 1:1. These findings add to the data on species characteristics of the chestnut goby in the Black Sea and indicate the need for a more accurate assessment of its conservation status given limited information on the population abundance and dynamics.

Keywords: chestnut goby, *Chromogobius quadrivittatus*, Black Sea, cryptobenthic species, length-weight relationships, species distribution

Acknowledgments: The work was performed under state assignment of IBSS on topic "Biodiversity as the basis for the sustainable functioning of marine ecosystems, criteria and scientific principles for its conservation" (state registration number 124022400148-4).

For citation: Karpova, E.P. and Abliazov, E.R., 2025. Distribution of the Chestnut Goby *Chromogobius quadrivittatus* (Steindachner, 1863) in the Black Sea and the Problem of its Range Expansion. *Ecological Safety of Coastal and Shelf Zones of Sea*, (2), pp. 149–158.

Распространение четырехполосого бычка *Chromogobius quadrivittatus* (Steindachner, 1863) в Черном море и проблема расширения его ареала

Е. П. Карпова [1] *, **Э. Р. Аблязов** [1, 2]

[1] *Институт биологии южных морей им. А. О. Ковалевского РАН, Севастополь, Россия*
[2] *Институт проблем экологии и эволюции им. А. Н. Северцова РАН, Москва, Россия*
* *e-mail: karpova_jey@mail.ru*

Аннотация
В условиях климатических изменений и нарастающего антропогенного давления редкие виды, обладающие уникальными экосистемными функциями, оказываются особенно уязвимыми. Одним из таких видов является четырехполосый хромогобиус *Chromogobius quadrivittatus*, чье присутствие в Черном море долгое время считалось эпизодическим. Настоящее исследование направлено на уточнение ареала, численности и экологических особенностей этого вида. Для этого с 2012 по 2022 г. проводились подводные наблюдения и отлов у побережья Крыма и Кавказа с применением техники апноэ, фотофиксации и ловушек – искусственных биотопов. Были зафиксированы четыре устойчивых местообитания вида у берегов Крыма и Кавказа, преимущественно в скально-каменистых биотопах на мелководье. Популяции демонстрировали мозаичное распределение и значительные межгодовые колебания численности. Максимальное обилие было зарегистрировано в 2016–2018 гг. в б. Казачьей (Севастополь) и составляло до трех особей на квадратный метр. С 2020 г. таких концентраций вида не отмечается. Предположительно, это результат увеличения численности каменного окуня *Serranus scriba*. В черноморских популяциях размерные характеристики рыб были близки к максимально известным, наблюдалась положительная аллометрия, созревали рыбы при достижении стандартной длины 45.5 мм, соотношение самцов и самок в выборке составляло 1:1. Полученные данные дополняют сведения о видовых характеристиках хромогобиуса в Черном море и указывают на необходимость более точной оценки его охранного статуса в условиях ограниченной информации о численности и динамике популяций.

Ключевые слова: четырехполосый хромогобиус, *Chromogobius quadrivittatus*, Черное море, криптобентический вид, линейно-весовые соотношения, распространение вида

Благодарности: работа выполнена в рамках государственного задания ФИЦ ИнБЮМ по теме «Биоразнообразие как основа устойчивого функционирования морских экосистем, критерии и научные принципы его сохранения» (№ гос. регистрации 124022400148-4).

Для цитирования: *Карпова Е. П., Аблязов Э. Р.* Распространение четырехполосого бычка *Chromogobius quadrivittatus* (Steindachner, 1863) в Черном море и проблема расширения его ареала // Экологическая безопасность прибрежной и шельфовой зон моря. 2025. № 2. С. 149–158. EDN RNTBAU.

Introduction

The ongoing degradation of ecosystems precipitated by climatic changes and increasing anthropogenic impact has led to a marked decline in biodiversity, with numerous species facing extinction. It is a well-documented fact that rare and small species are often the first to disappear. Despite the extensive research that has been conducted on the significance of biodiversity in ensuring ecosystem functionality, the role of these species remains a subject of debate. It is acknowledged that a limited number of species are capable of performing essential functions in a variety of transformative systems [1, 2]. The results obtained by these authors emphasize the importance of conserving rare species even in ecosystems with high diversity, which are thought to exhibit high functional redundancy. The hypothesis that common species can compensate for the loss of functions in ecosystems maintained by rare species has not been demonstrated. The role of rare and low abundance species extends beyond the aesthetic or taxonomic value of diversity; these species augment significantly the potential breadth of functions provided by ecosystems. Consequently, they are likely to ensure biodiversity against uncertainty arising from ecological restructuring due to climate change and ever-increasing anthropogenic pressure on ecosystems.

This is particularly evident in ecosystems characterised by low species diversity, a category that encompasses the Black Sea. In contrast, other ecosystems are likely to exhibit high functional redundancy. To illustrate this point, the number of fish species in the region is considerably lower than in the neighbouring Mediterranean basin, with only approximately 40 species being common and widespread. For rare species, data are definitely insufficient and often limited to records of isolated finds.

This also applies to one of the members of the Gobiidae family – the chestnut goby *Chromogobius quadrivittatus* (Steindachner, 1863). Based on isolated, generally few finds, its range includes the Eastern Atlantic, the Mediterranean, Aegean, Marmara and Black seas [1), 2), 3)] [3–7]. The history of findings of this species in the Black Sea is complex and long. It was first found in 1939 [8] in a salt lake near Novorossiysk, then in the coastal lagoons of Abrau and Sochi, and it was defined as a new scientific species and genus – *Relictogobius kryzanovskii* Ptschelina. Much later, the specimens were redefined as *Ch. quadrivittatus* [9] and the species has been granted the status of a Mediterranean alien. The following finds were discovered on the coast of the Gulf of Varna (Bulgaria) in 1957 [1)] and in coastal lakes between capes Bolshoi and Maly Utrish in 1971 [10]. Further attempts to find the goby in its former habitats on the Caucasian coast were unsuccessful [11], and

---

1) Georgiev, Z.M., 1961. [An Unknown Goby of Bulgarian Ichthyofauna – *Relictogobius kryzanowskii*]. *Izvestia na Tsentralniya Nauchnoizsledovatelski Institut po Ribovodstvo i Ribolov – Varna*, 1, pp. 141–145 (in Bulgarian).

2) Svetovidov, A.N., 1964. [*Fishes of the Black Sea*]. Moscow, Leningrad: Nauka, 551 p. (in Russian).

3) Vassilev, M., Apostolou, A., Velkov, B., Dobrev, D. and Zarev, V., 2012. *Atlas of Gobies (Gobiidae) in Bulgaria*. Sophia: IBER-BAS, 112 p.

it was concluded that the population had disappeared due to habitat degradation. However, the fish were soon found along the entire Black Sea coast of Turkey [7].

The goby was first recorded off the Crimean coast in 2012 in the underwater caves of the Tarkhankut Peninsula, and in subsequent years it was repeated in these habitats [12], with no fish observed near the open coast in this area. A few years later, the species was also identified in the vicinity of Sevastopol [4)] [13].

It is evident that the species under consideration is present in a relatively consistent manner along various sections of the Black Sea coast. However, it is noteworthy that the presence of the species has been documented in areas where it has not been previously recorded. Conversely, the occurrences of the species are sporadic and often do not recur in the same location. This species belongs to the group of cryptobenthic species, for which it is rather difficult to establish the naturalization status in different habitats. Furthermore, anthropogenic impact is considered to be the presumed cause of the species rarity [11].

The aim of this study is to obtain new data on the distribution and some ecological and ethological peculiarities of a rare species, the chestnut goby, and to specify the current status of the Black Sea population of this species.

Materials and methods

Observations were conducted as part of the monitoring program for ichthyofauna in the coastal zone of the Black Sea. The fish searches in the coastal water area were conducted through the utilization of diving techniques, specifically the apnoea method. Stony coastal substrates of the Crimean coast from the Tarkhankut Peninsula in the area of Mezhvodnoye village to Cape Opuk and near the Caucasian coast in the area of the *Utrish* Nature Reserve were surveyed. The transect method was used, with a transect length of 10 m and width of 1 m, running parallel to the shore at depths of 1.0, 1.0–2.0 and 2.0–3.0 m. When on the transect, both free bottom areas and rocks located on it, including their underside, were examined. Surveys were conducted regularly since 2013 on the same transects in Kazachya Bay (Sevastopol), in 2016–2019 – in the area of the *Utrish* State Nature Reserve, in the rest of the water area – episodically, once in 2–4 years. When possible, detected fish were caught with a hand net (hoop diameter 30 cm, mesh pitch 3 mm) or recorded with Nikon D800 (Taiwan) photographic equipment. In Sevastopol, in Kazachya and Karantinnaya bays and at berth No. 164, surveys were also carried out with the use of a trap – an artificial habitat (Patent No. 2624417) (Sevastopol). The traps were made according to the scheme of the utility model (Patent No. 162868). A total of 38 specimens of gobies were caught and examined by different methods.

Captured individuals were transported alive to the laboratory where biological analyses, including measurements (total TL and standard SL length, weight W), visual gender determination, were performed. Furthermore, the behaviour of the fish under aquarium conditions was observed after undergoing adaptation.

[4)] Boltachev, A.R., Karpova, E.P. and Pashkov, A.N., 2018. [Chestnut Goby *Chromogobius quadrivittatus* (Steindachner, 1863)]. In: I. V. Dovgal and V. V. Korzhenevskiy, eds., 2018. *The Red Data Book of Sevastopol*. Kaliningrad, Sevastopol: ROST-DOAFK, p. 368 (in Russian).

Results and discussion

From 2012 to 2022, four mosaic habitats of the chestnut goby were found near the Crimean and Caucasian coasts – in the vicinity of Cape Tarkhankut, in Sevastopol bays, in Laspinskaya Bay and in the area of Cape Bolshoi Utrish (Fig. 1).

In August 2013, during an expedition to the Tarkhankut Peninsula (western coast of Crimea), 15 individuals of the goby were found indicating that a population had been established there. The species inhabited underwater caves and grottoes, including small openings located on vertical walls in the lower part of caves, with the depth reaching up to 5–6 m.

The next finding was made in 2015 at berth No. 164 (Sevastopol) where traps simulating an artificial habitat were set in March after the end of winter storms. Mussel and oyster shells were used as filler. Traps were placed at 2–5 m depths along the berth and concrete tetrapod-shaped breakwaters. Three months later, in June, the traps were lifted and their contents were thoroughly searched resulting in the finding of several extremely rare species in the Black Sea including two individuals of *Ch. quadrivittatus*.

In Sevastopol, in Kazachya and Karantinnaya bays, the gobies were found during visual survey among limestone rubble piled on shell sand as well as in gaps between concrete blocks of hydraulic structures. Fish were usually found in depressions and holes leading under fairly large stones and sometimes on the sand next to their shelter – in calm conditions. All individuals were recorded in shallow water, at a depth of 0.5–1.5 m. Near the open coast in Laspinskaya Bay and in the area

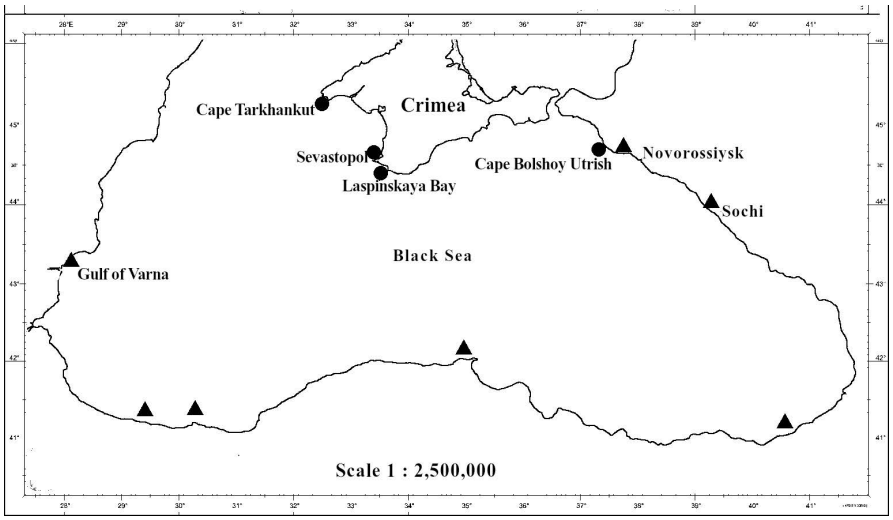

Fig. 1. The scheme of the locations of the chestnut goby finds in the Black Sea. Round markers are our findings, triangular markers are literary data

of Cape Bolshoi Utrish, fish were found in clumps of large rocks at the foot of boulders not subject to wave shear at 0.7–1.5 m depths in 2017 and 2018.

The maximum fish concentration was recorded in Kazachya Bay in 2016–2018 and reached 3 ind./m^2 and up to 10 individuals per transect. Fish were distributed very unevenly and could congregate in one small area and be absent from the rest of the transect. The gobies were predominantly recorded at shallow depths (0.5–0.8 m) in May and early June. Later, in July–October, fish were encountered at the same locations much less frequently and in numbers not exceeding 0.1 ind./m^2. Probably, as the water warmed up, they gradually migrated to deeper waters where it is much more difficult to detect them. Probably, therefore, the gobies were observed rarely and sporadically near the open shore, which does not make it possible to estimate the size of their populations.

Negative phototaxis associated with residence in darkened and twilight habitats was hypothesised for the gobies [11, 14]. However, according to our observations, fish are quite active also in sunlit areas and in calm conditions do not hurry to leave them. Probably, the behaviour noted by the researchers was more related to the general sensitivity of the species to stress factors and to the presence of observers. Most researchers classify the species as cryptobenthic [5, 7, 13], whose strategy is to hide and conceal themselves when any threatening factor (visual stimuli, water movement, etc.) appears.

We noted pronounced fluctuations in the abundance of this species. Fish were regularly recorded in the same habitat for 2–3 years, after which no individuals were found there. In the last 3–4 years, the gobies have become much rarer everywhere. Probably, one of the reasons for this was a sharp increase in the abundance of the rock bass *Serranus scriba* [14, 15] which occurs in various locations in large numbers including at shallow depths near the shore. At the same time, one large boulder can be used as a shelter by two to three rock bass individuals, which makes it unlikely that gobies live under such conditions as predators stalk their prey and do not let small fish leave their shelters in search of food. Negative impact of hydraulic construction on this species is unlikely as, according to our observations, the fish successfully exploit cracks between concrete blocks of berths and breakwaters made of artificial materials. The combination of factors such as cryptobenthic lifestyle, low abundance subject to sharp fluctuations and isolated finds in most Black Sea littoral countries can indicate that the range of the species covers the entire coastal part of the Black Sea where rocky and stony biotopes necessary for its successful survival are available and the lack of finds is mainly of a methodological nature.

It is possible to find little or no data on the biological and ecological characteristics of this species. Those papers where a maximum SL [5] of 66 mm is given for *Ch. quadrivittatus* [16], refer to a single study by P. J. Miller [3]. Individuals with sizes TL 35.0–71.1 mm, SL 28.7–60.3 and W 0.41–3.97 g were present in our findings. Consequently, the maximum sizes of the species in the Black Sea populations are close to those observed in the Mediterranean Sea. The relationship between total and standard fish length is described by the following equation: TL = 1.1427SL + 1.9413 with a high degree of approximation ($R^2 = 0.9938$) and length-weight relationships of the gobies (both genders) were expressed as follows: $W = SL^{3.11} \cdot 10^{-5}$ ($R^2 = 0.9772$). Fish exhibited positive allometry, which can be indicative of both species-specific traits and good feeding conditions. Fish matured at SL 45.5 mm, and the male-to-female ratio in the sample was 1:1.

As the fish matured, their colouration changed. In juvenile subjects with SL under 50 mm, the general body tone was olive with darker vertical stripes. The marble-like patterns on the head were bright, dark brown, the band at the base

Fig. 2. Specimens of *Ch. quadrivittatus* from Kazachya Bay (Sevastopol) with *TL* 42.5 mm (*a*) and 71.1 mm (*b*)

[5] Vasil'eva, E.D., 2007. *Fish of the Black Sea. Key to Marine, Brakish-Water, Euryhaline, and Anadromous Species with Color Illustration Collected by S. V. Bogorodsky*. Moscow: VNIRO Publishing, 238 p. (in Russian).

of the pectoral fin rays was dark, almost black, and the fins were yellow-olive in colour (Fig. 2, *a*). In larger individuals, the general body tone became brown, with very faint vertical stripes. The patterns on the head lost brightness and dark tone, and the fins also became lighter, up to the complete loss of the dark band on the pectoral fin, which is one of the defining characteristics of the species (Fig. 2, *b*).

The International Union for Conservation of Nature and Natural Resources has given this species LC (Least Concern) status. The question of whether this is appropriate, in the opinion of the authors of the article, is relevant in this case. As the chestnut goby leads a secretive way of life, it is extremely difficult to establish its number and population status. A more thorough evaluation can be found in the Red Data Book of Krasnodar Krai, where the species is categorized as Insufficiently Studied. This designation signifies that the reasons for its rarity have not been unequivocally determined, consequently precluding an accurate assessment of its extinction risk. The species is also included in the Red Data Book of the Republic of Crimea and the Red Data Book of the City of Sevastopol where it is assigned the 3rd category (rare species).

Conclusion

The conducted studies enabled to specify the current distribution and some features of the ecology of the chestnut goby *Chromogobius quadrivittatus* in the Black Sea. The species populations show mosaic distribution, predominantly in specific shelters in rocky and shaded habitats. Observed sharp fluctuations in abundance, limited number of finds and widespread fragmentation of the range indicate the potential vulnerability of the population. It has been found that despite its ability to master artificial structures, the species is under pressure from more abundant and aggressive inhabitants such as *Serranus scriba*, which may limit its distribution and maintenance of a stable population status. The contradiction between international Least Concern status and actual rarity in the Black Sea necessitates a reassessment of the level of threats and increased protection measures. These findings emphasize the importance of further monitoring and study of rare species that play a unique role in maintaining the sustainability and functional diversity of the regional marine ecosystems.

Compliance with ethical standards

In conducting this study, the authors claim to have adhered to all international, national or institutional guidelines relevant to the care and utilization of animals.

References

1. Mouillot, D., Bellwood, D.R., Baraloto, C., Chave, J., Galzin, R., Harmelin-Vivien, M., Kulbicki, M., Lavergne, S., Lavorel, S. [et al.], 2013. Rare Species Support Vulnerable Functions in High-Diversity Ecosystems. *PLoS Biology*, 11(5), e1001569. https://doi.org/10.1371/journal.pbio.1001569
2. Leitão, R.P., Zuanon, J., Villéger, S., Williams, S.E., Baraloto, C., Fortunel, C., Mendonça, F.P. and Mouillot, D., 2016. Rare Species Contribute Disproportionately to the Functional Structure of Species Assemblages. *Proceedings of the Royal Society B: Biological Sciences*, 283, 20160084. https://doi.org/10.1098/rspb.2016.0084

3. Miller, P.J., 1986. Gobiidae. In: P. J. P. Whitehead, M.-L. Bauchot, J.-C. Hureau, J. Nielsen and E. Tortonese, eds., 1986. *Fishes of the North-Eastern Atlantic and the Mediterranean*. Paris: UNESCO, Vol. 3, pp. 1019–1085.

4. Ahnelt, H., 1990. Chromogobius quadrivitatus, Chromogobius zebratus and Zebrus zebrus (Pisces, Gobiidae): Erstnachweise für Korsika (Frankreich) und Sardinien (Italien). *Annalen des Naturhistorischen Museums in Wien: Serie B: Botanik und Zoologie*, 91, B. 27–41.

5. Kovačić, M., 1997. Cryptobenthic Gobies (Pisces, Perficormes, Gobiidae) and Clingfishes (Pisces, Gobiesociformes, Gobiesocidae) in the Kvarner Area, Adriatic Sea. *Natura Croatica*, (6), pp. 423–435.

6. Van Tassel, J.L., 2001. Chromogobius (Teleostei: Gobiidae): A New Species from the Eastern Atlantic. *Copeia*, 4, pp. 1073–1080. https://doi.org/10.1643/0045-8511(2001)001[1073:CTGANS]2.0.CO;2

7. Engin, S., Seyhan, D., Akdemir, T. and Keskin, A.C., 2016. New Distribution Data for Two Cryptobenthic Gobiid Fish (Gobiidae) in the Turkish Coasts. *Journal of the Black Sea / Mediterranean Environment*, 22(1), pp. 110–118.

8. Pchelina, Z.M., 1939. [A New Goby Species from a Salt Lake of the Abrau Peninsula (the Black Sea Basin) Relictogobius kryzanovskii n.g., n.sp.]. *Doklady Akademii Nauk SSSR*, 23(6), pp. 586–589 (in Russian).

9. Miller, P.J., 1965. *Relictogobius kryzhanovskii* and the Penetration of Mediterranean Gobies into the Black Sea. *Nature*, 208(5009), pp. 474–475. https://doi.org/10.1038/208474a0

10. Pinchuk, V.I., 1987. [Taxonomic Notes on the Gobies (Perciformes, Gobiidae) of the Ukrainian Fauna]. *Vestnik Zoologii*, (5), pp. 30–35 (in Russian).

11. Pashkov, A.N., Reshetnikov, S.I. and Makhrov, A.A., 2013. On the Issue of Occurrence Frequency of the Chestnut Goby *Chromogobius quadrivittatus* (Steindachner, 1863) (Pisces, Gobiidae) in the Waters of Krasnodar Territory. In: O. A. Petrenko, ed., 2013. *Current Fishery and Environmental Problems of the Azov and Black Seas Region: Materials of VIII International Conference. Kerch, 26–27 June 2013*. Kerch: YugNIRO Publishers', pp. 83–87 (in Russian).

12. Kovtun, O.A., 2013. [A New Finding of the Rare Goby *Chromogobius quadrivittatus* (Actinopterygii, Perciformes, Gobiidae) in a Marine Underwater Cave of the Tarkhankut Peninsula (the Black Sea)]. *Marine Ekological Journal*, 12(1), p. 18 (in Russian).

13. Marin, I.N., 2018. New Records, Habitats and Features of Ecology Four-Banded Goby *Chromogobius quadrivittatus* (Steindachner, 1863) (Pisces: Gobiidae) Along the Russian Coasts of the Black Sea. *Ukrainian Journal of Ecology*, 8(4), pp. 320–322.

14. Karpova, E.P., Statkevich, S.V., Abliazov, E.R. and Gubanov, V.V., 2022. [Biodiversity of fish and decapod taxa of the Cape Martyan Nature Reserve (Crimea)]. In: V. N. Petrov, E. A. Borovichev, M. N. Kozhin and A. V. Marchenkov, 2022. *90 Years of Scientific Research in the Kandalaksha Reserve: History and Prospects. Abstracts of Reports of the Scientific-Practical Conference Devoted to the 90th Anniversary of the Kandalaksha State Reserve "90 Years of Scientific Research in the Kandalaksha Reserve: History and Prospects", Kandalaksha, 19–22 September 2022*. Apatity: Izd-vo FITs KNTs RAN, pp. 27–29. https://doi.org/10.37614/978.5.91137.470.9 (in Russian).

15. Kutsyn, D.N., Tamoikin, I.Yu., Samotoy, Yu.V. and Donchik, P.I., 2023. Age, Growth, and Maturity of Painted Comber Serranus Scriba (Serranidae) from the Crimea Region, the Black Sea. *Journal of Ichthyology*, 63(5), pp. 902–910. https://doi.org/10.1134/s0032945223050065

16. Kovačić, M., Renoult, J.P., Pillon, R., Svensen, R., Bogorodsky, S.V., Engin, S. and Louisy, P., 2022. Identification of Mediterranean Marine Gobies (Actinopterygii: Gobiidae) of the Continental Shelf from Photographs of *in situ* Individuals. *Zootaxa*, 5144, pp. 1–103. https://doi.org/10.11646/zootaxa.5144.1.1

Submitted 07.08.2024; accepted after review 21.10.2024;
revised 25.03.2025; published 30.06.2025

About the authors:

Evgeniia P. Karpova, Senior Research Associate, A. O. Kovalevsky Institute of Biology of the Southern Seas of RAS (2, Nakhimov av., Sevastopol, 299011, Russian Federation), PhD (Biol.), **ORCID ID: 0000-0001-9590-9302**, **Scopus Author ID: 26639409000**, **ResearcherID: T-5944-2019**, *karpova_jey@mail.ru*

Ernes R. Abliazov, Research Associate, A. O. Kovalevsky Institute of Biology of the Southern Seas of RAS (2, Nakhimov av., 299011, Sevastopol, 299011, Russian Federation), **ORCID ID: 0000-0002-8077-9848**, **Scopus Author ID: 57221542090**, **ResearcherID: AAS-2509-2021**, *e_ablyazov@mail.ru*

Contribution of the authors:

Evgeniia P. Karpova − collection of the material, analysis and discussion of the results, manuscript writing

Ernes R. Abliazov − processing of the material, analysis and discussion of the results, manuscript editing

All the authors have read and approved the final manuscript.

ISSN 2413-5577, Ecological Safety of Coastal and Shelf Zones of Sea, 2025, No. 2, pp. 159–174.

Original paper

Natural and Technogenic Risks Assessment of Arctic Nature Use for the Murmansk Region Coastal Zone

G. G. Gogoberidze [1], **E. A. Rumiantceva** [1] *, **I. A. Lednova** [2], **E. A. Efimenko** [1]

[1] *Murmansk Arctic University, Murmansk, Russia*
[2] *Peter the Great St. Petersburg Polytechnic University, St. Petersburg, Russia*
* *e-mail: rumkate@rambler.ru*

Abstract
Intensification of economic development of the Arctic coast of Russia increases the vulnerability of its coastal territories and coastal eco-socio-economic systems, exposed to a complex impact of natural and anthropogenic factors. Facing climatic changes and an increasing anthropogenic load, these Arctic territories require a comprehensive scientific system for analysing environmental and socio-economic risks of nature management to ensure their sustainable development. The study aims to develop a model of risk assessment that combines quantitative and qualitative indicator methods with a matrix method. The paper proposes an innovative matrix method of risk assessment based on a three-component structure (risk-source, risk-factor and risk-object). Each component of the system is characterised by a unique set of classification attributes, and the relationships between them are quantitatively assessed by the method of expert assessments on a five-point scale. The developed model of coastal management risks in the Russian Arctic contains two key matrices of risk components: risk-factor – risk-source and risk-object – risk-factor. This allows for a comprehensive analysis of risk formation processes. The model was applied in practice to 17 local coastal municipalities in the Murmansk Region. Using the developed methodology and model as a tool enables a thorough evaluation of the effectiveness of measures aimed at reducing environmental and socio-economic risks related to the Arctic coastal management. This approach provides a scientifically sound basis for improving territorial planning and forecasting the sustainability of Arctic coastal eco-socio-economic systems as an integrated whole, thus contributing to the sustainable development of Arctic coastal territories. Integrating the proposed model into management decision-making processes allows the dynamics of changes in the natural environment and socio-economic conditions to be taken into account in the mid- and long-term. This is particularly important for maintaining the balance in complex Arctic ecosystems.

Keywords: nature-use risks, social and economic risks, ecological and economic risks, coastal eco-socio-economic system, Arctic, integral risk indicator, nature-use ecology

Acknowledgements: The study was funded by Russian Science Foundation grant no. 24-17-20021, https://rscf.ru/en/roject/24-17-20021/, and Ministry of Education and Science of the Murmansk Oblast according to Agreement no. 199 as of 03.05.2024.

For citation: Gogoberidze, G.G., Rumiantceva, E.A., Lednova, I.A. and Efimenko, E.A., 2025. Natural and Technogenic Risks Assessment of Arctic Nature Use for the Murmansk Region Coastal Zone. *Ecological Safety of Coastal and Shelf Zones of Sea*, (2), pp. 159–174.

Оценка природных и техногенных рисков арктического природопользования для береговой зоны Мурманской области

Г. Г. Гогоберидзе [1], **Е. А. Румянцева** [1] *, **Ю. А. Леднова** [2], **Е. А. Ефименко** [1]

[1] *Мурманский арктический университет, Мурманск, Россия*
[2] *Санкт-Петербургский политехнический университет Петра Великого, Санкт-Петербург, Россия*
* *e-mail: rumkate@rambler.ru*

Аннотация
Интенсификация хозяйственного освоения арктического побережья России приводит к росту уязвимости прибрежных территорий, береговых эко-социо-экономических систем Арктической зоны Российской Федерации, подверженных комплексному воздействию природных и антропогенных факторов. В условиях климатических изменений и увеличения антропогенной нагрузки возникает необходимость в разработке комплексной научной системы анализа экологических и социально-экономических рисков природопользования для устойчивого развития прибрежных территорий Арктической зоны Российской Федерации. Цель исследования состоит в разработке такой модели оценки рисков, которая сочетает количественные и качественные индикаторные методики с матричной методикой. Предложена инновационная матричная методика оценки рисков, основанная на трехкомпонентной структуре (риск-источник, риск-фактор и риск-объект). Каждый компонент системы характеризуется уникальным набором классификационных признаков, а взаимосвязи между ними количественно оцениваются методом экспертных оценок по пятибалльной шкале. Разработанная модель рисков природопользования на побережье Российской Арктики содержит две ключевые матрицы составляющих риска: риск-фактор – риск-источник и риск-объект – риск-фактор, что позволяет проводить комплексный анализ рискообразующих процессов. Практическое применение модели проведено на примере 17 локальных приморских муниципальных образований Мурманской области. Применение разработанной методики и модели в качестве инструмента позволяет осуществлять комплексную оценку эффективности мер по снижению экологических и социально-экономических рисков, связанных с береговым арктическим природопользованием. Такой подход обеспечивает научно обоснованную базу для совершенствования территориального планирования и прогноза устойчивости арктических береговых эко-социо-экономических систем как единого комплекса, способствуя устойчивому развитию прибрежных территорий Арктики. Интеграция предложенной модели в процессы принятия управленческих решений дает возможность учитывать динамику изменений природной среды и социально-экономических условий в среднесрочной и долгосрочной перспективе, что особенно важно для сохранения баланса в сложных арктических экосистемах.

Ключевые слова: риски природопользования, социально-экономические риски, эколого-экономические риски, береговая эко-социо-экономическая система, Арктика, интегральный показатель риска, экология природопользования

Благодарности: исследование выполнено за счет гранта Российского научного фонда № 24-17-20021, https://rscf.ru/project/24-17-20021/ и Минобрнауки Мурманской области согласно Соглашения от 03.05.2024 № 199.

Для цитирования: Оценка природных и техногенных рисков арктического природопользования для береговой зоны Мурманской области / Г. Г. Гогоберидзе [и др.] // Экологическая безопасность прибрежной и шельфовой зон моря. 2025. № 2. С. 159–174. EDN XRRNBH.

Introduction

Economic development in the Arctic has increased the vulnerability of coastal ecosystems to natural and technogenic threats [1–5]. There is an urgent need to establish a scientific basis for analysing the risks associated with the nature use and their impact on the eco-socio-economic systems of the Arctic Zone of the Russian Federation (AZRF). One approach to such an analysis is to use a matrix in combination with quantitative and qualitative indicators. In the context of the Arctic, this approach can be implemented [1)] by using modern methodological tools, particularly cartographic and geoinformation methods [6–8] as well as marine spatial planning [9].

The concept of risk has many definitions in general, primarily relating to spheres of human activity that require assessment [2)] [5, 10]. In terms of nature use in Arctic conditions, risks are associated with the probability of a negative event occurring within a given timeframe, as well as the potential extent of damage. This damage can be measured in monetary terms or other absolute values, e. g. the area of exposed territory, volume of atmospheric emissions or the number of victims. A year is typically used as the time period for assessing nature-use risks.

A number of Arctic-specific issues need to be considered and addressed in risk assessment methodology [11–14]:

– creation of complex technical systems and the increased risk of nature use in the Arctic should be seen as the result of technological progress and increased use of natural resources;

[1)] Gogoberidze, G.G., Shilin, M.B. and Rumiantceva, E.A., 2020. [Principles of Classification of Nature Management Risks and their Interaction with Elements of the Coastal Eco-Socio-Economic System of the AZRF]. In: Rumiantceva, E.A., ed., 2020. *Regularities of Formation and Impact of Marine and Atmospheric Hazardous Phenomena and Disasters on the Coastal Zone of the Russian Federation under the Conditions of Global Climatic and Industrial Challenges ("Dangerous Phenomena – II") in memory of Corresponding Member RAS D.G. Matishov: Proceedings of the International Scientific Conference*. Rostov-on-Don, pp. 318–320 (in Russian).

[2)] Buyanov, V.P., Kirsan, K.A. and Mikhaylov, L.A., 2003. [*Riskology: Risk Management*]. Moscow: Ekzamen, 381 p. (in Russian).

– Arctic coastal nature use has a complex structure and is subject to unique risks that should be considered when developing territories and water areas;

– the impact of natural and anthropogenic risks on Arctic coastal eco-socio-economic systems poses a significant threat of cascading disasters and hierarchic systems catastrophes.

The coastal AZRF is characterised by two types of risk influencing nature-use processes: natural risks (as a consequence of natural hazards) and anthropogenic risks (including man-made disasters). While these types of risk to Arctic nature use are fundamentally different, they often occur together. This makes the Arctic region and its coastal zones unique in terms of the vulnerability of all components of coastal eco-socio-economic systems [15–17].

The study aims to develop a risk assessment model for Arctic nature use in coastal areas of the AZRF based on a risk assessment matrix in a sustainable nature use system. This will enable the spatial distribution of risk assessments to be obtained and the most important risk factors to be identified. The model will also be tested in seaside municipalities in the Murmansk region.

The article uses materials from conferences [1), 3)].

Methods

A matrix approach to the risk assessment of Arctic coastal nature use

Considering risk as infliction of harm with a certain probability, we can present it as a chain of three links [5, 16, 17].

1. Risk source.

The Arctic coastal zone is a complex eco-socio-system in which economic activity and nature use take place, and it contains potential sources of risk. The emergence of threats influences the region's sustainable development.

2. Risk factor.

The occurrence of negative factors transforms potential risks into specific events that threaten the objects and practices of nature use within the Arctic coastal system. Such threats originate from the risk source.

3. Risk object.

As an integral part of the Arctic coastal system, risk objects are exposed to negative factors that jeopardise their stable functioning and sustainability. An integrated

---

[3)] Gogoberidze, G.G. and Rumiantceva, E.A., 2023. Integrated Model of Risks of Arctic Nature-Use Management for the Russian Arctic Coastal Zone Based on the Interrelationship of Natural, Geomorphological and Technogenic Risk Factors. In: E. A. Rumiantceva, ed., 2023. [*Prevention and Elimination of Emergency Situations in the Arctic Zone of the Russian Federation : Proceedings of the Scientific-Practical Conference, 4–7 April 2023*]. Murmansk: MAGU, pp. 96–98 (in Russian).

approach to risk management is therefore required to ensure the long-term sustainability of the Arctic coastal zone.

It should be emphasised that the risk source and risk object in the Arctic coastal zone are closely bound, forming a sequence of interrelated risk incidents. Multi-stage accidents can be forecasted by applying the scenario method, whereby an initial hazard source initiates a risk factor that affects a vulnerable object. This object then becomes a generator of new risk factors, and the process repeats to form a hierarchical structure known as a risk tree.

Given the proposed structure, the following classification can be introduced [5, 17]:

1. Sources of risk:

– risk origin (the specific source generating the risk);

– controllability of risk reduction (the potential and effectiveness of measures aimed at reducing or eliminating risk);

– impact on the coastal eco-socio-economic system (the impact of risk on the environmental, social, and economic components of the coastal zone).

2. Risk factors:

– spatial coverage (the geographical area in which the risk occurs);

– time horizon of impact (duration of the period during which the risk has an impact);

– predictability (possibility of predicting the time and nature of the risk manifestation);

– probability of occurrence (frequency of risk occurrence in a given period).

3. Risk objects:

– the direct recipient of the risk (i. e. an element or system that is directly affected by the risk);

– the potential to induce a cascade of risks (the ability of a given risk to cause other, more complex risks);

– the position in the risk cascade (the position of the risk in the sequence of interrelated risk events);

– the scale of damage/consequences (the degree of negative consequences which may arise as a result of the risk occurence).

As a result, we made up a list of basic elements for each of the above risk components of the Arctic coastal eco-socio-economic system, as outlined in works [16–18]. This list generally contains:

– risk source (19 elements);

– risk factor (21 elements);

– risk object (18 elements).

Specialists assessed the relationships between the risk components using a scale from one to five [17]. Based on the obtained data, two matrices describing the components of the risk management process were developed:

– the first matrix is based on matching risk factors (in the rows) with sources of risk (in the columns). This 21 × 19 matrix is designed to numerically assess the intensity with which a certain risk factor is generated under the influence of each considered risk source;

– the second matrix is a structure in which the rows correspond to risk objects and the columns correspond to risk factors. This 18 × 21 matrix assesses the extent to which each risk factor may influence the correct and effective functioning of risk objects.

The key and minor risk elements for each matrix and structural component were determined based on summing up the values for the corresponding rows and columns.

The model of risks to Arctic nature use in the coastal AZRF

In accordance with the presented matrix approach for assessing the risk of nature use in Arctic coastal eco-socio-economic systems, the risk assessment methodology can be structured as an algorithm [5, 16].

1. The size of the risk matrices can be reduced by deleting the columns and rows corresponding to risk sources, risk factors and risk objects that are not available for a given local object.

2. The risk factors Ri are assessed using weight coefficients that are set according to the characteristics of the region under study [5]. Of note, the correction coefficients are actually matrices with a size coinciding with that of the matrices reflecting the ratio of risk elements.

The coefficients are calculated in accordance with criteria [16–18], based on analysis of the following data:

– information on past emergency situations of a natural or man-made origin. This analysis involves identifying the causes of these situations and assessing their consequences for the areas under consideration and adjacent territories;

– current and historical information on the situation of the study areas, obtained using satellite information. These analyses include the extent and types of development and infrastructure, coastline location, water's edge patterns and other spatial characteristics;

– information on the quantity and quality of infrastructure.

– plans for dealing with various emergency situations in the considered territories and adjacent areas;

– other information on the spatial and temporal features of the occurrence and dynamics of risk factors in the study territories.

3. The integral risk indicator R_{Int} is determined by summing all the risk factors R_i, adjusted by the appropriate territorial coefficients. It is calculated according to the formula

$$R_{Int} = \sum(R_i).$$

The key conceptual principles of the model for Arctic coastal nature-use risk assessment cover the following [5]:

1) the Arctic coastal eco-socio-economic system is a clearly defined geographical area. The boundaries of this system can be defined as follows, for example:

firstly, it may be a district-wide coastal municipality embracing adjacent marine areas;

secondly, the boundary may coincide with a coastal municipality consisting of settlements and including inland water bodies;

thirdly, the boundary could be a key geographical feature, such as a settlement with adjacent inland waters or other units characterised by interrelated environmental, social and economic aspects;

2) A non-dimensional method based on matrices describing risk components is used to assess the AZRF territorial object's exposure to hazardous events and calculate a comprehensive risk indicator. The first matrix, which compares risk factors and risk sources, shows how strongly each risk source influences the formation of the corresponding risk factor. The second matrix establishes the relationship between risk objects and risk factors and determines the impact level of each risk factor on the stable and effective functioning of the risk object in question. This approach allows a comprehensive assessment of the territory vulnerability and reveals key factors determining the level of risk.

To illustrate the process of determining the level of risk associated with activities in the Arctic coastal zone, we analysed some coastal territories in the Murmansk Region:

– the urban settlement of Kandalaksha. It is located in the southern Murmansk Region. The settlement's territory is divided by the Kola Peninsula: the northern part is on the peninsula while the southern one is on the mainland. To the southeast, the area borders Kandalaksha Bay;

– the rural settlement of Teriberka. It is located in the northern Murmansk Region and is washed by the Barents Sea from the north;

– the rural settlement of Ura-Guba. It is located in the Kola District of the Murmansk Region. The Ura River flows into the gulf of the same name here, and the Kislaya Guba tidal power station is located nearby.

The study territories vary considerably in terms of key physical geographical and socio-economic indicators. This allows us to assess the versatility of the proposed methodology with respect to different types of Arctic coastal territory.

For the urban settlement of Kandalaksha's territory and the adjacent water area, the initial matrices were slightly reduced: the risk factor–risk source matrix was reduced to 19 × 16, and the risk object–risk factor matrix was reduced to 16 × 19. This is due to the exclusion of risk factors and objects that are not typical of this area; while the number of risk factors was reduced by only two: earthquake hazard and iceberg hazard.

Risk factor assessments according to risk component matrices, taking territorial correction coefficients into account, showed that the most significant risk factors are as follows:

– fire (score 20.2);

– high water in river mouths / flooding of the territory (score 14.8);

– man-made accidents (score 13.7).

The risk factors that have a significant impact on this territory (an assessment score ranging from 12.2 to 10.0) include solid waste pollution (in particular chemical and household waste); infectious and epidemiological hazards; abnormally high temperatures (melting of glaciers and permafrost, and rising sea levels); emissions of chemical pollutants into the atmosphere. The integral risk assessment score for this territorial unit is 552.6.

For the rural settlement of Teriberka and the adjacent water area, the initial matrices are reduced: risk factor–risk source to 16 × 11 and risk object–risk factor to 11 × 16, due to the reduction in risk sources and risk objects not available in the area in question. The following items were also removed from the list of risk factors: earthquakes; the emission of chemical pollutants / toxic substances into the atmosphere; the emission of chemical pollutants / toxic substances onto land / into the hydrosphere; oil spills on land; and radiation contamination.

According to the risk component matrices, which take into account territorial correction coefficients, the following risk factors were found to be the most significant:

– fire (score 22.9);

– man-made accidents (score 14.0);

– high water in river mouths / flooding of the territory (score 12.0).

Other significant risk factors for the above territory (an assessment score ranging from 9.7 to 8.3) include an abnormal high temperature regime (melting of the ice cover and permafrost, and rising sea levels); infectious and epidemiological contamination; wave and ice loads; and abnormal (intensive) precipitation. The integral risk assessment score for the territorial entity is 379.2.

When analysing the territory of the rural settlement of Ura-Guba and the adjacent water area, the risk matrices were also optimised. The size of the risk factor–risk source matrix was reduced to 15 × 13, and that of the risk object–risk factor matrix was reduced to 12 × 15. Six risk factors were removed: earthquake, iceberg hazard, emission of chemical pollutants / toxic substances into the atmosphere and on land / into the hydrosphere, oil spill on land, and radiation contamination.

Analysis of risk factor assessments using matrix models, taking into account the correction coefficients determined for this territorial unit, revealed the following most significant risk factors:

– fire (score 15.2);

– man-made accidents (score 12.0).

Other risk factors affecting the territory under consideration (an assessment score ranging from 10.7 to 9.7) include solid waste pollution, in particular chemical ones; municipal solid waste; infectious and epidemiological contamination; and an abnormal high temperature regime (melting of the ice cover and permafrost, and rising sea levels). The integral risk assessment score for the territorial unit was 274.9.

The presented model for the analysis of risks associated with the exploitation of natural resources in the coastal AZRF allows not only establishing the geographical distribution of risk levels and identifying key risk factors, but also modelling predictive assessments of risks and their components based on different scenarios. This functionality is realised through the potential addition or deletion of major infrastructure units or their aggregations.

Results

Risk assessment of sustainable Arctic nature use for the coastal zone of the Murmansk Region

The developed model for assessing the risks of Arctic nature use in the coastal AZRF was tested on 17 coastal territorial units of the local management level of the Murmansk Region. Calculations were carried out according to the described methodology using examples for local municipalities of the urban settlement of Kandalaksha, the rural settlement of Teriberka and the rural settlement of Ura-Guba. This allowed us to analyse the obtained results in the form of non-dimensional assessments of risk and its components without detailing the calculations.

The main risk factors were identified for each territorial unit, and their contribution to the impact assessment of the study territory was considered. The contributions of natural and anthropogenic factors (excluding fire and infectious diseases) were assessed separately. The selection of factors such as fire and infectious diseases is conditioned by their special nature; these risks can be caused by natural or anthropogenic factors or by a combination of these.

The analysis results showed that the identified risk sources produce the risk factor in the Pechenga Municipal District most intensively. For this territory, the non-dimensional assessment score of the source–factor relationship exceeds 180 (Fig. 1).

The main reason for the increased risk level in this municipality is the combination of a relatively high population density and diverse landscapes. Consequently, the Pechenga Municipal District shows a higher intensity of risk factor production than other coastal districts in the Murmansk Region. The urban settlement

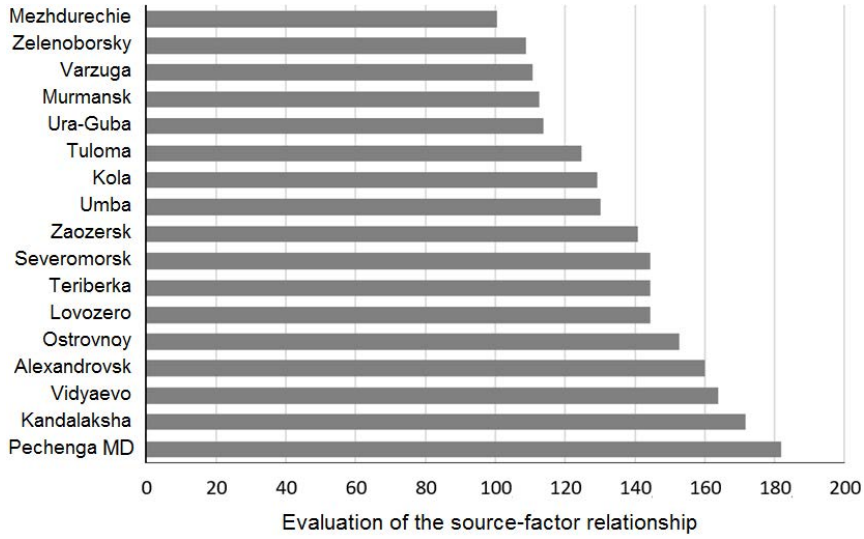

F i g . 1 . The degree of risk-factors production from exposure to risk-sources for the coastal local municipalities of the Murmansk region

of Kandalaksha is the second in terms of the degree of impact of identified risk sources with a source–factor relationship indicator of over 170. This high value is due to the reasons similar to those described for the Pechenga Municipal District. Kandalaksha is followed by the restricted administrative units of Vidyaevo and Aleksandrovsk with a source–factor correlation indicator of over 160 for each territory. The lowest indicator of risk factor production (slightly over 100) is registered for the rural settlement of Mezhdurechie.

When analysing the relationship between factors and objects in the coastal territories of the Murmansk Region, we assessed the potential impact of risk factors on the normal, effective functioning of risk objects. The objects of Kandalaksha were found to be the most vulnerable. The non-dimensional assessment score for this area exceeded 380, indicating a high risk (Fig. 2).

As for the Pechenga Municipal District, where the non-dimensional indicator was over 340, this result can be explained by a significant number of risk-prone objects concentrated in a densely populated coastal area of diverse topography. These factors together substantially influence the normal, effective functioning of the risk objects located in the region. The risk zone also encompasses objects in Murmansk, Teriberka and the restricted administrative units of Vidyaevo, Alexandrovsk, Severomorsk, Zaozersk and Ostrovny as well as in Kola and Tuloma. In these territories, the assessment scores range from over 310 to approximately 200.

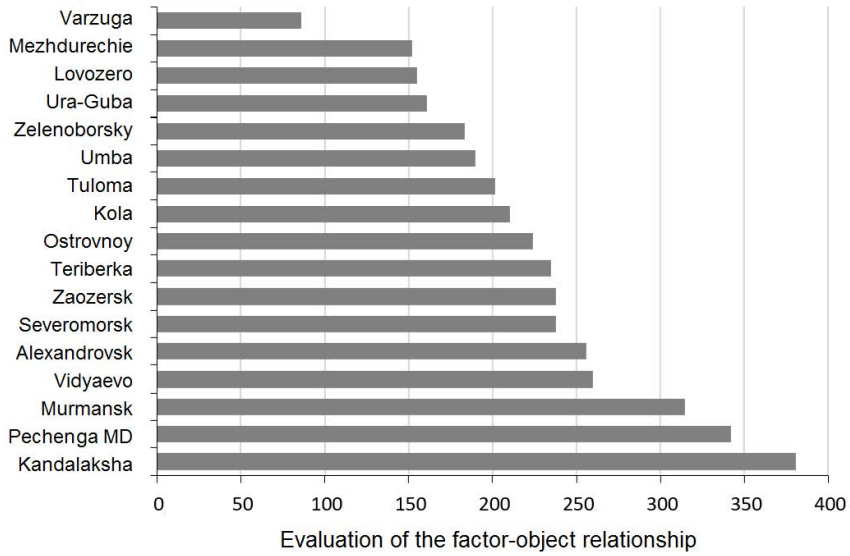

F i g . 2 . The degree of impact of the risk-factors on the normal effective functioning of risk objects for the coastal local municipalities of the Murmansk region

The lowest risk assessment score (over 85) was noted in the rural settlement of Varzuga. This is due to the small number of objects in the area with dispersed population with a homogeneous landscape. Taken together, these factors suggest that the potential risks have an insignificant impact on the normal and effective operation of risk objects in this region.

Analysis of the comprehensive risk assessment for the nature use in coastal areas of Murmansk Region municipalities revealed that Kandalaksha's coastal zone is at the highest risk. The integral risk assessment score for this area exceeds 550 (Fig. 3). This indicates that the occurrence probability for natural or man-made risks in this municipality is approximately 10%.

The coastal systems of the restricted administrative units of Aleksandrovsk and Vidyaevo as well as the Pechenga municipality and Murmansk are significantly influenced by risk factors, with integral assessment scores ranging from 410 to over 520. The lowest impact of risk factors is observed in the rural settlement of Varzuga, where the score is below 200 and the occurrence probability for adverse events (hazards) is 3%. Generally, the distribution of integral risk assessment values indicates a higher occurrence probability for various risks in relatively densely populated areas with a large number of functioning objects and a diverse landscape.

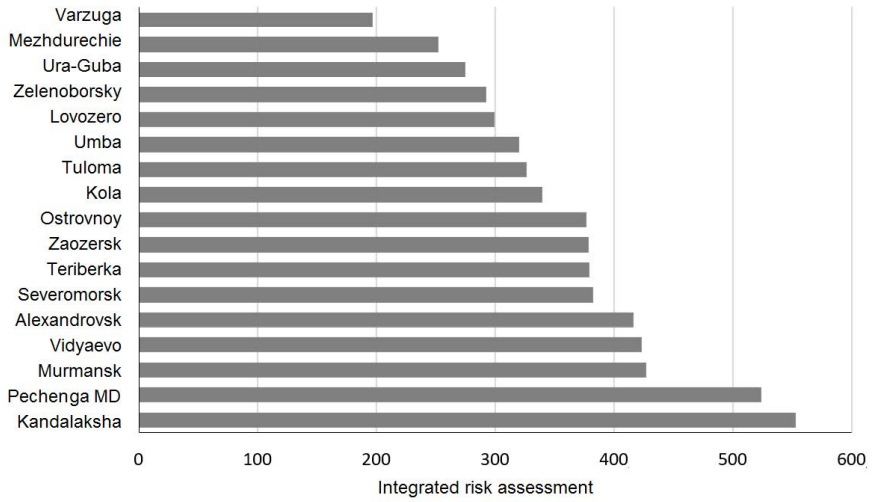

Fig. 3. Integrated risk assessment for the coastal local municipalities of the Murmansk region

Having analysed the key risk factors differentiated by their impact on Arctic nature use objects in each seaside municipality, we can identify the following features:

– fires have the greatest impact on the objects of the Pechenga Municipal District (with a 9% probability of occurrence). The rural settlement of Varzuga is the least vulnerable to this factor;

– the risk of high water in river mouths / flooding of the territory is also minimal in Varzuga;

– nature-use objects of the urban settlement of Kandalaksha have the highest (9%) probability of man-made accident risk among all objects of the Murmansk Region;

– infectious and epidemiological contamination is the most probable (9%) in objects of the Arctic coastal eco-socio-economic system of the Pechenga Municipal District compared to other municipalities of the Murmansk Region. The lowest vulnerability to this factor is observed in Varzuga.

The analysis revealed differences in the degree to which natural and anthropogenic risk factors (excluding fires and infectious diseases) influence the seaside municipalities of the Murmansk Region. The Pechenga Municipal District demonstrated the highest contribution of natural factors (over 260, corresponding to a 9% occurrence probability of an adverse natural phenomenon). This is due to a large number of natural risk factors present in the district compared to other coastal municipalities. The urban settlement of Kandalaksha has the greatest contribution of anthropogenic factors (over 235, which corresponds to approximately 12% occurrence

probability of an adverse event). This is due to the concentration of a large number of technogenic objects in a relatively densely populated area. The rural settlement of Varzuga shows minimum values of the complex contribution of both natural (approximately 4% probability) and anthropogenic (approximately 2% probability) factors. Thus, this settlement is the safest of the 17 coastal municipalities of the Murmansk Region.

Conclusion

The model developed for assessing risks associated with natural resource use in the coastal AZRF is based on a matrix methodology for assessing sustainability risks in nature use. The model provides a spatial map of risk assessment scores and identifies key risk factors. It considers a database of criteria, types, sources and objects of risk, as well as their spatial scale and the nature of their impact. It also allows for the assessment of different combinations of individual risk factors, such as the impact of natural, anthropogenic and other factors.

It is possible to create cartographic materials and graphic models reflecting the eco-socio-economic systems of Arctic coastal territories. This approach has been successfully implemented using the Murmansk Region as an example.

Within the Russian Science Foundation project, the level of territorial risk associated with the nature use was assessed. This allowed developing recommendations for informed managerial decisions as to territorial planning and the rational use of available resources. The resulting cartographic and graphic materials can be used to optimise management and ensure the sustainable development of the Arctic region.

The proposed model is a valuable tool for analysing risk dynamics and determining the overall level of risk associated with the commissioning or dismantling of large infrastructure units or their complexes. The implementation of such a scenario implies the development of a forecast of changes in the risk components values and corrective factors, which, in turn, allows obtaining an integral risk assessment. Introducing the presented methodology and model will optimise territorial planning procedures and ensure the sustainability of Arctic coastal eco-socio-economic complexes. The improvement of this methodology and model is dependent on analysing the risks of nature use and adapting to changes in environmental and socio-economic spheres. This will provide flexibility when carrying out similar risk assessments within the set tasks.

REFERENCES

1. Detter, G.F. and Iliasov, R.M., 2018. Evaluation of the Results of Approbation of the Model of Integrated Coastal Zone Management on the Example of the Yamal-Nenets Autonomous District. *Scientific Bulletin of the Yamal-Nenets Autonomous District*, (4), pp. 118–125 (in Russian).
2. Donskikh, D.V., Melnikov, A.O. and Lyui, K.E., 2023. Sustainable Development of the Arctic Region: Main Theoretical Aspects. *National Security*, (4), pp. 39–51 (in Russian).
3. Filimonova, I.V., Ivanova, M.V., Kuznetsova, E.A. and Kozmenko, A.S., 2023. Assessment of Effectiveness of New Economic Growth Centers in the Arctic. *Arctic and North*, (50), pp. 66–88. https://doi.org/10.37482/issn2221-2698.2023.50.66 (in Russian).
4. Morgunov, B.A., Terentiev, A.A. and Kozeltsev, M.L., 2019. Assessment of Transboundary Risks and Global Effects of Climate Change and Economic Activities in the Basins of the Arctic Seas. *Izvestiya Rossiiskoi Akademii Nauk. Seriya Geograficheskaya*, (2), pp. 100–108. https://doi.org/10.31857/S2587-556620192100-108 (in Russian).
5. Gogoberidze, G.G., Shilin, M.B. and Rumyantseva, E.A., 2021. Natural and Technology-Related Risks of Environmental Management in the Coastal Eco-Socio-Economic Systems of the Arctic Zone of the Russian Federation. *Regional Economics: Theory and Practice*, 19(2), pp. 360–383. https://doi.org/10.24891/re.19.2.360 (in Russian).
6. Kuzmin, S.B. and Lopatkin, D.A., 2020. Mapping Nature Management Risk in the Russian Federation Districts. *Geodesy and Carthography*, 81(9), pp. 14–29. https://doi.org/10.22389/0016-7126-2020-963-9-14-29 (in Russian).
7. Kulygin, V.V., 2018. Development of the Geoinformational Resource of Natural Hazards Risks for Marine Economic Activities. *InterCarto. InterGIS*, 24(1), pp. 158–166. https://doi.org/10.24057/2414-9179-2018-1-24-158-166 (in Russian).
8. Gogoberidze, G.G., Kosyan, R.D. and Rumiantceva, E.A., 2020. Method for Comprehensive Assessment of the Stability of Coastal Eco-Socio-Economic Systems on the Indicator Approach. *Ecological Safety of Coastal and Shelf Zones of Sea*, (3), pp. 122–141. https://doi.org/10.22449/2413-5577-2020-3-122-141 (in Russian).
9. Ershova, A.A., Vitsentii, A.V., Gogoberidze, G.G., Shishaev, M.G. and Lomov, P.A., 2018. Marine Spatial Planning: Possibilities for Maritime Areas and Adjacent Waters of the Murmansk Oblast. *National Interests: Priorities and Security*, 14(2), pp. 269–287. https://doi.org/10.24891/ni.14.2.269 (in Russian).
10. Akimov, V.A., Novikov, V.D. and Radaev, N.N., 2001. [*Natural and Man-Made Emergencies: Hazards, Threats, Risks*]. Moscow: Delovoy Ekspress, 344 p. (in Russian).
11. Balandin, D.A., Balandin, E.D. and Pytkin, A.N., 2019. The Priorities of Spatial Development of the Arctic Territories. *Journal of International Economic Affairs*, 9(3), pp. 1735–1746. https://doi.org/10.18334/eo.9.3.40926 (in Russian).
12. Lazhentsev, V.N., 2018. Socio-Economic Space and Territorial Development of the North and the Arctic of Russia. *Economy of Regions*, 14(2), pp. 353–365. https://doi.org/10.17059/2018-2-2 (in Russian).
13. Porfiryev, B.N. and Leksin, V.N., 2017. Drifting to Socially-Oriented Economy and Sustainable Development of the Russian Arctic: the Input of Technological Modernization. *MIR (Modernization. Innovation. Research)*, 8(S4), pp. 629–639. https://doi.org/10.18184/2079-4665.2017.8.4.629-639 (in Russian).
14. Tsukerman, V.A. and Goryachevskaya, E.S., 2017. On the Methodology of Assessing the Innovation Development Level of the Regions of the Arctic and the North. *Sever i Rynok: Formirovanie Ekonomicheskogo Poryadka*, (3), pp. 57–68 (in Russian).

15. Bakaev, A.A. and Sakharova, S.M., 2024. Assessment of the State Management Effectiveness of Socio-Economic Development of the Arctic Zone of the Russian Federation Based on a System of Balanced Indicators. *Central Russian Journal of Social Sciences*, 19(1), pp. 150–171. https://doi.org/10.22394/2071-2367-2024-19-1-150-171 (in Russian).
16. Rumiantceva, E.A., Gogoberidze, G.G., Lednova, Yu.A. and Efimenko, E.A., 2024. Assessment of Risks of Nature Management in the Coastal Zone of the Murmansk Region Based on the Matrix-Indicator Approach. *Ekologiya. Ekonomika. Informatika. Seriya: Sistemny Analiz I Modelirovanie Ekonomicheskikh I Ekologicheskikh Sistem*, 1(9), pp. 92–95 (in Russian).
17. Gogoberidze, G., Rumiantceva, E. and Shilin, M., 2021. Risk Assessment of the Arctic Coastal Nature Management Based on the Matrix Approach. *Russian Arctic*, 15, pp. 5–16. https://doi.org/10.24412/2658-4255-2021-4-05-16 (in Russian).
18. Gogoberidze, G.G., Rumiantceva, E.A. and Shilin, M.B., 2021. Classification Features and Specific Forms of Components of Nature-Management Risks for the Coastal Eco-Socio-Economic System of the Arctic Zone of the Russian Federation. In: SSC RAS, 2021. *Regularities of Formation and Impact of Marine and Atmospheric Hazardous Phenomena and Disasters on the Coastal Zone of the Russian Federation under the Conditions of Global Climatic and Industrial Challenges ("Dangerous Phenomena – III") in Memory of Corresponding Member RAS D.G. Matishov: Proceedings of the International Scientific Conference (Rostov-on-Don, 15–19 June 2021)*. Rostov-on-Don: SSC RAS Publishers, pp. 123–126 (in Russian).

Submitted 07.08.2024; accepted after review 14.10.2024;
revised 25.03.2025; published 30.06.2025

About the authors:

George G. Gogoberidze, Leading Research Associate, Murmansk Arctic State University (15 Kapitana Egorova St., Murmansk, 183038, Russian Federation), DSc (Econ.), Associate Professor, **ORCID ID: 0000-0002-0537-0268, Scopus Author ID: 6507697703, ResearcherID: E-6597-2014**, *gogoberidze.gg@gmail.com*

Ekaterina A. Rumiantceva, Senior Research Associate, Murmansk Arctic State University (15 Kapitana Egorova St., Murmansk, 183038, Russian Federation), PhD. (Phys.-Math.), **ORCID ID: 0000 -000 3-29 16-3092, Scopus Author ID: 57205164298, ResearcherID: T-2221-2018**, *rumkate@rambler.ru*

Yulia A. Lednova, Associate Professor, Higher School of Hydrotechnical and Power Engineering, Peter the Great St. Petersburg Polytechnic University (29Б, Politekhnicheskaya St., Saint Petersburg, 195251, Russian Federation), PhD (Geogr.), **ORCID ID: 0000-0003-2051-1994, Scopus Author ID: 56076423700, ResearcherID: H-3062-2014,** *lednovajulia@mail.ru*

Ekaterina A. Efimenko, Research Engineer, Murmansk Arctic State University (15 Kapitana Egorova St., Murmansk, 183038, Russian Federation), **ORCID ID: 0009-0007-3557-1937**, *efimenkoea@mauniver.ru*

Contribution of the authors:

George G. Gogoberidze – general scientific supervision of the study, study goals and objectives statement, development of methodology and approaches, development of matrix approach and risk model, formulation of directions for further study, discussion of the work results, conclusion drawing, preparation of the manuscript

Ekaterina A. Rumiantceva – development of the matrix approach, analysis of the computational results, discussion of the article materials and work results, preparation of the manuscript, text revision

Yulia A. Lednova – literature review on the study problem, development of the matrix approach, collection of information for calculations, formulation of directions for further study, discussion of the article materials and work results, conclusion drawing, text revision

Ekaterina A. Efimenko – collection of information for calculations, discussion of the article materials and work results, conclusion drawing, text revision

All the authors have read and approved the final manuscript.